Dissection of the Epigenetic Asymmetry in Mouse Zygotes

Inauguraldissertation

zur
Erlangung der Würde eines Doktors der Philosophie
vorgelegt der
Philosophisch–Naturwissenschaftlichen Fakultät
der Universität Basel

von

Rico Kunzmann
aus Zürich, ZH

Basel, 2012

Originaldokument gespeichert auf dem Dokumentenserver der Universität Basel
edoc.unibas.ch

Dieses Werk ist unter dem Vertrag „Creative Commons Namensnennung-Keine kommerzielle Nutzung-Keine Bearbeitung 2.5 Schweiz“ lizenziert. Die vollständige Lizenz kann unter
creativecommons.org/licences/by-nc-nd/2.5/ch
eingesehen werden.

Genehmigt von der Philosophisch-Naturwissenschaftlichen Fakultät
auf Antrag von

Prof. Dr. Susan Gasser	Dr. Antoine Peters	Dr. Gunter Reuter
(Fakultätsverantwortlicher)	(Referent)	(Koreferent)

Basel, den 13.12.2011

Dr. Martin Spiess
(Dekan)

Namensnennung-Keine kommerzielle Nutzung-Keine Bearbeitung 2.5 Schweiz

Sie dürfen:

das Werk vervielfältigen, verbreiten und öffentlich zugänglich machen

Zu den folgenden Bedingungen:

Namensnennung. Sie müssen den Namen des Autors/Rechteinhabers in der von ihm festgelegten Weise nennen (wodurch aber nicht der Eindruck entstehen darf, Sie oder die Nutzung des Werkes durch Sie würden entlohnt).

Keine kommerzielle Nutzung. Dieses Werk darf nicht für kommerzielle Zwecke verwendet werden.

Keine Bearbeitung. Dieses Werk darf nicht bearbeitet oder in anderer Weise verändert werden.

- Im Falle einer Verbreitung müssen Sie anderen die Lizenzbedingungen, unter welche dieses Werk fällt, mitteilen. Am Einfachsten ist es, einen Link auf diese Seite einzubinden.

- Jede der vorgenannten Bedingungen kann aufgehoben werden, sofern Sie die Einwilligung des Rechteinhabers dazu erhalten.
- Diese Lizenz lässt die Urheberpersönlichkeitsrechte unberührt.

Die gesetzlichen Schranken des Urheberrechts bleiben hiervon unberührt.

Die Commons Deed ist eine Zusammenfassung des Lizenzvertrags in allgemeinverständlicher Sprache: http://creativecommons.org/licenses/by-nc-nd/2.5/ch/legalcode.de

Haftungsausschluss:
Die Commons Deed ist kein Lizenzvertrag. Sie ist lediglich ein Referenztext, der den zugrundeliegenden Lizenzvertrag übersichtlich und in allgemeinverständlicher Sprache wiedergibt. Die Deed selbst entfaltet keine juristische Wirkung und erscheint im eigentlichen Lizenzvertrag nicht. Creative Commons ist keine Rechtsanwaltsgesellschaft und leistet keine Rechtsberatung. Die Weitergabe und Verlinkung des Commons Deeds führt zu keinem Mandatsverhältnis.

Quelle: http://creativecommons.org/licenses/by-nc-nd/2.5/ch/ Datum: 3.4.2009

Table of Contents

Abbreviations....4

1. Summary....7

2. Introduction....11

  2.1 Chromatin States....12

    2.1.1. Euchromatin....14

    2.1.2. Heterochromatin....15

      2.1.2.2. Constitutive Heterochromatin....15

      2.1.2.1. Facultative Heterochromatin....16

  2.2. Heterochromatin Formation and Maintenance in Model Organisms....17

    2.2.1. Fungi....17

      2.2.1.1. *S. cerevisiae*....17

      2.2.1.2. *S. pombe*....18

      2.2.1.3. *N. crassa*....21

    2.2.2. Animals....22

      2.2.2.1. *D. melanogaster*....22

      2.2.2.2. *M. musculus*....33

  2.3. (Hetero-) Chromatin dynamics in the mouse zygote....45

    2.3.1. Spermatogenesis....45

    2.3.2. Oogenesis....46

    2.3.3. The Zygote....47

      2.3.3.1. Asymmetry of Histones in the Zygote....49

      2.3.3.2. Asymmetry of Global Histone Marks....52

      2.3.3.3. Asymmetry at PCH in the Mouse Zygote....52

      2.3.3.4. DNA ‘demethylation’ in the Mouse Zygote....55

      2.3.3.5. Maternal-to-Zygotic Transition....56

  2.4. Scope of the thesis....57

3. Results....59

  3.1. Unpublished Manuscript: PRC1 targeting to constitutive heterochromatin and its dependency with the *Suv39h/Hp1*β pathway in mouse zygotes....59

3.2. Additional Results 90

3.2.1. Additional Results: PRC1 targeting to constitutive heterochromatin and its dependency with the *Suv39h/Hp1β* pathway in mouse zygotes 90

3.2.1.1. FRAP of Cbx2 at Heterochromatin in Suv39h-dn ESC. 90

3.2.1.2. Polycomb from an evolutionary point of view 93

3.2.1.3. Exogenously provided Hp1β restores PCH asymmetry in Hp1β^{m-z+} zygotes 100

3.2.1.4. The Effect of SUV39H Activity in Mouse Zygotes on the PCH Asymmetry 104

3.2.2. Size Difference of Maternal and Paternal Pronuclei 109

3.2.3. Impact of Epigenetic Repressors on Zygotic 5mC to 5hmC conversion 117

4. Discussion 128

5. References 134

Appendix 156

Acknowledgements 162

Curriculum Vitae 163

Abbreviations

aa	amino acid
ARS	autonomously replicating sequences
bp	base pair
CD	chromodomain
CDS	chromoshadow domain
ChIP	chromatin immuno-precipitation
cKO	conditional knock out
DAPI	4,5-diamidino-2-phenylindole
DNA	deoxyribonucleic acid
Dnmt	DNA methyl transferase
EdU	5-ethynyl-2'-deoxyuridine
E(var)	enhancer of variegation
ETn	early transposons
FISH	fluorescent *in situ* hybridization
FRAP	fluorescence recovery after photobleaching
Gb	giga base
GFP	green fluorescent protein
GV	germinal vesicle
HML	hidden MAT left
HMR	hidden MAT right
HMT	histone methyltransferase
IAP	intracisternal A-particle
ICM	inner cell mass
kb	kilo base

KD	knock down
K_d	dissociation constant
KO	knock out
LINE	long interspersed element
LTR	long terminal repeat
lncRNA	long non-coding RNA
lincRNA	large intergenic non-coding RNA
Mb	mega base
MBD	methyl-CpG binding domain
MII	metaphase II oocyte
miRNA	micro RNA
ncRNA	non-coding RNA
NPB	nucleolar precursor body
NSN	non-surrounding nucleolus oocyte
ORC	origin replication complex
ORI	DNA replication origin
PcG	Polycomb group
PCH	pericentromeric heterochromatin
PEV	position effect variegation
PGC	primordial germ cells
PHD	plant homeotic domain
piRNA	Piwi-interacting RNA
PN	pronucleus
PRC	Polycomb repressive complex
PRE	Polycomb response element
rDNA	ribosomal DNA

RIP	repeat-induced point mutation
RITS	RNA-induced transcriptional silencing
RNAi	RNA interference
SET	Suppressor of variegation, Enhancer of Zeste, Trithorax
SINE	short interspersed element
SIR	silent information regulator
SN	surrounding nucleolus oocyte
Su(var)	suppressor of variegation
SUMO	small ubiquitin-related modifier
TrxG	Trithorax group
Xi	inactivated X
ZGA	zygotic genome activation
H2AK119ub1	histone H2A lysine 119 mono-ubiquitination
H3K9me3	histone H3 lysine 9 tri-methylation
3C	chromosome conformation capture
5mC	5-methyl cytosine
5hmC	5-hydroxy-methyl cytosine

1. Summary

PRC1 targeting to heterochromatin and its dependency with the Suv39h/Hp1β pathway in mouse zygotes.

Constitutive heterochromatin in mouse is mainly detected around the centromeres of chromosomes. It consists of highly abundant, repetitive AT-rich DNA. These repeats are called major satellite repeats. They are marked by the epigenetic, repressive Suv39h pathway in various cell types. In mouse zygotes, maternal pericentric heterochromatin (PCH) displays the marks of the Suv39h pathway: tri-methylation of lysine 9 on histone tail H3 (H3K9me3), H4K20me3 and Hp1β (Santos et al., 2005) (Figure 1.1). Paternal PCH on the other hand does not exhibit the Suv39h marks. It is enriched for proteins of another major epigenetic repressive complex: the Polycomb repressive complex 1 (PRC1) (Puschendorf et al., 2008) (Figure 1.2). This complex, consisting of Polycomb group proteins (PcG), has been shown to be important for gene repression (Lewis, 1978). In mouse zygotes, however, PRC1 also represses paternal transcription of major satellite repeats. It has been shown to mark paternal PCH immediately after fertilization (Puschendorf et al., 2008).

The first major question addressed in this thesis is how PRC1 is targeted to PCH. We show that PRC1 targeting to paternal PCH is dependent on two protein modules of Cbx2, a core member of PRC1 in early mouse zygotes. The first module is the N-terminal chromodomain (CD), which preferentially binds H3K27me3 (Kaustov et al., 2011), a histone mark that appears on paternal PCH in the late zygotic stages. The second module is an AT-hook motif, which is located just C-terminal of the CD. AT-hook motifs have been shown to bind the minor groove of AT-rich DNA sequences, therefore, the AT-rich major satellite repeats are putative target sequences for this motif. Indeed, treatment of zygotes with dystamicin, a compound that binds AT-rich DNA sequences, diminishes PRC1 enrichment at paternal PCH in early zygotes. Furthermore, insertion of a point mutation into either the CD or the AT-hook results in reduced heterochromatin enrichment. Nevertheless, only the introduction of point mutations into both modules results in complete loss of enrichment. Additionally, the Cbx2 targeting to PCH is Ezh2 and RNA independent. By performing fluorescence recovery after bleaching (FRAP) experiments, we show that overexpressed Cbx2 at heterochromatin is dynamic with an average half recovery time of 7 seconds. Upon introduction of point mutations into either the CD or AT-hook modules, the dynamics strongly increase, suggesting weaker binding. Finally, we show

that among all five Cbx paralogs in mouse, only Cbx2 contains an AT-hook motif, which is highly conserved from fish to humans. Thus, this targeting mechanism of PRC1 is strictly Cbx2 dependent.

The second major question addressed in this thesis concerned the hierarchy of the two major epigenetic, repressive pathways at PCH in mouse zygotes. Zygotes that are deficient for the Suv39h2 histone methyltransferase (HMT), as well as embryonic stem cells (ESCs) lacking both Suv39h1 and Suv39h2 HMTs and therefore any downstream mark, exhibit PRC1 enrichment at paternal and maternal PCH and at chromocenters in ESCs, respectively. These observations suggest a hierarchy between the two epigenetic, repressive pathways. We show that Hp1β, a downstream member of the Suv39h pathway, but not the Suv4-20 HMTs, actively prevents PRC1 members from binding to maternal PCH. In *Hp1β* maternally deficient zygotes (*Hp1β*$^{m\text{-}z+}$) as in *Suv39h2*$^{m\text{-}z+}$ zygotes, PRC1 members strongly localize to maternal PCH, despite the presence of the H3K9me3 and H4K20me3 maternal histone marks. Furthermore, we show that enhancing the affinity of the Cbx2 CD for H3K9me3 by a single amino acid (aa) exchange enables its co-localization with members of the Suv39h pathway on maternal PCH and in wild type (wt) ESC, respectively. We show that this aa residue confers the H3K27me3 specificity of Cbx2. Interestingly, this aa residue is conserved in Cbx2 among eumetazoa.

Taken together, we propose a simple targeting mechanism for PRC1 to heterochromatin, based on a CD and an AT-hook motif. A similar targeting mechanism for PRC1 can be envisioned for the AT-rich DNA of euchromatin. Furthermore, we map the interdependency of the Suv39h pathway with PRC1 to the CDs of Hp1β and Cbx2.

Size Difference of Maternal and Paternal Pronuclei

Although the maternal and the paternal genomes are equally large, the paternal pronucleus (PN) is bigger than the maternal PN. This suggests that DNA in the maternal PN is more compacted. Interestingly, this size difference is not only observed in PN5 zygotes but throughout zygotic development, which suggests that it is maintained by proteins present in the zygote.

Here we show that the size difference between maternal PN and paternal PN is due to Hp1β. The maternal PN is smaller than the paternal PN because of Hp1β, putatively bound to maternal H3K9me3. In *Hp1β*$^{m\text{-}z+}$ zygotes, this size difference is lost. Microinjection of recombinant Hp1β into *Hp1β*$^{m-z+}$ zygotes reestablishes the size decrease of maternal PN, suggesting that it is a zygotic phenotype. Furthermore, the maternal and paternal PN sizes of wt zygotes can be decreased by the presence and the enzymatic activity of abundant exogenously provided proteins of the Suv39h pathway.

Impact of Epigenetic Repressors on Zygotic 5mC to 5hmC conversion

Within a few hours after fertilization, the paternal genome rapidly loses its global 5mC DNA methylation (Mayer et al., 2000a; Oswald et al., 2000; Santos et al., 2002). The maternal genome remains DNA methylated in the zygote. A maternal factor called PGC7/Stella was identified to protect the maternal DNA methylation state (Nakamura et al., 2007). Recently, it was shown that paternal 5mC is converted to 5hmC by the Tet3 proteins (Gu et al., 2011).

Zygotes, which were maternally deficient for either PcG proteins or members of three H3K9 HMT pathways, were analyzed for their maternal and paternal 5mC and 5hmC content. The most evident effect on the 5mC to 5hmC conversion in zygotes was observed in maternally deficient *G9a* and *Hp1β* zygotes. In both lines, enhanced conversion of maternal 5mC was observed. This suggests that G9a and even more so Hp1β protect maternal 5mC from conversion to 5hmC.

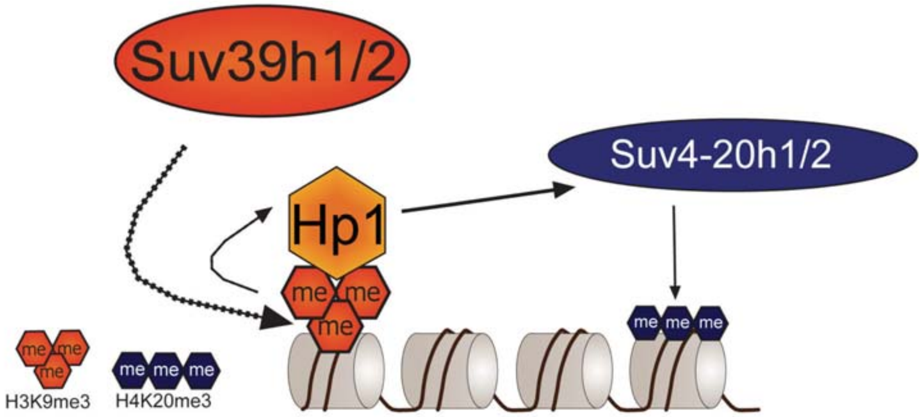
Suv39h1/2
Hp1
Suv4-20h1/2
me
me
me
me me me
H3K9me3
H4K20me3

Figure 1.1: Cartoon showing the canonical, heterochromatin associated Suv39h pathway, which is highly conserved among metazoan. The Suv39h HMTs tri-methylate H3K9me3. This chromatin mark is bound by the CD of the Hp1 orthologs. They, in turn, recruit the Suv4-20h HMTs, which tri-methylate H4K20.

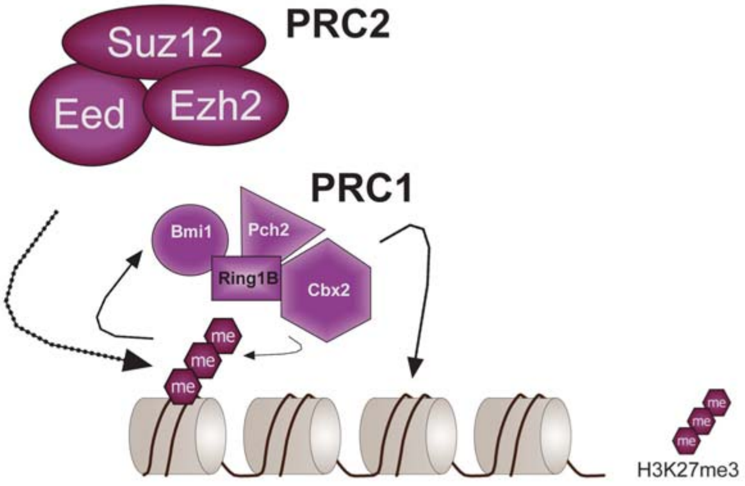
Suz12
PRC2
Eed
Ezh2
PRC1
Bmi1
Pch2
Ring1B
Cbx2
me
me
me
H3K27me3

Figure 1.2: Cartoon of the two main complexes formed by PcG: PRC1 and PRC2. Shown are the core members of PRC1 and PRC2 present in the mouse zygote. In this simplified model, Ezh2 of PRC2 tri-methylates H3K27me3. This mark is bound by the PRC1 member Cbx2, which then recruits the other complex members via its PcBox.

2. Introduction

Emil Heitz: distinction of euchromatin and heterochromatin

In the late 1920s Emil Heitz (1892-1965 (Passarge, 1979; Zacharias, 1995)), a cytological geneticist, to use his terminology, fixed moss material in 2/3 of alcohol and 1/3 of acetic acid. He stained it in carmine acetic acid and prepared single cell layers. By putting gentle pressure to the cover slip he obtained the best metaphase spreads free of cytoplasm (Heitz, 1926, 1928a, b, 1933a). Applying this method, the longitudinal differentiation of mitotic chromosomes became apparent. He further stained cells throughout the cell cycle. Regions that continuously showed dense staining were named heterochromatin, while regions that showed no staining, thus decondensed during interphase, were called euchromatin (Heitz, 1928a). Later, Heitz started a series of cytological investigations searching for heterochromatin in somatic cell nuclei of *Diptera* (Figure 2.1). He showed that heterochromatin was a general phenomenon occurring in both animals and plants (Heitz, 1933b).

Spencer W. Brown: definition of the 'heterochromatin state'

A few decades after Heitz, another geneticist, Spencer Brown, makes the following statement in a report on heterochromatin (Brown, 1966): "…probably all chromosome regions are potentially capable of becoming heterochromatic, but in most organisms only certain segments will usually so respond during development. We must, therefore, regard euchromatin and heterochromatin as states rather than substances."

Scientists to this day continue to study the heterochromatic state, how dynamic it is, how it is established, structured and maintained throughout cell cycles. Many proteins have been shown to be important for these processes. I will highlight the function of Hp1 within the Suv39h pathway in epigenetic silencing and oppose it to the function of PcG proteins in this respect.

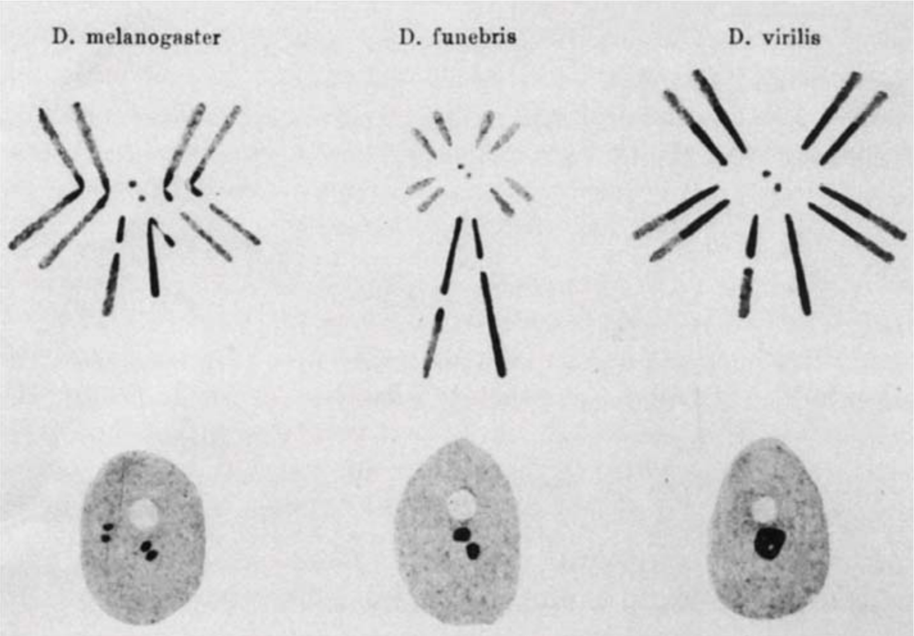

Figure 2.1: Chromatin structure of three *Drosophila* species. Darkly stained chromosomal regions during metaphase indicate heterochromatin. In interphase nuclei the heteropycnotic material is associated with chromocenters (adapted from Heitz, 1934, Figure 9 and 1935, Figure7).

2.1 Chromatin States

The genomic DNA of eukaryotic nuclei is packaged by histones into chromatin. Two H3-H4 histone dimers interact to form a stable tetramer, which is in turn flanked by two H2A-H2B dimers. Together they form the so-called histone octamer. 146 base pairs (bp) of DNA is wrapped 1.7 times in superhelical turns around such a histone octamer (Davey et al., 2002; Luger et al., 1997). This structure is referred to as a nucleosome. The nucleosomal histones interact with each other through a histone fold domain (Davey et al., 2002). The nucleosomal arrangement results in a fiber 11 nm in diameter, which represents the lowest level of chromatin organization in the nucleus (Luger et al., 1997). The binding of linker histones H1 protects the internucleosomal linker DNA (Woodcock et al., 2006), and organizes the nucleosomal arrangement into a more condensed 30 nm fiber, which is referred to as the second structural level of chromatin organization (Robinson et al., 2006). Two models for the 30 nm fiber have been proposed. The solenoid model suggests that chromatin is arranged in a superhelical path in which a nucleosome interacts with its fifth and sixth neighbor nucleosome (Widom and Klug, 1985). In the zigzag model, chromatin is arranged in a zig-zag manner such that one nucleosome in the fiber binds to the second neighbor nucleosome (Dorigo et al., 2004; Schalch et al., 2005; Williams et al., 1986). The folding of a chromatin fiber into a next higher level is less understood. For example, some microscopic studies have identified larger fiber-like structures in mammalian nuclei ranging from 60-80nm in interphase and up to 750 nm in metaphase cells (Kireeva et al., 2004). In addition to that, recent technological advances in chromosome conformation capture (3C) based methods enable to map the three-dimensional chromosome organization at a resolution of several kb (Sanyal et al., 2011).

The folding of a chromatin fiber into a higher level is putatively influenced by epigenetic modifiers and their chromatin signature. A prominent, functionally important feature of a chromatin signature is the post-translational modifications of histones. Such modifications occur on all four core histones. The ones best studied localize to the unstructured N-terminal tail of histone H3 and H4, which are extruded from the core of the nucleosome. Depending on which modification marks the chromatin, it appears either more or less condensed.

Another functionally important chromatin feature is DNA methylation. A methyl group is added to the position 5 of the cytosine ring (5mC). In mammals, genome wide profiles of DNA methylation show that cytosine methylation occurs in the context of CpG dinucleotides. Most cytosines of intergenic regions, coding regions and repeats in the CpG context are methylated (reviewed in (Guibert, 2009)).

Furthermore, the grade of condensation of chromatin has been implicated with the accessibility of the transcription machinery, and thus transcription in general. This refers also to Heitz' original observation: "Euchromatin is genicly active, heterochromatin genicly passive" (Heitz, 1929). This, although, as we know by now, is not entirely valid.

2.1.1. Euchromatin

Euchromatin is less compacted than heterochromatin and generally highly transcriptionally active. It has been suggested that higher-order chromatin structures inhibit polymerases and DNA repair factors (Campos and Reinberg, 2009). Accordingly, nucleosomal arrays impede transcription *in vitro* (Morse, 1989). Nevertheless, euchromatin is not nucleosome free (Schones et al., 2008). On the contrary, it remains nucleosome dense *in vivo*. Access to the DNA for the transcription-, replication– and repair-machinery is ensured by the displacement of nucleosomes via chromatin remodeling factors (Workman, 2006). Post-translational modifications of the histone tails influence the recruitment of chromatin-modifying effectors as well as the local chromatin structure (Campos and Reinberg, 2009). Histone modifications that have been implicated with transcribed euchromatin include acetylation, H3K4me3 at transcription start site (Barski et al., 2007) and H3K36me3 within gene bodies (Bannister et al., 2005). Additionally, histone variants H3.3 (Tagami et al., 2004) and H2A.Z (Suto et al., 2000) are enriched at euchromatin.

In addition to specific histone modifications within euchromatin, cytosine residues of euchromatin are methylated in the CpG context. Around 40 % of the mammalian promoters are CpG poor. The CpG dinucleotides within these promoters are usually DNA methylated irrespective of the transcriptional activity of the associated gene, suggesting that low DNA methylation does not prevent transcription (Meissner et al., 2008). The other 60 % of promoters are enriched for CpG dinucleotides. Most of them remain unmethylated even when the associated gene is not expressed, suggesting that they are protected from DNA methylation, independent of transcription (Meissner et al., 2008). Recent studies, though, show that also a fraction of high CpG content promoters are hypermethylated in various somatic cell types, which coincides with transcriptional repression (Illingworth et al., 2008; Shen et al., 2007; Weber et al., 2007).

2.1.2. Heterochromatin

Two major distinct heterochromatic types have been defined: constitutive and facultative heterochromatin.

2.1.2.2. Constitutive Heterochromatin

The chromatin of lower eukaryotes is almost entirely in a euchromatic conformation. Only regions that ensure genome integrity, such as telomeres and centromeres, are in a heterochromatic conformation and are referred to as constitutive heterochromatin (Grewal and Jia, 2007; Grunstein, 1998). In higher eukaryotes the same chromosomal regions are kept in a heterochromatic conformation. Additionally, a large portion of the genome consists of repetitive and non-coding sequences, resulting in an increase in genome size (Kent et al., 2002). Most of these repetitive sequences are in a constitutive heterochromatin conformation, in order to ensure genome stability (Lehnertz et al., 2003). The most prominent, constitutively silenced chromosomal domains are localized around the centromeres, thus they are called pericentromeric. They are largely devoid of genes and enriched for repetitive elements. In mouse, these are the so-called major satellite repeats (Lehnertz et al., 2003). They contribute to centromere function and chromosome segregation (Malik and Henikoff, 2009; Peng and Karpen, 2008; Peters et al., 2001). Despite the condensed state of pericentromeric heterochromatin, transcription at these genomic regions is possible and in some cases also required for the establishment of constitutive heterochromatin (Grewal and Elgin, 2007), as discussed in 2.2. The transcript levels, though, remain low.

Many proteins involved in the formation and maintenance of heterochromatin were first identified in genetic screens for position effect variegation (PEV) in *Drosophila*. Around 150 loci, so-called suppressor of variegation (Su(var)) genes, are thought to be involved in heterochromatin formation in *Drosophila* (Eissenberg and Reuter, 2009; Schotta et al., 2003). They will be discussed in more detail in 2.2.2.1. Other components of heterochromatin are the histone variants H1.0 and H2A/Z, chromatin binders like the Hmga1/2 proteins, nucleosome remodelers like Atrx and proteins involved in DNA methylation like the DNA methyltransferases (DNMT) and methyl-CpG binding domain (MBD) 1, -2, -4 proteins, as well as DNA methylation itself (Fodor et al., 2010).

2.1.2.1. Facultative Heterochromatin

Using cytological staining methods, facultative heterochromatin is either indistinguishable from constitutive heterochromatin, like the inactive X chromosome, or is restricted to a region that cannot be distinguished from euchromatin. Therefore, it has been proposed that facultative heterochromatin adopts a wide range of chromatin condensation states (Trojer and Reinberg, 2007). Similar to constitutive heterochromatin, facultative heterochromatin is transcriptionally inactive. Nevertheless, facultative, silent chromatin regions are able to de-condense and become transcriptionally active within a temporal (e.g. developmental stages), spatial (e.g. nuclear localization) or parent of origin (e.g. monoallelic gene expression) specific manner (Trojer and Reinberg, 2007).

A classic example of facultative chromatin is the inactive X-chromosome present in mammalian, female cells. Before gastrulation, one of the X-chromosomes, randomly chosen, is stably silenced. This state is maintained throughout the life of the organism (Trojer and Reinberg, 2007). Similar mechanisms have been reported to achieve the repression of autosomal imprinted genomic loci. These silencing mechanisms will be discussed in more detail in 2.2.2.2. Other well studied regions of facultative heterochromatin are the clustered *Hox* genes, which exhibit a pattern of transcriptionally active and inactive genes. Once this pattern is established, it is maintained throughout developmental stages (Lewis, 1978).

The pathways involved in the setting up of facultative heterochromatin will be discussed in more detail in 2.2.2.1 and 2.2.2.2. Generally, a non-coding RNA (ncRNA) or a specific DNA sequence is implicated in the recruitment of the proteins, like the PcG proteins, that maintain the silenced state. The maintenance of facultative heterochromatin is also associated with DNA methylation and repressive histone marks.

2.2. Heterochromatin Formation and Maintenance in Model Organisms

2.2.1. Fungi

2.2.1.1. *S. cerevisi*ae

The 16 chromosomes of budding yeast, *S. cerevisiae*, are too small for the visualization of heterochromatin by the cytological stainings used by Heitz. Nevertheless, they display chromosomal regions, which appear to be more condensed (Loo and Rine, 1994; Weiss and Simpson, 1998), replicate late in S-phase (Bianchi and Shore, 2007) and localize in foci at the nuclear periphery (Gotta et al., 1996; Palladino et al., 1993). These dense regions are found at the telomeres of chromosomes and at the silent mating loci.

Telomeres

Yeast telomeres consist of around 300 bp, containing a short single stranded 3' overhang and double stranded, irregular repeats (reviewed in (Buhler and Gasser, 2009)). They are free of nucleosomes. It has been shown that these DNA repeats associate with the N-terminus of the non-histone protein RAP1 (Conrad et al., 1990). The subtelomeric, heterochromatic regions on the other hand are only moderately repetitive, and they are nucleosomal (Vega-Palas et al., 1998). Interestingly, chromatin in these regions is hypoacetylated at lysine residues of histones H2B, H3 and H4. Furthermore, the highly conserved H3K4 methylation and H4K16 acetylation marks, which are associated with transcribed DNA regions, are absent from subtelomeric histones (reviewed in (Buhler and Gasser, 2009)). The hypoacetylation of histones suggests localization specific activity of histone deacetylases. Indeed, SIR2, a conserved NAD-dependent histone deacetylase, specifically deacetylates subtelomeric H4K16, in addition to other acetylated residues on the histone tails of H3 and H4 (Blander and Guarente, 2004). The hypoacetylation enables binding of the silent information regulatory (SIR) complex, consisting of SIR2/3/4, which ensures transcriptional repression of subtelomeric regions (Cubizolles et al., 2006).

Mating Type Loci

There are three mating type loci in *S. cerevisiae*: *HMLα* (hidden MAT left), MAT and *HMRa* (hidden MAT right). Whereas *HMLα* and *HMRa* are the silenced loci, the MAT locus, displaying either α or a, is the active locus. The silenced loci carry the information for the two mating types α and a. Sterility screens identified *SIR1, 2, 3* and *4* as being essential for the repression of the silent loci (Rusche et al., 2002). Interestingly, the origin recognition complex (ORC), consisting of six subunits (Orc1-6), which plays a crucial role in the initiation of DNA replication at the AT-rich autonomously replicating sequences (ARS), has been shown to be involved in silencing elements of HMR (Bell et al., 1993; Foss et al., 1993b; Micklem et al., 1993).

Summary

Taken together, subtelomeric heterochromatin formation in *S. cerevisiae* histone tails relies on the absence of active histone marks. The canonical pathway associated with heterochromatin formation in metazoa, the Su(var) pathway, is absent in *S. cerevisiae*.

2.2.1.2. *S. pombe*

In fission yeast, like in budding yeast, telomeres and the mating type loci are epigenetically silenced. In addition, the outer repeats of the centromeres are also subject to epigenetic silencing (Grewal and Jia, 2007).

The Su(var) pathway in S. pombe

The assembly of subtelomeric and pericentromeric heterochromatin as well as at the silent mating type loci, requires deacetylation of histone tails H3 and H4 (Shankaranarayana et al., 2003), similar to *S. cerevisiae*. Sir2 proteins act cooperatively with Clr3, a NAD-independent histone deacetylase, throughout the silent regions. The most significant deacetylation sites are H3K14 acetylation for Clr3 and H3K9 acetylation for Sir2 (Wiren et al., 2005). This, subsequently, enables activity of the histone lysine methyltransferase Clr4, an ortholog of the mammalian Suv39h HMT, which tri-methylates histone H3K9. This histone mark is present at pericentromeric and subtelomeric DNA as well as at the silent mating-type loci (Nakayama et al., 2001). Methylation of H3K9 by Clr4 creates a binding site for proteins with CDs, like Swi6, Chp1 and 2, or Clr4 itself. From these CD containing proteins, Swi6 and Chp2 display high sequence similarity. They both belong to the HP1 protein family. These four CD containing proteins are detected at pericentromeric and subtelomeric heterochromatin and contribute to heterochromatin assembly (Partridge et al., 2000; Partridge et al., 2002; Thon and Verhein-Hansen, 2000). Interestingly, H3K4 acetylation plays a role in the transition of H3K9 methylation occupancy from Chp1/Clr4 to Chp2/Swi6, creating a CD switch between a more transcriptionally active heterochromatic state (Clr4/Chp1) and an inactive state (Swi6/Chp2) (Xhemalce and Kouzarides, 2010). In respect to Swi6/Chp2, it was shown that Swi6 is expressed abundantly and plays a dose-dependent role in forming a repressive structure through its self-association property, whereas Chp2 is expressed at low levels only and does not show this simple dose-dependent repressive activity, but it contributes to the recruitment of chromatin modulating factors. Furthermore, it was shown that the disruption of the balance between Swi6 and Chp2 is critical for heterochromatin assembly (Sadaie et al., 2008). Interestingly, the recognition of H3K9 methylation *in vitro* relies on an interface between two Swi6 CDs (Canzio et al., 2011). This interaction causes Swi6 to tetramerize on a nucleosome. Strengthening this CD-CD interaction results in enhanced heterochromatin silencing and heterochromatin spreading *in vivo* (Canzio et al., 2011). Additionally, Swi6 also dimerizes. This dimerization occurs via its C-terminal chromoshadow domain (CSD) (Cowieson et al., 2000). CSD domains have been shown to be involved in protein-protein interactions (Smothers and Henikoff, 2000).

Targeting the Su(var) pathway to heterochromatin

Non-coding transcripts of repeat elements, processed by the RNAi pathway, have been shown to target the heterochromatin machinery to these repeats (Hall et al., 2002; Volpe et al., 2002). Interestingly, Swi6 associates with a set of nuclear proteins and with non-coding centromeric transcripts. It is required for efficient RNAi-dependent processing of these transcripts. Chp2, on the other hand, associates with the SHREC histone deacetylase complex

(SHREC2). It is needed for histone H3K14 deacetylation and mediates transcriptional repression by limiting RNA polymerase II access to heterochromatin (Motamedi et al., 2008). Interestingly, Chp1 contributes to *de novo* heterochromatin formation at all sites, but it contributes to its maintenance only at the centromeres (Sadaie et al., 2004), suggesting that pericentromeric heterochromatin is less stable than subtelomeric heterochromatin in *S. pombe*, relying on constant signals for *de novo* heterochromatin formation for proper heterochromatin assembly. Strikingly, Chp1 is a core member of an RNAi effector complex termed RNA-induced initiation of transcriptional gene silencing (RITS) that is required for heterochromatin formation. It resides together with Ago1, the fission yeast Argonaute homolog, and Tas3, a previously undescribed protein (Verdel et al., 2004). Later, it was shown that RNAi contributes to *de novo* heterochromatin formation at all heterochromatic sites, while, like shown for Chp1, it is also required for maintenance on pericentromeric heterochromatin. Additionally, genetic deletion of RNAi components results in loss of H3K9 methylation and Swi6 at pericentromeric heterochromatin (Volpe et al., 2002).

Similar to *S. cerevisiae*, DNA replication origins (ORI) in *S. pombe* coincide with AT-rich islands. Interestingly, they also occur at the mating type loci, centromeres and subtelomeric regions (Segurado et al., 2003). One of the orc proteins, Orc4, contains an AT-hook motif (Lee et al., 2001), which might target ORC to the AT-rich ORI and possibly also to the AT-rich mating type loci, centromeres and subtelomeric regions, possibly linking replication origins and transcriptional silencing. Nevertheless, AT-richness is not the only determinant for ORC localization, since DNA stretches with similar AT-richness display different ORC occupancy (Bell, 2002).

Summary

While heterochromatin in *S. cerevisiae* does not contain histone marks associated with repression, heterochromatin maintenance in *S. pombe* displays the canonical marks of the highly conserved Su(var) pathway. Furthermore, the RNAi pathway has been implicated in *de novo* establishment of heterochromatin. Possibly, also ORC plays a role in transcriptional silencing.

2.2.1.3. N. crassa

The filamentous fungus *Neurospora crassa* is not as widely studied as *S. cerevisiae* or *S. pombe*. However, in respect to heterochromatin formation, it exhibits a feature that is not present in either *S. cerevisiae* or *S. pombe*, but that contributes to gene silencing and heterochromatin formation in mammals: DNA methylation. Therefore, *N. crassa* can be used as a model organism to study DNA methylation mechanisms.

DNA methylation

Heterochromatin in *N. crassa* is mostly detected around centromeres and near telomeres. The underlying DNA sequences are usually relics of invasive DNAs (e.g. transposons, retrotransposons, viruses) (Selker, 2009). A defense system, called repeat-induced point mutation (RIP), protects the *Neurospora* genome from such invasive DNA and ensures genome stability (Foss et al., 1993a; Selker et al., 2003). RIP senses duplicated regions in the genome and rapidly mutates them by G:C to A:T conversion during its reproductive phase. The remaining cytosines at altered regions are typically methylated (Selker et al., 2003). This methylation is not restricted to symmetrical sequences, unlike in most vertebrates (Selker and Stevens, 1985). In addition to DNA methylation, such heterochromatic sites also show hypoacetylated histones, methylated H3K9 and HP1 enrichment (Bhaumik et al., 2007). Furthermore, colocalization of DNA methylation, H3K9me3 and HP1 was observed on 44 discrete heterochromatic domains (Lewis et al., 2009).

Genetics of DNA methylation

The treatment of *Neurospora* with Trichostatin-A, an inhibitor of HDACs, causes selective loss of DNA methylation (Selker, 1998). This was the first observation that DNA methylation is linked to histone modifications in *Neurospora*. Genetic studies then identified two mutants *defective in DNA methylation*, *dim-2* and *dim-5*, which abolish DNA methylation in vegetative tissue (Foss et al., 1993a; Tamaru and Selker, 2001). DIM-2 was then shown to be the only DNA methyltransferase in *Neurospora*. *dim-5*, on the other hand, encodes for a histone methyltransferase, which tri-methylates H3K9. While *Neurospora* strains deficient for *dim-5* show loss of DNA methylation, strains deficient for *dim-2* do not show any alteration of H3K9 methylation, which shows that *dim-5* is upstream of *dim-2* (Tamaru and Selker, 2001). Unlike the homologous HMTs in mammals and Drosophila, *dim-5* does not contain a CD. Nevertheless, there are proteins in *Neurospora* that contain CDs, among them an HP1 ortholog. Inactivation of hpo, the gene that codes for HP1, does not globally affect H3K9 methylation (Lewis et al., 2009), but it results in the loss of DNA methylation in vegetative tissues (Freitag et al., 2004a). Additionally, it was shown that the CSD of HP1 interacts with two PXCXL-like domains of DIM-2 (Honda and Selker, 2008), linking *dim-5* with HP1 and *dim-2*.

Summary

In *Neurospora*, not only the Su(var) pathway is implicated in the maintenance of heterochromatin, but also DNA methylation. Interestingly, genetic analysis showed that the two pathways are linked. How DIM-5 is targeted to heterochromatin remains unknown for the moment. Unlike in *S. pombe*, where the RNAi pathway is implicated in heterochromatin assembly, the RNAi pathway in *N. crassa*, although present, is not required for either the initiation or maintenance of heterochromatin (Freitag et al., 2004b).

2.2.2. Animals

2.2.2.1. *D. melanogaster*

In *Drosophila*, around 1/3 of the genome is considered to be in heterochromatic conformation. Of the four chromosomes of *D. melanogaster*, the entire Y chromosome, most of the small fourth chromosome, which is referred to as the ‘dot’ chromosome, as well as 40 % of the X chromosome and the pericentromeric 20 % of the large autosomes are heterochromatic.

Position Effect Variegation

A few years after Heitz’ first cytological stainings, Muller, a *Drosophila* geneticist, used X-rays as a mutagen in *Drosophila* and observed the following phenotype: the fly eyes displayed red and white spots. Thus, the eye color was variegating (Muller, 1930). The gene responsible for this variegating eye color was called the *white* gene, referring to the phenotype observed in the mutant state (wild type flies have red eyes). It was concluded that the *white* gene itself was not damaged in flies with a variegating phenotype, since the red pigment was still produced in some cells (Figure 2.2.B). Later analysis of polytene chromosomes in mutant fly lines revealed either an inversion or a rearrangement of the chromosome with one part of the inverted sequence close to the *white* gene and the other one close to pericentromeric heterochromatin. Therefore, this genetic incident was called position-effect variegation (PEV) (Figure 2.2.A and 2.2.C). The vicinity of the *white* gene to the pericentric heterochromatin resulted in its silencing in some cells, while in others expression remained, which suggested that heterochromatic organization is able to spread along the chromosome (Baker, 1968; Lewis, 1950; Morgan, 1942). PEV has been shown to occur also in yeast and mammals, but has been used to study heterochromatin formation mostly in *Drosophila*.

In the 1950s, Schultz, another *Drosophila* geneticist, identified dominant modifier mutations of the *white*^{m4} line (Schultz, 1950). In this line, originally generated by Muller, the variegated phenotype is sensitive to modifiers. Importantly, its chromosomal inversion does not interfere with the viability of the flies, since the euchromatic and heterochromatic breakpoints do not reside in essential DNA sequences (Appels and Hilliker, 1982) (A. Ebert and G. Reuter, unpublished). Since this time, several modifier screens using EMS, X-rays or P-elements have been performed using similar fly lines (Reuter and Wolff, 1981; Sinclair D.A.R, 1983; Wustmann et al., 1989) in order to identify proteins, which act as enhancers of white variegation, *E(var)*, or suppressors of white variegation, *Su(var)*. A large number of genes has been identified that are putatively involved in PEV. 15-20 of them have been molecularly described. Well studied are two so-called haplo-triplo dosage-dependent modifier genes *Su(var)2-5* and *Su(var)3-9*. Haplo-triplo means that the loss of one copy of gene leads to the loss of PEV, while the presence of three copies enhances PEV (Figure 2.3). This suggests that the protein amount of such genes is required in a stoichiometric amount.

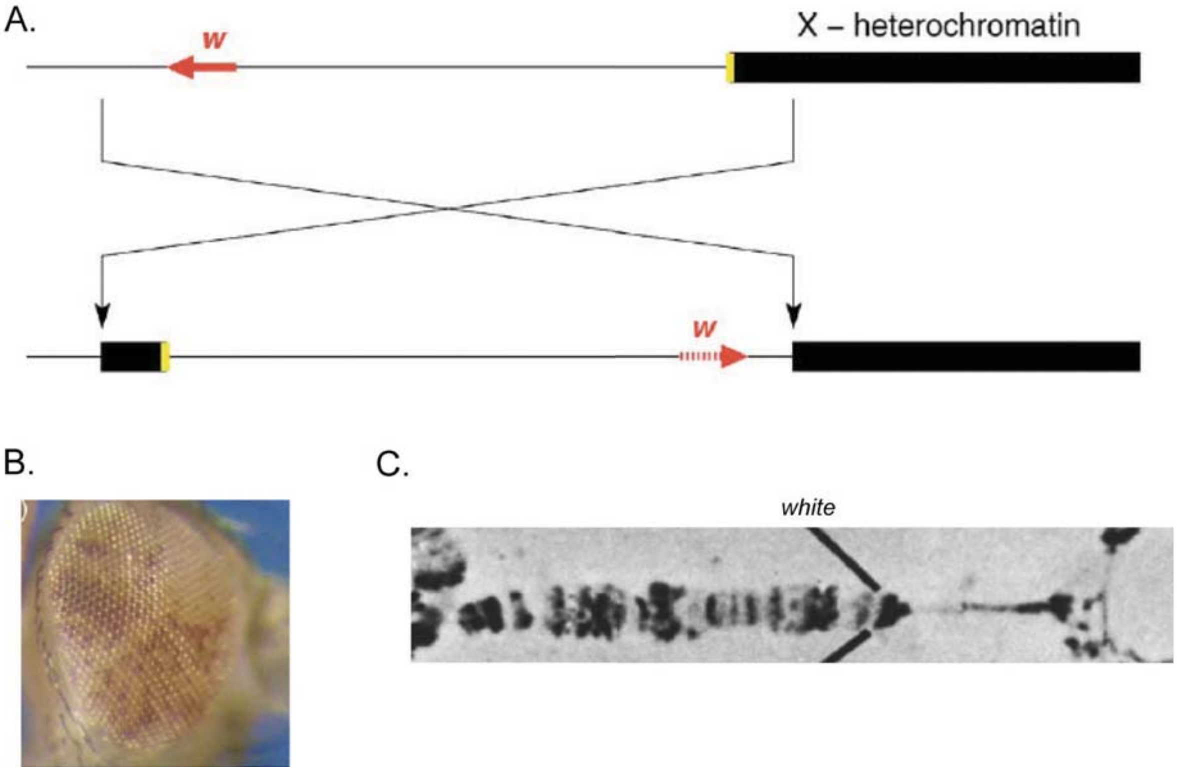

Figure 2.2: PEV in the *In(1)w*^{m4} fly line. **A.** Relocalization of the *white* gene in the *w*^{m4} line. **B.** Variegation for *white*. A white eye color indicates silencing. **C.** Hetero-chromatinisation of the *white* gene visible by a condensed and underreplicated chromosome structure (adapted from: Schotta, et al, 2003).

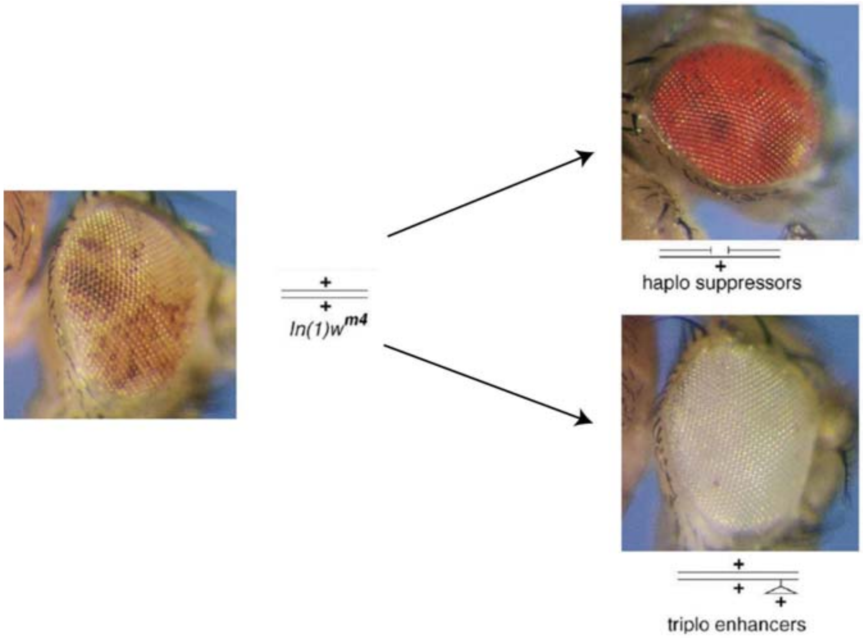

Figure 2.3: Dosage effect of PEV modifier genes in the *In(1)w*^{m4} fly line. Deletion of one gene copy results in dominant suppression, whereas gain of one copy of the same gene causes a triplo-enhancer effect (like observed for Su(var)2-5 and Su(var)3-9) (adapted from: Schotta et al, 2003).

Su(var)2-5

The *Drosophila Su(var)2-5* gene encodes HP1, one of the first heterochromatin associated proteins cloned (James and Elgin, 1986). Mutations in *Su(var)2-5* are recessive lethal at the third larval instar (Eissenberg and Hartnett, 1993). Mutant larvae approaching that stage show loss of heterochromatin silencing (Lu et al., 2000). Interestingly, in *Su(var)2-5* mutant flies, the expression of two essential genes, which are located within a heterochromatic region, is reduced. This suggests that HP1 is also required for normal transcriptional activation of such heterochromatic genes (Lu et al., 2000). It was shown that the CD as well as the CSD of *Drosophila* HP1 is sufficient for localization to heterochromatin *in vivo* (Platero et al., 1995; Powers and Eissenberg, 1993). Point mutations in the CD (in particular Y24F and V26M) of HP1 inactivate its ability to contribute to heterochromatin silencing (Platero et al., 1995). Similarly, deletion studies of the CSD also resulted in the inability of heterochromatin silencing (Eissenberg and Hartnett, 1993; Eissenberg et al., 1992). The first crystal structure of a CD was obtained from *Drosophila* HP1 (Jacobs and Khorasanizadeh, 2002). It showed that it consists of two antiparallel β-sheets at the N-terminus, which are linked by short α-helices with a third antiparallel β-sheet (Figure 2.4.A). The HP1 CD preferentially binds H3K9me3 with a dissociation constant (K_d) of 4 μM. The methylated histone tail is bound by a 'cage' formed by three aromatic residues (Tyr23, Trp45 and Tyr48) (Figure 2.4.A). But not only methylated K9 is important for the binding of the HP1 CD. Also preceding and following aa residues of the histone H3 tail (TARK^{9}S) form hydrogen bonds with the hydrophobic cavitiy of the CD (Jacobs and Khorasanizadeh, 2002). Furthermore, HP1 is highly phosphorylated *in vivo*. This phosphorylation influences its heterochromatin binding and silencing activity (Zhao and Eissenberg, 1999; Zhao et al., 2001).

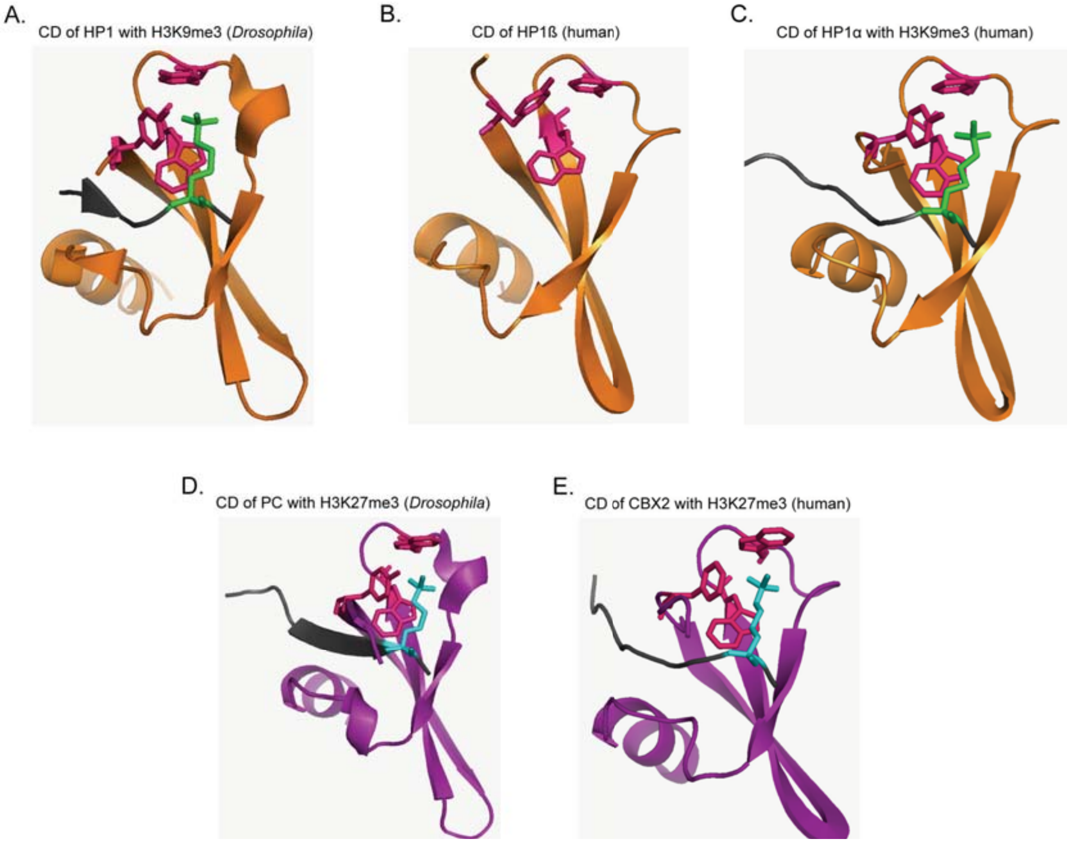
A.
CD of HP1 with H3K9me3 (*Drosophila*)
B.
CD of HP1ß (human)
C.
CD of HP1α with H3K9me3 (human)
D.
CD of PC with H3K27me3 (*Drosophila*)
E.
CD of CBX2 with H3K27me3 (human)

Figure 2.4: Protein structures of selected *Drosophila* and human CDs. **A.** CD of *Drosophila* HP1 bound to an H3K9me3 modified peptide (adapted from Jacobs et al, 2001). **B.** CD of human HP1β, crystal without the H3 peptide (adapted from Kaustov et al, 2011). **C.** CD of human HP1α bound to an H3K9me3 modified peptide (adapted from Kaustov et al, 2011). **D.** CD of *Drosophila* PC bound to an H3K27me3 modified peptide (adapted from Fischle et al, 2003). **E.** CD of human CBX2 with an H3K27me3 modified peptide (adapted from Kaustov et al, 2011). Color code: orange: CD of HP1 and homologs; violet: CD of PC and homologs; grey: H3 peptide; green: H3K9me3; cyan: H3K27me3; pink: aromatic cage residues.

Su(var)3-9 and Su(var)4-20

Similar to *Su(var)2-5*, a mutation in the *Su(var)3-9* gene also results in the loss of heterochromatin silencing (Tschiersch et al., 1994). SU(VAR)3-9 contains a CD motif, like HP1, and a SET domain, which displays histone methyltransferase activity. Yeast two-hybrid screens, using SU(VAR)3-9 as bait, showed that its N-terminus interacts with the CSD of HP1 (Schotta et al., 2002). Interestingly, in *Su(var)3-9* mutants, HP1 localization at pericentric heterochromatin is drastically reduced, whereas in HP1 null mutants, SU(VAR)3-9 is not restricted to heterochromatin anymore, but dispersed across the chromosomes, suggesting an interdependence of the two proteins. Nevertheless, *Su(var)3-9* dominates the PEV modifier effects, indicating that it is epistatic (Schotta et al., 2002). Later, a H4K20 methyltransferase was described in mammals and shown to act as a PEV also in *Drosophila* within the Su(var) pathway (Schotta et al., 2004). This SU(VAR)4-20 histone methyltransferase has been described to act downstream of HP1 in *Drosophila*.

The Dot Chromosome

The fourth chromosome of *D. melanogaster* is referred to as the ‘dot’-chromosome or Muller’s F-element (Muller, 1930), because it is the smallest chromosome of *Drosophila* with a length of only 4.2 Mb (Locke and McDermid, 1993). Interestingly and in contrast to other autosomes in *Drosophila*, its gene rich regions display features of euchromatin and heterochromatin (Riddle and Elgin, 2006). For example, the euchromatin of the dot chromosome replicates late, lacks recombination (although it contains a number of important genes) and shows high H3K9 methylation, altogether features of heterochromatin. Nevertheless, the euchromatin remains transcriptionally active and does not show any PEV induction (Riddle and Elgin, 2006). Thus, no spreading of heterochromatin is observed. The dot chromosome contains also more repetitive sequences than the other *Drosophila* autosomes (Wilson et al., 2008). Most of these repeats consist of fragments derived from transposable elements (Slawson et al., 2006). These repetitive elements are not arranged in blocks of heterochromatin, but appear interspersed with genes. This arrangement is similar to the one observed in mammalian chromosomes, where repetitive elements and genes appear in proximity to each other along the chromosome arms. Therefore, transcriptional regulation of genes on the dot chromosome in *Drosophila* is also achieved in repeat-rich genomic regions. Nevertheless, it is more characteristic to mammalian genomes. The repetitive elements, though, are transcriptionally silenced in order to ensure genomic stability. Unlike in *N. crassa*, where DNA methylation is involved in the silencing of such elements, in *Drosophila* there is only sparse DNA methylation observed (Lyko et al., 2006). Nevertheless, HP1 and H3K9me2 strongly stain the dot chromosome. While polytene chromosomes in SU(VAR)3-9 mutants globally lack H3K9me2, this mark is not affected on the dot chromosome (Schotta et al., 2002), where it is set by another methyltransferase named EGG (also known as ESET) (Seum et al., 2007; Tzeng et al., 2007). In lines mutant for *egg*, HP1, H3K9me2 and painting of fourth (POF), a protein that specifically associates with the dot chromosome (Larsson et al., 2001), are strongly diminished (Tzeng et al., 2007). Similarly, in POF mutants, the dot chromosome lacks H3K9me2 and HP1 to a large degree (Tzeng et al., 2007), and in HP1 mutants, there is no POF enrichment on the dot chromosome and H3K9me2 is redistributed (Johansson et al., 2007). All this genetic evidence suggests an interdependence of the three players, which remains to be unraveled.

Targeting of the Su(var) pathway to heterochromatin

The proteins identified in PEV screens helped in understanding the heterochromatin setup on a molecular and biochemical level, which led to models of how to define heterochromatin and how DNA sequences are transcriptionally silenced. Nevertheless, it is not known yet, how this heterochromatin assembly machinery is targeted to specific DNA stretches and not to others. There are two general models that might explain this specific targeting: either through binding of a sequence specific protein present in the complex, or alternatively through the targeting via non-coding transcripts.

One example supporting the first possibility is the protein D1, an AT-hook containing protein. AT-hook motifs have been described to bind AT-rich DNA sequences. The type III satellite DNA in the centromeric heterochromatin region of the X-chromosome in *Drosophila* displays such AT-richness, and D1 was shown to bind them (Aulner et al., 2002). Furthermore, mutations in D1 cause suppression of variegation (Aulner et al., 2002). A more recent report challenges these results though, suggesting no PEV effect of D1 (Weiler and Chatterjee, 2009). Furthermore, no association of D1 with the Su(var) pathway has been described. In addition to D1, ORC might play a role in targeting HP1 to AT-rich DNA sequences as already observed in yeast. In *Drosophila*, ORC consists of five subunits (Orc1-5). It was shown that Orc2 colocalizes with HP1 at pericentromeric heterochromatin (Pak et al., 1997). Surprisingly, Orc2 mutants even exhibit a Su(var) phenotype, which strongly suggests a role of ORC in heterochromatin organization (Huang et al., 1998; Loupart et al., 2000; Pak et al., 1997). Later it was shown that hypophosphorylated HP1 forms a complex together with ORC (Orc1, 3 and 6) and an HMG-like HP1/ORC-associated protein (HOAP). The N-terminus of HOAP contains similarity to an HMG box, which binds AT-rich satellite sequences in vitro (Badugu et al., 2003; Huang et al., 1998; Shareef et al., 2001), suggesting a targeting mechanism of HP1 to AT-rich satellites, like it was proposed for D1. However, this targeting mechanism cannot explain the heterochromatin formation of various, variable transposable elements as they appear on the dot chromosome, but only less specific targeting to abundant AT-rich repeats.

Alternatively, ncRNA transcripts of the transposable elements recruit proteins that set up heterochromatin. This could provide a more specific targeting of the heterochromatin formation complexes. For example, POF shows similarity to RNA-binding proteins, which might link transcription of repeats with the association of POF and, therefore, HP1 and EGG (Riddle et al., 2009). Another targeting mechanism could involve the RNAi machinery, which has been shown to be important for heterochromatin formation in *S.pombe* (as discussed in 2.2.1.2.) and in plants (Verdel et al., 2009). Homologs of the RNAi pathway have also been identified in *Drosophila* (Riddle and Elgin, 2008). Interestingly, in somatic cells, it was shown that mutations in *piwi*, *aubergine*, or *spindle-E*, which encode RNAi components, show weak loss of silencing (Pal-Bhadra et al., 2004). Furthermore, these mutations result in the reduction of H3K9 methylation and delocalization of HP1 (Pal-Bhadra et al., 2004). Especially, the PIWI-associated RNAs (piRNA), whose presence correlates with the emergence of germ cells in evolution have been shown to be involved in transposon control (Aravin et al., 2007). In yeast 2-hybrid studies, PIWI has been shown to directly interact with the CSD of HP1 (Brower-Toland et al., 2007). In a proposed model (Riddle and Elgin, 2006), long non-coding transcripts from transposons, such as *flamenco*, are generated (Brennecke et al., 2007; Sarot et al., 2004) and processed to short piRNAs by the proteins of the PIWI-clade, AGO3, AUB and PIWI (Brennecke et al., 2007; Gunawardane et al., 2007; Saito et al., 2006). The generated piRNAs might target the heterochromatin machinery to the complementary transposon DNA sequence via the CSD of HP1, resulting in transcriptional silencing. However, this model is limited to the germline due to the germ cell specific presence of piRNAs. For the soma, despite the weak suppression of variegation effect of RNAi components, it is still debated, whether they have a function in heterochromatin formation or whether, once heterochromatin formation is initiated in the germ line, this state is maintained in the presence of the members of the *SU(VAR)* proteins in somatic cells.

Polycomb Group Proteins: PcG

While the SU(VAR) pathway has been implicated in silencing of pericentromeric heterochromatin and repeats, another pathway, consisting of the PcG proteins, originally identified in *Drosophila*, has been shown to be critical for gene silencing. The anterior-posterior axis in *Drosophila* and other metazoans is set by the expression pattern of HOX genes. This leads to the segment specific expression pattern of the HOX genes, which is maintained throughout the development of the fly. Interestingly, this pattern is maintained even after the transcriptional activators or repressors (e.g. retinoic acid, or proteins of gap or pair-rule genes (Small et al., 1992)), are gone (Deschamps et al., 1999). Genetic analysis of the HOX gene cluster then identified *trans*-acting regulators responsible for this maintenance. One of the first PcG Proteins, which also gave them its name, was *Polycomb* (PC) (Lewis, 1978). Misregulation of PcG proteins leads to the upregulation of HOX genes, which results in a phenomenon called homeotic transformation, where one body segment is convertent into another one (Denell, 1978; Sato et al., 1983). Therefore, PcG were proposed to act as repressors of HOX genes in *trans*. Besides PcG proteins, another group of trans-acting regulators, named Trithorax Group Proteins (TrxG), which function antagonistically to PcG, maintaining active transcription of HOX genes, were identified. Furthermore, PcG phenotypes are partially rescued by trxG mutations, suggesting, indeed, that they are involved in the maintenance of the expression state, but not its establisment (Moehrle and Paro, 1994).

PRC1 and 2

PcG proteins have been characterized to form two major protein complexes: PRC1 and 2 (Beisel and Paro, 2011). Different variants of PRC2 complexes have been purified from *Drosophila* embryos. They all contain four core members (Levine et al., 2004). First, Enhancer of Zeste (E(Z)) (Jones and Gelbart, 1990; Shearn et al., 1978) is a SET containing histone methyltransferase that tri-methylates H3K27 (Cao et al., 2002; Czermin et al., 2002). It interacts via a C5 domain with the Suppressor of Zeste12 (SU(Z)12), which contains C2H2-type zinc finger and a carboxy terminal VEFS domain (Birve et al., 2001). Additional components include ESC and p55, which contain five and six WD40 repeats, respectively (Hennig et al., 2005; Struhl, 1981), and are necessary for protein-protein interactions with the other core members

(Tie et al., 1998). Finally, Nurf55 contains a WD40 propeller, which has been shown to interact with SU(Z)12 (Schmitges et al., 2011). Together with SU(Z)12, it is required for nucleosome assembly of PRC2 (Schuettengruber et al., 2007).

The PRC1 repressor complex contains stoichiometric amounts of the four core members: Polycomb (PC), Polyhomeotic (PH), Posterior Sex Combx (PSC), and Ring1 (dRing/SCE) (Shao et al., 1999). PC possesses sequence similarity to HP1 (Paro and Hogness, 1991). Both proteins contain an N-terminal CD (Cowell and Austin, 1997). While the CD of HP1 strongly binds H3K9 methylation, the CD of PC preferentially binds methylated H3K27 (Min et al., 2003), in particular H3K27me3 with which it interacts with a K_d of 5 µM (Fischle et al., 2003). The PC CD is thought to distinguish its methylation target on the H3 tail via an extended recognition groove that binds five additional residues preceding the ARKS motif (LATKAARK^{27}S) (Figure 2.4.D). In order to study the domains involved in targeting these regions to chromatin, a chimeric protein with the CD of PC and the CSD of HP1 fused to β-galactosidase has been generated. This protein targets β-galactosidase to both HP1 and PC binding sites. It also mislocalizes endogenous HP1 to euchromatic PC sites and endogenous PC to heterochromatin, which suggests importance of the CD of PC and the CSD of HP1 in protein-protein interactions (Platero et al., 1996). Furthermore, and not in full agreement with the previous study, the exchange of the CD of HP1 with the CD of PC shows exclusion of the chimeric protein with H3K9me2, while exchange of the CD of PC with the CD of HP1 results in displacement of PC to H3K9me2 sites, suggesting that the CD targets the proteins to specific domains (Fischle et al., 2003).

PH (Dura et al., 1985) contains a zinc finger and a SAM domain, which have been shown to participate in interactions with other proteins (Min et al., 2003). This supports the results, where PcG proteins have been detected and might act in foci called PcG bodies (Saurin et al., 1998). Third, there is PSC, which contains a C3HC4 ring finger motif. This motif might be involved in protein-protein interactions and shows homology to the murine Bmi1 oncogene (Brunk et al., 1991). The final component of PRC, RING1 (Breen and Duncan, 1986) has only been detected via biochemical purification as part of this complex. It is thought to play a structural role (Francis et al., 2001; Lavigne et al., 2004). It contains a RING domain that mediates E3 ubiquitin ligase activity, resulting in mono-ubiquitination of histone H2A at K119 (Wang et al., 2004a).

Targeting PcG proteins

As with targeting of the Su(var) pathway to constitutive heterochromatin, various PcG targeting mechanisms in *Drosophila* have been investigated. A number of DNA binding proteins have been found to associate with PcG proteins. For example, pleiohomeotic (PHO) and pleiohomeiotic-like (PHOL) encode DNA-binding proteins (Brown et al., 2003; Brown et al., 1998). Additionally, DNA specific modules, referred to as Polycomb response elements (PRE), have been shown to be involved in the control of the transcriptional status of target genes. The number and order of PRE consensus motifs is not conserved between different PREs. They are mostly a few hundred base pairs (bp) long and contain motifs, which are recognized by DNA binding proteins like PHO and PHOL (Ringrose and Paro, 2007; Schwartz and Pirrotta, 2007). In a study of the *ubx* PRE, it was shown that PHO/PHOL recruit E(Z), which leads to H3K27 methylation. This in turn is the binding site for PC of PRC1 (Wang et al., 2004b). Moreover, inactivation of E(Z) results in the loss of PRC1 from polytene chromosomes (Czermin et al., 2002), and likewise PCH binding is competed with H3K27me3 peptides (Ringrose et al., 2004). These observations lead to the model of sequential targeting of the two complexes. Nevertheless, recent results suggest that PcG recruitment is more complex. For example, PcG sites in polytene chromosomes are stained normally in *pho/phol* double mutants (Brown et al., 2003). Additionally, PHO/PHOL binding sites are insufficient to tether PcG protein *in vivo* (Brown et al., 2003; Dejardin et al., 2005). Mapping of the chromosomal distribution of *Drosophila* candidate DNA-binding factors for PcG recruitment showed that PHO exhibits strong binding to silenced regions, whereas PHOL preferentially binds to PREs of active promoters, which questions the function of PHOL in recruiting PcG proteins to silenced PREs (Schuettengruber et al., 2009). Furthermore, in ChIP analysis it was shown that PRC1 and PRC2 peak at PREs, while H3K27me3 is distributed along the transcribed region and spans often several kilo bases (kb) (Kahn et al., 2006; Papp and Muller, 2006; Schwartz et al., 2006), suggesting that they act partly also independently. Finally, PRC1 and PRC2 members have not been found to physically interact. Additionally, it remains unknown for the moment, how PRC1 and 2 bound to PRE, which are often far away from their target promoters, maintain silencing of transcription on a molecular level. It has been suggested that PRE bound complexes form loops to contact their target promoter (Bantignies et al., 2003; Cleard et al., 2006; Lanzuolo et al., 2007; Vazquez et al., 2006).

Summary

In summary, the Su(var) pathway is conserved also in *Drosophila*. It is essential for constitutive heterochromatin silencing. The piRNA pathway has been implicated in heterochromatin formation in the germ line, but not necessarily in somatic cells, suggesting that formation in the germ line is sufficient and that there is possibly no *de novo* heterochromatin formation in somatic cells required anymore. In addition to the Su(var) pathway, the PcG pathway was identified in *Drosophila*. It has been shown to be essential for gene silencing. PREs have been shown to be crucial for the targeting of the two PcG complexes PRC1 and PRC2.

2.2.2.2. *M. musculus*

All of the *Mus musculus* subspecies show the same karyotype of 20 pairs of chromosomes with 19 autosomal pairs and the X and Y sex chromosomes. This number was first determined by Painter (Painter, 1928). All 19 autosomes as well as the X chromosome are acrocentric, meaning that the centromere is adjacent to one telomere (Figure 2.5). This makes it more difficult to distinguish the chromosomes. Nevertheless, there are several staining procedures, which differentially stain the chromosomes. The use of the dye Giemsa, for example, results in darkly stained chromosomal bands, called G bands. The G bands underlying DNA condenses early in the cell cycle, replicates late and is relatively A:T rich. In contrast, there are R-bands, which show a Giemsa negative staining. The R-band associated DNA condenses late, replicates early and is G:C rich (Bickmore and Sumner, 1989). Housekeeping genes, for example, are located in R bands. The two band types are also associated with different repeats: G-bands contain the long interspersed elements (LINE-1) elements, while R-bands contain short interspersed elements (SINE) elements.

Repeats and Single Genes

Renaturation analysis of mouse DNA revealed that 5% of the genome renatures almost one million times faster than the bulk DNA. This class represents the satellite DNA. These highly repetitive DNA sequences are thought to consist of the centromeric sequences, comprising the euchromatin-proximal major satellite repeat (234 bp long) and the telomere proximal minor repeat (120 bp long) found on some chromosomes (Horz and Altenburger, 1981; Joseph et al., 1989; Wong and Rattner, 1988). In the mouse sequencing project, the major satellite repeats were detected in only 3.6% of the reads, which is lower than estimated previously in density gradient experiments, where major satellites comprise around 5.5%, or approximately 8 Mb per chromosome, which suggests that each centromere contains 35'000 copies (Davisson, 1989; Waterston et al., 2002). The minor satellite repeats were poorly represented in the mouse genome project. Previous reports suggest that they are present in around 50-100'000 copies in the whole genome (Davisson, 1989; Waterston et al., 2002). These two satellite repeats appear to have a common ancestor (Silver, 1995). This first class of DNA that renatures very fast is followed by a second class of DNA, which consists of various types of repeats. Their copy number varies from few up to hundreds of thousands. It comprises four classes of transposable elements: the autonomous long interspersed nucleotide elements (LINE), the LINE-dependent, RNA-derived short interspersed nucleotide elements (SINE), retrovirus-like elements with long terminal repeats (LTRs) and DNA transposons (Smit, 1999; Waterston et al., 2002). LINE-1 elements are present at more than 80'000 chromosomal sites. This family of retrotransposons is very old and has also been detected in protists and plants. Full-length LINE-1 elements are 7 kb in length, however, most are reduced in size to 500 bp and are non-functional in respect to transposition (Martin, 1991). SINE elements comprise two subfamilies of repetitive elements, B1 and B2, which are 140 and 190 bp long respectively and do not code for a reverse transcriptase. Thus they are dependent on elements such as LINE-1 for reverse transcription. They are thought to have evolved from small cellular RNA species, such as tRNAs. The B1 element is repeated 150'000 times, and the B2 90'000 times (Hasties, 1998). The third repeat class contains the long terminal repeat (LTR) elements. Among them, the MaLR with 388'000 copies, which are still active in mouse, the intracisternal-A particles (IAP), the early-transposons (ETn), which are highly abundant and active and the mouse mammary tumour virus, which is also still active, but present in only a few copies (Hamilton and Frankel, 2001; Waterston et al., 2002). The fourth group of DNA transposons is small in mouse compared to the primate lineage. It consists of four lineage-specific families (Waterston et al., 2002). Finally, the bulk of DNA that renatures latest includes the unique sequences, consisting of genes, pseudogenes, simple sequence repeats, which are perfect or near-perfect tandem repeats, and other low copy number repeats (Breslauer et al., 1986; Davisson, 1989; Silver, 1995). Furthermore, sequencing the mouse genome showed that it contains altogether around

2.5 giga bases (Gb). Interestingly, in respect to transcription, it has been shown for humans that a large proportion of its genome is transcribed (Birney et al., 2007). Therefore, it is possible that also a large amount of the mouse genome is transcribed, while only a fraction of the transcribed RNA is actually translated. Finally, it has been suggested that the mouse genome contains 30’000 protein-coding genes (Waterston et al., 2002).

Suv39h1 and Suv39h2

The SET domain, originally characterized in SU(VAR)3-9, E(Z) and TRX, from SUV39H1 was the first domain shown to methylate H3K9 (Rea et al., 2000). Many other SET containing proteins have since been shown to specifically methylate lysine residues of histones and other proteins. In mouse, there are two forms of the *Drosophila* SU(VAR)3-9 methyltransferase. Both have H3K9me activity. Furthermore, as in *Drosophila*, they contain a CD that preferentially binds the mark that they set: H3K9me3, which might result in a positive feedback loop. While Suv39h1 has been shown to modulate chromatin dynamics in somatic cells, Suv39h2 displays a more specific expression pattern, with high expression during oogenesis, spermatogenesis and in early preimplantation embryos (Aagaard et al., 2000; O'Carroll et al., 2000; Puschendorf et al., 2008; Rea et al., 2000). Both proteins strongly localize to the major satellite repeats. They mark and silence pericentromeric heterochromatin (Lachner et al., 2001; Lehnertz et al., 2003; Peters et al., 2001). A mouse deficient for both Suv39h HMTs shows loss of H3K9 methylation at pericentromeric heterochromatin, impaired viability and chromosomal instability that is associated with an increased tumor risk (Peters et al., 2001). Additionally, it shows a loss of enrichment for downstream members of the Suv39h pathway at pericentromeric heterochromatin (Lachner et al., 2001; Schotta et al., 2004). More recently, Suv39h1 has also been shown to repress pluripotency genes in trophoblast stem (TS) cells, which are primed by PRC1 and the RNA polymerase in ES cells (Alder et al., 2010). Nevertheless, Suv39h and PcG remain mutual exclusive, as in other silenced chromatin regions (Alder et al., 2010).

The three Hp1 paralogs: Hp1α, Hp1β and Hp1γ

Like the SU(VAR)3-9 gene, SU(VAR)5-2 was multiplied during evolution. Vertebrates, from fish to humans, contain three Hp1 isoforms: Hp1α, Hp1β and Hp1γ (also known as: Cbx5, Cbx1 and Cbx3 respectively). All three contain the highly conserved N-terminal CD that strongly binds H3K9me3 (Lachner et al., 2001), a less conserved hinge domain and the conserved C-terminal CSD that carries out various functions. The measured K_d of Hp1α, Hp1β and Hp1γ towards H3K9me3 are 30 µM, 5 µM and 15 µM, respectively (Kaustov et al., 2011) (Figure 2.4.B and 2.4.C). The CSD of Hp1β was the first to be crystalized (Brasher et al., 2000). The structure strongly resembles that of a CD with three β-sheets, but with two C-terminal α-helices instead of one. Unlike CDs it was crystallized as a homodimer. The aa residues involved in dimerization were mapped to the dimer interface (e.g. Hp1β^{I161}). Furthermore, an intact, dimeric CSD is required for interaction with Caf1 and Tif1β proteins (Brasher et al., 2000). The linker domain among the three isoforms is less conserved. It is flexible and exposed to the surface (Singh and Georgatos, 2002). Furthermore, it has been shown to bind RNA (Muchardt et al., 2002). Knock-out (KO) mice for each of the Hp1 isoforms have been generated. An *Hp1α* KO mouse does not show any severe phenotypes compared to wild-type littermates, suggesting redundant function with its homologs (Aucott et al., 2008; Brown et al., 2010). *Hp1β* deficient mice are perinatal lethal due to respiratory failure. Furthermore, defective development of the cerebral neocortex and neuromuscular junctions was observed (Aucott et al., 2008). Hp1γ function is required for male germ cell survival and spermatogenesis (Brown et al., 2010). More specifically, centromere clustering and synapsis are affected in *Hp1γ* deficient spermatocytes. This Hp1γ function has been shown to be within the G9a pathway (Takada et al., 2011). It is interesting to note that *Suv39h*-dn animals live, whereas *Hp1β* deficient mice die perinatally. This is similar to the situation observed in *Drosophila*, where HP1 mutants die at the third larval instar stage, whereas SU(VAR)3-9 mutants remain viable, as discussed above. This suggests that the essential function of Hp1β is not within the Su(var) pathway (Billur et al., 2010). While Hp1γ has been described to localize to euchromatin, Hp1α and β both localize to euchromatin as well as to heterochromatin (Bartova et al., 2007; Horsley et al., 1996; Minc et al., 1999; Nielsen et al., 1999). The heterochromatin localization of Hp1β is cell cycle dependent. Phosphorylation of H3S10 reduces the affinity of the Hp1β CD for H3K9me3 greatly. This might explain the displacement of chromatin bound Hp1β into the cytoplasm in metaphase chromosomes (Fischle et al., 2005; Hirota et al., 2005). Another histone mark that has been reported to modulate Hp1α function is phosphorylation of H3Y41 by Jak2. It prevents Hp1α, but not Hp1β, from binding to chromatin (Dawson et al., 2009). Furthermore, as in *Drosophila*, the Hp1 isoforms themselves are phosphorylated. Some sites are phosphorylated in a cell cycle specific manner (Minc et al., 1999), while others are implicated with other functions, like general chromatin binding (Hiragami-Hamada et al., 2011). For example, Hp1γ^{S83} phosphorylation impairs its silencing activity and is a marker of transcriptional elongation (Lomberk et al., 2006), while Hp1β^{S51}

phosphorylation has been implicated in Hp1β mobilization during the initiation of the DNA damage response (Ayoub et al., 2008). Another post-translational modification, SUMOylation, has been shown to promote targeting of Hp1α to pericentromeric heterochromatin (Maison et al., 2011). Such SUMO-modified Hp1 proteins were shown to bind ncRNA of major satellite transcripts (Maison et al., 2011). Interestingly, the SUMOylation sites are within the hinge domain, which has been shown to bind RNA previously (Maison et al., 2002; Muchardt et al., 2002). Notably, SUMOylation of Hp1α was shown to be critical for Hp1α targeting to pericentric domains (Maison et al., 2011). Besides the association with RNA, the Hp1 isoforms have also been shown to interact with many proteins. For example, it was shown that gene silencing by the sex determination transcription factor SRY is mediated by a Krab-O protein that recruits the Kap1 co-repressor, which binds the CSD of Hp1 via its PxVxL motif (Peng et al., 2009). Another example is the p150 subunit of the chromatin assembly factor 1 (Caf-1), which has been shown to promote delivery of Hp1α to heterochromatic sites during replication (Quivy et al., 2004).

Suv4-20h1 and Suv4-20h2

The most downstream member of the Su(var) pathway described so far, are the two Suv4-20h histone methyltransferases. The Suv4-20h proteins both contain a SET domain that tri-methylates H4K20 (Schotta et al., 2004). The proteins as well as the histone mark they set, localize to pericentromeric heterochromatin (Schotta et al., 2004). *Suv4-20*-dn embryos are born smaller than wt littermates and die perinatally a few hours after birth, probably due to an alveolar defect in the lungs. They have lost nearly all H4K20me2 and H4K20me3. Furthermore, the genome-wide transition to an H4K20me1 state in these mutants results in increased sensitivity to damaging stress (Schotta et al., 2008). The interaction of the Suv4-20h enzymes with Hp1 isoforms suggests a sequential mechanism to establish H3K9 and H4K20 tri-methylation at pericentromeric heterochromatin (Schotta et al., 2004). This interaction domain was mapped to the CSD of Hp1 and aa 347-435 of Suv4-20h2 (Souza et al., 2009).

Targeting Su(var)

Targeting of the Su(var) pathway to the AT-rich major satellite repeats of the pericentromeric heterochromatin is not well understood currently. As in *Drosophila*, DNA binding proteins or ncRNAs, in this case transcripts of the major satellite repeats, are candidate mechanisms investigated (Probst and Almouzni, 2011). This will be discussed in more detail in 2.3.3.3. Furthermore, ORC (Orc1-5) has also been shown to interact with Hp1 and associate with heterochromatin in mammals, similar to *Drosophila* (Auth et al., 2006; Deng et al., 2007; Prasanth et al., 2004; Prasanth et al., 2010). Interestingly, *Orc2* and *Orc3* deficiency results in loss of Hp1α enrichment at heterochromatin and abnormal chromosome condensation. *Orc1* and *Orc5* deficiency, on the other hand, results in redistribution of Hp1α around the nucleolar periphery (Prasanth et al., 2010). Recently, an ORC associated, WD40 containing protein called Orca has been shown to play a crucial role in heterochromatin organization (Bartke et al., 2010; Shen et al., 2010; Vermeulen et al., 2010). Orc and Orca are both enriched at H3K9me3 of satellite repeats. Surprisingly, it was also shown that this complex binds H3K9me3, H3K27me3 and H4K20me3 (Vermeulen et al., 2010). Furthermore, the recruitment of ORC is DNA methylation dependent (Bartke et al., 2010).

In addition to ORC, several studies have identified ncRNAs as being involved in targeting Su(var) in mouse. Interestingly, like in *Drosophila*, piRNA clusters have been detected in the germline of male mice. They were shown to be important for spermatogenesis, and they have been implicated in transposon control (Aravin et al., 2006; Aravin et al., 2007; Watanabe et al., 2006). Deficiency of *Mili* or *Miwi2*, murine homologs of *Piwi*, results in de-repression and loss of methylation of transposons in the male germline (Carmell et al., 2007). Furthermore, in mouse oocytes, 20-24nt transcripts derived from retroelements were detected (Watanabe et al., 2006). It has also been shown that deletion of *Dicer* results in an increase of major and minor satellite transcripts, with no detectable change in DNA or H3K9 methylation (Kanellopoulou et al., 2005; Murchison et al., 2005). More recent studies have identified some DNA methylation changes following *Dicer* deletion, but these changes were mediated via the miRNA pathway and not via siRNA (Benetti et al., 2008; Sinkkonen et al., 2008). Therefore, as in *Drosophila*, small RNAs are implicated with controlling repetitive elements in the germline. For the moment, though, there is only little evidence for a role in somatic cells. Furthermore, a recent study associates Hp1β and Hp1γ as well as Suv39h1 and Eset with long intergenic non-coding (linc) RNA (Guttman et al., 2011), which might specifically recruit them to their targets.

Dynamics of Su(var)

The dynamics of Suv(39) pathway have been studied extensively. Fluorescent recovery after photobleaching (FRAP) experiments for Suv39h1 in fibroblast cells revealed a substantial population of immobile Suv39h1 at pericentromeric heterochromatin. The average half recovery time for Suv39h1 at heterochromatin was 19 seconds. This stable binding is mediated by the SET domain. Furthermore, DNA demethylation, achieved by treatment with the DNA methyltransferase inhibitor 5-aza-C, increased the dynamics of Suv39h1, but not that of Hp1β (Krouwels et al., 2005), suggesting that DNA methylation stabilizes the localization of Suv39h1 at heterochromatin. The Hp1 isoforms on the other hand are highly dynamic at heterochromatin with a half recovery time of 2.5 seconds. This dynamic interaction depends on Suv39h. In addition, the CD and the CSD of Hp1 are both needed *in vivo* for binding chromatin (Cheutin et al., 2003). Dynamics of Hp1α in human cells were also measured in relation to dynamics of ORC subunits. Whereas Orc2, Orc3 and Hp1α displayed high dynamics with half recovery times of 4-5 seconds, Orc1 is more stably bound to heterochromatin (Prasanth et al., 2010). The same study showed that Orc1 and Orc3 physically interact with Hp1α (Prasanth et al., 2010). Further analysis identified a low-mobility fraction of the Hp1 isoforms (t1/2= 10 sec) (Schmiedeberg et al., 2004). In 4-cell embryos, the Hp1β dynamics are rather stable, with a half recovery time of 9 seconds, which is similar to the low-mobility fraction measured in cells, suggesting, altogether, more stably bound proteins at heterochromatin in embryos than in cells (Yamazaki et al., 2007). Another study showed high mobility of Hp1 with slightly different dynamics during the cell cycle. Suv4-20h2, though, remained strongly bound to pericentromeric heterochromatin throughout the cell cycle. Only 8.4% of Suv4-20h2 recovered after 30 seconds (Souza et al., 2009), suggesting that it is stably bound to heterochromatin.

DNA methylation in mouse

Pericentromeric heterochromatin and other repetitive sequences in mouse is DNA methylated. It has been shown that this plays a critical role in silencing transcription of retrotransposons during embryonic development and spermatogenesis (Bourc'his and Bestor, 2004; Walsh et al., 1998). In mammals, DNA methylation occurs mostly on cytosines in a CpG context, unlike in *Neurospora*. Chemically, this means that carbon 5 of a cytosine receives a methyl group. This is catalyzed by so-called DNA methyltransferases. Early experiments showed that DNA methylation silences the expression of viral genomes and that embryonic cells have the capability to *de novo* methylate DNA (Jahner et al., 1982; Stewart et al., 1982). *Dnmt3a* and *Dnmt3b* were identified to be the *de novo* methyltransferases, as ES cells lacking both proteins were unable to *de novo* methylate proviral genomes and repetitive elements

(Okano et al., 1999). Loss of *Dnmt3a* causes postnatal lethality, male sterility and failure to establish methylation imprints in male and female germ cells (Li, 2007). Furthermore, cells lacking *Dnmt3a* or an associated regulatory factor, *Dnmt3l*, fail to establish distinct methylation patterns at imprinted genes (Hata et al., 2002; Kaneda et al., 2004). *Dnmt3b* deficiency on the other hand leads to demethlyation of minor satellite DNA and embryonic lethality around E14.5 (Li, 2007). Deficiency for both *de novo* methyltransferases results in early embryonic lethality (Okano et al., 1999). Furthermore, Dnmt3a methylates SINE-B1 elements, while Dnmt3a and Dnmt3b cooperate to methylate IAP and LINE-1 elements (Kato et al., 2007). *Dnmt1*, the founding member of DNA methyltransferase family, is needed for the maintenance of DNA methylation. It recognizes hemimethylated sites and methylates the cytosine of the newly synthesized DNA strand. Loss of *Dnmt1* results in severe genome-wide hypomethylation and lethality during gastrulation (Li et al., 1992; Li, 2007). Furthermore, it results in abnormal expression of imprinted genes, ectopic X-chromosome inactivation and activation of silent transposons (Li, 2007). Interestingly, it was shown that Suv39h1 interacts *in vitro* and *in vivo* with Dnmt3a, via its PHD-like motif. Additionally, H1β binds Dnmt1 and Dnmt3a. This directly links DNA methylation with histone methylation (Fuks et al., 2003). It has subsequently been shown that silencing of the *Survivin* gene coincides with recruitment of G9a, another H3K9 methyltransferase, and Hp1 in wt cells, but not in *Dnmt1* deficient cells, suggesting that the Hp1 Dnmt1 interaction mediates silencing of euchromatic genes (Smallwood et al., 2007).

During mammalian development there are two waves of global DNA methylation reprogramming. Both waves include the active removal of 5mC. One occurs immediately after fertilization, where the paternal pronucleus (PN) actively loses 5mC (Mayer et al., 2000a; Oswald et al., 2000; Santos et al., 2002). The second wave occurs when the primordial germ cells (PCG) migrate to the genital ridge around E11.5 (Lees-Murdock and Walsh, 2008; Sasaki and Matsui, 2008). Since the description of these two waves of loss of 5mC in mouse a search for an enzyme responsible for this DNA ‘demethylation,’ as it has been described in plants (Gehring et al., 2006), has occured. Many mechanisms and enzymes have been reported to be involved in this process in mammals (Wu and Zhang, 2010). Most recently, the Ten-eleven translocation (Tet) proteins have been implicated with DNA demethylation (discussed in (Veron and Peters, 2011)). The model proposed for these proteins activity is that the Tet proteins hydroxy-methylate 5-methylcytosine (5mC) to 5 hydroxmethylcytosine (5hmC). This 5hmC modification is thought to be an intermediate state that can be either removed or changed back into 5mC. The near future will bring more insight into this model.

PcG in mouse

Like in *Drosophila*, PcG proteins form two distinct complexes in mice. PRC2 comprises the SET domain containing histone methyltransferases Ezh1 and Ezh2 (E(Z) homologs), embryonic ectoderm development Eed (ESC homologs), Suz12 (SU(Z)12 homolog) and RbAp 48/46 (homologs of NURF55) (Faust et al., 1995; Niswander et al., 1988; O'Carroll et al., 2001; Pasini et al., 2004). Mice deficient for any PRC2 core member are inviable. They die during early post-implantation development with severe developmental and proliferative defects (Faust et al., 1995; O'Carroll et al., 2001; Pasini et al., 2004). Loss of *Ezh2* reduces di- and tri-methylation globally. Ezh1 displays only weak H3K27me2/3 activity (Margueron et al., 2008). It is thought to be responsible for mono-methylation of H3K27 mainly (Shen et al., 2008). Eed must be involved in all three H3K27 methylation states, since its deletion results in loss of all H3K27 methylation states. Recently, a crystal structure revealed that Ezh2 binds to the WD domain of Eed (Han et al., 2007).

PRC1 contains the following core members, depending on the cell type: Cbx2, Cbx4, Cbx6, Cbx7 and Cbx8 (PC homologs; it must be noted again that *Cbx1*, *Cbx3* and *Cbx5* are other gene names for *Hp1α*, *Hp1β* and *Hp1γ*, which belong to another family of CDs), Ring1a and Ring1b (dRING homologs), Phc-1-3 (PH homologs) and Bmi1, Pcgf1-7 and Mel18 (PSC homologs) (Sawarkar and Paro, 2010). Deletion of several PRC1 members leads to homeotic transformations (Akasaka et al., 1996; Core et al., 1997; del Mar Lorente et al., 2000; van der Lugt et al., 1994).

PRC2 mediated H3K27me3 provides a binding site for the N-terminal CD of some of the Cbx homologs. Interestingly, different K_ds for H3K27me3 and H3K9me3 have been determined for the five paralogs. One study measured strong H3K27me3 binding for the CDs of Cbx2 and Cbx7, similarly strong H3K9me3 binding for the CDs of Cbx2, Cbx4 and Cbx7 and no binding of the CDs of Cbx6 and Cbx8 (Bernstein et al., 2006). Another study measured equally strong H3K27me3 binding for CBX2, CBX4 and CBX7, but binding to H3K9me3 only by CBX4 and CBX7 and again no binding of the CDs of CBX6 and CBX8 (this study analyzed the human CDs, which are all fully conserved compared to the mouse CD)(Kaustov et al., 2011) (Figure 2.4.E). Thus, the strong H3K27me3 binding of the PC CD is not conserved in mouse. Additionally, H3 peptide permutation arrays revealed greater sequence tolerance of the Cbx CDs. Comparison of the human CBX CD crystal structures with the HP1 CD crystal structures revealed that two conserved aa residues form a hydrophobic clasp in the CBX orthologs, while the aa residues at the same position in HP1β form polar fingers surrounding the peptide in the HP1 orthologs (Kaustov et al., 2011). Nevertheless, this does not explain why some Cbx CDs bind more strong to H3K27me3 than to H3K9me3. C-terminal, all five Cbx homologs contain a conserved PcBox, a motif necessary for the interaction with Ring1a and Ring1b (Garcia et al., 1999; Whitcomb et al., 2007). Besides these two motifs, the conservation of the five homologs is low.

Cbx2, which is predominantly expressed in oocytes and pre-implantation embryos, contains an AT-hook motif located just to the C-terminal end to the CD (Senthilkumar and Mishra, 2009; Whitcomb et al., 2007). Moreover, it has been implicated in maintenance of the inactive X chromosome (Plath et al., 2004) and phosphorylation of a conserved residue in the CD results in specificity changes for methylated histone H3 in specific cell types (Hatano et al., 2010). Interestingly, loss of *Cbx2* in mice has been reported to lead to a male-to-female sex reversal (Katoh-Fukui et al., 1998).

Cbx4 on the other hand binds the transcriptional co-repressor C-terminal binding protein (CtBP) (Sewalt et al., 1999). It is the only Cbx homolog to contain an E3 SUMO ligase, including CtBP as a target (Kagey et al., 2003; Roscic et al., 2006). Furthermore, it has been described as a repressor of C-Myc (Satijn et al., 1997).

While *Cbx6* has not been studied thoroughly, *Cbx7* and *Cbx8* have been shown to be involved in maintaining the repression of the *Ink4-Arf* locus, which regulates cellular proliferation and senescence (Dietrich et al., 2007; Gil et al., 2004). Binding of Cbx8 to *Ink4-Arf* depends on Bmi1, while binding of Cbx7 is Bmi1 independent (Dietrich et al., 2007; Gil et al., 2004). *Cbx7* KD increases the Arf and Ink4a expression which causes impairment of cell growth (Gil et al., 2005). Interestingly, a study has also shown that Cbx7 together with Suv39h2 suppress the *p16Arf-p15* locus in gastric cancer cell lines. Mutation of the Cbx7 CD and the PcBox abolishes Cbx7 binding and H3K9me3 formation at this locus. In addition, siRNA KD of *Suv39h2* blocked the repressive effect of Cbx7 on *p16* transcription (Li et al., 2010). Surprisingly, in these cancer cell lines, polycomb and Su(var), which have been described to be distinct, co-localize to this gene.

Mel-18 and *Bmi1* (two of the PSC homologs in mammals) mutants display similar but nevertheless unique homoeotic phenotypes (Akasaka et al., 1996; van der Lugt et al., 1994). Only 30% of *Bmi1*-regulated genes were found to be co-regulated by *Mel-18* and vice-versa

(Wiederschain et al., 2007). Strangely, *Bmi1* was shown to be oncogenic (Haupt et al., 1991), while *Mel-18* is associated with tumor-suppressor function (Sparmann and van Lohuizen, 2006). Both proteins form stable PRC1 complexes, but only Bmi1 has been shown to positively regulate H2AK119 ubiquitination by Ring1b (Cao et al., 2005).

The two mammalian Ring proteins, Ring1a and Ring1b, also exhibit different functions. *Ring1a* heterozygous mutant mice exhibit classical homeotic transformations (del Mar Lorente et al., 2000), while *Ring1b* heterozygous mutant mice do not show such a phenotype (Voncken et al., 2003). Nevertheless, *Ring1b* null embryos do not live beyond E10.5 (Voncken et al., 2003). Such *Ring1b*$^{m+z-}$ embryos show global reduction of H2A ubiquitination, with only some staining remaining on the X-chromosome, while *Ring1a/Ring1b* double KO cells show a complete loss of H2A ubiquitination (de Napoles et al., 2004), suggesting certain redundancy of the two mammalian Ring proteins.

Finally, the mammalian polyhomeotic homologs have not been studied thoroughly yet, but Phc3, for example, has been suggested to act as a suppressor of colony formation of tumor cells (Iwata et al., 2010).

PcG targeting in mice

How PcG are recruited to their targets is still poorly understood. Unlike in *Drosophila*, the existence of PREs in mammals has been questioned. Only recently, the first vertebrate PRE was identified. This PRE recruits PRC1 and PRC2 to repress *MafB* gene expression. Interestingly, PRC1 is recruited to this PRE with higher affinity than PRC2. Furthermore, a palindromic double Pho-binding site was present in the mouse sequence (Sing et al., 2009). Its function in respect to PcG targeting remains to be unraveled. Another study describes a 44 kb region corresponding to the *Zfpm2* locus. It initiates *de novo* recruitment of PRC2. A CpG island within this locus is both necessary and sufficient for PRC2 recruitment. Furthermore, two 1 kb *E. coli* DNA fragments with a GC content comparable to a mammalian CpG island were capable of recruiting PRC2 when integrated into the mouse ESCs. This suggests that GC-rich elements recruit PRC2 in mouse ESCs (Mendenhall et al., 2010). Nevertheless, large-scale ChIP data sets for chromatin modifications and PRC1 and 2 members showed that PcG target regions do not contain a simple arrangement of consensus motifs (Barski et al., 2007; Boyer et al., 2006; Bracken et al., 2006; Guenther et al., 2007; Ku et al., 2008; Lee et al., 2006). Overlap with pluripotency transcription factors Oct4, Sox2 and Nanog suggests importance of DNA transcription factors in recruiting PcG (Lee et al., 2006). Furthermore, one can envision, that PRC1 or 2 themselves bind target DNA, for example via the AT-hook motif of Cbx2, in a similar mechanism as it was described for the AT-hook motif containing protein D1 in *Drosophila* (Aulner et al., 2002).

Another possible targeting mechanism could involve ncRNAs. A prominent example of targeting the repression machinery by a ncRNA is the X-inactivation specific transcript (*Xist*) (Borsani et al., 1991; Brockdorff et al., 1991; Brown et al., 1991). Xist transcript accumulates on the inactivated X (Xi). It is required for the initiation of silencing (Marahrens et al., 1997; Penny et al., 1996), but not for the maintenance of gene repression on Xi in differentiated cells (Brown and Willard, 1994; Csankovszki et al., 1999; Wutz and Jaenisch, 2000). The transition from initiation to maintenance involves DNA methylation and PcG mediated chromatin modifications, the latter of which is *Xist* binding dependent (Wutz, 2011).

Other examples of ncRNA dependent PcG targeting include short ncRNAs (50-200 nt), derived from upstream elements of the transcription start site of PcG repressed loci (Kanhere et al., 2010) and long nc (lnc) RNAs. One well studied lncRNA called ANRIL is encoded by the *Ink4b/Arf* locus. It has been shown to bind Cbx7. Together with the recognition of H3K27 methylation, binding to ANRIL RNA contributes to Cbx7 function, and disruption of either interaction impacts the ability of Cbx7 to repress the *Ink4b/Arf/Ink4a* locus (Yap et al., 2010). In addition to Cbx7, also Cbx4, Cbx6 and Cbx8 have been reported to bind to RNA (Bernstein et al., 2006).

Another example is a 2.2 kb large intergenic non-coding RNA (lincRNA) expressed by the *HoxC* locus, called HOTAIR. Depletion of HOTAIR diminishes targeting of PRC2 and H3K27 methylation to *HoxD* and results in its de-repression (Rinn et al., 2007). More recently, RNA-Suz12 and RNA-Ezh2 complexes were crosslinked and immunoprecipitated. Altogether, 24 lincRNAs (around 10% of the ES cell lincRNAs) were strongly enriched for these Polycomb components (Guttman et al., 2011). Another study shows association of approximately 20 % of the around 3’000 identified lincRNA with PcG (Khalil et al., 2009).

Summary

Although more complex in mice, the major features of epigenetic silencing at constitutive heterochromatin, facultative heterochromatin or at single loci are conserved within metazoan. The targeting of either the Su(var) pathway or PcG proteins is not well understood yet, but ncRNAs as well as DNA binding factors have been implicated in it. Unlike in *Drosophila*, DNA methylation is a third major component of transcriptional silencing in mice. Furthermore, several studies have linked the Su(var) pathway with DNA methylation, whereas the Su(var) pathway and PcG remain exclusive with only few single exceptions further discussed in 2.4.

2.3. (Hetero-) Chromatin dynamics in the mouse zygote

2.3.1. Spermatogenesis

Spermatogenesis can be divided into three major phases: mitotic proliferation of spermatogonial stem cells, reduction of chromosomal number by meiosis and the morphological transformation of the haploid germ cell into a spermatozoon (de Kretser et al., 1998).

Various epigenetic processes take place during male germ cell development. Paternally imprinted genes are DNA methylated (Davis et al., 1999; Li et al., 2004). All members of the DNMT family have been implicated in this process (Li et al., 1993; Li et al., 1992; Sasaki et al., 2000). Furthermore, transposable elements are silenced by DNA methylation before and during early steps of spermatogenesis. This prevents genomic instability (Bourc'his and Bestor, 2004; Suetake et al., 2004). Besides DNA methylation, histone methylation is implicated in spermatogenesis. *Suv39h*-dn mice undergo apoptosis at the pachytene stage of meiotic prophase as a consequence of incomplete homolog pairing and synapsis (Peters et al., 2001). Additionally, *G9a* mutant mice are sterile (Tachibana et al., 2007). Furthermore, centromere clustering and synapsis was affected in *G9a* as well as in *Hp1γ* deficient spermatocytes (Takada et al., 2011). This implicates importance of H3K9 methylation during spermatogenesis.

In the post-meiotic stages of spermatogenesis, the haploid round spermatids undergo cytoplasmic metamorphosis and chromatin remodeling. This includes transcriptional silencing and condensation of the chromatin into a volume of about 5% of that of a somatic cell nucleus, which is assisted by double strand breaks and histone-to-protamine exchange (Doenecke et al., 1997; Govin et al., 2004; Marushige and Marushige, 1975). Protamines are small basic arginine- and cysteine-rich proteins, which are spermatid-specific (Wouters-Tyrou et al., 1998). Nevertheless, the histone-to-protamine exchange is not complete. Around 1% of nucleosomes are retained in mouse and 15% in humans (Tanphaichitr et al., 1978; Wykes and Krawetz, 2003). The importance of these retained histones is not understood. Recent studies show that the retained histones carry post-translational modifications and are associated with specific promoters (Brykczynska et al., 2010; Hammoud et al., 2009). This suggests a model, in which histone marks are transmitted via the paternal germline to the embryo, assuring correct gene expression (Brykczynska et al., 2010).

2.3.2. Oogenesis

During female gametogenesis, the diameter of an oocyte increases up to 8 times, while its volume increases more than 100-fold. Concomitantly, the maternal genome is highly transcribed and transcripts accumulate (De Leon et al., 1983). In mouse oocytes, more than 5’000 different transcripts are detected (Evsikov et al., 2006; Kocabas et al., 2006). Many transcripts are directly translated, some of which have been cataloged in proteomic profiling (Latham et al., 1991; Vitale et al., 2007). These proteins ensure early embryonic development. They nurture the embryo until the major zygotic genome activation (ZGA) occurs in the late 2-cell stage, upon which the embryo relies on its own transcripts and proteins (Tadros and Lipshitz, 2009).

Oogenesis initiates during fetal development around embryonic day E13.5 after the primordial germ cells (PGC) have entered the genital ridge. The PGCs divide mitotically, which leads to the generation of oogonia. In turn, they enter meiosis and begin forming primordial follicles (Acevedo and Smith, 2005). Around 10’000 oocytes remain to assure functional gametes for the reproductive phase of the female. The fully grown oocytes, called germinal vesicle (GV) oocytes, are divided into two populations based on their chromatin organization (De La Fuente et al., 2004a). The non-surrounded nucleolus (NSN) oocyte is characterized by a diffuse chromatin configuration. NSN-oocytes are still immature and cannot be fertilized. They then develop to the surrounded-nucleolus (SN) oocyte configuration. This transition is accompanied with the cessation of transcription and the rearrangement of the peri- and centromeric DNA into a ring like structure, surrounding the ribosomal DNA (rDNA). A similar PCH arrangement is observed in the zygote (Figure 2.5) and the early 2-cell embryo. This ring-like structure in the oocyte shows reduced histone acetylation (De La Fuente et al., 2004b) and enrichment for the histone variant macroH2A (Chang et al., 2005). It is bound by the chromatin remodeler Atrx, which is needed for proper chromosome segregation during meiosis (De La Fuente et al., 2004b), and is enriched for the histone marks established by the Su(var) pathway and Hp1β. Finally, the SN-GV oocyte completes the first meiotic division and then arrests in metaphase of the second meiotic division (MII oocytes), ready to be fertilized by the sperm. Once fertilized, the second meiotic division is completed and the maternal pronucleus is formed.

2.3.3. The Zygote

At the onset of mouse development, a spermatozoon fertilizes a mature oocyte. Fertilization triggers a cascade of crucial events in embryonic development. Sperm entry initiates Ca^{2+} spiking, which leads to the activation of a signaling pathway that triggers the resumption of the cell cycle (Jones, 1998). The second meiotic division is completed, and the maternal genome is now haploid. At the same time, paternal chromatin undergoes major remodeling events and finally forms a pronucleus (PN), similar to the maternal PN. Initially, both PN are small in size and far apart from each other. During zygotic development, the chromatin of both PN decondenses (in wt zygotes the paternal PN is the larger), and they move towards each other and the center of the zygote. Based on the PN morphology, zygotic substages have been defined (Adenot et al., 1997; Santos et al., 2002). PN0 refers to the zygote right after fertilization. It is characterized by maternal chromosome segregation and paternal sperm decondensation. PN1 pronuclei are small and reside at the periphery of the embryo. PN2/3 pronuclei display an increased size and have started to migrate toward the center of the embryo. PN4 pronuclei are close to each other and PN5 refers to large central pronuclei. At the end of zygotic development, the pronuclear membranes break down and the two parental genomes fuse during the first mitotic division. However, maternal and paternal genomes will be indistinguishable by global chromatin marks only by the 4-8 cell stage (Mayer et al., 2000b; Puschendorf et al., 2008).

As in oogenesis, PCH is arranged in a ring-like structure surrounding the nucleoli (Probst et al., 2007; Zuccotti et al., 1995) (Figure 2.5). Only oocytes with this PCH organization develop beyond the two-cell stage when fertilized *in vitro*, thus this structure correlates with the developmental competence of the embryo (De La Fuente et al., 2004a; Zuccotti et al., 2002). As the maternal PN forms, individual minor satellite signals can be resolved by DNA fluorescence *in situ* hybridization (FISH) experiments, suggesting absence of association of the centromeres (Figure 2.6). In PN2, the major satellites align and form a discontinuous ring, surrounding the nucleolar precursor bodies (NPB) with insertion of some minor satellites between the major satellite repeats (Probst et al., 2007) (Figure 2.6). Paternally in PN1, the minor satellite repeats remain tightly associated with pericentromeric repeats in the center of the nucleus, with no association with the recently formed NPB observed. In paternal PN during PN2, the major satellite repeats form a continuous ring with the minor satellites on either side, surrounding the NPB (Probst et al., 2007) (Figure 2.6).

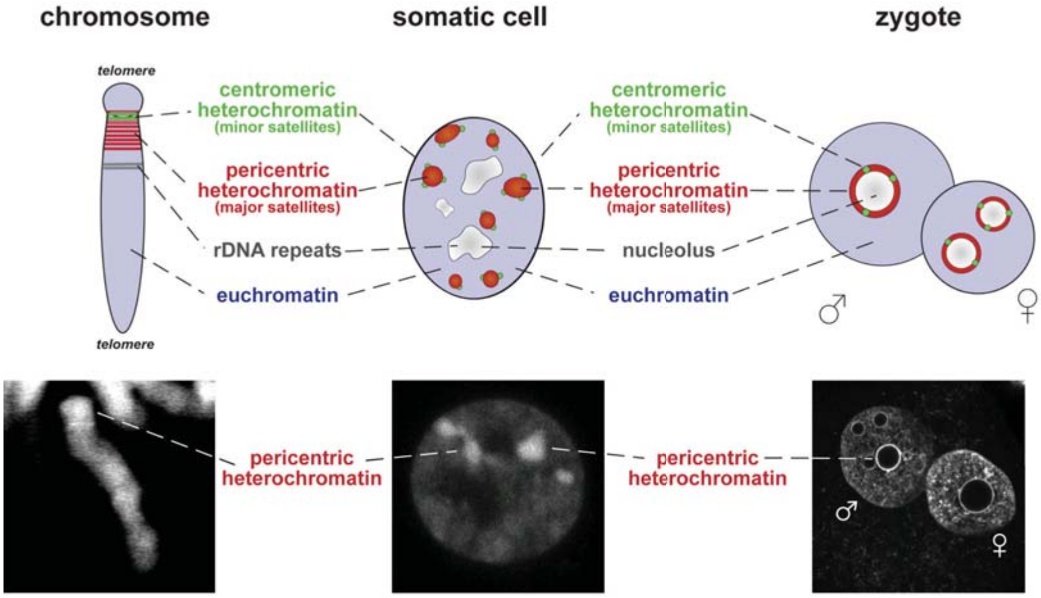
chromosome
somatic cell
zygote
telomere
centromeric heterochromatin (minor satellites)
pericentric heterochromatin (major satellites)
rDNA repeats
euchromatin
telomere
centromeric heterochromatin (minor satellites)
pericentric heterochromatin (major satellites)
nucleolus
euchromatin
♂
♀
pericentric heterochromatin
pericentric heterochromatin
♂
♀

Figure 2.5: Top: cartoon of chromosomal regions of an acrocentric chromosome, a somatic cell and a zygote in mouse. **Bottom:** DNA (visualized by DAPI) arrangement of an acrocentric metaphase chromosome, an ES cell and a PN5 zygote.

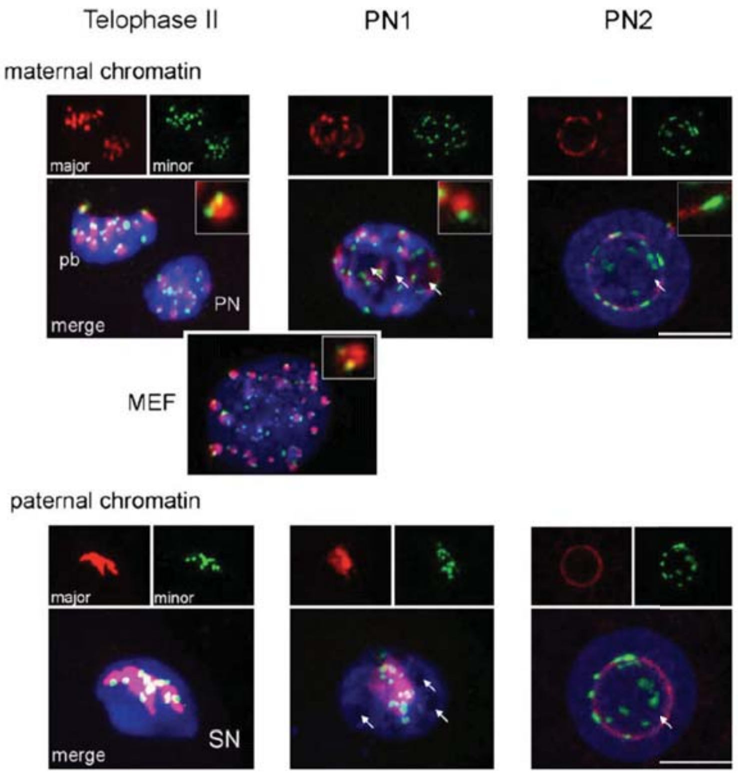

Figure 2.6: Organisation of satellite repeats in maternal and paternal chromatin of mouse zygotes. DNA-FISH for major (red) and minor (green) satellite repeats. DNA was visualized with DAPI (blue). pb: second polar body; PN: pronucleus; SN: sperm nucleus (PN0); arrows indicate the NPB. A mouse embryonic fibroblast (MEF) cell is shown for comparison. Scale bar: 10 µm. Adapted from Probst et al, 2007.

2.3.3.1. Asymmetry of Histones in the Zygote

Within 30 minutes after sperm entry, the protamines are shed from the paternal DNA (van der Heijden et al., 2005). As the sperm head decondenses, presence of the histone H3.3 chaperone Hira is observed (van der Heijden et al., 2005) and the replication independent H3 variant H3.3 is incorporated into the male PN right after fertilization (Torres-Padilla et al., 2006). Maternally, the DNA remains wrapped around the canonical histone variants H3.1/2, as inherited by the oocyte (van der Heijden et al., 2005). These canonical histone variants H3.1/2, which differ from H3.3 by five and four aa residues, respectively, are incorporated by a replication dependent pathway (Ahmad and Henikoff, 2002). Recently, it was also shown that these two variants are also incorporated in the context of DNA repair (Polo et al., 2006). This incorporation is mediated by the Caf-1 complex and Asf-1 (Tagami et al., 2004). In agreement with this model, microinjection of tagged H3.1 into zygotes before pronuclear formation, only results in incorporation in S-phase, whereas microinjected tagged H3.3 mRNA can be incorporated into the paternal PN already during its formation (Santenard and Torres-Padilla, 2009).

Interestingly, mouse oocytes fertilized with human sperm show dots of H3.1/2 staining in the paternal PN before DNA synthesis, suggesting that retained histones in human sperm remain chromatin bound even after the global protamine-to-histone exchange in the zygote (van der Heijden et al., 2008). It is possible that these H3.1/2 histones are post-translationally modified and serve as templates for the propagation of a paternally inherited chromatin state. For mouse oocytes fertilized by mouse sperm, no such paternal H3.1/2 staining has been observed so far (van der Heijden et al., 2005). Recently, we stained mouse oocytes fertilized with mouse sperm immediately after fertilization and in later pronuclear stages, using an antibody specific for H3.1 and H3.2. We detect a dot-like staining from decondensing mouse sperm onwards (Figure 2.7.A), suggesting inheritance of paternal H3.1/2 histones, which remain bound to paternal chromatin. In later pronuclear stages, the dot-like staining throughout the nucleus is maintained, while patches of stainings on or within the paternal ring structure become apparent (Figure 2.7.B). The shape and localization of these patches strongly resemble DNA-FISH signals from minor satellite repeats (Probst et al., 2007). Furthermore, in order to exclude that these H3.1/2 dots and patches are due to DNA lesions, the zygotes were incubated in 5-ethynyl-2'-deoxyuridine (EdU), which is incorporated into newly synthesized DNA. No *de novo* DNA synthesis was observed in these regions (Figure 2.7.B). Additionally, incubation in EdU allowed us also to analyze the replication timing of putatively paternally inherited H3.1/2. While the small euchromatic dots are replicated early (Figure 2.7.C), the patches around or within the NPB are late-replicative, consistent with their being minor satellite repeats (Figure 2.7.D). Whether those retained histones serve any function in pre-implantation development remains to be investigated. A recent study, however, showed that histone H3.3, in particular residue K27 is crucial for early development (Santenard and Torres-Padilla, 2009). Micro-injection of $H3.3^{K27R}$-GFP into zygotes resulted in a developmental arrest at the 2-cell stage, aberrant transcription of pericentromeric transcripts and mislocalization of Hp1β in 2-cell embryos (Santenard et al., 2010). Therefore, it is possible that the paternally inherited H3.1K27me3 and H3.2K27me3 serve as a template for spreading K27 methylation paternally. Injection of excess $H3.3^{K27R}$ would disable this propagation, which might lead to the observed phenotype.

The asymmetry of the histones is finally resolved during the first DNA synthesis in the zygote, a few hours after fertilization, when the canonical cell cycle dependent H3.1/2 histones are globally incorporated maternally and paternally (Santenard et al., 2010; van der Heijden et al., 2005).

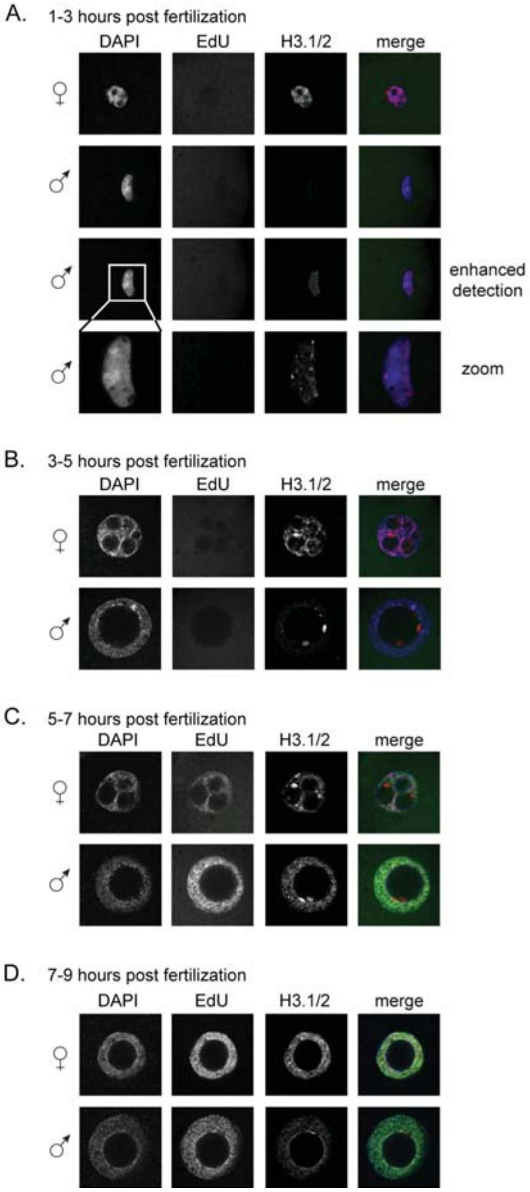
A.
1-3 hours post fertilization
DAPI
EdU
H3.1/2
merge
♀
♂
♂
enhanced detection
♂
zoom
B.
3-5 hours post fertilization
DAPI
EdU
H3.1/2
merge
♀
♂
C.
5-7 hours post fertilization
DAPI
EdU
H3.1/2
merge
♀
♂
D.
7-9 hours post fertilization
DAPI
EdU
H3.1/2
merge
♀
♂

Figure 2.7: Immunofluorescence analysis of H3.1 and H3.2 presence in paternal PN of *in vitro* fertilized zygotes. DNA was visualized by DAPI. H3.1 and H3.2 presence was visualized by an antibody raised against both canonical histones (antibody name: #34). DNA synthesis and repair was scored by incorporation of EdU, which is incorporated into DNA during active DNA synthesis and repair. Zygotes were incubated in 10 µM EdU from fertilization onwards. **A.** Zygotes fixed after 1-3 hours post fertilization. The H3.1 and H3.2 staining is only visible with enhanced detection. **B.** Zygotes fixed 3-5 hours post fertilization. Neither DNA synthesis nor DNA repair is observed in these zygotes, whereas the paternal H3.1 and H3.2 staining is evident. **C.** Zygotes fixed 5-7 hours post fertilization. DNA synthesis initiated. The H3.1 and H3.2 patches are late replicative. **D.** Zygotes fixed 7-9 hours post fertilization. DNA synthesis is nearly completed. The paternal H3.1 and H3.2 patches were replicated.

2.3.3.2. Asymmetry of Global Histone Marks

Not only core histones are arranged asymmetrically in the mouse zygote, but also post-translational modifications of the histone tails vary between the maternal and the paternal PN. While maternal histone marks are mostly inherited from the oocyte, the major part of paternal marks are set up *de novo*, after or with the global *de novo* incorporation of the H3.3 histones. Many HMT are not present or active in the zygote. This leads to the differential epigenetic signatures of the maternal and the paternal PN. Upon paternal histone H3.3 incorporation, strong lysine acetylation is observed (Adenot et al., 1997; Santos et al., 2005; Sarmento et al., 2004; van der Heijden et al., 2006). At this early stage, the paternal PN still lacks histone methylation marks, while the maternal PN exhibits the inherited H3K4, H3K9, H3K27 and H4K20 methylation. The first methylation mark to appear paternally is H4K20me1 (van der Heijden et al., 2005). This is followed by mono-methylation of H3K4, H3K9 and H3K27, later di- and eventually tri-methylation. Interestingly, Ezh2 and Eed are present during PN1 in the paternal PN, but nonetheless H3K27me3 appears only around PN3/4 concurrent with DNA replication (Erhardt et al., 2003; Santos et al., 2005). Paternal acquisition of H3K9me2/3 is even further delayed, with H3K9me2/3 appearing only around the 4-cell stage (Lepikhov and Walter, 2004; Liu et al., 2004; Merico et al., 2007; Yeo et al., 2005). Interestingly, transferring a paternal PN into enucleated GV or MII stage oocytes resulted in its *de novo* H3K9 di-methylation, suggesting that the HMT is active before fertilization, but not afterwards (Liu et al., 2004). Surprisingly, the maintenance of asymmetric H3K9me2 is an active process that depends on protein synthesis and zygotic transcription, as *de novo* methylation in the male PN occurred when either protein synthesis or gene expression was inhibited by cycloheximide or α-amanitin (Liu et al., 2004).

2.3.3.3. Asymmetry at PCH in the Mouse Zygote

In addition to this global asymmetry of histone marks, also PCH in the zygote displays asymmetric features. The maternal PCH is enriched for the histone marks of the canonical Su(var) pathway, H3K9me3 and H4K20me3 (Probst et al., 2007; Santos et al., 2005). Furthermore, Hp1β, but not Hp1α or Hp1γ localizes to PCH (Meglicki et al., 2008; Puschendorf et al., 2008; Santos et al., 2005) (Figure 2.8). Since the paternal PCH does not contain these marks, it is possible that the Suv39h and Suv4-20 HMTs remain absent in the zygote, until they are transcribed and translated form the zygotic genome upon ZGA. It is also possible, though, that the maintenance of the PCH asymmetry is an active process, as was described for H3K9me2 (Liu et al., 2004). Thus, only the maternally inherited chromatin displays the features of heterochromatin as it is observed in most cell types. Recently, it was shown that paternal PCH within this developmental phase is marked by PcG proteins (Puschendorf et al., 2008) (Figure 2.8). This was the first study, which described wt constitutive heterochromatin as a target of PcG proteins. Earlier, it was shown that ESCs lacking both *Suv39h* HMTs possess constitutive heterochromatin with H3K27me3 enrichment (Peters et al., 2003). Interestingly, PRC1 is detected at paternal PCH already in decondensing sperm, prior to PRC2, where it remains throughout the zygotic stages, and diminishes only by the 4-8 cell stage from paternal PCH, when Su(var) marks also paternal PCH. PRC2 localizes to paternal PCH from PN4/5 pronuclear stage onwards only (Puschendorf et al., 2008). Thus, PRC1 is targeted to paternal PCH before it is enriched for H3K27me3. Furthermore, it was shown that PRC1 at paternal PCH represses the transcription of the major satellite repeats, since *Ring1b*$^{m-z+}$ show enhanced transcription of the paternal major satellite repeats. Thus, PRC1 possibly ensures sufficient silencing of the paternal repeats, backing up the Su(var) pathway paternally in this function, but, nevertheless, keeping the parental heterochromatin domains epigenetically distinct.

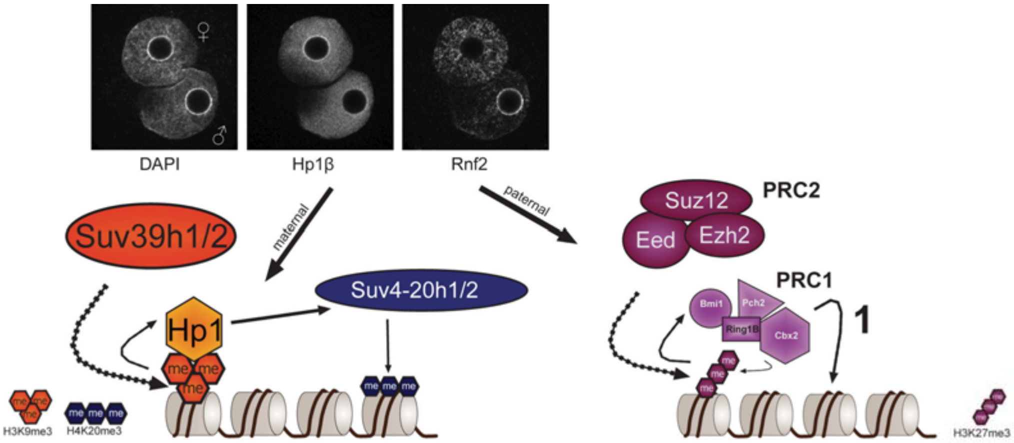

Figure 2.8: Asymmetry of the Suv39h pathway and PcG proteins observed at PCH of mouse zygotes. DNA is visualized by DAPI. The depicted zygote was stained with an antibody raised against Hp1β representing the Suv39h pathway. It strongly stains maternal PCH. Additionally, the zygote was stained with an antibody against the PRC1 member Rnf2, which stains paternal PCH.

Interestingly, in zygotes deficient for *Suv39h-2*, the maternal PCH lacks any marks established by the Su(var) pathway. Instead, PRC1 members are now detected not only at paternal PCH, but also at maternal PCH (Figure 2.9). This suggests that the Su(var) pathway prevents PRC1 from binding to maternal PCH in wt mouse zygotes (Puschendorf et al., 2008). Surprisingly, in *Suv39h-2*$^{m\text{-}z+}$ zygotes, where PRC1 localizes to maternal PCH, the transcriptional level of maternal major satellite repeats is not enhanced, suggesting an additional level of transcriptional regulation maternally, which has not been detected so far. *Suv39h2*$^{mz+}$*/Ring1b*$^{mz+}$-dn zygotes have not been analyzed in this respect so far. Despite the upregulation of the major satellite transcripts in *Ring1b* deficient mice, they do not show a severe phenotype in preimplantation embryos and are lethal only after implantation (Voncken et al., 2003), suggesting that repression of major satellite repeats by PRC1 is not crucial for preimplantation development. Nevertheless, correct repression/expression of these major satellite repeats has been suggested to be involved in setting up the canonical heterochromatin configuration paternally. These non-coding transcripts of heterogenous length are transcribed from the 234bp long AT-rich major satellite subunits. They have been implicated in recruiting Hp1β to paternal PCH. Indeed, in PN5 zygotes, little paternal PCH enrichment of Hp1β, which is independent of the Su(var) pathway, is observed, coinciding with transcription of major satellites (Probst et al., 2010; Santos et al., 2005). This has been suggested to be crucial for the formation and maturation of paternal PCH (Probst and Almouzni, 2011). This hypothesis is strengthened by the observation that the hinge domain of Hp1α binds RNA (Maison et al., 2002; Muchardt et al., 2002). Additionally, in 2-cell embryos, co-localization of HP1β with forward and reverse major satellite transcripts from putative paternal origin is observed (Probst et al., 2010). Finally, this might lead to the targeting of the Suv39h HMT in the 4-cell embryo and the epigenetic equalization of maternal and paternal constitutive heterochromatin.

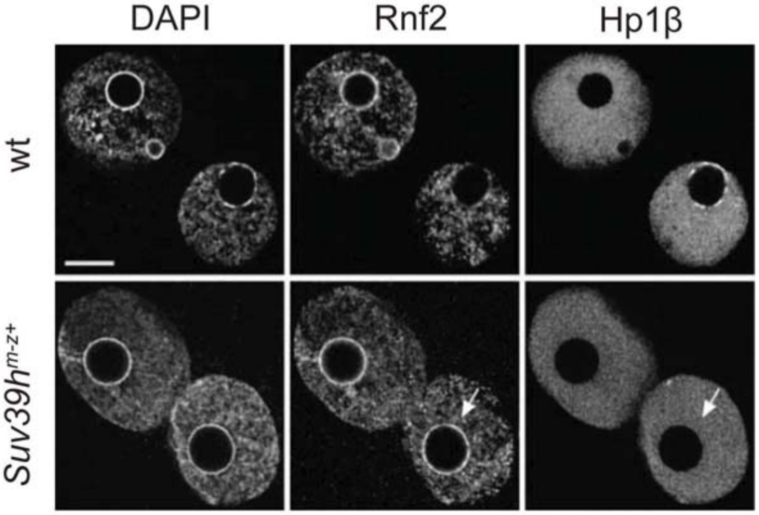

Figure 2.9: PRC1 enrichment at paternal and maternal PCH in *Suv39h2*$^{m\text{-}z+}$ zygotes. DNA is visualized by DAPI. Hp1β staining represents the Suv39h pathway. It is not enriched at maternal PCH in *Suv39h2*$^{m\text{-}z+}$ zygotes (arrow), whereas Rnf2 (Ring1b) as a member of PRC1 is enriched at maternal and paternal PCH in *Suv39h2*$^{m\text{-}z+}$ zygotes (arrow).

2.3.3.4. DNA ‘demethylation’ in the Mouse Zygote

Paternal chromatin differs in respect to DNA methylation from maternal chromatin. Within a few hours after fertilization (prior to the first zygotic S-phase), the paternal genome rapidly loses its global DNA methylation (Mayer et al., 2000a; Oswald et al., 2000; Santos et al., 2002), implying an active mechanism of DNA demethylation. In contrast, the maternal genome is only passively DNA demethylated via DNA replication and synthesis. This is due to the absence of the maintenance DNA methyltransferase Dnmt1 at this stage (Reik, 2007). *De novo* methylation occurs then specifically only in the inner cell mass (ICM) of the blastocyst, whereas lower levels of methylation are detected in the trophectoderm (Santos et al., 2002). Nevertheless, the paternal DNA is not fully demethylated. Paternally imprinted genes (Olek and Walter, 1997), pericentromeric heterochromatin (Rougier et al., 1998; Santos et al., 2002; Santos et al., 2005) and the IAP retrotransposons (Lane et al., 2003) are excluded from active DNA demethylation. The maintenance of this DNA methylation is thought to involve both, an oocyte specific *Dnmt1* isoform as well as the somatic *Dnmt1* (Cirio et al., 2008; Gaudet et al., 2004; Hirasawa et al., 2008; Kurihara et al., 2008). Since only paternal DNA is demethylated in the mouse zygote, it was suggested that maternal DNA is protected from this process. Indeed, a maternal factor essential for early development called *PGC7/Stella* was identified as being involved in the protection of the DNA methylation state of several imprinted loci and of the epigenetic asymmetry (Nakamura et al., 2007). Furthermore, a number of proteins have been implicated in DNA demethylation (Guibert, 2009). More recently, it was shown that 5mC can be hydroxylated to form 5hmC (Kriaucionis and Heintz, 2009; Tahiliani et al., 2009). 5hmC might reflect an intermediate DNA modification before it is fully demethylated or re-methylated. This hydroxylation can be performed by the dioxygenases Tet1, Tet2 and Tet3. IF stainings in wt zygotes indeed revealed the appearance of 5hmC paternally from PN3 onwards as 5mC disappears (Iqbal et al., 2011; Wossidlo et al., 2011). Furthermore, *PGC7/Stella* deficient zygotes, which lack maternal 5mC protective protein, show 5mC erasure and concomitant 5hmC appearance in maternal and paternal PN (Wossidlo et al., 2011). The paternal 5hmC enrichment in the male PN of zygotes is further diluted in a replication-dependent manner during preimplantation development (Inoue and Zhang, 2011). Finally, Tet3 was also shown to be enriched in the paternal PN. In *Tet3* deficient zygotes, the paternal genome conversion of 5mC to 5hmC fails to occur and the level of 5mC remains constant (Gu et al., 2011).

2.3.3.5. Maternal-to-Zygotic Transition

Most reprogramming taking place in the zygote is due to the activity of maternally provided proteins. A first wave of zygotic transcription is observed at the late zygote stage, known as the minor ZGA. This is followed by the major ZGA in the 2-cell embryo. Genome activation is accompanied by a global degradation of maternally inherited transcripts at the 2-cell stage, which restricts the period of time in which those maternal transcripts function. Furthermore, it allows the embryo to replace oocyte-specific transcripts with those required for embryonic development (Aoki et al., 1997; Knowles et al., 2003; Schultz, 2002; Stitzel and Seydoux, 2007).

2.4. Scope of the thesis

The recent discovery that implicates PcG proteins in constitutive heterochromatin localization and repression of major satellite transcripts raised the question, how these proteins are targeted to the major satellite repeats. Together with Mareike Albert (maiden name Puschendorf), we analyzed their targeting mechanism. We already had indications that this targeting is dependent on two modules of Cbx2: the CD and the AT-hook motif. It was then my part of the project to provide further and more detailed insight into this targeting mechanism by analyzing it in wt and transgenic zygotes, by microinjection of recombinant mRNA, performing life imaging and analyzing the targeting modules in an evolutionary context.

The larger scope of my project was to map the interdependency of the Suv39h and the PcG pathways. It is interesting to note the similarities between these two major epigenetic repressive pathways. Both contain proteins with SET domains (Suv39h1, Suv39h2, Suv4-20h1, Suv4-20h2 and Ezh1 and Ezh2). These proteins ‘write’ their signature onto chromatin by tri-methylating specific aa residues of the histone tails (H3K9me3, H4K20me3 and H3K27me3, respectively). In a next step, proteins containing a CD specific for one of these marks, ‘read’ them and bind to them. Thus, HP1 family members bind to H3K9me3, while the PC orthologs bind either H3K27me3 or both H3K9me3 and H3K27me3. Furthermore, ‘readers’ from both families have been described to bind RNA (Bernstein et al., 2006; Maison et al., 2002; Muchardt et al., 2002). Finally, in a mechanism not fully understood for the moment, the presence of both of these pathways at chromatin results in transcriptional silencing.

Altogether, these two pathways share many similarities. Generally, this suggests that epigenetic silencing of chromatin is most efficiently achieved using this model of ‘writers’ and ‘readers.’ Nevertheless, the two pathways were originally identified in very different experiments. While the members of the Su(var) pathway were identified by screens for mutants affecting PEV, the PcG pathway mutants were shown to result in homeotic transformations, suggesting already that their targets are different. Interestingly, they have not been shown to colocalize and may be mutually distinct. Only recently, a study suggested H3K9me3 (mediated by Eset though and not by Suv39h) at the Hox gene cluster, a classical PcG target (Bilodeau et al., 2009). Nevertheless, this colocalization of the H3K9me3 histone mark with a PcG target does not necessarily mean colocalization of the two pathways. It is quite possible, that the H3K9me3 histone mark is set in temporal window where no PcG proteins are present. Another study that identified colocalization of the two pathways at a gene was performed in cancer cell lines, which by their nature may not display normal chromatin dynamics (Li et al., 2010). Besides these two studies, no report of colocalization of the two pathways has been published, despite the publication of hundreds of studies examining each of these pathways. In the mouse zygote, however, Su(var) and PcG share constitutive heterochromatin as a target. Interestingly, zygotes that lack *Suv39h2* and, therefore, any downstream signal from this pathway, show enrichment of PRC1 at maternal PCH. This suggests that there is a interdependency at heterochromatin of the two pathways, with the Su(var) pathway upstream of PRC1, blocking PRC1 from binding to maternal PCH. Thus, it was the scope of my PhD to analyze, dissect and possibly overcome the interdependency of these two major epigenetic pathways.

In addition to the epigenetic asymmetries discussed so far, there is also a morphological asymmetry in respect to the size of the maternal and paternal PN. Although the maternal and the paternal genomes are equally large, the paternal PN is bigger. This suggests that DNA in the paternal PN is less compacted. Interestingly, this size difference is not only observed in PN5 zygotes but throughout zygotic development, which suggests that it is maintained by proteins present in the zygote. Therefore, we wondered what impact epigenetic repressors have on the size of maternal and paternal PN.

Finally, it has been shown that the paternal genome loses its global 5mC DNA methylation within a few hours after fertilization (Mayer et al., 2000a; Oswald et al., 2000; Santos et al., 2002). The maternal genome remains DNA methylated in the zygote. Recently, it was shown that paternal 5mC is converted to 5hmC by the Tet3 proteins (Gu et al., 2011). Epigenetic repressors have been associated with DNA methylation as well as with 5mC to 5hmC conversion in various cell types. Thus, it was the scope of my thesis to analyze the global impact of epigenetic repressors on the 5mC to 5hmC conversion of paternal DNA in the mouse zygote.

3. Results

3.1. Unpublished Manuscript: PRC1 targeting to constitutive heterochromatin and its dependency with the *Suv39h/Hp1β* pathway in mouse zygotes

Rico Kunzmann,[1#] Mareike Albert,[1,#,$] Lilia Kaustov,[2] Jean-Francois Spetz,[1] Stuart H. Orkin[3], Gunnar Schotta[4], Cheryl Arrowsmith[2] and Antoine H.F.M. Peters[1‡]

[1] Friedrich Miescher Institute for Biomedical Research, Maulbeerstrasse 66, 4058 Basel, Switzerland

[2] Ontario Cancer Institute, Campbell Family Cancer Research Institute and Department of Medical Biophysics, University of Toronto, Ontario M5G 1L7, Canada

[3] Department of Pediatric Oncology, Dana Farber Cancer Institute, Harvard Stem Cell Institute and HHMI, Harvard Medical School, USA

[4] Munich Center for Integrated Protein Science (CiPSM) and Adolf-Butenandt-Institute, Ludwig-Maximilians-Universität München, Schillerstrasse 44, 80336 Munich, Germany.

[#] These authors contributed equally to this work.

[$] Present address: Biotech Research and Innovation Centre (BRIC), Centre for Epigenetics, University of Copenhagen, Ole Maaløes Vej 5, 2200 Copenhagen, Denmark

[‡] Corresponding author: Antoine Peters

Phone: +41 61 6978761, Fax: +41 61 6973976, Email: antoine.peters@fmi.ch

Keywords:

Constitutive heterochromatin, Polycomb Repressive Complex 1, Cbx2, HP1β, Chromodomain, AT hook

Abstract

In early pre-implantation mouse embryos, parental genomes are epigenetically distinct despite their genetic resemblance. While pericentromeric heterochromatic (PCH) regions of maternal chromosomes are marked by *Suv39h*-mediated H3K9 trimethylation (H3K9me3), paternal PCH structure and function are controlled by maternally provided proteins of the Polycomb repressive complex 1 (matPRC1). *Suv39h*-dependent H3K9me3 established during oogenesis constitutes a dominant intergenerational signal for PCH formation in the embryo. In absence of this signal, like at the paternal genome, matPRC1 functions as a repressive back-up mechanism. The molecular mechanisms underlying matPRC1 localization to paternal and exclusion from maternal PCH are unknown. Here, we show that Cbx2 directs matPRC1 to PCH in mouse zygotes and *Suv39h* double null embryonic stem cells. Cbx2 targeting depends on its chromo domain (CD), binding to *Ezh2*-mediated H3K27me3, and the neighboring AT-hook, binding to DNA, likely major satellites underlying paternal PCH. The CD of Cbx2 prevents DNA binding by the AT-hook when PCH is marked by H3K9me3/Hp1. However, the $\mathrm{Cbx2}^{\mathrm{A14V}}$ mutant with moderate H3K9me3 affinity localizes to PCH marked by H3K9me3/Hp1β. In *Hp1β* maternally deficient zygotes lacking HP1β protein, matPRC1 strongly localize to maternal PCH that is still marked by H3K9me3 and H4K20me3. Thus, Hp1β prevents matPRC1 from binding to maternal PCH. Together, our data indicate that the CD and AT-hook motifs of Cbx2 function together as one reader domain that modulates matPRC1 binding to chromatin by integrating local histone modification states. Our work elucidates the mechanism underlying the molecular hierarchy of Suv39h/Hp1 over PRC1, two major chromatin repressive pathways in flies and mammals.

INTRODUCTION

The Suv39h pathway has been associated with constitutive heterochromatin in pluripotent and in somatic cell types. It is conserved from *S. pombe* to humans. Within this pathway, the Suv39h histone methyltransferases (HMT) specifically tri-methylate histone tail H3K9 (Rea et al., 2000). Deficiency for the two mammalian *Suv39h* histone HMTs result in loss of H3K9me3 at constitutive heterochromatin (Peters et al., 2001). In the wild-type background, the H3K9me3 histone mark is bound by the chromodomains (CD) of heterochromatin protein 1 (Hp1) family members (Jacobs and Khorasanizadeh, 2002; Lachner et al., 2001). Three murine Hp1 proteins have been described: Hp1α, Hp1β and Hp1γ, of which Hp1α and β localize to heterochromatin. Furthermore, Hp1 form homo- and/or heterodimers via their C-terminal chromoshadow domain (CSD), which is linked to the CD by an unstructured hinge domain, which itself has been described to bind RNA (Muchardt et al., 2002). Finally, the Hp1 proteins recruit the Suv4-20h methyltransferases, which tri-methylate H4K20 (Schotta et al., 2004). These three proteins reflect the canonical Suv39h pathway.

Facultative heterochromatin displays a more wide range of chromatin condensation states than constitutive heterochromatin. Most studied is the inactivated X chromosome. One of the X chromosomes in female cells is stably silenced before gastrulation and this state is maintained throughout life. This maintenance of silencing is assured by the Polycomb group (PcG) proteins. PcG proteins were first shown in *Drosophila* to repress the HOX gene cluster and localize to a various number of other repressed genes (Lewis, 1978; Schuettengruber and Cavalli, 2009). They are mainly detected in two complexes: Polycomb Repressive Complexes (PRC) 1 and PRC2. Vertebrate PRC1 comprises of four core subunits, which all have their founding member in *Drosophila*: PC homologs (Cbx2, Cbx4, Cbx6, Cbx7, Cbx8), dRING homologs (Ring1a, Rnf2), PSC homologs (Bmi1, Pcgf1-6, Mel18) and PH homologs (Phc1-3) (Sawarkar and Paro, 2010). PRC1 binding to target loci is thought to be crucial for the establishment of transcriptional silencing. The molecular mechanism that underlies the repression is widely studied. Interestingly, the Ring proteins were shown to ubiquitinate histone H2A, which compacts chromatin (Wang et al., 2004a). Furthermore, Cbx2 contains a charged region that compacts chromatin (Grau et al., 2011). PRC2 comprises the core components Ezh2, Suz12 and Eed (Schuettengruber and Cavalli, 2009), while Suz12 and Eed are both required for complex stability and for the methyltranserferase activity of Ezh2 (Pasini et al., 2004). In the canonical model, Ezh2 tri-methylates histone tail H3K27. This histone mark is recognized by the CD of a Cbx homolog, which in turn recruits PRC1.

In the mouse zygote, an asymmetry, in respect to maternal and paternal chromatin, is observed for the Suv39h and the PcG proteins (Puschendorf et al., 2008). In mouse zygotes and early 2-cell embryos the pericentromeric heterochromatin from various chromosomes form a ring like structure, surrounding the rDNA, unlike in most other cell types where they would cluster to form so-called chromocenters. This ring like structure consists of the AT-rich major satellite repeats. Maternal PCH displays the canonical heterochromatin marks: H3K9me3, H4K20me3 and Hp1β (Santos et al., 2005). Paternal PCH within this developmental phase is marked by PcG proteins, where they repress transcription of the major satellite repeats (Puschendorf et al., 2008). In respect to heterochromatin targeting and localization, unlike in other cell types, PRC1 is detected already in decondensing sperm (PN0) prior to PRC2 at paternal PCH, which is detected only in late zygotes (PN4-5) (Puschendorf et al., 2008), suggesting a PRC1 function independent of PRC2. PRC1 and 2 remain at paternal PCH up to the 4-8 cell stage (Puschendorf et al., 2008), upon which the ring like arrangement of PCH is restructured to chromocenters and maternally as well as paternally inherited heterochromatin is marked by the Suv39h pathway.

Taken together, in the mouse zygote constitutive heterochromatin, the classical Suv39h target, was shown to be also a target of PcG. This observation raises the question how PcG proteins are targeted to PCH in the paternal PN. And even more, how and why they specifically localize to paternal PCH? Interestingly, in maternally deficient *Suv39h2* mouse zygotes, PRC1 is targeted to maternal as well as to paternal PCH (Puschendorf et al., 2008). This suggests that there is a negative interaction and a hierarchy between the Suv39h pathway and PRC1. Thus, PRC1 is prevented from binding to maternal PCH by a component of the Suv39h pathway.

In this study, we elucidate how PRC1 is targeted to paternal PCH and why it does not localize to maternal PCH.

RESULTS

Cbx2 mediates matPRC1 targeting to constitutive heterochromatin in *Suv39h* dn ES cells

We have previously shown that the localization of the matPRC1 complex at constitutive heterochromatic regions of the paternal genome in early embryos can be recapitulated by over-expression of matPRC1 proteins in embryonic stem cells that are deficient for the two *Suv39h* HMTs (Puschendorf et al., 2008). In order to investigate whether any of the four core matPRC1 members would target the other matPRC1 components to heterochromatin, we overexpressed the individual components in *Suv39h* dn and wild-type control ESCs and measured by immunofluorescence microscopy their localization at chromocenters, which represent clusters of pericentromeric heterochromatic regions of different chromosomes (PCH) (Figure 3.1A). Among the four overexpressed matPRC1 proteins, only Cbx2 showed strong enrichment at PCH in *Suv39h* dn ESC (Figure 3.1A). In contrast, neither Cbx2 nor any other matPRC1 member localized to PCH in wild-type ESCs. This dependence of Cbx2 localization to PCH on *Suv39h* deficiency phenocopies the localization of the matPRC1 complex in zygotes (Puschendorf et al., 2008), suggesting an important function for Cbx2 in targeting matPRC1 to PCH in preimplantation mouse embryos.

The mouse genome encodes five Cbx orthologs of the *Drosophila* POLYCOMB (PC) protein which are part of functionally distinct PRC1 complexes (Beisel and Paro, 2011). To address whether Cbx4, Cbx6, Cbx7 and Cbx8 localize to PCH under similar conditions as the Cbx2, we over-expressed them individually in wild-type and *Suv39h* dn ESCs. None of the other PC orthologs, however, localized to chromocenters in any condition (Figure 3.1.B). To test the interdependencies for heterochromatic targeting of Cbx2 and other matPRC1 components, we co-transfected matPRC1 components with Cbx2 into *Suv39h* dn ESC cells. We observe that Cbx2 is required for PCH localization of endogenous Rnf2 and that Cbx2 and Rnf2 are both required for localization of Bmi1 or Phc2 to PCH (data not shown). These dependencies are consistent with known protein-protein interactions between PRC1 components (Bardos et al., 2000; Garcia et al., 1999; Whitcomb et al., 2007). In summary, among the five Pc Cbx proteins, Cbx2 has the unique ability to target the matPRC1 complex to PCH in *Suv39h* dn ESCs.

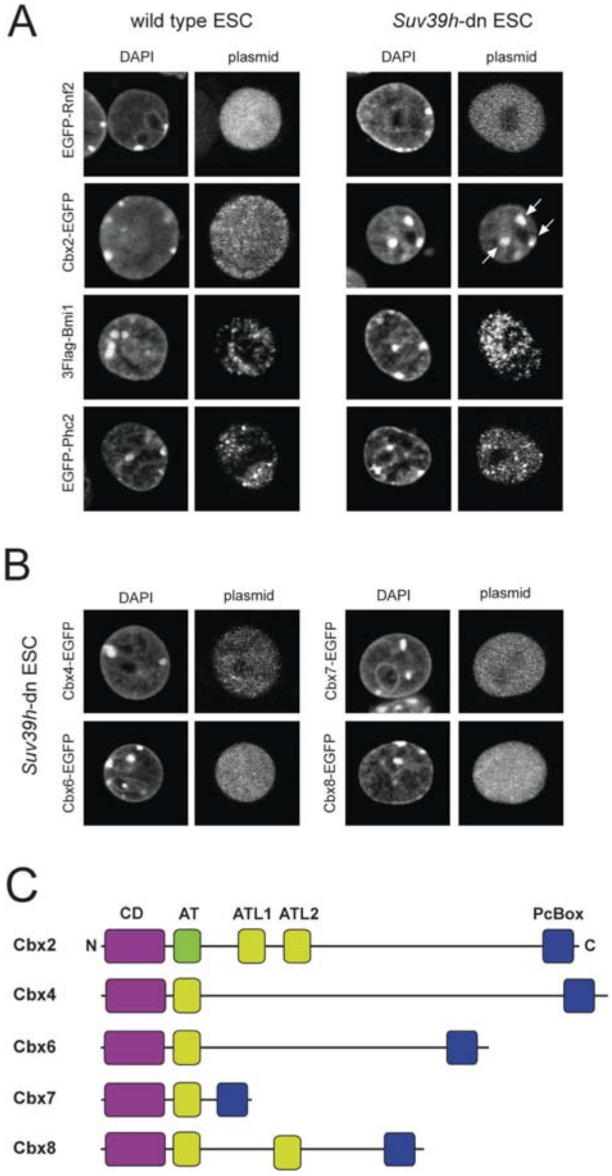
A
wild type ESC
Suv39h-dn ESC
DAPI
plasmid
DAPI
plasmid
EGFP-Rnf2
Cbx2-EGFP
3Flag-Bmi1
EGFP-Phc2
B
Suv39h-dn ESC
DAPI
plasmid
DAPI
plasmid
Cbx4-EGFP
Cbx6-EGFP
Cbx7-EGFP
Cbx8-EGFP
C
CD
AT
ATL1
ATL2
PcBox
Cbx2
N
C
Cbx4
Cbx6
Cbx7
Cbx8

Figure 3.1. Cbx2 is targeted to heterochromatin in *Suv39h* dn ESC. A. Immunofluorescence characterization of wt and *Suv39h* dn ESC overexpressing tagged PRC1 components. Overexpressed 3Flag-Bmi1 was detected using an antibody against flag. For EGFP tagged proteins, the EGFP was detected. **B.** Immunofluorescence characterization of *Suv39h* dn ESC overexpressing EGFP-tagged PC homologs: Cbx2, 4, 6, 7, 8. The EGFP signal was detected. **C.** Schematic representation of the 5 PC homologs in mammals. Chromodomains in purple, AT-hook motifs in green, AT-hook like motifs in light green, PcBox in blue.

Chromodomain and AT-hook of Cbx2: promising PCH targeting modules

Sequence comparison of the five Cbx proteins shows a N-terminal CD and a C-terminal Polycomb Box (Pc-box) (Whitcomb et al., 2007) (Figure 3.1.C). Among Cbx proteins, the Pc-box is unique to homologues of the PC protein (Senthilkumar and Mishra, 2009). This domain mediates the interaction of Cbx2 and Cbx8 with Ring1 (Bardos et al., 2000; Schoorlemmer et al., 1997) and is in flies required for PC function (Breiling et al., 1999).

CDs preferentially bind methylated histone residues via an aromatic cage, composed of three aromatic residues (Figure 3.2.A) (Fischle et al., 2003; Jacobs et al., 2001). While CDs of mammalian HP1 homologs strongly bind to H3K9me3, CDs of mouse and human CBX proteins have reduced binding affinities for H3K27me3 and/or H3K9me3 (Bernstein et al., 2006; Kaustov et al., 2011). The relative affinities of mammalian PC homologues for these modifications vary between the different Cbx proteins (Bernstein et al., 2006; Kaustov et al., 2011). For example, while CBX2 binds to H3K27me3, CBX4 and CBX7 have higher affinity for H3K9me3 relative to H3K27me3 peptides (Kaustov et al., 2011). Given that PCH in *Suv39h* dn ESC is marked by H3K27me3, the CD of Cbx2 is the first candidate for targeting Cbx2 to PCH.

Unique to Cbx2 is an AT-hook motif that is separated from the CD by a 15 amino acid linker with a predicted alpha-helix configuration (Figure 3.2.A) (Kaustov et al., 2011). AT-hook motifs are known to bind to the minor groove of a variety of AT-rich DNA sequences (Reeves, 2001). Despite the relaxed specificity, the AT-hook containing protein HMGA1 binds to DNA with nanomolar affinity (Reeves and Nissen, 1990) and methylation interference studies located its binding site to the minor groove of AT tracts (Thanos and Maniatis, 1992). The AT-hook motif of Cbx2 contains the core sequence GRP that is necessary for the recognition and binding of AT-rich DNA in the minor groove of the helix (Reeves and Nissen, 1990) (Figure 3.2.A, B). The other four Cbx proteins lack this consensus sequence. Instead, they contain only an AT-hook like motif that is unlikely to bind AT-rich DNA (Figure 3.2.B). Likewise, Cbx2 contains two AT-hook like (ATL) motifs lacking the GRP core consensus sequence. Since major satellite repeats in mouse cells are AT-rich, the AT-hook of Cbx2 represents the second candidate for targeting Cbx2 to chromo centers in mouse *Suv39h*-dn ESCs.

Cbx2 targeting to PCH in *Suv39h* dn ESC depends on its chromodomain and AT-hook

To test the function of the CD in PCH targeting, we mutated one of its three aromatic residues that is essential for H3K27me3 binding (F12A; Figure 3.2.C) (Bernstein et al., 2006).

We transiently transfected *Suv39h* dn ES cells with full length Cbx2-EGFP and Cbx2^{F12A}-EGFP constructs and scored the enrichment of the EGFP fusion proteins at PCH relative to euchromatin (Figure Supp 3.1). While Cbx2-EGFP was strongly enriched at PCH in many cells, heterochromatic enrichment was significantly reduced for the Cbx2^{F12A}-EGFP protein (Figure 3.2.D, E), demonstrating that the CD of Cbx2 contributes to targeting to PCH. Nevertheless, heterochromatin localization was not impaired by the F12A mutation in all cells suggesting that binding of the CD to H3K27me3 is not solely responsible for Cbx2 localization at PCH.

We subsequently tested the importance of the AT-hook motif for heterochromatin targeting by introducing several different point mutations (Figure 3.2.C). Compared to Cbx2^{F12A}-EGFP, mutation of the AT-hook “GRP” consensus sequence into “AAA” or just of a single residue (G78R or G78L) reduced PCH enrichment in even more cells. None of these mutations, however, completely abrogated heterochromatic enrichment (Figure 3.2.D, E).

A comparable point mutation in the first ATL motif of Cbx2 (G137R) did not impair heterochromatin enrichment. Likewise, mutations in both ATL motifs of Cbx2 (G137R, G165R) did not extravagate the reduction in PCH binding caused by mutations in the AT-hook alone (Figure 3.2.D, E). Thus, only the AT-hook of Cbx2 and not its two ATL motifs contributes to binding of Cbx2 to PCH in *Suv39h* dn ES cells.

To test whether the CD and AT together confer Cbx2 full binding capacity to PCH, we transfected *Suv39h* dn ES cells with a Cbx2-EGFP construct containing point mutations in both domains and observed a complete loss of heterochromatin targeting (Figure 3.2.D, E). Furthermore, an EGFP fusion reporter protein harboring only the CD and AT-hook domains displayed PCH enrichment comparable to the full length Cbx2-EGFP protein while PCH binding of single domain fusion proteins was strongly diminished (Figure Supp 3.2). Therefore, these data evidently demonstrate that the CD and AT-hook of Cbx2 are sufficient for PCH targeting in *Suv39h* dn ES cells. Further, the data reveal an additive, potentially cooperative effect of the two modules in Cbx2 targeting to chromatin in ESCs.

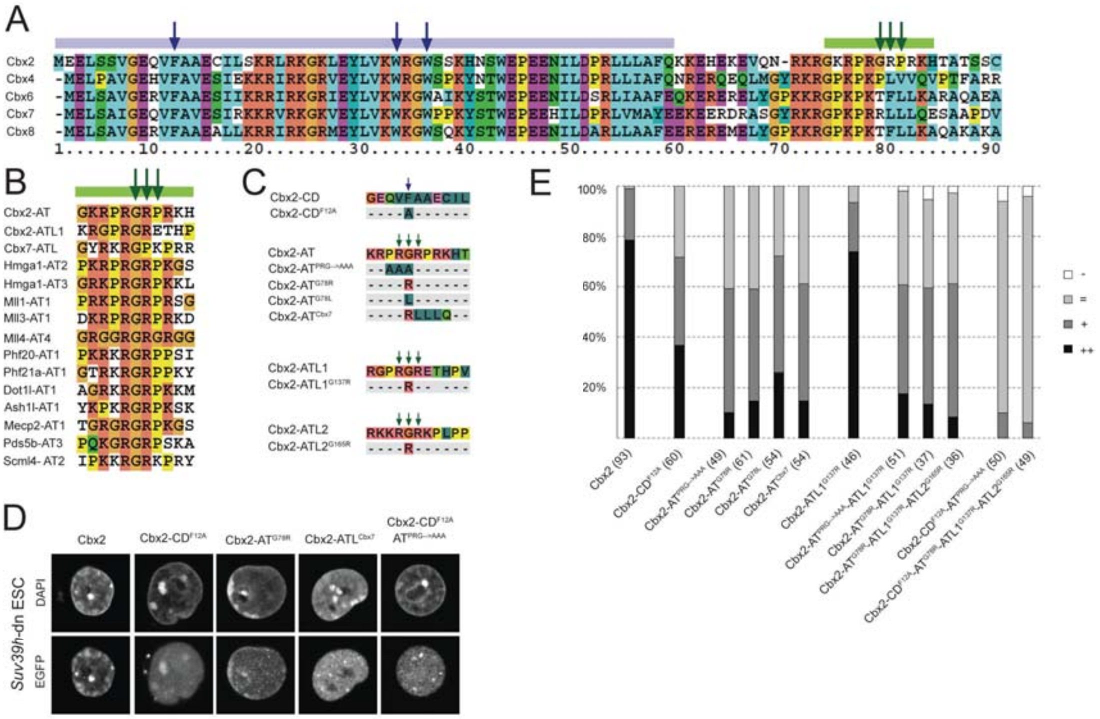

Figure 3.2: Cbx2 targeting to heterochromatin in *Suv39h* dn ESC depends on its chromodomain and first AT-hook. A. Alignment of the first 90 amino acids of the five mouse Pc homologs. The blue line highlights the N-terminal chromodomain. Blue arrows indicate the aromatic caging residues required for methyl-lysine binding. The Cbx2 AT-hook 1 is marked by a green line. Green arrows indicate the central RGR core. **B.** Alignment of AT-hook motifs detected in various proteins. **C.** Point mutations introduced into the Cbx2 chromodomain and AT-hooks. Blue arrow indicates the caging residues, green arrows highlight the central RGR core of the AT-hooks 1, 2 and 3. **D.** Selection of overexpressed Cbx2 mutation constructs in Suv39h-dn ESC. DAPI and direct GFP signals are shown for a representative cell. **E.** Quantification of heterochromatin enrichment in Suv39h-dn ESC for each construct.

Cbx2 targeting to eu- and heterochromatin in zygotes

In order to test the importance of the CD and AT-hook domains for Cbx2 targeting to heterochromatin in pre-implantation embryos, we micro-injected mRNA of various Cbx2-EGFP reporter constructs into early mouse zygotes shortly after fertilization. We subsequently cultured these zygotes until the stage just prior to the first cleavage division (pro-nuclear stage 5; PN5) and scored enrichment of the Cbx2-EGFP reporters at PCH sequences of the paternal genome. Full length Cbx2-EGFP was strongly enriched at paternal PCH, like the endogenous protein (Figure 3.3.A). Unlike in *Suv39h* dn ESCs, the F12A point mutation in the CD did not impair localization to PCH, suggesting a greater contribution of the AT-hook to PCH binding in zygotes. This finding is consistent with the reported *Ezh2*-independent targeting of matPRC1 to paternal PCH (Figure 3.3.A) (Puschendorf et al., 2008). Indeed, Cbx2-EGFP remains strongly enriched at paternal PCH in *Ezh2* maternally deficient (*Ezh2*$^{m\text{-}z+}$) zygotes in which H3K27me3 fails to be established on the paternal PN due to absence of the maternally provided enzyme (Figure 3.3.B).

On the other hand, the G78R mutation in the AT-hook reduces paternal PCH enrichment in wt zygotes (Figure 3.3.A), but to a lesser extent than observed in *Suv39h* dn ESC (Figure 3.3.B). This possibly hints to a stronger compensatory back-up mechanism provided by the CD binding to H327me3 that is not revealed by the F12A mutant alone. To test this, we first analyzed the F12A-G78R double mutant in wild-type zygotes (Figure 3.3.A). Secondly, to circumvent potential negative effects of the two point mutations on protein stability, we tested the G78R construct in *Ezh2*$^{m\text{-}z+}$ zygotes lacking H3K27me3 at paternal PCH (Figure 3.3.B). In both cases we observed a dramatic decrease in EGFP reporter localization at paternal heterochromatin compared to control conditions. We conclude that the CD and AT-hook of Cbx2 are the major determinants of Cbx2 localization to PCH in mouse preimplantation embryos. Compared to *Suv39h* dn ESCs, either domain can compensate better for the deficiency of the other domain in mouse zygotes.

To assess the importance of the AT-hook in heterochromatin targeting without mutating its sequence, we aimed at interfering with its ability to interact with DNA. We therefore treated early zygotes and *Suv39h* dn ESCs with distamycin, a small compound that binds to the minor groove of DNA and that impairs binding of AT-hook containing proteins to AT-rich satellites in Drosophila (Susbielle et al., 2005). In decondensing sperm nuclei of just fertilized oocytes, heterochromatic localization of the endogenous matPRC1 components Cbx2 and Rnf2 was abrogated in a distamycin concentration depend manner (Figure 3.3.C). Likewise, exogenous Cbx2-EGFP was dislocalized from chromocenters of *Suv39h* dn ESCs while heterochromatic localization of H3K9me3 and HP1β was unaffected in wild type ESCs (Figure Supp 3.4). These data underscore the importance of the Cbx2 AT-hook in heterochromatic targeting of the matPRC1 complex *in vivo*.

To further rule out a contribution of RNA transcripts to the targeting of PRC1 to heterchromatin, we micro-injected RNaseA directly into the paternal PN. RT-PCR analysis of transcripts of housekeeping genes demonstrated activity of the injected RNaseA (Figure Supp 3.3). However, we did not observe loss of matPRC1 members from paternal PCH in RNase A injected zygotes (Figure Supp 3.3), excluding a major role for RNA in PCH targeting of matPRC1.

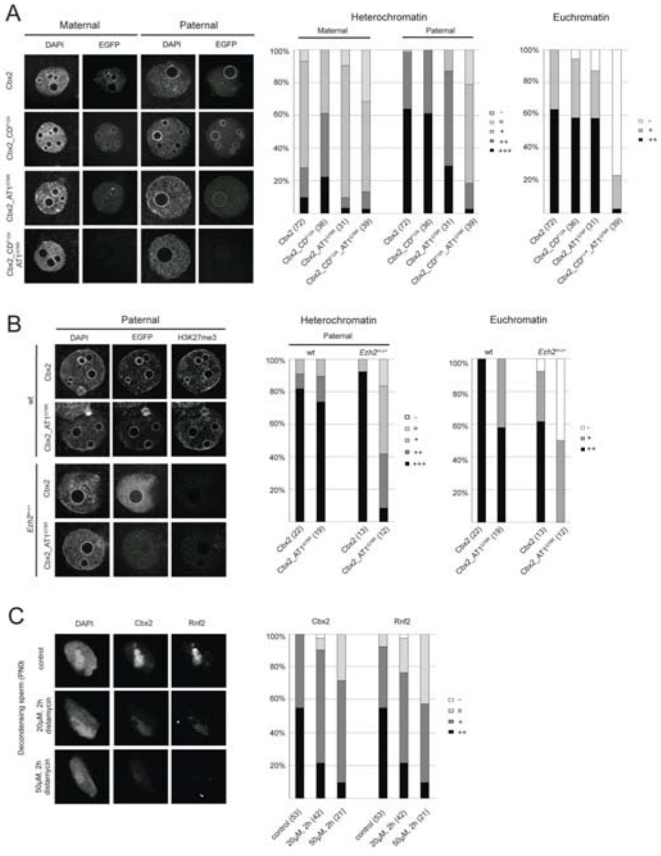
A
Maternal
Paternal
DAPI
EGFP
DAPI
EGFP
Cbx2
Cbx2_CD
Cbx2_AT1
Cbx2_CD AT1
Heterochromatin
Maternal
Paternal
100%
80%
60%
40%
20%
-
+
++
+++
Cbx2 (72)
Cbx2_CD (36)
Cbx2_AT1 (31)
Cbx2_CD_AT1 (39)
Euchromatin
B
Paternal
DAPI
EGFP
H3K27me3
wt
Ezh2
Cbx2
Cbx2_AT1
Heterochromatin
Paternal
wt
Ezh2
Euchromatin
Cbx2 (22)
Cbx2_AT1 (19)
Cbx2 (13)
Cbx2_AT1 (12)
C
DAPI
Cbx2
Rnf2
Decondensing sperm (PN0)
control
20μM, 2h distamycin
50μM, 2h distamycin
Cbx2
Rnf2
control (53)
20μM, 2h (42)
50μM, 2h (21)

Figure 3.3: Cbx2 targeting to heterochromatin in zygotes. A. Micro-injection of EGFP-tagged Cbx2 mutation constructs. Shown are representative maternal and paternal PN5 pronuclei for each construct. On the right, quantification of maternal and paternal PCH enrichment for each construct. On the far right, quanification of euchromatic EGFP-signal for each construct. **B.** Immunofluorescence analysis for Cbx2 and Rnf2 enrichment at heterochromatin in untreated and distamycin (20mM and 50mM) treated PN0 zygotes. Shown are representative decondensing spermheads. Below, quantification of Cbx2 and Rnf2 enrichment at heterochromatin. **C.** Micro-injection of EGFP tagged Cbx2 constructs into *Ezh1* deficient *and Ezh1/2* deficient zygotes. Shown are representative maternal and paternal PN5 pronuclei for both construct. Below left, quantification of paternal PCH enrichment; below right, quantificaiton of euchromatin signal.

Finally, unlike in *Suv39h* dn ES cells, Cbx2-EGFP containing the F12A and G78R point mutations failed to enrich at euchromatin of paternal pronculei in wild-type zygotes (Figure 3.3.A). Similarly, euchromatic staining was also lost for Cbx2-EGFP containing the G78R mutation in the AT-hook in *Ezh2*$^{m-z+}$ zygotes lacking H3K27me3 (Figure 3.3.B). In *Ezh2*$^{m-z+}$ zygotes the euchromatic localization pattern of Cbx2-EGFP appeared qualitatively less distinct than in wild- type control zygotes, arguing for a role of the CD - H3K27me3 interaction in specifying euchromatin binding (Figure 3.3.B).

Altogether, these data indicate that Cbx2 is targeted to pericentromeric heterochromatin of the paternal genome and to euchromatin in one-cell embryos by its AT-hook motif binding the minor groove of DNA and by its CD binding to H3K27me3, which is catalyzed *de novo* by the maternally provided Ezh2 protein.

The CD of Cbx2 regulates DNA binding of the AT-hook by integrating histone modification states

In wild-type ESCs, transiently overexpressed Cbx2-EGFP does not accumulate at chromocenters (Figures 3.1.A, 4.A). Surprisingly, Cbx2-EGFP containing the F12A mutation in its CD is enriched at PCH in wild type ESCs to a similar extent as in *Suv39h* dn ESCs (Figure 3.4.A). Combining the F12A and G78R mutations leads to a complete loss of PCH enrichment in wild-type ESCs indicating that the AT-hook mediates PCH enrichment of the Cbx2-CD^{F12A} protein in wt cells (Figure 3.4.A). To test whether the gain in PCH binding in wild-type ESCs is specifically due to the inability of the CD^{F12A} to bind methylated histones, we generated a CD-AT-EGFP reporter protein in which we mutated another residue (W33) that is also required for the formation of the “aromatic cage”, the histone methylation binding site of the CD. Indeed, we observed for the CD$^{Cbx2-W33A}$-AT^{Cbx2}-EGFP reporter a similar gain in PCH enrichment that was dependent on a functional AT-hook as we observed for the CD$^{Cbx2-F12A}$-AT^{Cbx2}-EGFP reporter in wt ESCs (Figure 3.4.B). Furthermore, we obtained a similar result in zygotes, where the F12A mutation leads to Cbx2-EGFP enrichment at maternal PCH in the presence of H3K9me3, H4K20me3 and HP1β (Figure 3.3.A). Together, these data show that the CD of Cbx2 prevents binding of the AT-hook to PCH defined by the *Suv39h* dependent pathway.

Based on these results, we wondered what mechanism underlies the inhibition of DNA binding of the AT-hook by the CD of Cbx2. Phylogenetic studies indicate that the 15 amino acid linker sequence between the CD and AT in Cbx2 homologs is partly conserved from fish to human. Based on this notion we hypothesize that the CD and AT-hook function as one molecular unit in which DNA binding of the AT-hook is determined by the CD integrating the status of chromatin at neighboring nucleosomes. While the *Suv39h*-dependent state characterized by the presence of H3K9me3, H4K20me3 and Hp1 proteins is inhibitory, nucleosomes carrying H3K27me3 or none of the three modifications are proficient states for DNA binding by the AT-hook of Cbx2. This model raises the questions whether the inhibitory capacity of CD^{Cbx2} is specific towards the AT-hook of Cbx2, whether it depends on the length of the linker sequence and whether it is specific to the CD of Cbx2. Furthermore, it asks what molecular mechanism underlies this inhibition of DNA binding by the *Suv39h* dependent chromatin state? Is it histone methylation and/or HP1 proteins?

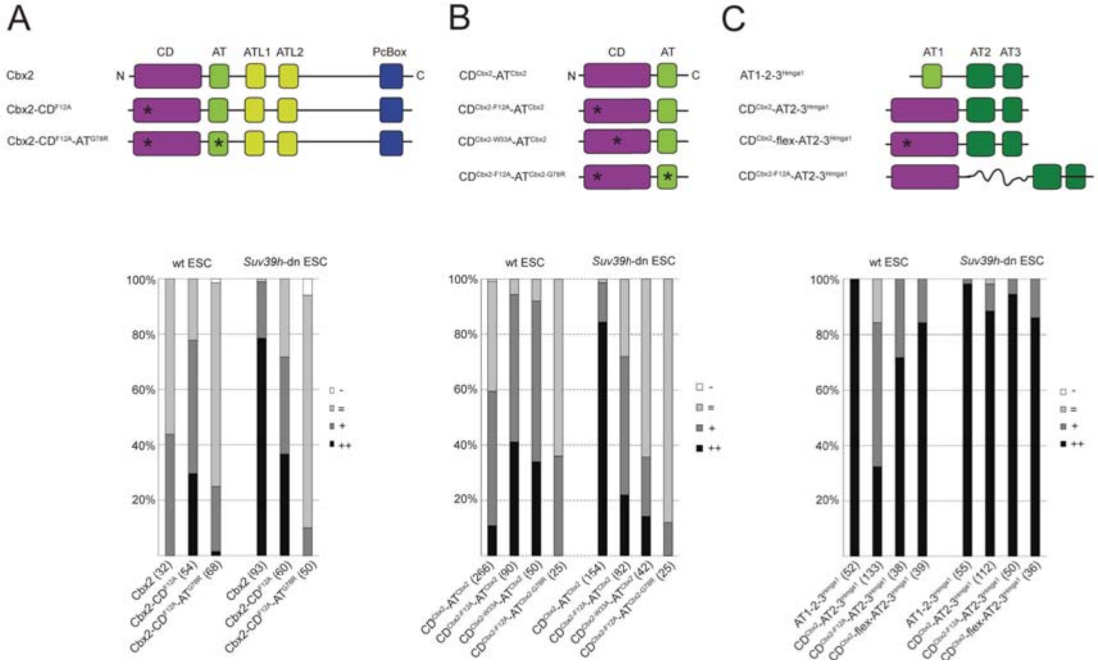

Figure 3.4: The Cbx2 chromodomain blocks PCH accumulation in wt ESC. A. Schematic representation of the Cbx2 full length constructs. Quantification of heterochromatin enrichment in wt and *Suv39h* dn ESC. B. Schematic representation of the Cbx2 reporter constructs and quantification of heterochromatin enrichment in wt and *Suv39h* dn ESC. **C.** Schematic representation of the Cbx2-Hmga fusion constructs analyzed and quantification of heterochromatin enrichment in wt and *Suv39h* dn ESC. Asteriks indicate the location of the inserted mutation.

$\mathrm{CD}^{\mathrm{Cbx2}}$ and $\mathrm{AT}^{\mathrm{Cbx2}}$ function as one molecular unit

To investigate whether or not the $\mathrm{CD}^{\mathrm{Cbx2}}$ modulates DNA binding of more potent AT-hook motifs, we linked it to the AT-hooks number 2 and 3 of HMGA1, which have been described to have high affinity to DNA (Reeves, 2001). While HMGA1-EGFP itself strongly localized to heterochromatin in wild-type conditions, as reported before (Amirand et al., 1998; Martelli et al., 1998), the CD of Cbx2 reduced heterochromatin localization of the $\mathrm{CD}^{\mathrm{Cbx2}}$-$\mathrm{AT2/3}^{\mathrm{HMGA1}}$-EGFP reporter in wild-type but not in *Suv39h* dn ESCs (Figure 3.4.C). As for the $\mathrm{CD}^{\mathrm{Cbx2\text{-}F12A}}$-$\mathrm{AT}^{\mathrm{Cbx2}}$ reporter (Figure 3.4.B), the F12A mutation restored localization of the $\mathrm{CD}^{\mathrm{Cbx2\text{-}F12A}}$-$\mathrm{AT2/3}^{\mathrm{HMGA1}}$-EGFP reporter to chromocenters in wild-type ESCs (Figure 3.4.C). These results indicate that the CD of Cbx2 effectively inhibits binding of neighboring AT-hooks to DNA in the context of a *Suv39h* dependent chromatin configuration.

To test whether this inhibitory effect is alleviated by spatial separation of the CD and AT-hooks, we replaced the linker sequence by a 30 amino acid long flexible linker (ten ‘TGS’ repeats). We observed a similar gain in heterochromatin localization for the $\mathrm{CD}^{\mathrm{Cbx2}}$-flex-$\mathrm{AT2/3}^{\mathrm{HMGA1}}$-EGFP as for the $\mathrm{CD}^{\mathrm{Cbx2\text{-}F12A}}$-$\mathrm{AT2/3}^{\mathrm{HMGA1}}$-EGFP reporter in wild type ESCs (Figure 3.4.C). Together, these data support the model in which the CD and AT-hook in Cbx2 function as one molecular entity that integrates the chromatin state for DNA binding.

The CDs of Cbx4 and Cbx7 lack chromatin sensing ability

Next we addressed whether the inhibitory effect of $\mathrm{CD}^{\mathrm{Cbx2}}$ is conserved among Cbx2 orthologs. The CDs of these orthologs and of the *Drosophila* PC exhibit different binding affinities for H3K9me3 and H3K27me3 (Bernstein et al., 2006; Kaustov et al., 2011). While $\mathrm{CD}^{\mathrm{Cbx2}}$ and $\mathrm{CD}^{\mathrm{dPC}}$ bind to H3K27me3 only, the CDs of Cbx4 and Cbx7 bind with intermediate K_ds to histone peptides tri-methylated at H3K9 and H3K27 (Kaustov et al., 2011). These H3K9me3 affinities are, however, at least one order of magnitude higher than those of the CDs of HP1 proteins (Bernstein et al., 2006; Kaustov et al., 2011). Consistently, we failed to detect Cbx4 and Cbx7 at PCH in wild-type ESCs while HP1α and HP1β were detectable (data not shown). Given these K_d values, we hypothesized that linking $\mathrm{CD}^{\mathrm{Cbx4}}$ or $\mathrm{CD}^{\mathrm{Cbx7}}$ to $\mathrm{AT}^{\mathrm{Cbx2}}$ would enable localization to chromocenters in wild-type ESC. In agreement, we observed strong PCH enrichment of $\mathrm{CD}^{\mathrm{Cbx4}}$- $\mathrm{AT}^{\mathrm{Cbx2}}$-EGFP and $\mathrm{CD}^{\mathrm{Cbx7}}$-$\mathrm{AT}^{\mathrm{Cbx2}}$-EGFP. Furthermore, the chimaeric $\mathrm{CD}^{\mathrm{dPC}}$ -$\mathrm{AT}^{\mathrm{Cbx2}}$-EGFP was significantly less frequently localized to PCH in wild-type ESCs (Figure 3.5.A). Together, these data suggest that the DNA binding capacity of the Cbx2 AT hook motif depends on the relative affinity of the adjacent CD for H3K27me3 versus H3K9me3.

Alanine 14 defines the histone methylation binding and chromatin targeting specificity of Cbx2

To prove this hypothesis, we aimed at increasing the affinity of CD^{Cbx2} for H3K9me3 by changing one or more of its amino acids and assessing the level of PCH enrichment in wt ESCs. Sequence comparison of CDs of mammalian Cbx and Suv39h proteins revealed several amino acid variations between classes of proteins with different histone methylation binding affinities (Figure 3.5.B). However, analysis of crystal structures of all CBX CDs (Kaustov et al., 2011) indicate that most variant amino acids are not in contact with the H3 N-terminus and may therefore not be critical for direct recognition of methylated residues. A few residues though, which are located within the hydrophobic cavity that embraces the methylated H3 tail, differ between the CDs of Cbx2 and Cbx4/Cbx7 (Figure 3.5.B). Particularly residue 14 (Cbx2 nomenclature), which is located C-terminally of the F12 “aromatic cage” residue in a highly conserved region, caught our interest. This residue is an alanine in the CDs of Cbx2, Cbx6, Cbx8 and dPC, while it is a valine in the CDs of Cbx4 and Cbx7, as well as in the CDs of the mammalians Hp1 isoforms, dHP1 and the Suv39h HMTs (Figure 3.5.B). In light of our PCH localization data (Figure 3.5.A), this residue may play a key role in specifying binding to H3K27me3 or H3K9me3.

In agreement, the A14V point mutation revealed strong enrichment of the CD^{Cbx2_A14V}-AT^{Cbx2}-EGFP reporter at chromocenters in wild-type ESCs, supporting the notion that $Cbx2^{A14}$ confers binding specificity towards H3K27me3 (Figure 3.5.C). Interestingly, as for Cbx2, the A14V mutation within the CD^{dPC}-AT^{Cbx2}-EGFP construct resulted in significant enrichment at chromocenters in wt ESCs, indicating functional conservation of that residue in fly PC (Figure 3.5.C). Inversely, replacing the valine of CD^{Cbx4} and CD^{Cbx7} by an alanine (V13A) caused reduction in chromocenter enrichment of wild-type ESCs (Figure 3.5.C). Finally, to assess the *in vivo* relevance of A14 in modulating chromatin binding, mRNA encoding Cbx2 or Cbx2-CD^{A14V} was micro-injected into mouse zygotes. As in ESCs, the Cbx2-CD^{A14V} construct was significantly enriched at maternal PCH in comparison to the Cbx2 construct (Figure 3.5.D).

Based on these cellular results, we measured the K_ds between methylated histone peptides and Cbx2, Cbx4 and Cbx7 CD constructs containing an alanine or valine at positions 14 or 13 (Figure 3.5.E). For Cbx2, the A14V mutation decreased the K_d for H3K9me3 while leaving its K_d for H3K27me3 intact. In contrast, V13A in Cbx4 and Cbx7 results in a strong increase in K_d values for H3K9me3 and H3K27me3.

In summary, alanine 14 in Cbx2 plays a crucial role in specifying binding of Cbx2 to H3K27me3, and to constitutive heterochromatin in mouse ESCs and early embryos. By enhancing the binding affinity of CD^{Cbx2} for H3K9me3 using the A14V mutation, Cbx2 localizes to maternal PCH and to chromocenters in wt ESCs, marked by components of the Suv39h pathway like H3K9me3, H4K20me3 and HP1 proteins.

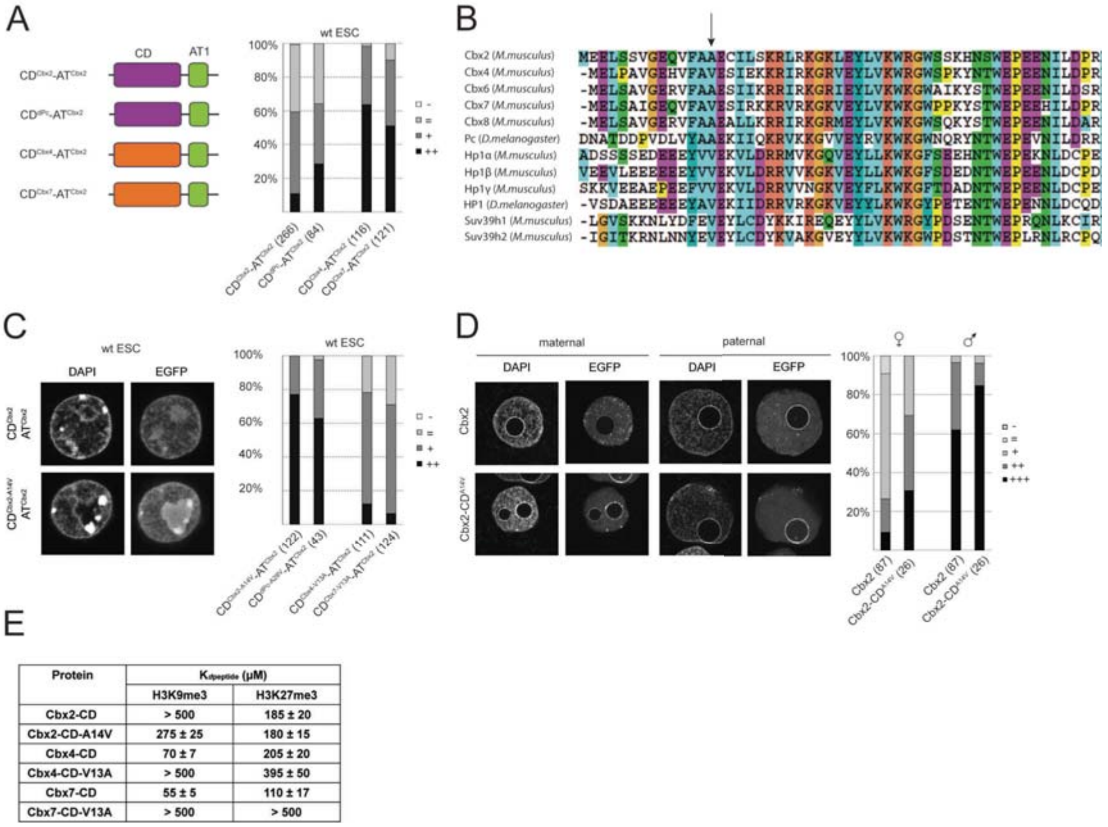

Protein	$K_{d peptide}$ (µM)	
	H3K9me3	H3K27me3
Cbx2-CD	> 500	185 ± 20
Cbx2-CD-A14V	275 ± 25	180 ± 15
Cbx4-CD	70 ± 7	205 ± 20
Cbx4-CD-V13A	> 500	395 ± 50
Cbx7-CD	55 ± 5	110 ± 17
Cbx7-CD-V13A	> 500	> 500

Figure 3.5: The Cbx2_A14V mutation enhances H3K9me3 binding affinity and gets targeted to wt ESC and maternal PCH. A. Schematic representation of fusion reporter construct. Right: quantification of heterochromatin enrichment for the indicated reporter constructs. **B.** Alignment of the CD of PC and its mouse homologues as well as HP1 and its mouse homologues, together with the CDs from the Suv39h methyltransferases. **C.** Representative IF staining for the Cbx2_CD_A14V_AT1 reporter construct in wt ESC. Right: quantification of heterochromatin enrichment for the indicated constructs. **D.** Repre-sentative IF staining for the Cbx2_CD_A14V_AT1 reporter construct in wt PN5 zygotes. Right: quantification of heterochromatin enrichment for this construct. **E.** Dissociation constant values (K_d) measured by fluorescence polarization for CD from Cbx proteins with methylated peptides and their mutants are shown. Interactions were designated as >500 uM when the values were too weak to accurately estimate a K_d value.

Hp1β but not Suv4-20h HMTs prevents PRC1 binding to maternal PCH in zygotes

To investigate which component in the *Suv39h* pathway prevents PRC1 members from binding to PCH in wild-type ESCs and at maternal chromosomes in zygotes, ESC or zygotes deficient for the downstream members of the *Suv39h* pathway were analyzed. In mammals, the Suv4-20 HMTs mediate H4K20me2 and H4K20me3 at euchromatin and at PCH (Schotta et al., 2004). In early pre-implantations embryos, changes in PCH associated H4K20me3 levels suggest that these enzymes are not active in early embryos. Nonetheless, maternal PCH in zygotes is marked by H4K20me3 that is presumably inherited from oocytes (Figure 3.6.B). Thus, this modification and/or downstream binding factors could, in principle, prevent PRC1 binding to maternal PCH. To test this model, *Suv4-20* dn ESCs, which lack H4K20me3 but still contain H3K9me3 and HP1 proteins at chromocenters, were transiently transfected with Cbx2-EGFP. Like in wt ESCs, no enrichment of recombinant Cbx2 at chromocenters in *Suv4-20* dn ESCs was observed (Figure Supp. 3.5). This indicates that neither the Suv4-20 HMTs nor H4K20me3 or any downstream acting factor prevent PRC1 binding to heterochromatin.

Next, the role of Hp1 proteins, acting upstream of the Suv4-20h HMTs and downstream of the Suv39h HMTs, were tested in respect to PRC1 heterochromatin binding. In mouse, three Hp1 orthologs are expressed in most cell types including ESCs. Chromocenters are predominantly marked by Hp1α (Cbx5) and Hp1β (Cbx1), but not by Hp1γ (Cbx3). In mouse zygotes, Hp1β enrichment at maternal PCH that is dependent on *Suv39h2* expression in oocytes is observed. It correlates with H3K9me3 enrichment at maternal PCH (Figure Supp. 3.5) (Puschendorf et al., 2008). Hp1β localization at euchromatin of both pronuclei is independent of Suv39h2 activity in oocytes. We failed to detect Hp1α by IF in zygotes while Hp1γ displayed weak euchromatic staining (Figure 3.6.B). Given that only Hp1β is localized to maternal PCH, mice that are conditionally deficient for *Hp1β* during oogenesis and lack the maternal protein during pre-implantation development were generated. In such *Hp1β* maternally deficient (*Hp1β*$^{m\text{-}z+}$ or *Cbx1*$^{m\text{-}z+}$) zygotes, neither Hp1α nor Hp1γ were significantly up-regulated (Figure 3.6.B). Furthermore, H3K9me3 was still enriched at maternal PCH like in wt zygotes while H4K20me3 levels were slightly reduced (Figure 3.6.B). Subsequently, *Hp1β*$^{m\text{-}z+}$ zygotes were stained for Rnf2, Cbx2 and Bmi1, the core components of the matPRC1 complex (Puschendorf et al., 2008). Strong enrichments for all three members on maternal and paternal PCH were observed in absence of Hp1β protein (Figure 3.6.C).

Together, these data demonstrate that matPRC1 binds to maternal PCH in the presence of H3K9me3 and H4K20me3. In wild-type mouse zygotes, Hp1β prevents matPRC1 from binding to maternal PCH, presumably by binding to H3K9me3 and inhibiting Cbx2 binding to major satellite DNA sequences.

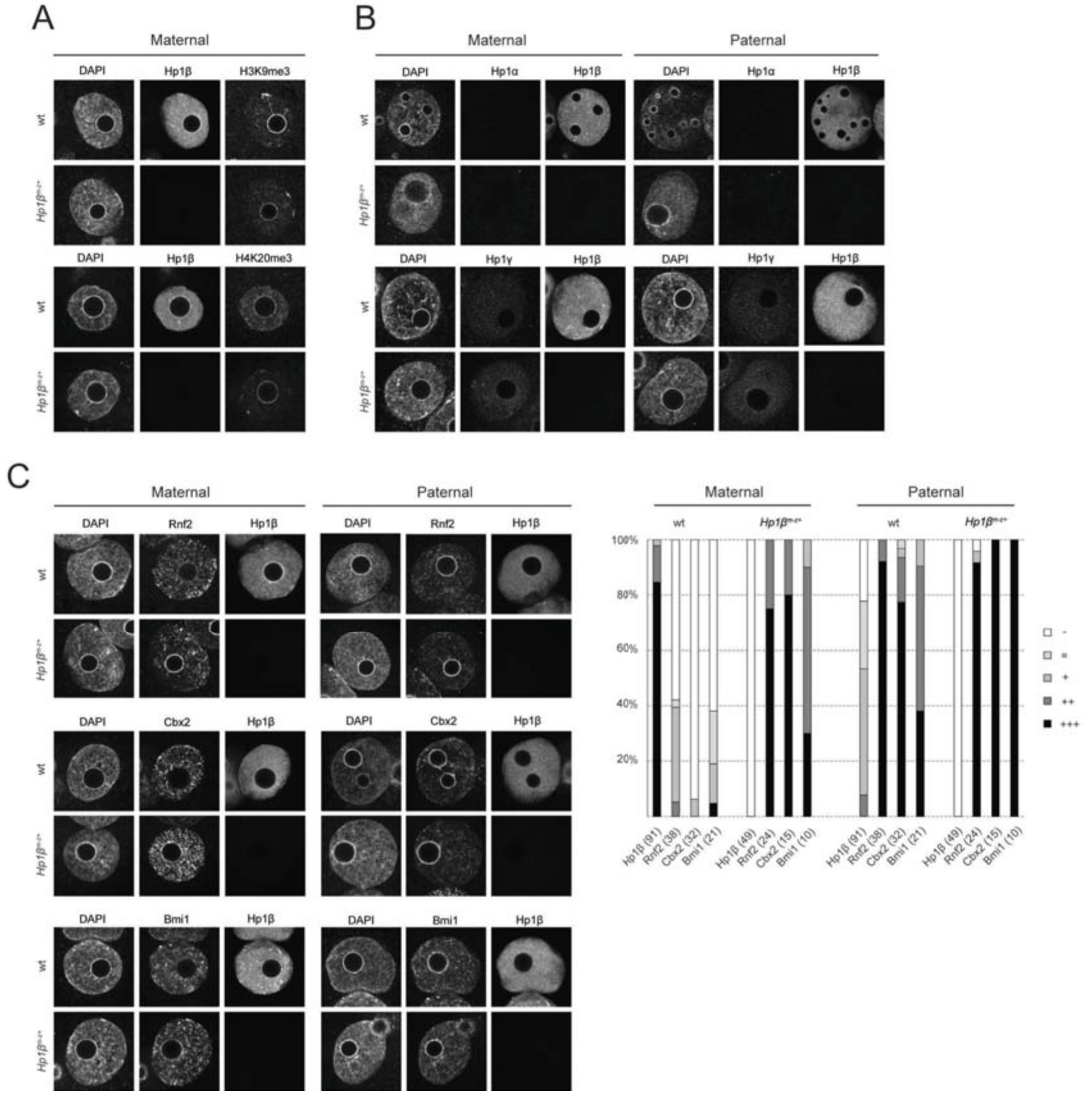
A
Maternal
DAPI
Hp1β
H3K9me3
wt
Hp1β^m-z+
DAPI
Hp1β
H4K20me3
wt
Hp1β^m-z+
B
Maternal
Paternal
DAPI
Hp1α
Hp1β
DAPI
Hp1α
Hp1β
wt
Hp1β^m-z+
DAPI
Hp1γ
Hp1β
DAPI
Hp1γ
Hp1β
wt
Hp1β^m-z+
C
Maternal
Paternal
DAPI
Rnf2
Hp1β
DAPI
Rnf2
Hp1β
wt
Hp1β^m-z+
DAPI
Cbx2
Hp1β
DAPI
Cbx2
Hp1β
wt
Hp1β^m-z+
DAPI
Bmi1
Hp1β
DAPI
Bmi1
Hp1β
wt
Hp1β^m-z+
Maternal
Paternal
wt
Hp1β^m-z+
wt
Hp1β^m-z+
100%
80%
60%
40%
20%
-
=
+
++
+++
Hp1β (91)
Rnf2 (38)
Cbx2 (32)
Bmi1 (21)
Hp1β (49)
Rnf2 (24)
Cbx2 (15)
Bmi1 (10)
Hp1β (91)
Rnf2 (38)
Cbx2 (32)
Bmi1 (21)
Hp1β (49)
Rnf2 (24)
Cbx2 (15)
Bmi1 (10)

Figure 3.6: PRC1 localizes to maternal PCH in *Hp1β* maternally deficent zygotes. A. Immunofluorescence analysis for the presence of maternal histone marks in wt and *Hp1β*$^{m-z+}$ zygotes, in respect to PRC1 localization. **B.** Immuno-fluorescence analysis of wt and *Hp1β*$^{m-z+}$ PN5 zygotes for the three mammalian Hp1 isoforms. **C.** Immunofluorescence analysis of wt and *Hp1β*$^{m-z+}$ PN5 zygotes for Hp1 and PRC1 components.

DISCUSSION

In *Drosophila*, the core PRC1 complex consists of four subunits. In vertebrates, each of these proteins has multiple orthologs that are thought to serve different functions during development (Whitcomb et al., 2007). For example, the five mammalian orthologs of dPC are present in biochemically distinct PRC1-like complexes in human cell lines (Vandamme et al., 2011), which originate likely from variations in primary sequences of the different Cbx proteins (Senthilkumar and Mishra, 2009). All five orthologs contain N-terminally localized chromodomains that display different *in vitro* binding affinities for histone H3 peptides marked by H3K9me3 or H3K27me3 (Bernstein et al., 2006; Kaustov et al., 2011). These affinities are, however, at least one order of magnitude lower than those of mammalian and fly Hp1 proteins or dPC (Bernstein et al., 2006; Fischle et al., 2003). Up to date, it is unknown whether the various Cbx proteins would target PRC1 complexes to distinct sets of targets genes in response to local histone methylation profiles.

Targeting of matPRC1: additive functions of the CD and AT-hook of Cbx2

By using EGFP-tagged Cbx proteins in embryonic stem cells and mouse pre-implantation embryos, we show here that Cbx2 mediates binding of the matPRC1 complex to constitutive heterochromatin in a parental specific manner. As proposed by Senthilkumar and Mishra (Senthilkumar and Mishra, 2009), we demonstrate that Cbx2 is a protein with two functional chromatin reader domains, the CD and the closely neighboring AT-hook, that are sufficient for targeting to paternal heterochromatin. By combining mutation analysis of the CD and AT-hook with *Ezh2* maternal deficiency we are the first to demonstrate the importance of the specific interaction between the CD and H3K27me3 for chromatin binding and localization of Cbx2 at euchromatin and PCH *in vivo*. The observed H3K27me3 selectivity is consistent with *in vitro* binding specificity reported previously (Bernstein et al., 2006; Kaustov et al., 2011). Likewise, mutations analysis and competition experiments with distamycin indicate that the AT-hook of Cbx2 mediates direct binding to the minor groove of AT-rich DNA.

Cbx2 is unique among Cbx proteins of the PcG family in having two reader domains. It allows the protein to bind to constitutive PCH regions that is composed of AT-rich major satellite sequences and marked by H3K27me3, as observed at paternal chromosomes in early embryos and in *Suv39h* dn ESCs (Peters et al., 2003; Puschendorf et al., 2008). In contrast, the CDs of

Cbx4 and Cbx7 proteins which display moderate binding affinities to H3K9me3 and H3K27me3 (Bernstein et al., 2006; Kaustov et al., 2011) do not direct binding to PCH, neither in wild type nor *Suv39h* dn ESCs. Addition of the AT-hook of Cbx2, however, resulted in efficient targeting of the chimaeric reporter to PCH in wild-type cells, arguing that only the combination of these CDs and the AT-hook provides the protein sufficient affinity to compete with Hp1 proteins for binding to H3K9me3-labeled major satellites.

Chromatin sensing by the CD/AT-hook module

It is increasingly recognized that chromatin proteins or complexes are bound to chromatin through multiple (weak) interactions with identical or different posttranslational modifications on histones and sometime directly with DNA (Ruthenburg et al., 2011; Yun et al., 2011). The CD/AT-hook double reader module of Cbx2 is particularly interesting since it harbors an intrinsic ability to promote binding under H3K27me3 conditions while inhibiting binding under H3K9me3/Hp1 conditions. Our linker insertion experiments suggest that the short peptide linker between the two domains is critical for the inhibitory function (Figure 3.4). We propose that the two reader domains actually function as one molecular unit assessing the local histone methylation and Hp1 state for binding.

Evolutionary conservation

In zygotes, the CD and AT-hook are together required for proper targeting of Cbx2 to euchromatin (Figure 3.3). These data suggest that both modules are important for proper PRC1 mediated gene repression during pre-implantation development. Supporting a gene regulatory function is the notion that the CD and the AT-hook motif are conserved between Cbx2 homologs among vertebrates. Interestingly, all Cbx2 orthologs contain at least one AT-hook like motif that is moderately conserved among vertebrates (data not shown) supporting the idea that AT-hook sequence arose prior to gene duplication and speciation. Additionally, the exon-exon organization as well as the distance between the CD and the AT-hook in Cbx2 is conserved from zebrafish to men (data not shown). Finally, the A14 and V13 amino acids in mammalian Cbx2, respectively Cbx4 and Cbx7 proteins that are critical for histone methylation binding specificity are evolutionary conserved. Together, these data suggest that Cbx2 acquired early during evolution the ability to sense chromatin states, placing Cbx2/PRC1 complexes functionally subordinate to the Suv3h/Hp1 pathway.

Exceptions to this rule are bilateral animals such as *Drosophila* in which the AT-hook is absent (data not shown). The loss of the AT hook in dPC is likely compensated by the increased affinity of the CD for H3K27me3 (Fischle et al., 2003). The absence of the AT-hook suggests that the molecular hierarchy as observed in mouse is non-functional in *Drosophila*. Furthermore, the multiple gene duplications of Cbx genes within vertebrates point to a more diverse mode of gene regulation by distinct PRC1 complexes in these organisms.

Transcriptional regulatory functions

In mouse, Cbx2 is predominantly expressed in oocytes and in early pre-implantation embryos while Cbx7 and other Cbx proteins are more highly expressed later during development in a tissue specific manner (Wu et al., 2009; Zeng et al., 2004). Cbx2 is similarly expressed during early development of zebrafish (Kawamura et al., 2002). In mouse early embryos, matPRC1 is initially preferentially localized to the paternal genome. This asymmetric labeling correlates with the absence of H3K9me2 and H3K9me3. At later stages, however, the parental asymmetry in H3K9me2/3 states is resolved and the paternal matPRC1 specific labeling as well. Given the matPRC1 mediated repression of major satellite sequences specifically at the paternal genome (Puschendorf et al., 2008), the fluorescence labeling data may indicate an early role for H3K9 specific HMTs and PRC1 complexes in regulating parental specific gene repression.

Recently, it was shown that repressed somatic lineage regulators like Hox, Gata and Sox factors that carry bivalent chromatin modifications (like H3K4me2, H3K27me3 and Rnf2 occupancy) in ESCs are also marked by H3K4me2 and H3K27me3 in trophectodermal stem cells (TSCs). Nonetheless, Rnf2 was not enriched at these genes in TSCs. Instead, they were marked by Suv39h1-mediated H3K9me3 and DNA methylation (Alder et al., 2010). These data support a model in which cross talk between H3K9me3/Hp1 and PRC1 pathways may regulate gene specific repression in a lineage specific manner. Our current molecular understanding of this cross talk will direct future experiments addressing the role of both pathways in transcriptional regulation.

EXPERIMENTAL PROCEDURES

Constructs

Constructs for N-terminal enhanced GFP (EGFP) fusion proteins of Rnf2 and Phc2 in the EGFP-C2 backbone (BD Biosciences) were obtained from K. Isono, the 3Flag Bmi1 construct in the pCAGIPuro vector was obtained from M. Endoh. The C-terminally enhanced GFP fusion proteins of Cbx2, Cbx4, Cbx6, Cbx7, Cbx8 in the EGFP-N1 backbone (BD Biosciences) were obtained from E. Bernstein (Bernstein et al., 2006). Point mutation of the Cbx2 CD and AT-hooks were generated by site-directed mutagenesis. Approximately 25bp long primers containing the mutation in the centre were used for amplification with Phusion Taq (Finnzymes). The PCR reaction was digested with the methylation sensitive restriction enzyme Dpn1 (New England BioLabs) to remove the original construct and subsequently used for transformation. Successful mutagenesis was performed by sequencing. The Cbx2 truncation constructs were generated by PCR from the Cbx2-EGFP construct. For the Cbx4, Cbx7 CD fusion constructs with the Cbx2 AT-hook, a Pst1 site was introduced between the CD of Cbx2 and the Cbx2 AT-hook for cloning. The CDs of Cbx4 and Cbx7 were amplified by PCR. Hmga1 was cloned by PCR from NIH3T3 cDNA. For microinjection, the constructs were cloned into a pcDNA3.1-poly(A) vector kindly provided by K. Yamagata (Yamagata et al., 2005).

Antibodies

For immunofluorescence analysis the following antibodies were used: anti-GFP (Roche, 1:200), anti-flag-M2 (Sigma, 1:500), anti-M33 (Cbx2; Otte, 1:500), anti-Rnf2 (Koseki, 1:500), anti-Bmi1 (Upstate, 1:100), anti-Hp1α (Euromedex, 1:500), anti-Hp1β (Serotec, 1:500), Hp1γ (Euromedex, 1:500), anti-H3K9me3, anti-H3K27me3, and anti-H4K20me3 (Jenuwein, 1:500). The primary antibodies were used in combination with cross-absorbed Alexa 488-, 568-, or 633-coupled secondary antibodies (Molecular Probes).

Mice and Cell Lines

Zygotes used for microinjection experiments were obtained from CD1 mice, if not cited otherwise. Mice maternally deficient for *Ezh2* have been reported previously (Puschendorf). Mice conditionally ablated for Cbx1 were obtained by blastocyst aggregation using ESC generated by Eucomm. To produce maternally deficient *Hp1β* mice, *Cbx1*$^{F/F}$ mice that carried the *Zp3-cre* recombinase transgene were generated. Housing and handling of mice conformed to the Swiss Animal Protection Ordinance, chapter 1.

Wild-type, *Suv39h*-dn (Lehnertz et al., 2003; Peters et al., 2001) and *Suv4-20h*-dn (Schotta et al., 2004) ES cells were cultured in DMEM medium with 4.5g/l glucose (Gibco) containing 15% FCS (fetal calf serum, Chemicon), penicillin, streptomycin, 2mM L-glutamine, 0.1mM 2β-mercaptoethanol, non-essential amino acids and 1mM sodium pyruvate (Gibco). ES cells were transfected with fusion constructs using Lipofectamine 2000 (Invitrogen) and after approximately 16h were seeded on poly-L-lysine coated coverslips, fixed with PFA and mounted in Vectashield containing DAPI (Vector).

Collection, *in vitro* fertilization (IVF) and culture of mouse embryos

Mouse oocytes and embryos were derived from superovulated 5-10 week old females according to standard procedures (Hogan 1994). For IVF, females were injected with PMSG (5U, Intervet) and 48h later with hCG (5U each, Intervet). M-II oocytes were then collected 14h after hCG injection. Sperm was obtained from 10-16 week old control males. Capacitation was carried out in human tubular fluid (HTF) containing 7.5 mg/ml BSA for 2h. IVF was performed in HTF containing 7.5 mg/ml BSA for 2h. If not *in vitro* fertilized, CD1 mice were mated and zygotes were isolated from the ampullae. Thereafter, the embryos were cultured in KSOM medium plus amino acids (Chemicon) in a humidified atmosphere of 5% CO_2 until required. Zygotes were substaged according to morphology of pronuclei using criteria as defined previously (adenot 1997, santos 1997). In brief, PN0 refers to oocytes immediately after fertilization and PN5 refers to large central pronuclei. For distamycin treated PN0 zygotes, fertilization was performed in HTF containing 7.5 mg/ml BSA supplemented with 20μM Distamycin (Sigma, #D6135) for 2h.

Microinjection

For *in vitro* transcription the plasmids were linearized and the mMessage mMachine T7 kit (Ambion, AM1344) was used. The synthesized mRNA was diluted to the optimal concentration using nuclease-free water (Ambion, AM9937). 2-4 pl mRNA (100ng/μl) was microinjected into the cytoplasm of *in vitro* fertilized CD1 zygotes using the Eppendorf FemtoJet injector system. Zygotes were then cultured in KSOM medium plus amino acids (Chemicon) under a 5% CO2 atmosphere at 37ºC and fixed at late zygotic stages (PN5). For micro-injection of RNaseA, zygotes were isolated 20h after hCG injection from CD1 mice and further cultured in M2 medium until the late pronuclear stage (PN4/5, 26h after hCG). RNase A (Roche, #109169) was dissolved in TE buffer (pH 8.0) at 2 mg/ml. Approximately 5 pl of RNaseA were micro-injected into the paternal pronucleus. Control zygotes were injected with TE buffer into the paternal pronucleus. Following micro-injection, zygotes were cultured for further 15 min.

Immunofluorescence Staining

Before fixation of embryos, the zona pellucida was removed by incubation in acidic tyrode for 30 seconds. Embryos were washed twice in FHM, fixed for 15 min in 4% paraformaldehyde in PBS (pH 7.4) and permeabilized with 0.2% Triton-X 100 in PBS for 15 min at room temperature (RT). Fixed embryos were blocked at least 4 hours at RT in 0.1% Tween-20 in PBS containing 2% BSA and 5% normal goat serum, and were then incubated with primary antibodies in blocking solution overnight at 4ºC. Embryos were washed three times for 30 min in 0.1% Tween-20 in PBS containing 2% BSA before application of secondary antibodies for 1 h at RT followed by three washing steps for 30 min in 0.1% Tween-20 in PBS containing 2% BSA in the dark. Embryos were mounted in Vectashield containing DAPI (Vector).

ES cells were trypsinized and placed on poly-L-lysine coated coverslips for 10 min to attach. Cells were fixed with 2% paraformaldehyde in PBS (pH 7.4), permeabilized in 0.1% Triton-X100 in 0.1% sodium citrate and blocked for 30 min in 0.1% Tween-20 in PBS containing 2% BSA and 5% normal donkey serum at RT. Incubation with primary and secondary antibodies as well as mounting was performed as described above.

Microscopy and Image Analysis

Immunofluorescence stainings of embryos were analyzed using the laser scanning confocal microscopes LSM510 META (Zeiss; software: LSM Image Browser) and LSM700 (Zeiss; software: ZEN, 2009). One confocal slice through the maximal radius of each (pro-) nucleus was scanned. The images were projected using ImageJ. For numerical evaluation, all images of embryos and cells were analyzed individually and scored as follows: (-) no staining; (=) equal staining at heterochromatin and euchromatin; (+) weakly enriched; (++) clearly enriched; (+++) strongly enriched staining at heterochromatin versus euchromatin.

RNA isolation and RT-PCR

RNA was isolated from 15 embryos. The embryos were transferred into Trizol and 100ng of E.coli RNA was added to each sample as carrier. RNA was isolated according to the manufacturer's instructions. Briefly, reverse transcription was performed using random primers (200ng) and SuperScript II RNase H Reverse Transcriptase (Invitrogen). For PCR reactions, cDNA corresponding to 0.2 embryos was used as a template. 30 amplification cycles were performed using Taq DNA polymerase (Qiagen), PCR products were resolved on a 2% agarose gel and subsequently detected via SYBR green I staining (Molecular Probes; 1:10’000). Fluorescence was detected on a Typhoon 9400 scanner (Amersham Biosciences). The following primers and cycle numbers were used:

Actb: F: 5’-TGGGAATGGGTCAGAAGGACT, R: 5’-GGGTCATCTTTTCACGGTTGGC
Gapdh: F: 5’-AACAACCCCTTCATTGACCTC, R: 5’-TTCTGAGTGGCAGTGATGGC
Dap: F: 5’-GATCTATACGCAACCGGAACC, R: 5’-ACAAGAATTTCCGCAGTACCC

Fluorescence Polarization

Chromodomains of Cbx2 (9-66), Cbx4 (8-65) and Cbx7 (8-62) were amplified by PCR from the Mammalian Gene Collection clones and were subcloned into a modified pET28a-LIC vector. The recombinant proteins and their corresponding mutants were overexpressed as N-terminal His6-tagged proteins at RT using *E. coli* BL21 (DE3) Codon plus RIL (Stratagene) as a host organism. These expressed proteins were purified by Talon (BD) affinity chromatography under native conditions and eluted with buffer containing 500mM Imidazole followed by size exclusion chromatography using a HiLoad 26/60 Superdex-75 column (GE Healthcare). The proteins were monomeric in solution as determined by size exclusion chromatography. The final samples were prepared in buffer containing 20 mM Tris (pH 8), 250 mM NaCl, 1mM DTT, 1mM TCEP, 1 mM Benzamidine, 0.5 mM PMSF.

H3K9Me3 (ARTKQTARK(me3)STGGKA) and H3K27Me3 (QLATKAARK(me3)SAPATG) were synthesized, N-terminally labeled with fluorescein and purified by Tufts University Core Services (Boston, MA, USA). Binding assays were performed in 10 µl volume at a constant labeled peptide concentration of 40 nM, and Cbx protein concentrations at saturation ranging from 800 to 1300 µM in buffer containing 20 mM Tris pH 8.0, 250 mM NaCl, 1 mM DTT, 5mM BME (B-Mercaptoethanol), 1mM Benzamidine, 1 mM PMSF, 0.01% Tween-20. Fluorescence polarization assays were performed in 384 well plates using Synergy 2 microplate reader (BioTek, Vermont, USA). The excitation wavelength of 485nm and the emission wavelength of 528 nm were used. The data was corrected for background of the free labeled peptides. To determine K_d values, the data were fit to a hyperbolic function using Sigma Plot software (Systat Software, Inc., CA, USA). The K_d values represent averages ± standard errors for at least three independent experiments.

SUPPLEMENTAL INFORMATION

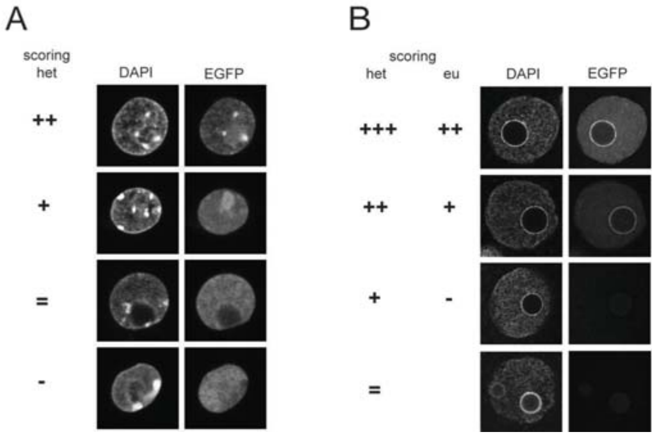

Figure Supp 3.1: Scoring of heterochromatin enrichment in chromocenters and in PCH. A. Scoring of heterochromatin enrichment in wt and Suv39h-dn ESC. ++: strong enrichment; +: weak; =: equally enriched as euchromatin; -: less enriched than euchromatin. **B.** Scoring of heterochromatin and euchromatin enrichment in zygotes. Shown are paternal PN5 pronuclei. Heterochromatin: +++: very strong, ++: strong; +: weak; =: equal to euchromatin; -: weaker than euchromatin (not observed). Euchromatin: ++: strong; +: weak; -: no signal.

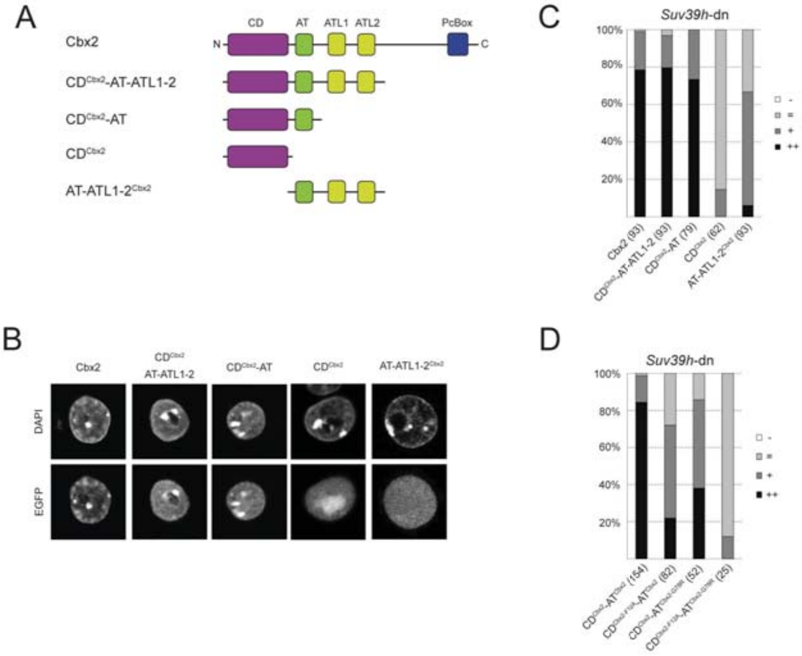

Figure Supp 3.2: The Cbx2 CD and AT-hook1 are sufficient for heterochromatin targeting. A. Schematic representation of the truncated Cbx2 constructs analysed. **B.** Representative IF pictures of transiently transfected *Suv39h* dn ESC with truncated constructs as indicated. **C.** Analysis of transiently transfected *Suv39h* dn ESC with truncated constructs as indicated. **D.** Analysis of transiently transfected *Suv39h* dn ESC for the Cbx2_CD_AT1 reporter construct.

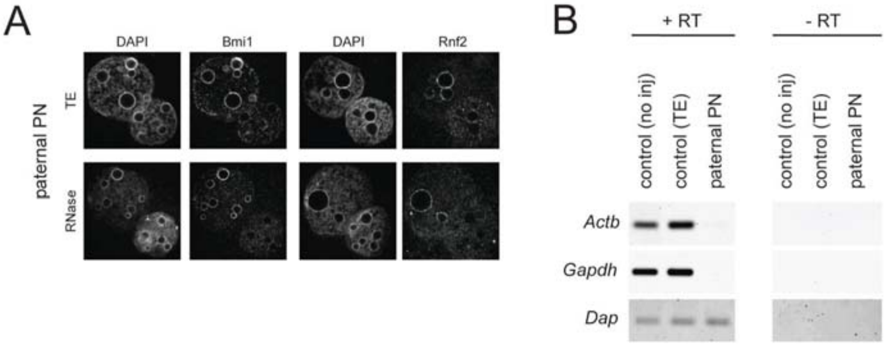
A
DAPI
Bmi1
DAPI
Rnf2
paternal PN
TE
RNase
B
+ RT
- RT
control (no inj)
control (TE)
paternal PN
control (no inj)
control (TE)
paternal PN
Actb
Gapdh
Dap

Figure Supp 3.3: PRC1 localization to paternal PCH is RNA-independent in zygotes. A. Immunofluorescence staining for PRC1 members in RNaseA microinjected zygotes. RNase A was injected into the paternal pronucleus. **B.** RT-PCR of control, TE- and RNaseA microinjected paternal pronuclei. Actb and Gapdh are strongly decreased following RNase treatment, whereas a spike control (Dap) remains unchanged.

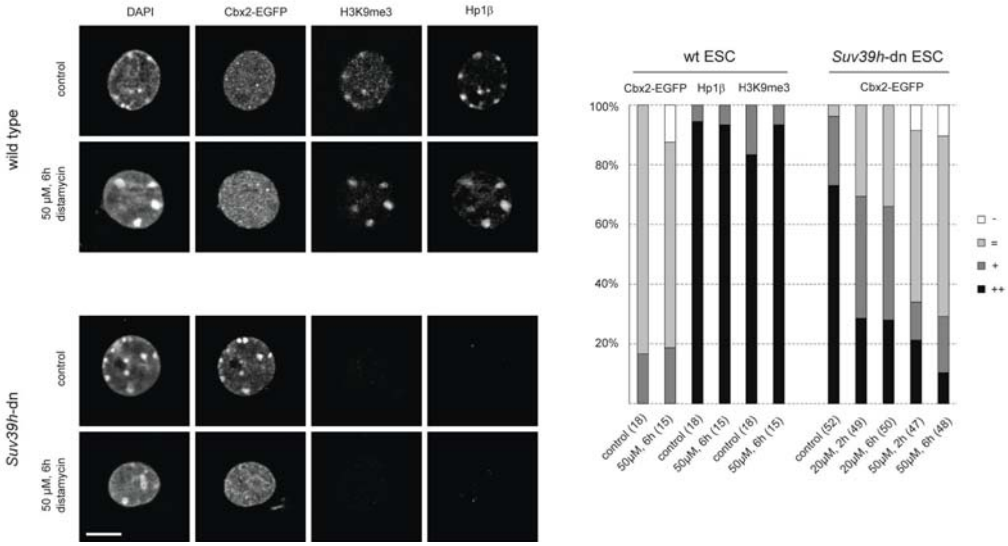

Figure Supp 3.4: Cbx2 enrichment in *Suv39h* dn ESC at chromocenters is sensitive to distamycin treatment. Top: Distamycin treatment of wt ESC does not affect chromocenter localization of H3K9me3 and Hp1β. Bottom: Distamycin treatment results in loss of Cbx2 enrichment at chromocenters in *Suv39h* dn ESC. Right: Data analysis of distamycin treated wt and *Suv39h* dn ESC.

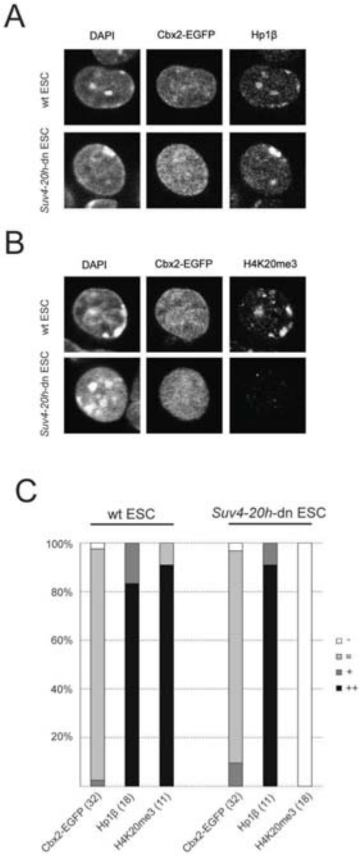
A
DAPI
Cbx2-EGFP
Hp1β
wt ESC
Suv4-20h-dn ESC
B
DAPI
Cbx2-EGFP
H4K20me3
wt ESC
Suv4-20h-dn ESC
C
wt ESC
Suv4-20h-dn ESC
100%
80%
60%
40%
20%
Cbx2-EGFP (32)
Hp1β (18)
H4K20me3 (11)
Cbx2-EGFP (32)
Hp1β (11)
H4K20me3 (18)
□ -
▨ =
▨ +
■ ++

Figure Supp 3.5: Suv4-20h methyltransferases do not block Cbx2 from binding to heterochromatin in ES cells. Top left: immunofluorescent analysis of wt ESC. Bottom left: immunofluorescent analysis of *Suv4-20h* dn ESC. Right: Scoring of Cbx2 heterochromatin enrichment in wt and *Suv4-20h* dn ESC.

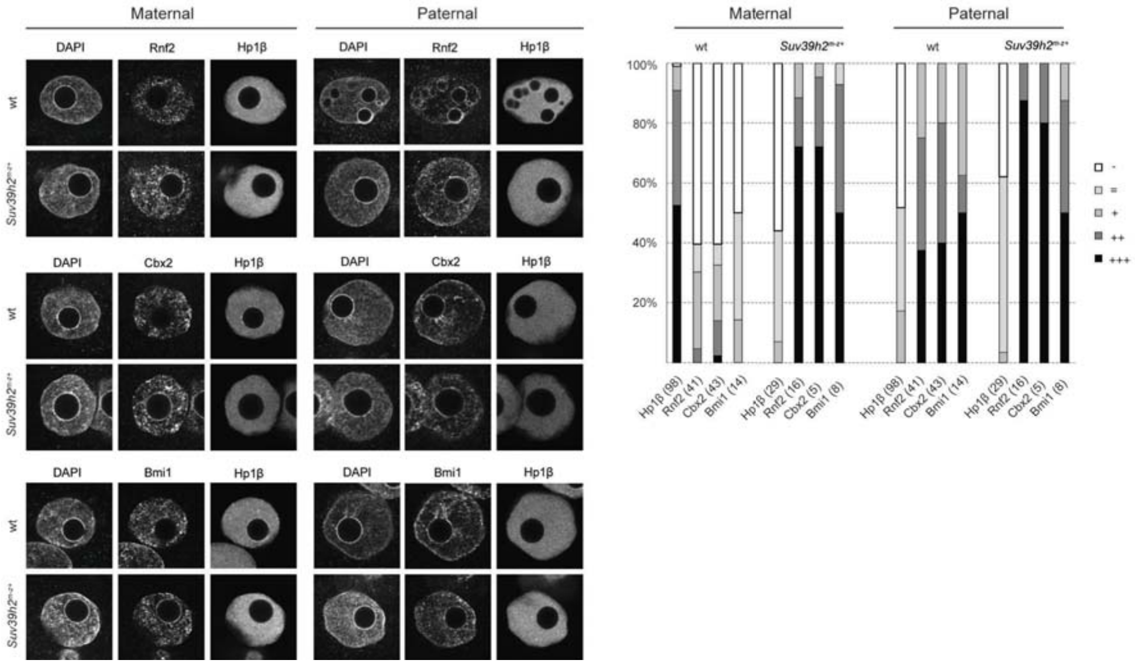
Maternal
Paternal
DAPI
Rnf2
Hp1β
Cbx2
Bmi1
wt
Suv39h2m-z+
100%
80%
60%
40%
20%
Hp1β (98)
Rnf2 (41)
Cbx2 (43)
Bmi1 (14)
Hp1β (29)
Rnf2 (16)
Cbx2 (5)
Bmi1 (8)
□ -
▨ =
▨ +
▨ ++
■ +++

Figure Supp. 3.6: PRC1 localizes to maternal PCH in *Suv39h2* maternally deficent zygotes. Left: Immunofluorescence analysis of wt and *Suv39h2*$^{m\text{-}z+}$ PN5 zygotes for the PRC1 members, Rnf2, Cbx2 and Bmi1 together with Hp1β. Right: analysis of wt and *Suv39h2*$^{m\text{-}z+}$ PN5 zygotes of Hp1 and PRC1 components.

ACKNOWLEDGMENTS

We thank A. Otte, H. Koseki and T. Jenuwein for providing antisera and K. Isono, M. Endoh, E. Bernstein and K. Yamagata for plasmids. We are grateful to B. Knowles for providing *Zp3-cre* transgenic mice. We acknowledge excellent assistance by F. Zilbermann and FMI colleagues L. Gelman (microscopy), Hans Ruedi Hotz (bioinformatics), B. Heller-Stilb and P. Kopp (animal facility).

AUTHOR CONTRIBUTIONS

R.K., M.A. and A.H.F.M.P. conceived and designed the experiment. R.K., M.A. and L.K. performed the experiments. S.H.O. provided Ezh2 floxed mice and G.S. provided *Suv4-20h* dn ESCs. R.K., M.A., L.K., C.A. and A.H.F.M.P. analyzed the data. R.K. and A.H.F.M.P. wrote the manuscript.

3.2. Additional Results

3.2.1. Additional Results: PRC1 targeting to constitutive heterochromatin and its dependency with the *Suv39h/Hp1β* pathway in mouse zygotes

3.2.1.1. FRAP of Cbx2 at Heterochromatin in Suv39h-dn ESC.

Rico Kunzmann and Laurent Gelman

Introduction

Dynamics of the Suv39h pathway proteins at heterochromatin have been analyzed in various cell types by FRAP experiments, as introduced in 2.2.2.2. One can conclude from these experiments, that the SET domains of the HMTs ensure stable binding. The Hp1 paralogs on the other hand are highly mobile, with only a small fraction of them exhibiting lower dynamics. Generally, these experiments show that the epigenetic heterochromatin state is dynamic. Based on these results, we wondered how dynamic PRC1, especially Cbx2, at heterochromatin is. Furthermore, we wanted to test to what extend the two targeting modules of Cbx2, the CD and the AT-hook motif, influence its dynamics at heterochromatin. To measure the targeting dynamics, we performed FRAP experiments in *Suv39h*-dn ESC overexpressing various Cbx2 constructs.

Results

The *Suv39h*-dn ESCs were transiently transfected with Cbx2-EGFP, Cbx2-CD^{F12A}-EGFP or Cbx2-AT^{G78R}-EGFP. After an incubation time of 24 hours, the EGFP enriched heterochromatin foci were bleached and the recovery time was measured (Figure 3.7.A.). The average half recovery time for full length EGFP tagged Cbx2 was measured to be 7 seconds (Figure 3.7.B). In comparison, half recovery time for Hp1 is measured between 2.5 – 4 seconds (Cheutin et al., 2003; Prasanth et al., 2010). Thus, the turnover of Cbx2 proteins at heterchromatic foci is slower than the turnover of Hp1 proteins. Nevertheless, in comparison to the dynamics of HMTs (half recovery time greater than 19 seconds (Krouwels et al., 2005; Souza et al., 2009)), Cbx2 can be considered to be dynamic at heterochromatin.

Furthermore, our results suggest the existence of three populations of Cbx2 proteins at heterochromatic foci. The first population consists of highly mobile Cbx2 proteins with half recovery times between 4 – 6 seconds (Figure 3.7.C.). The second population consists of a more stably bound fraction of Cbx2 proteins with half recovery times ranging from 13 to 20 seconds (Figure 3.7.C.). A third population of Cbx2 proteins is immobile. This is visualized by the plateau, which is reached 60 seconds after bleaching, just below 70 % of the initial intensity (Figure 3.7.B.). It suggests that up to 30 % of Cbx2-EGFP proteins remain bound to the bleached heterchromatic foci within this time frame.

Interestingly, FRAP analysis in *Suv39h*-dn ESC for constructs containing either a non-functional CD or a non-functional AT-hook revealed higher dynamics as well as overall higher recovery rate than full length Cbx2. Surprisingly, point mutations in both targeting modules of Cbx2 resulted in a similar reduction of half recovery times to 2 seconds in average and a recovery over 80 % after 60 seconds (Figure 3.7.B.). This suggests that both modules are similarly important for targeting dynamics of Cbx2. The individual half recovery times for these two constructs revealed one major population around 3 seconds (Figure 3.7.C.).

Discussion

Taken together, Cbx2 dynamics at heterochromatic foci of *Suv39h*-dn ESC is of high velocity. Interestingly, it is not as high as for the major population measured for the Hp1 isoforms. It suggests that Cbx2 is bound more stably to heterochromatic foci than Hp1. This is surprising, especially in light of the K_d measured for the CDs of Hp1 and Cbx2. Whereas the CD of Hp1 binds to H3K9me3 in the µM range, the CD of Cbx2 binds to H3K27me3 at least ten fold weaker. Therefore, the AT-hook motif of Cbx2 accounts for this lower dynamic. Upon insertion of a point mutation into the AT-hook motif of Cbx2, the velocity increases to a level comparable to Hp1 dynamics. Nevertheless, it does not fully reflect the K_d measurements, suggesting that there are additional factors that influence the dynamics of CD containing proteins at heterochromatin. Furthermore, the insertion of a point mutation into the CD also enhances the dynamics. Therefore, the two protein modules together account for the Cbx2 dynamics. This is in agreement with our analysis of Cbx2 constructs in fixed *Suv39h*-dn ESC.

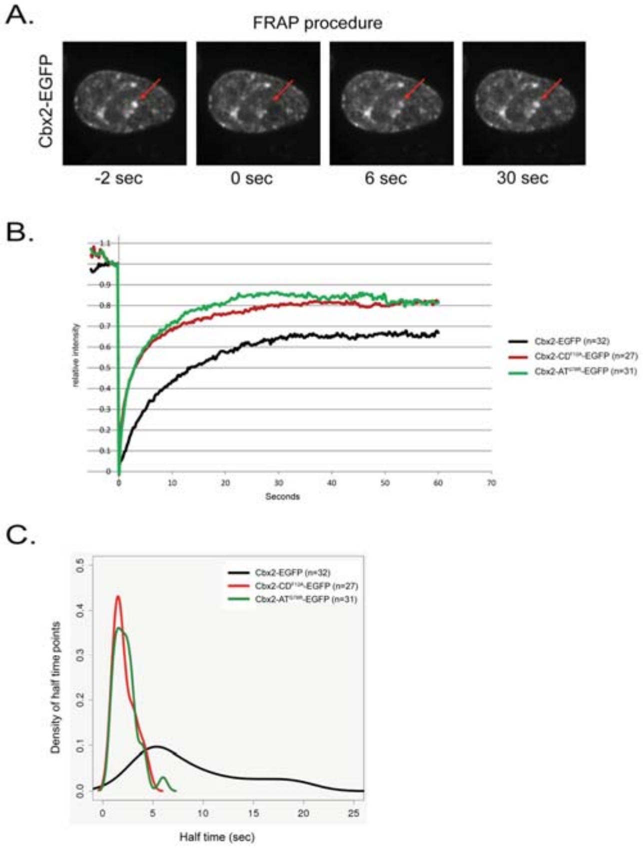

Figure 3.7: FRAP analysis of various Cbx2-EGFP constructs in *Suv39h*-dn ESC. A. Example of the experimental procedure. Distinct foci with high EGFP intensity were photobleached and recovery time was measured. **B.** Quantitative FRAP analysis for Cbx2-EGFP, Cbx2-CD^{F12A}-EGFP and Cbx2-AT^{G78R}-EGFP at heterochromatin in *Suv39h*-dn ESC over a period of 60 seconds. **C.** Representation of the half recovery time values for the individual measurments of Cbx2-EGFP, Cbx2-CD^{F12A}-EGFP and Cbx2-AT^{G78R}-EGFP at the photobleached foci.

A substantial amount of Cbx2-EGFP proteins at heterochromatic foci is less dynamic or even immobile. The detection of this immobile fraction is not simply due to technical issues, because the recovery rate Cbx2-CD^{F12A}-EGFP or Cbx2-AT^{G78R}-EGFP proteins from bleached foci is above 80 % after 60 seconds, whereas Cbx2-EGFP recovers only up to 70 %. Thus, this immobile fraction, as well as the heterochromatic foci displaying slow half recovery times, is Cbx2-EGFP specific. It depends on the two functional targeting modules. This immobile fraction might facilitate the targeting of other PRC1 members, whereas the more mobile fraction might not be PRC1 complex bound. Indeed, we never measured the ability of Cbx2-CD^{F12A}-EGFP or Cbx2-AT^{G78R}-EGFP to target other PRC1 members in fixed cells. It might be that targeting of other PRC1 members is more severely affected in cells transfected with Cbx2-CD^{F12A}-EGFP or Cbx2-AT^{G78R}-EGFP than in cells transfected with Cbx2-EGFP. This could be determined by measuring the dynamics of Cbx2 and other PRC1 members at heterochromatin simultaneously. Furthermore, the immobile fraction could also function as a template for other Cbx2 proteins, creating a positive feed-back loop.

Material and Methods

The *Suv39h*-dn ESC were transiently transfected using Lipofectamin as described before. For imaging, cells were plated on Ibidi plates (Ibidi, Germany), grown 24 hours in ESC medium and imaged on a spinning disc confocal setup comprising an Olympus IX81 (Olympus, Japan) microscope equipped with a Yokogawa CSU-X1 scan head, a 491nm laser line, a PlanApo 100x/1.45 TIRFM oil immersion objective, an ASI MS-2000 with Z-piezo stage, a Semrock Di01-T488/568-13x15x0.5 dichroic, a Semrock FF01-525/40-25 emission filter and a Cascade II EM-CCD camera (Photometrics). The setup was enclosed in a heating box and temperature was set at 37°C and controled with a "Box" element (Life Cell imaging, Basel). The sample was covered with a plate dispensing humidified air containing 5% CO2 at a flux rate of 6 l/hour controlled with a "Brick" element (Life Cell imaging, Basel). Final pixel size was 94nm. FRAP was performed using a Rapp-Optoelectronic module equipped with a 473 laser. The results were analyzed using ImageJ.

3.2.1.2. Polycomb from an evolutionary point of view

Rico Kunzmann and Hans-Rudolf Hotz

Five PC orthologs have been described in mouse: Cbx2, Cbx4, Cbx6, Cbx7 and Cbx8 (Cbx1, Cbx3 and Cbx5 are orthologs of Hp1). With the increase of genomic size and organism complexity gene duplication and subsequent functional divergence is a commonly observed phenomenon. This is also true for the different PC mouse paralogs. As described in 2.2.2.2., they display different functions, and they are expressed in a temporally and spatially controlled manner.

Chromosomal arrangement

Interestingly, mouse *Cbx2*, *Cbx4* and *Cbx8* are all three located within 80 kb on chromosome 11. In addition, also *Cbx6* and *Cbx7* are within 200 kb on chromosome 15 (Figure 3.2.). Together, this implies at least three gene duplications. In order to investigate whether this gene order is evolutionary conserved, we compared the chromosomal arrangement of the PC orthologs in various vertebrate species, from fish to humans. The sequential arrangement as well as the orientation of *Cbx2*, *Cbx4* and *Cbx8* on one chromosome and *Cbx6* and *Cbx7* on another chromosome is conserved among human, chicken (bird) and the anole lizard (reptile) (Figure 3.8). Unfortunately, the genome of *Xenopus tropicalis* (amphibian) is not fully sequenced yet. Thus, sequenced scaffolds have not been assigned to chromosomes. Nevertheless, *Cbx6* and *Cbx7* are in proximity on one aligned scaffold in the same orientation as in mouse. Also, *Cbx4* and *Cbx8* are close to each other on another aligned scaffold, whereas *Cbx2* was sequenced on different scaffold. Nevertheless, once the genome is sequenced, it is possible, that *Cbx2* turns out to be on the same chromosome as *Cbx4* and *Cbx8*, just in greater distance to them than in other tetrapods. In zebrafish, finally, this chromosomal arrangement is not fully conserved. Zebrafish contains at least eight Cbx genes. The existence of several isoforms of one paralog in fish is possibly due to genome duplications. For six of the paralogs, a protein has been described (Figure 3.8). The eight Cbx genes show a chromosomal arrangement slightly different to the one observed in tetrapods. Although the gene order of *Cbx2*, *Cbx8a* and *Cbx4* on chromosome 3 is conserved, *Cbx2* is in great distance to *Cbx8a* and *Cbx4*, and it is also differentially orientated compared to tetrapods. Interestingly, *Cbx6b* and *Cbx7a* are also located on chromosome 3 within 300 kb of each other and 6 Mb apart from *Cbx8a* and *Cbx4* (Figure 3.8). This means that the five Cbx genes once were all on the same chromosome and only in tetrapods, Cbx7 and Cbx6 were separated to another chromosome via chromosomal translocation. In zebrafish, the additional Cbx paralogs are on chromosome 6 (*Cbx8b*), chromosome 12 (*Cbx7b*) and chromosome 22 (*Cbx6a*). Taken together, the chromosomal arrangement detected in mouse is conserved among tetrapods (the exact Cbx2 location in *Xenopus* still has to be determined), and partly also within vertebrates (Figure 3.8).

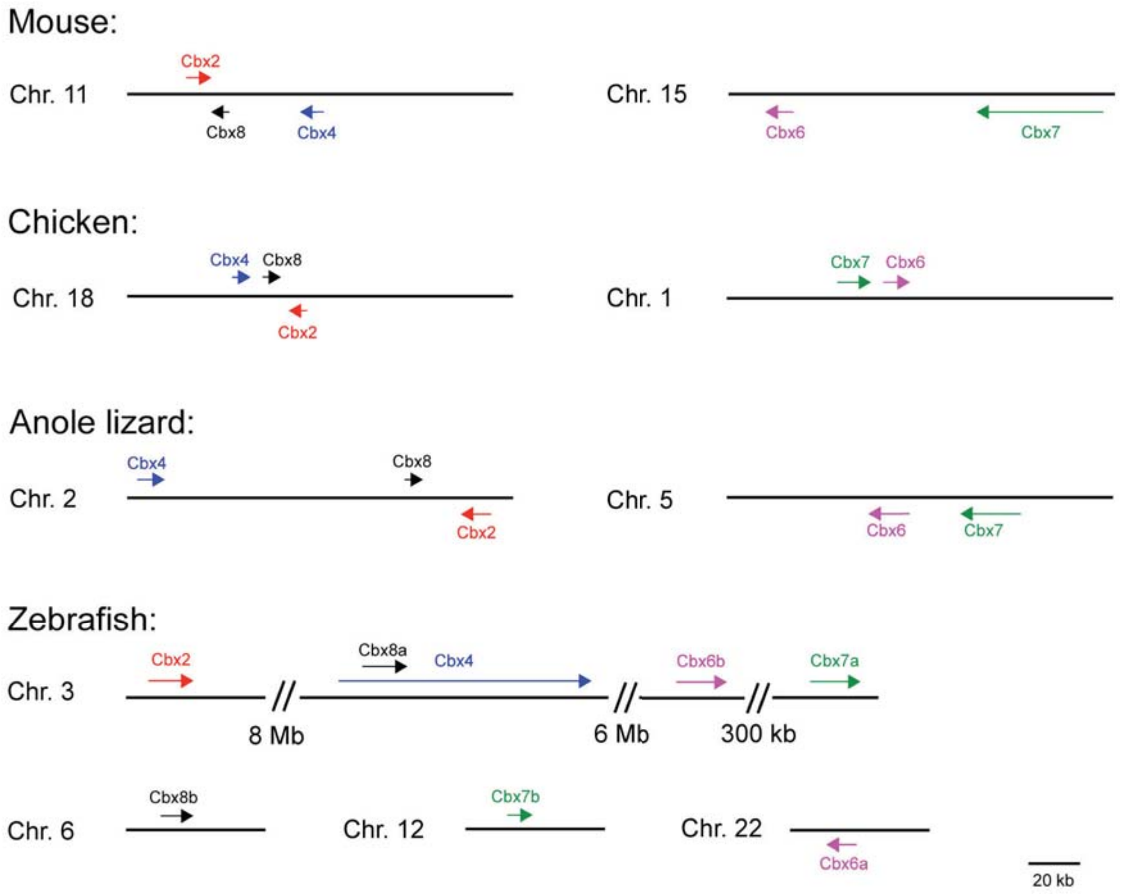
Mouse:
Chr. 11
Cbx2
Cbx8
Cbx4
Chr. 15
Cbx6
Cbx7
Chicken:
Chr. 18
Cbx4
Cbx8
Cbx2
Chr. 1
Cbx7
Cbx6
Anole lizard:
Chr. 2
Cbx4
Cbx8
Cbx2
Chr. 5
Cbx6
Cbx7
Zebrafish:
Chr. 3
Cbx2
Cbx8a
Cbx4
Cbx6b
Cbx7a
8 Mb
6 Mb
300 kb
Chr. 6
Cbx8b
Chr. 12
Cbx7b
Chr. 22
Cbx6a
20 kb

Figure 3.8: Chromosomal arrangement of the five Cbx paralogs of mouse, chicken, the anole lizard and zebrafish.

Polycomb evolution

Alignment of the five mouse paralogs showed that solely Cbx2 contains an AT-hook motif, whereas Cbx4, Cbx6, Cbx7 and Cbx8 contain AT-hook-like motifs only. Furthermore, Cbx2, Cbx6 and Cbx8 contain an alanine at position 14, ensuring H3K27me3 specificity (at least for Cbx2), while Cbx4 and Cbx7 contain a valine, displaying binding preference for H3K9me3, as described before. Also, the exon exon boundaries of the first four exons, which encode for the CD, are highly conserved between all five paralogs (Figure 3.9.A.). These exon exon boundaries are conserved among vertebrates from fish to mammals (Figure 3.9.B. and C.). Furthermore, all zebrafish paralogs show great similarity to its mouse ortholog. Additionally, Cbx2 in fish is the only paralog that contains an AT-hook motif and position 14 is like in mouse an alanine in Cbx2, Cbx6 and Cbx8 and a valine in Cbx4 and 7 (Figure 3.9.B.). Comparison of a number of fish species with mouse Cbx2 again showed conservation of A14, the AT-hook motif and the exon exon boundaries. Surprisingly, A13, which is highly conserved among the mouse Cbx paralogs, is mutated to an aspartate in fish Cbx2, suggesting lower evolutionary constraint on aa A13 than on aa A14 (Figure 3.9.C.).

Cbx2 orthologs have also been described in early deuterstomia. The sea urchin (Echinodermata) shows perfect conservation of the CD with A14 and the exon exon boundaries of the first four exons. Furthermore, of the two Cbx2 paralogs described in Sea urchins, one of them already contains an AT-hook like motif, suggesting that the Cbx2 AT-hook evolved convergent to other AT-hook motifs containing proteins from an imperfect sequence. It also suggests that the AT-hook is evolutionary younger than the CD with the A14 and the exon exon boundaries (Figure 3.9.E.).

Alignment of mouse Cbx2 with different *Drosophila* species and other arthropods (all protostomia) displayed a different exon exon structure. Nevertheless, the primary amino acid structure remained conserved, encoding for a CD with A14. Furthermore, neither an AT-hook motif nor an AT-hook like motif (Figure 3.9.D.) was detected in the protostomia species investigated. The Water flea (a mandibulata like *Drosophila*, but from the crustacean family; it must be noted that the A14 of the Water flea is shifted N-terminally by three aa), and the Deer tick (also an arthropod, but a chelicerata) showed conservation of the first three exon junctions. The Honey bee on the other hand shows conservation of only the first two exon boundaries. Finally, only the first exon exon boundary is conserved in *Drosophila* (Figure 3.9.D.).

Importantly two Cbx2 transcripts were also detected in the Sea anemone, a cnidaria. This animal is placed in the tree of life before the separation into the two major bilateria groups of protostomia and deuterostomia. Thus, it is the oldest organism that contains a Cbx paralog described so far. Surprisingly, the CD with A14 as well as the exon exon boundaries is fully conserved for one of the two isoforms with mouse Cbx2, while the other isoform shows at least partial exon exon boundary conservation. Both isoforms do not contain an AT-hook like motif (Figure 3.9.E). Finally, this protein sequence in Sea anemones strongly suggests that the exon exon boundaries are conserved beyond bilateria, and that the protostomia species lost these boundaries.

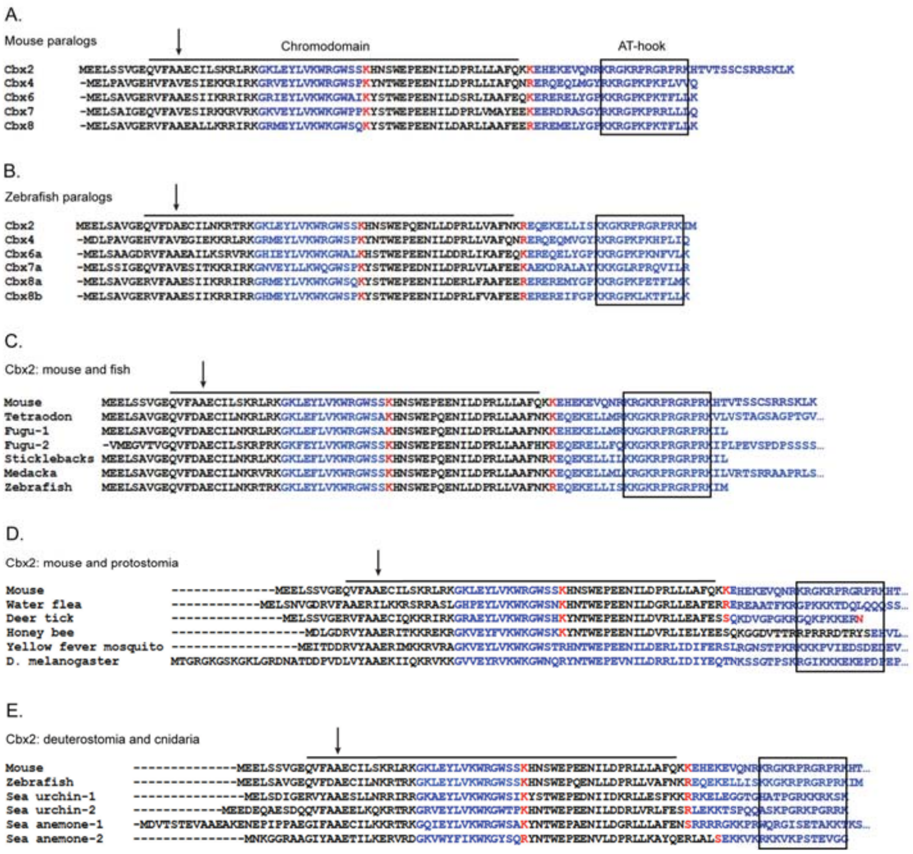
A.
Mouse paralogs
Chromodomain
AT-hook
Cbx2
Cbx4
Cbx6
Cbx7
Cbx8
B.
Zebrafish paralogs
Cbx2
Cbx4
Cbx6a
Cbx7a
Cbx8a
Cbx8b
C.
Cbx2: mouse and fish
Mouse
Tetraodon
Fugu-1
Fugu-2
Sticklebacks
Medacka
Zebrafish
D.
Cbx2: mouse and protostomia
Mouse
Water flea
Deer tick
Honey bee
Yellow fever mosquito
D. melanogaster
E.
Cbx2: deuterostomia and cnidaria
Mouse
Zebrafish
Sea urchin-1
Sea urchin-2
Sea anemone-1
Sea anemone-2

Figure 3.9: Alignments of the the mouse Cbx paralogs and orthologs displaying the first four exons. **A.** Mouse Paralogs, exon 1 to exon 4 (CBX2: ENSMUSP00000026662; CBX4: ENSMUSP00000026665; CBX6: ENSMUSP00000105255; CBX7: ENSMUSP00000105245; CBX8: ENSMUSP00000026663); **B.** Zebrafish Paralogs, exon 1 to exon 4 (Cbx2: ENSDARP 00000066052; Cbx4: ENSDARP00000095047; Cbx6: ENSDARP00000117129; Cbx7: ENSDARP00000055427; Cbx8a: ENSDARP00000095045; Cbx8b: ENSDARP 00000093874); **C.** Mouse Cbx2 and Fish orthologs, exon 1 to exon 4 (mouse: ENSMUSP 00000026662; Tetraodon: ENSTNIP00000014215; Fugu-1: ENSTRUP 00000004914; Fugu-2: ENSTRUP 00000008095; Sticklebacks: ENSGACP00000019004; Medacka: ENSORLP 00000001129; Zebrafish: ENSDARP00000066052); **D.** Mouse Cbx2 and selected Protostomia (arthropods) orthologs, exon 1 to exon 4 according to mouse (mouse: ENSMUSP00000026662; Water flea (Daphnia pulex): P191862; Deer tick (Ixodes scapularis): ISCW012843; European honey bee (Apis mellifera): GB12523; Yellow fever mosquito (Aedes aegypti): AAEL014098; *D.melanogaster*: FBpp0078059); **E.** Mouse Cbx2 (a late deuterostomia), a Cnidaria (before protostomia and deuterostomia division), an early deuterostomia (Sea urchin) and Zebrafish (a deuterstomia) (mouse: ENSMUSP00000026662; Zebrafish: ENSDARP00000066052; Sea urchin (Strongylocentrotus purpuratus): 020586, 020946; Sea anemone (Nematostella vectensis): v1g238789, v1g243415); arrow: amino acid residue 14 according to mouse Cbx2; long bar: chromodomain; short bar: AT-hook motif. Colors of aa residues: black and blue letters distinguish exons; red letters display exon exon junctions within a codon.

Furthermore, for the Sea anemone as well as for the Sea urchin two Cbx2 homologs have been described. Firstly, this suggests that a Cbx2-like protein was the founding member of the Cbx protein family. Secondly, it also suggests that the protostomia lineage lost one of the Cbx2 gene copies during evolution (Figure 3.10.A.). Interestingly, we did not detect any Cbx homolog in *C. elegans* (Nematodes), *Schistosoma mansoni* (Platyhelminthes) and *Oikopleura dioica* (Urochrodata), as described previously (Schuettengruber et al., 2007) (Figure 3.10.B). This implies that those species lost several Cbx gene copies. Therefore, the loss of Cbx genes during evolution occurred several times. And thirdly, the founding member of the Cbx proteins might be even older than the Cnidarians, and upon Cnidarian evolution an early, first gene duplication must have taken place, resulting in the two Cbx2 Cnidarian homologs (Figure 3.10.A).

Discussion

Taken together, the chromosomal arrangement of the Cbx paralogs is conserved among the tetrapod model organisms (the correct localization of Cbx2 in *Xenopus* still needs to be determined). Furthermore, the first 3 exon junctions of the Cbx paralogs, coding for the CD, are highly conserved from cnidarians to humans, but diverged in the protostomia lineage. The CD with aa residue A14 remains preserved in the deuterostomia and the protostomia lineage, though. Finally, the AT-hook motif, putatively evolved from an AT-hook like motif, originates in early deuterostomia. It is unique for the Cbx2 orthologs, suggesting importance of the AT-hook motif from fish to humans, in respect to Cbx2 function (Figure 3.10.A).

Cbx2 has been described to function within the PRC1 complex. The presence of two Cbx homologs in Cnidarians raises the question, whether or not other PRC1 members are present in Cnidarians. Interestingly, for the Cnidarian Sea anemone a Ring homolog as well as a Ph homolog has been described, whereas it is not known presently if it contains also a Bmi1 homolog (Schuettengruber et al., 2007). Nevertheless, the presence of three of the four core PRC1 members in the Sea anemone strongly suggests the presence of PRC1 itself. Furthermore, the Sea anemone also contains a partial Hox gene cluster, the well described target of PRC1 in other species. It is possible that the maintenance of silencing of this Hox gene cluster in the Sea anemone is dependent on PRC1.

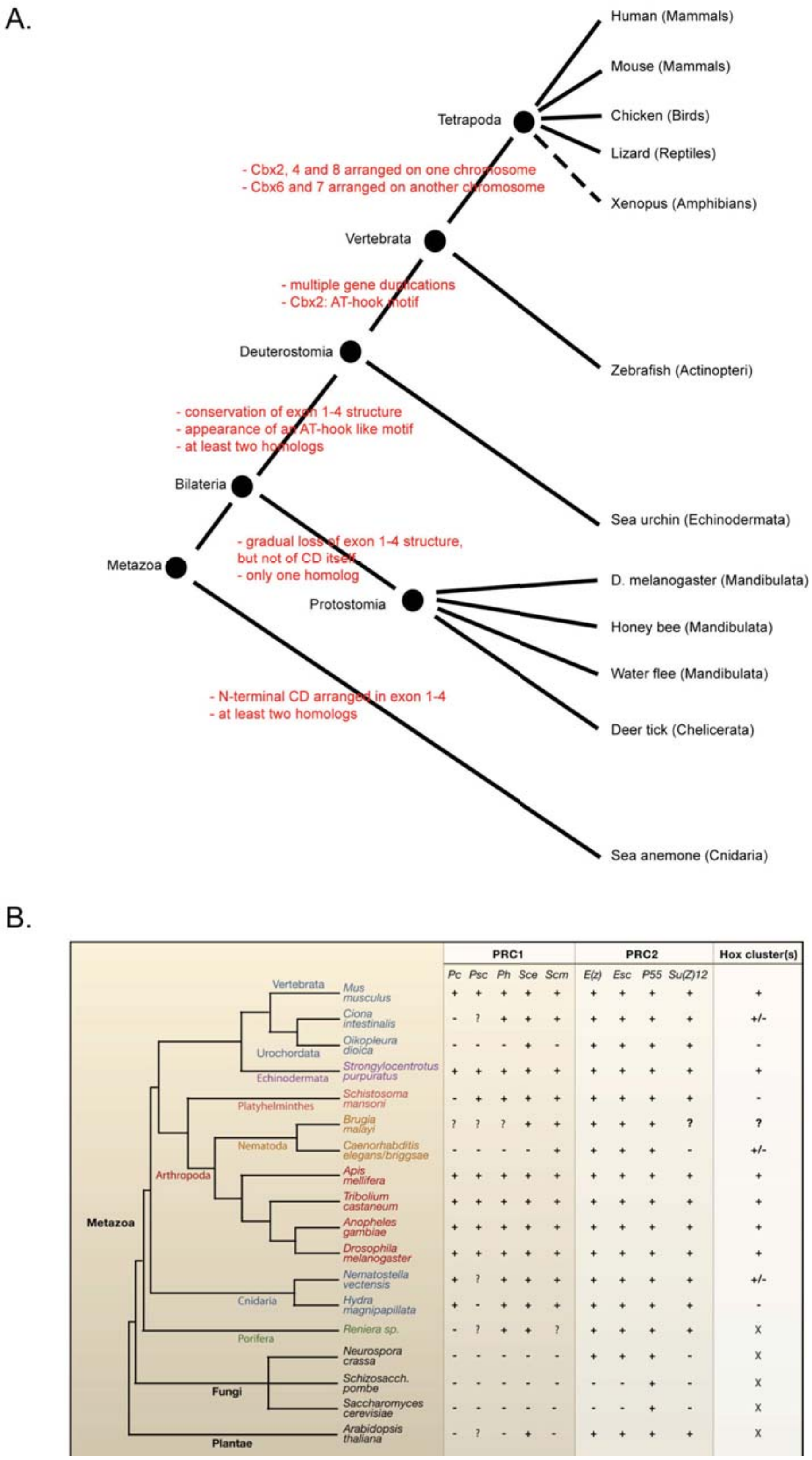
A.
Human (Mammals)
Mouse (Mammals)
Chicken (Birds)
Lizard (Reptiles)
Xenopus (Amphibians)
Tetrapoda
- Cbx2, 4 and 8 arranged on one chromosome
- Cbx6 and 7 arranged on another chromosome
Vertebrata
- multiple gene duplications
- Cbx2: AT-hook motif
Deuterostomia
Zebrafish (Actinopteri)
- conservation of exon 1-4 structure
- appearance of an AT-hook like motif
- at least two homologs
Bilateria
Sea urchin (Echinodermata)
- gradual loss of exon 1-4 structure,
but not of CD itself
- only one homolog
Metazoa
Protostomia
D. melanogaster (Mandibulata)
Honey bee (Mandibulata)
Water flee (Mandibulata)
Deer tick (Chelicerata)
- N-terminal CD arranged in exon 1-4
- at least two homologs
Sea anemone (Cnidaria)
B.
Metazoa
Vertebrata
Urochordata
Echinodermata
Platyhelminthes
Nematoda
Arthropoda
Cnidaria
Porifera
Fungi
Plantae

	PRC1					PRC2				Hox cluster(s)
	Pc	*Psc*	*Ph*	*Sce*	*Scm*	*E(z)*	*Esc*	*P55*	*Su(Z)12*	
Mus musculus	+	+	+	+	+	+	+	+	+	+
Ciona intestinalis	-	?	+	+	+	+	+	+	+	+/-
Oikopleura dioica	-	-	-	+	-	+	+	+	+	-
Strongylocentrotus purpuratus	+	+	+	+	+	+	+	+	+	+
Schistosoma mansoni	-	+	+	+	+	+	+	+	+	-
Brugia malayi	?	?	?	+	+	+	+	+	?	?
Caenorhabditis elegans/briggsae	-	-	-	-	+	+	+	+	-	+/-
Apis mellifera	+	+	+	+	+	+	+	+	+	+
Tribolium castaneum	+	+	+	+	+	+	+	+	+	+
Anopheles gambiae	+	+	+	+	+	+	+	+	+	+
Drosophila melanogaster	+	+	+	+	+	+	+	+	+	+
Nematostella vectensis	+	?	+	+	+	+	+	+	+	+/-
Hydra magnipapillata	+	-	+	+	+	+	+	+	+	-
Reniera sp.	-	?	+	+	?	+	+	+	+	X
Neurospora crassa	-	-	-	-	-	+	+	+	-	X
Schizosacch. pombe	-	-	-	-	-	-	-	+	-	X
Saccharomyces cerevisiae	-	-	-	-	-	-	-	+	-	X
Arabidopsis thaliana	-	?	-	+	-	+	+	+	+	X

Figure 3.10: A. Phylo-genetic tree of selected organism displaying Pc evolution within metazoa. Black nodes indicate common ancestor. The branch lengths do not represent evolutionary distance between orga-nisms. Red letters indicate evolutionary events. **B.** Phylogenetic distribution of the PRC1, PRC2 and Hox gene clusters. Adapted from Schuettengruber et al., 2007.

3.2.1.3. Exogenously provided Hp1β restores PCH asymmetry in Hp1β^{m-z+} zygotes

Introduction

In wt zygotes, Hp1β, putatively bound to H3K9me3, is strongly enriched at maternal PCH, while PRC1 localizes to paternal PCH. In zygotes maternally deficient for Hp1β, though, PRC1 members localize to paternal and also to maternal PCH. Therefore, Hp1β prevents PRC1 binding to maternal PCH. To test whether this blocking effect takes place directly by Hp1β in the zygote, or whether it appears to be indirect or relies on an Hp1β function during oocyte development, recombinant N-terminal myc tagged Hp1β was micro-injected into zygotes right after fertilization. These zygotes were then analyzed for PRC1 localization and possible restored asymmetry.

Results

In zygotes, which were microinjected with recombinant Hp1β, endogenous Cbx2 at maternal PCH was reduced in comparison to *Hp1β*$^{m-z+}$ zygotes microinjected with water (Figure 3.11.A and 3.11.B). This suggests that the epigenetic asymmetry can be directly rescued and restored in the zygote by Hp1β. It must be stated though, that recombinant Hp1β never reached the same level of maternal PCH enrichment as endogenous Hp1β in wt zygotes (Figure 3.11.A and 3.12.A). This reduced targeting might be due to the lack of post-translational, cell cycle dependent modifications of recombinant Hp1β, such as phosphorylation. In contrast, in 2-cell embryos the enrichment of recombinant Hp1β at heterochromatin is equally strong as endogenous Hp1β (data not shown).

Next, we asked whether Hp1β dimerization and potential higher order organization of chromatin is required to prevent Cbx2 from binding to maternal heterochromatin. To address this question, we microinjection of Hp1β^{I161E}, an Hp1β construct that lacks the ability to form homo- and heterodimers, did not result in the reduction of Cbx2 at maternal PCH (Figure 3.11.B). Localization of Hp1β^{I161E} to maternal PCH, though, was even lower than the localization of full length recombinant Hp1β (Figure 3.11.A and 3.12.A). Thus, we cannot conclude whether the inability to rescue the asymmetry is due to the inability to form homo- and heterodimers or due to inefficient targeting of Hp1β^{I161E} to PCH.

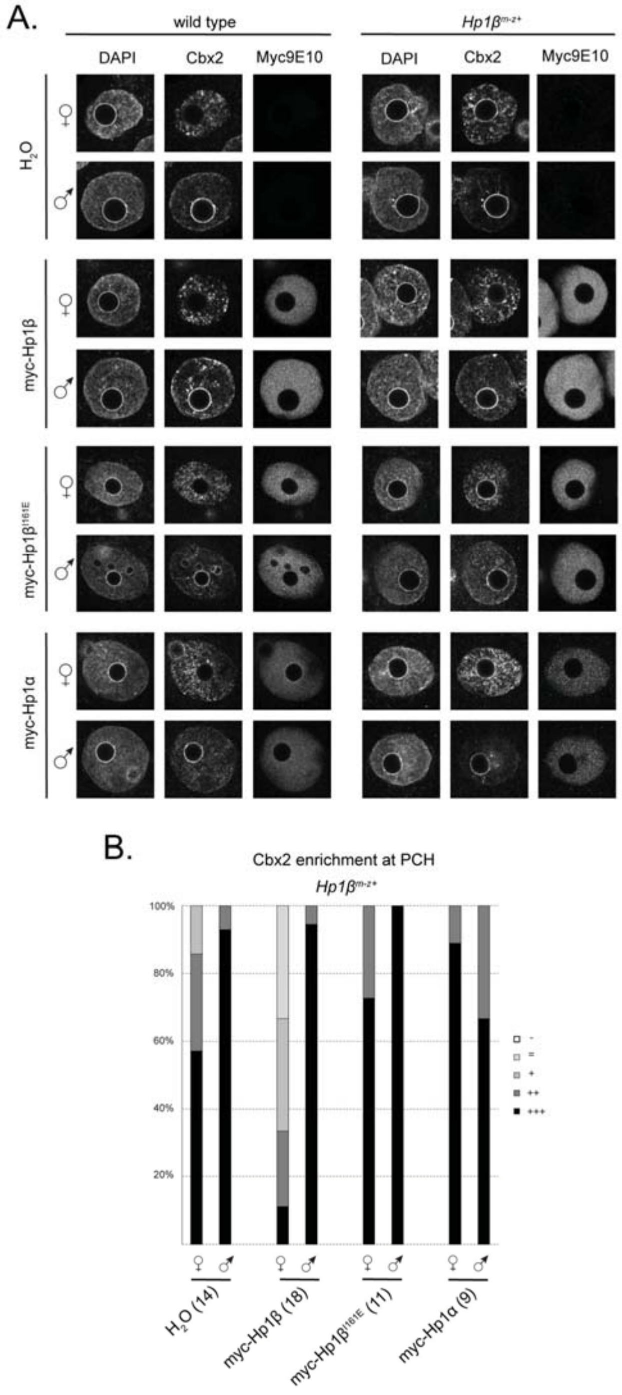
A.
wild type
Hp1β^m-z+
DAPI
Cbx2
Myc9E10
DAPI
Cbx2
Myc9E10
H2O
myc-Hp1β
myc-Hp1β^I161E
myc-Hp1α
♀
♂
B.
Cbx2 enrichment at PCH
Hp1β^m-z+
100%
80%
60%
40%
20%
-
=
+
++
+++
H2O (14)
myc-Hp1β (18)
myc-Hp1β^I161E (11)
myc-Hp1α (9)

Figure 3.11: Microinjection of recombinant myc tagged Hp1 constructs into wt and *Hp1β*$^{m\text{-}z+}$ zygotes. **A.** Representative confocal images of wt and *Hp1β*$^{m\text{-}z+}$ zygotes microinjected with myc tagged Hp1β, Hp1β^{I161E} and Hp1α mRNA or H_2O. DNA was visualized by DAPI. PRC1 localization by an antibody against Cbx2 and the recombinant construct by a myc9E10 antibody. **B.** Graph displaying the Cbx2 enrichment at maternal and paternal PCH of *Hp1β*$^{m\text{-}z+}$ zygotes.

Interestingly, microinjection of Hp1α, an Hp1 isoform, which is not present in wt zygotes, into *Hp1β*$^{m\text{-}z}$ zygotes did not restore the epigenetic asymmetry (Figure 3.11.B), suggesting that the blocking effect of Hp1β toward PRC1 is Hp1β specific. However, enrichment of recombinant Hp1α in *Hp1*$^{m\text{-}z+}$ zygotes at PCH was low, as observed for Hp1β^{I161E} (Figure 3.11.A and 3.12.A). Therefore, we cannot formally conclude whether restoring the asymmetry by Hp1α in *Hp1β*$^{m\text{-}z+}$

zygotes fails due to insufficient PCH targeting or because Hp1α cannot prevent Cbx2 from binding to maternal PCH. Interestingly though, enrichment of recombinant Hp1α at maternal PCH was high in wt zygotes. This suggests that Hp1α targeting to maternal PCH in wt zygotes is Hp1β dependent.

Discussion

Taken together, the epigenetic asymmetry in *Hp1β*$^{m\text{-}z+}$ zygotes is restored upon microinjection of recombinant Hp1β, whereas it is not restored by a construct that lacks the ability to form homo- and heterodimers (Hp1β^{I161E}) or by Hp1α. Therefore, Hp1β directly prevents PRC1 from binding to maternal PCH in the mouse zygote. This asymmetry is set up *de novo* in the zygote. Surprisingly, the exogenously provided Hp1α was recruited to maternal PCH only in the presence of Hp1β in wt zygotes. Therefore, targeting of exogenously provided Hp1α to maternal PCH depends on Hp1β in the mouse zygote (Figure 3.12.A). The endogenously present Hp1β might be post-translationally modified. This might enhance the targeting efficiency of exogenously provided, putatively unmodified, Hp1α. Nevertheless, there is no such dependency of exogenously provided Hp1β observed in respect to PCH targeting (Figure 3.12.A). In wt as well as in *Hp1β*$^{m\text{-}z+}$ zygotes, recombinant Hp1β is enriched at maternal PCH to a similar degree. Therefore, this specificity in zygotes must be due to sequence differences between the two paralogs (Figure 3.12.B). Mutational analysis of recombinant Hp1α might identify the aa residues responsible for this specificity.

Material and Methods

Recombinant myc tagged Hp1β, Hp1β^{I161E} and Hp1α mRNA or H_2O was microinjected into cytoplasm of IVF zygotes right after fertilization at a concentration of 7.5 ng/μl as previously described.

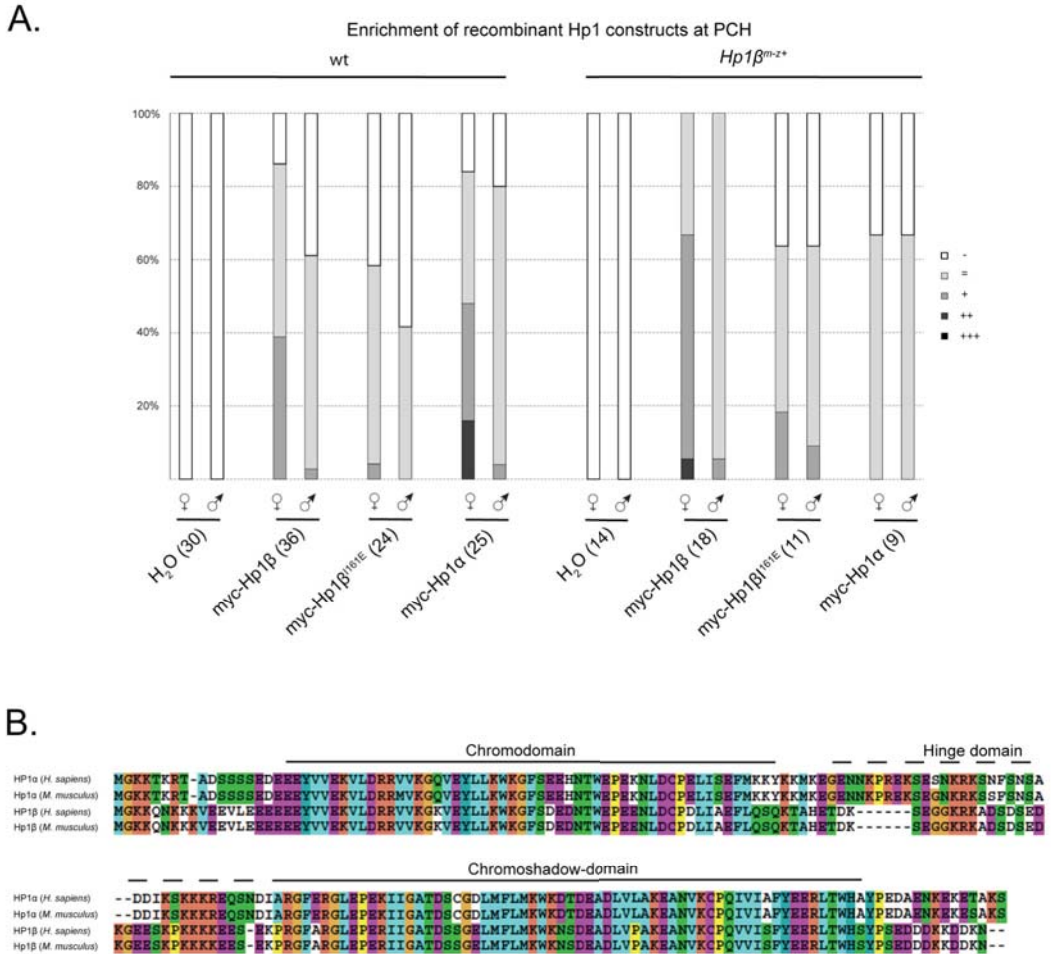

Figure 3.12: A. Graph displaying the enrichment of Hp1 constructs at PCH in wt and *Hp1β*$^{m\text{-}z+}$ zygotes. The enrichment was scored based on the myc9E10 antibody staining. **B.** Alignment of the mouse and human Hp1α and Hp1β homologs.

3.2.1.4. The Effect of SUV39H Activity in Mouse Zygotes on the PCH Asymmetry

Introduction

In the paternal PN of wt zygotes there is no H3K9me3 detected in IF stainings. This lack of paternal H3K9me3 propagation suggests absence of the Suv39h and other H3K9me3 HMTs. One can also envision that the maintenance of asymmetric H3K9me3 is an active process that depends on zygotic transcription and protein synthesis, as it has been described for the asymmetric H3K9me2 (Liu et al., 2004). This would be in agreement with the detection of mRNA of Suv39h2 in zygotes (Puschendorf et al., 2008). To test whether asymmetric H3K9me3 is due to the absence of the HMTs and its enzygmatic activity, we microinjected myc-tagged human SUV39H1 and mouse Suv39h2 mRNA into wt zygotes.

Results

Whereas microinjection of water did not affect the PCH asymmetry with conventional maternal Hp1β and H3K9me3 and paternal Cbx2 enrichment (Figure 3.13.A, Figure 3.14.A), microinjection of 100ng/µl SUV39H1 mRNA resulted in the loss of PCH asymmetry. Interestingly, recombinant human SUV39H1 was not only targeted to paternal PCH, but also tri-methylated H3K9 at paternal PCH (Figure 3.14.B). Furthermore, paternal PCH got highly enriched for Hp1β (Figure 3.13.B). Surprisingly, this *de novo* paternal localization of the Su(var) pathway did not result in the loss of paternal Cbx2 enrichment. On the contrary, Cbx2 enrichment was now also observed at PCH of maternal PN (Figure 3.13.B). Microinjection of a hyperactive SUV39H1 construct (SUV39H1^{H320R}) revealed an even stronger abolishment of the PCH asymmetry, displaying high enrichment of the Suv39h pathway and PRC1 equally strong at maternal and paternal PCH (Figure 3.13.C, Figure 3.8.C). Microinjection of an inactive SUV39H1 (SUV39H1^{H324L}), however, did not result in paternal H3K9me3 (Figure 3.14.D) and did not affect the PCH asymmetry (Figure 3.13.D). Thus, the loss of PCH asymmetry is dependent on the activity of SUV39H1.

Furthermore, microinjection of 100ng/µl Suv39h2 mRNA resulted in the enrichment of the Su(var) pathway paternally and colocalization with Cbx2 (Figure 3.13.E, Figure 3.14.E). Interestingly and in contrast to microinjection of SUV39H1, Cbx2 was still prevented from binding to maternal PCH (Figure 3.13.E). Thus, the asymmetry remained at least maternally intact upon Suv39h2 microinjection.

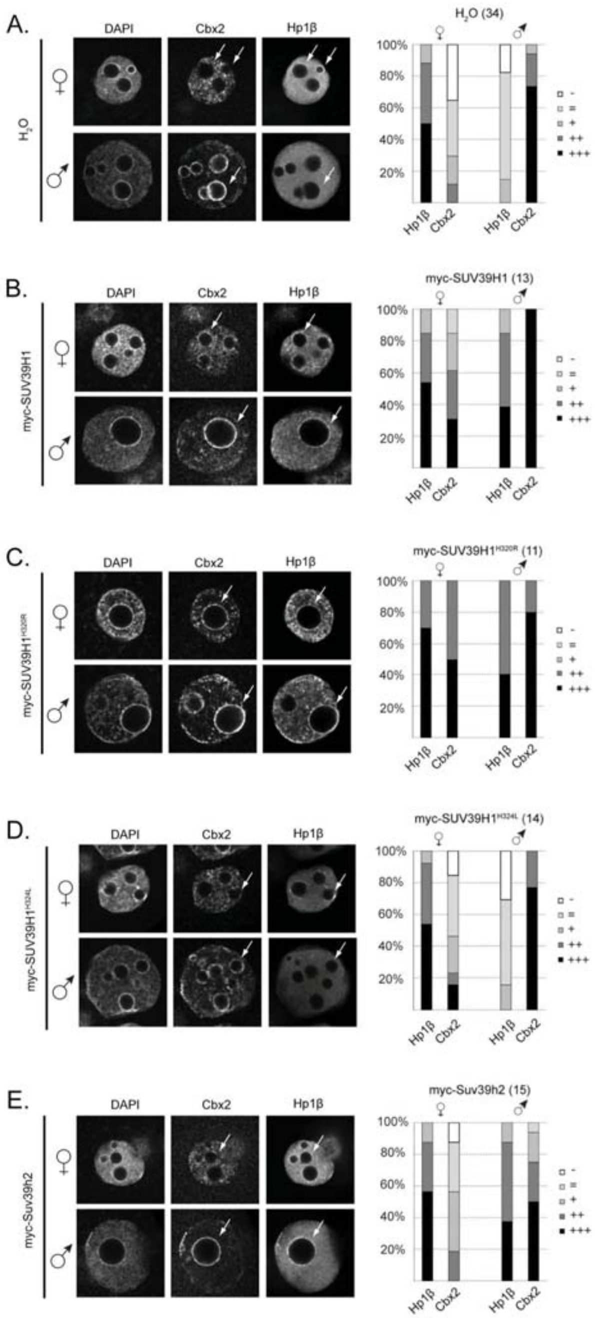
A.
B.
C.
D.
E.
DAPI
Cbx2
Hp1β
H_2O
myc-SUV39H1
myc-SUV39H1^{H320R}
myc-SUV39H1^{H324L}
myc-Suv39h2
♀
♂
H_2O (34)
myc-SUV39H1 (13)
myc-SUV39H1^{H320R} (11)
myc-SUV39H1^{H324L} (14)
myc-Suv39h2 (15)
100%
80%
60%
40%
20%
Hp1β
Cbx2
-
=
+
++
+++

Figure 3.13: Microinjection of recombinant myc-tagged SUV39H1 and Suv39h2 constructs into wt zygotes. Zygotes were stained Hp1β and Cbx2 (determination of PCH asymmetry). **A.** Microinjection of H_2O. **B.** Microinjection of myc-tagged SUV39H1. **C.** Microinjection of myc-tagged SUV39H1^{H320R}, which displays enhanced H3K9me3 activity. **D.** Microinjection of myc-tagged SUV39H1H324L, which lacks H3K9me3 activity. **E.** Microinjection Suv39h2.

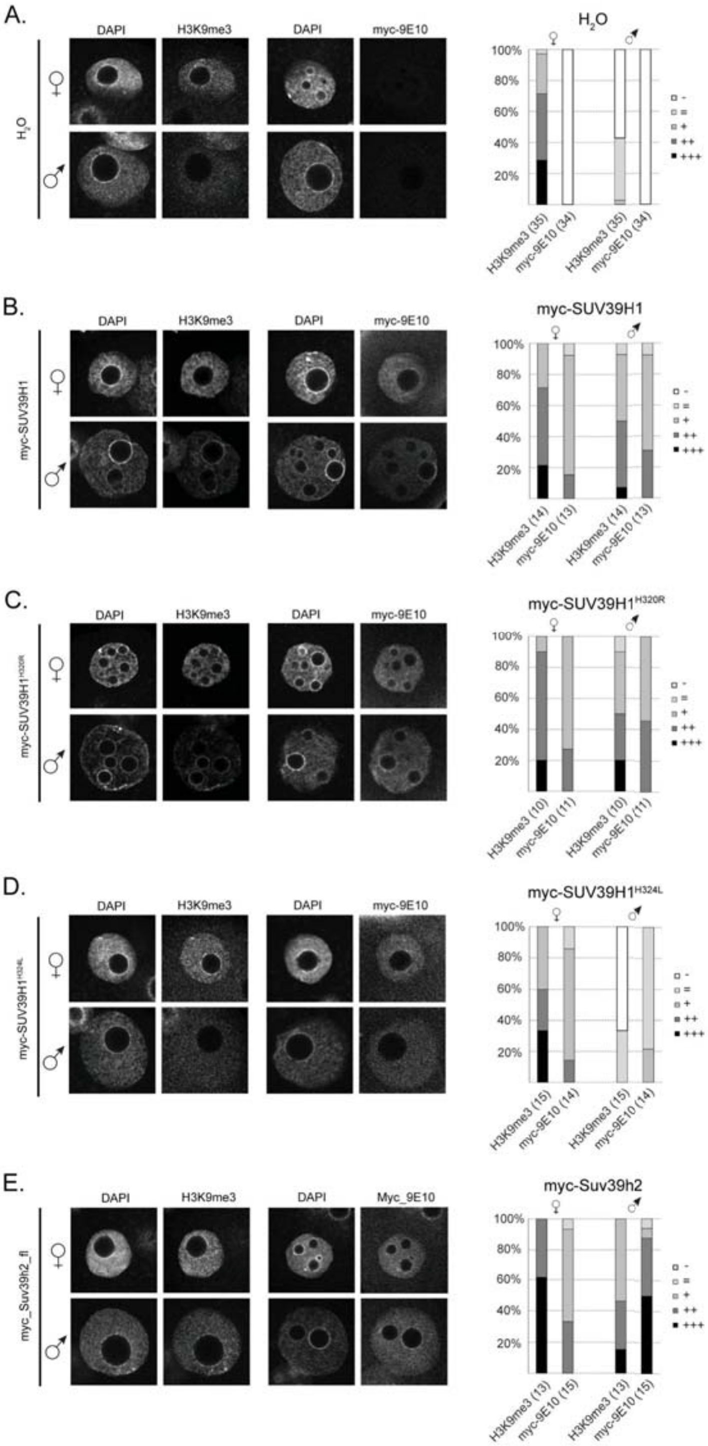
A.
DAPI
H3K9me3
DAPI
myc-9E10
H$_2$O
♀
♂
100%
80%
60%
40%
20%
H3K9me3 (35)
myc-9E10 (34)
H3K9me3 (35)
myc-9E10 (34)
□ -
□ =
□ +
■ ++
■ +++
B.
myc-SUV39H1
H3K9me3 (14)
myc-9E10 (13)
H3K9me3 (14)
myc-9E10 (13)
C.
myc-SUV39H1^{H320R}
H3K9me3 (10)
myc-9E10 (11)
H3K9me3 (10)
myc-9E10 (11)
D.
myc-SUV39H1^{H324L}
H3K9me3 (15)
myc-9E10 (14)
H3K9me3 (15)
myc-9E10 (14)
E.
myc-Suv39h2
myc_Suv39h2_fl
Myc_9E10
H3K9me3 (13)
myc-9E10 (15)
H3K9me3 (13)
myc-9E10 (15)

Figure 3.14: Microinjection of recombinant myc-tagged SUV39H1 and Suv39h2 constructs into wt zygotes. Zygotes were stained with antibodies raised against myc9E10 in order to detect the recombinant protein and H3K9me3 (detection of the HMT activity). **A.** Microinjection of H_2O. **B.** Microinjection of myc-tagged SUV39H1. **C.** Microinjection of myc-tagged SUV39H1^{H320R}, which displays enhanced H3K9me3 activity. **D.** Microinjection of myc-tagged SUV39H1H324L, which lacks H3K9me3 activity. **E.** Microinjection Suv39h2.

Upon Suv39h HMT activity in the mouse zygote, the asymmetry for the Su(var) pathway and PcG proteins at PCH is resolved. The two pathways colocalize at the PCH of maternal and paternal PN. This result is highly surprising and unexpected, and it raises more questions than it answers.

It has been shown for the Hp1 isoforms that they are highly dynamic at heterochromatin with half recovery times around 2.5 seconds and that their dynamics rely on the Suv39h HMT. In 4-cell embryos, the dynamic of Hp1β at heterochromatin is reduced. Half recovery times of 9 seconds were measured. This decrease of mobility in early preimplantation embryos might be due to the absence of Suv39h HMT activity. This implies that Hp1β is bound stronger to heterochromatin in the absence of Suv39h HMT activity. Therefore, in addition to the high affinity for H3K9me3 of Hp1β, this low mobility might lead to a more fixed chromatin configuration at maternal PCH in early embryos, which putatively results in the maternal and paternal asymmetry at PCH. Upon Suv39h HMT activity, though, Hp1β at PCH might become more dynamic. The enhanced dynamic of the Suv39h pathway together with the high content of PRC1 proteins in zygotes compared to other cell types might result in this colocalization at PCH.

This does not explain the result for microinjected Suv39h2 where Hp1β, putatively bound to H3K9me3, and Cbx2 colocalize paternally, but not maternally. Thus, the abundant presence of Suv39h2 keeps Cbx2 from maternal PCH, by an unknown Suv39h2 specific mechanism, while SUV39H1, the major embryonic HMT does not distinguish maternal and paternal PCH in this respect. Interestingly, sequence alignments of the human and mouse Suv39h HMT display a basic stretch of aa, which is specific to the C-terminus of Suv39h2. Human SUV39H2 does not contain this basic stretch (Figure 3.15). Therefore, it would be interesting to microinject human SUV39H2, in order to test whether or not this specificity is due to this basic C-terminus. Interestingly, overrepresentation of basic aa have been shown to correlate with the compaction capability for members of the PRC1 complex (Grau et al., 2011). Thus, the basic aa stretch of mouse Suv39h2 might also result in a higher level of compaction maternally compared to SUV39H1. This, together with the inherited maternal heterochromatic state might prevent colocalization with PRC1 proteins.

Further investigation and comparison of the two Suv39h HMT, the importance of the Suv39h pathway and PcG proteins in chromocenter formation and heterochromatin maturation in late 2-cell, analysis of targeting mechanisms of the Suv39h pathway to paternal PCH might give more insight into these unexpected observations. Altogether, though, they show that the Suv39h pathway and PcG proteins under these circumstances colocalize.

Materials and Methods

Plasmids containing the myc-tagged SUV39H1 and Suv39h2 ORFs were obtained from T. Jenuwein. mRNA was generated as described before and 100ng/μl were individually microinjected into the cytoplasm of wt C57BL/6 zygotes. They were fixed at the PN5 zygotic stage. Zygotes were stained with antibodies against myc-9E10, H3K9m3, Hp1β and Cbx2. Confocal images were taken with a LSM 700 microscope (Zeiss, Germany). Enrichment at maternal and paternal PCH was scored using ImageJ.

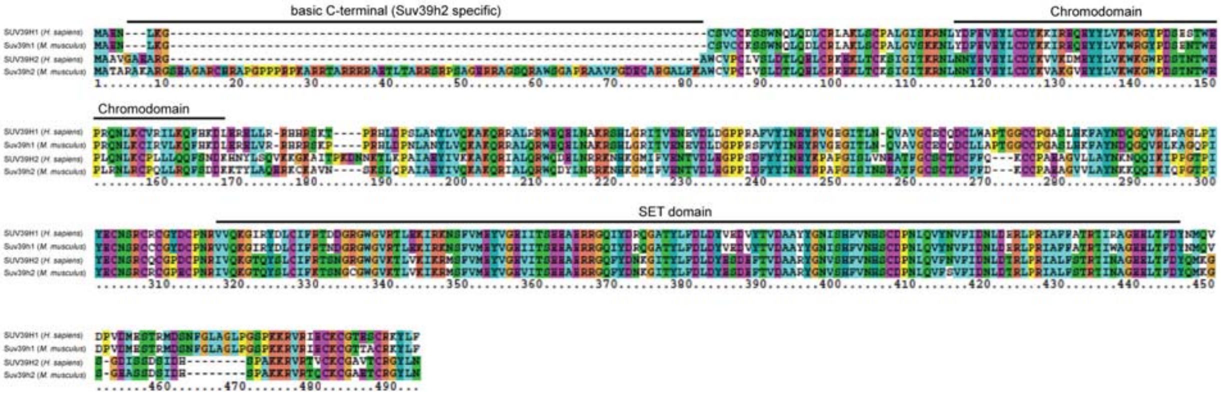
basic C-terminal (Suv39h2 specific)
Chromodomain
Chromodomain
SET domain
SUV39H1 (H. sapiens)
Suv39h1 (M. musculus)
SUV39H2 (H. sapiens)
Suv39h2 (M. musculus)

Figure 3.15: Sequence alignment of the human and mouse Suv39h proteins. Domains are indicated above the sequence.

3.2.2. Size Difference of Maternal and Paternal Pronuclei

In addition to the epigenetic asymmetries discussed so far, there is also a morphological asymmetry in respect to the size of the maternal and paternal PN. The distinction of the maternal and the paternal PN is usually determined in a first step by their relative size difference, with the paternal PN being bigger than the maternal PN. This size difference is visualized by DAPI, which intercalates with DNA. DAPI dense regions are thought to consist of DNA within more condensed chromatin than weakly stained DAPI regions.

Although the maternal and the paternal genomes are equally large, the paternal PN is bigger. This suggests that DNA in the paternal PN is less compacted. Indeed, DAPI stainings of paternal PN display more dispersed weak staining patterns than maternal PN DAPI stainings. Interestingly, this size difference is not only observed in PN5 zygotes but throughout zygotic development, which suggests that it is maintained by proteins present in the zygote. Furthermore, paternal DAPI dense regions are usually limited to PCH. To emphasize whether it is indeed the paternal PN that is bigger than the maternal PN in a mouse model, further analysis is needed (e.g. DNA methylation status, H3K9me2/3 or PRC1 stainings). To date, no KO or cKO mouse model, neither maternally nor zygotically deficient for a gene, has been described that results in the increase of maternal and/or paternal PN size or the decrease of maternal and/or paternal PN.

Histone variants

The compaction of DNA into higher order chromatin involves epigenetic regulators (Trojer and Reinberg, 2007). After the protamine to histone exchange in the paternal PN, maternally provided H3.3 histones are incorporated paternally, whereas maternal DNA remains wrapped around the canonical H3.1/2 histone variants. Thus, it is possible that global H3.3 incorporation does not compact chromatin to the same level as H3.1/2. Nevertheless, after the first round of DNA synthesis in the zygote, where H3.1/2 variants are incorporated also paternally, the size difference of maternal and paternal PN persists. Finally, it is possible that the global paternal histone content is lower than the maternal histone content, which might result in the relative size difference.

Transcriptional activity

The major ZGA takes place in the 2-cell embryo. Nevertheless, minor transcription has been observed from S-phase zygotes onwards. Interestingly, the transcriptional levels of the paternal PN are 4 to 5 times higher than in the maternal PN (Aoki et al., 1997). This enhanced paternal transcription might be in relationship to the putatively less compacted chromatin of the bigger paternal PN. Therefore, the transcriptional machinery might have better access to paternal transcription start sites than to maternal transcription start sites. Additionally, it is known that the paternal PN is enriched for histone H4 acetylation in comparison to the maternal PN (Adenot et al., 1997). The elevation of global acetylation in the zygote led also to enhanced maternal transcription (Wiekowski et al., 1993). This suggests that the transcriptional asymmetry is due to acetylation, resulting in a more transcription favorable chromatin state of the paternal PN. Nevertheless, this hyperacetylation in zygotes has not been reported to have any effect on the PN size.

DNA methylation

It is also possible that the active, global, paternal DNA demethylation is responsible for this pronuclear size difference. But neither PGC7/Stella mutants, which lack protection of the maternal DNA from demethylation, nor TET3 mutants, which do not show 5mC to 5hmC conversion paternally, an effect on the relative size difference between the maternal and the paternal PN have been described (Gu et al., 2011; Nakamura et al., 2007). Furthermore, late PN5 stage zygotes show less relative size difference of the maternal and the paternal PN in comparison to earlier PN stages, whereas active paternal DNA demethylation is completed by then and the two PN are highly asymmetric in respect to DNA methylation. Therefore, it is unlikely that the global paternal hydroxymethylation of 5mC residues is responsible for the size difference of the two maternal and the paternal PN.

Suv39h pathway

It is possible that the size difference between the maternal and the paternal PN is due to the absence of repressors paternally, such as the Su(var) pathway. Therefore, we analyzed the size of maternal and paternal PN of *Hp1β*$^{m-z+}$ zygotes and compared them to the PN sizes of wt zygotes. The maternal PN was determined by H3K9me3 and euchromatic PRC1 staining. Interestingly, the analysis of *Hp1β*$^{m-z+}$ zygotes displayed a significantly bigger maternal PN. In *Hp1β*$^{m-z+}$ zygotes the size of maternal and the paternal PN are identical. They are similar to the size of the paternal PN in wt zygotes (Figure 3.16.A, B and C).

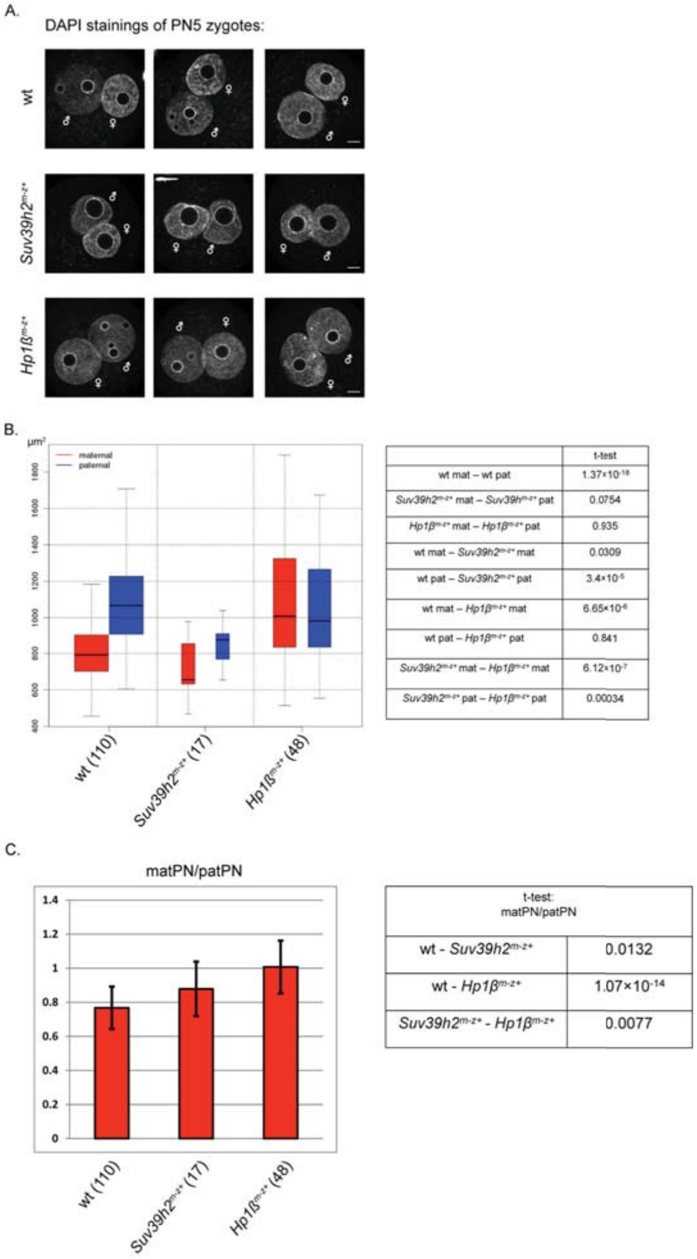

	t-test
wt mat – wt pat	1.37×10^{-18}
Suv39h2^{m-z+} mat – *Suv39h*$^{m-z+}$ pat	0.0754
Hp1β^{m-z+} mat – *Hp1β*$^{m-z+}$ pat	0.935
wt mat – *Suv39h2*$^{m-z+}$ mat	0.0309
wt pat – *Suv39h2*$^{m-z+}$ pat	3.4×10^{-5}
wt mat – *Hp1β*$^{m-z+}$ mat	6.65×10^{-6}
wt pat – *Hp1β*$^{m-z+}$ pat	0.841
Suv39h2^{m-z+} mat – *Hp1β*$^{m-z+}$ mat	6.12×10^{-7}
Suv39h2^{m-z+} pat – *Hp1β*$^{m-z+}$ pat	0.00034

t-test: matPN/patPN	
wt - *Suv39h2*$^{m-z+}$	0.0132
wt - *Hp1β*$^{m-z+}$	1.07×10^{-14}
Suv39h2^{m-z+} - *Hp1β*$^{m-z+}$	0.0077

Figure 3.16: The effect of *Suv39h2* and *Hp1β* maternal deficiency on the PN size. **A.** Representative images of the DNA from wt, *Suv39h2*$^{m-z+}$ and *Hp1β*$^{m-z+}$ PN5 zygotes. DNA was visualized by DAPI. Bar = 10µm. **B.** Graph displaying sizes of wt, *Suv39h2*$^{m-z+}$ and *Hp1β*$^{m-z+}$ PN5 zygotes, including t-test values for the three mouse lines. **C.** Relative size differences between maternal and paternal PN (matPN/patPN) of the three mouse lines, including p-values.

Based on this result, we wondered whether the phenotype observed for *Hp1β*$^{m\text{-}z+}$ zygotes is within the Suv39h pathway. Therefore, PN sizes of *Suv39h2*$^{m\text{-}z+}$ zygotes were analyzed. Based on weak maternal euchromatic H3K9me3 and euchromatic PRC1 staining, the maternal PN was determined. Strangely, both PN of *Suv39h2*$^{m\text{-}z+}$ zygotes were smaller than wt zygotes (Figure 3.16.B). Generally, one would expect that maternal loss of the heterchromatic H3K9me3 HMT would result rather in the size increase of a PN than in its decrease. For the moment, we do not have an explanation for this observation. Also, the distance between the maternal and the paternal PN is not changed in *Suv39h2*$^{m\text{-}z+}$ compared to wt zygotes. This suggests that there is no developmental delay in the *Suv39h2*$^{m\text{-}z+}$ zygotes, which could explain this size difference. Despite the reduction in size of both PN, the relative size difference between the maternal and the paternal PN was less obvious in *Suv39h2*$^{m\text{-}z+}$ zygotes compared to wt zygotes, although not significantly (Figure 3.16.C). The examination of additional *Suv39h2*$^{m\text{-}z+}$ zygotes will resolve whether or not the loss of the size difference between maternal and paternal PN in *Hp1β*$^{m\text{-}z+}$ zygotes is within the Suv39h pathway.

Altogether, the equal size of maternal and paternal PN in *Hp1β*$^{m\text{-}z+}$ zygotes suggests that the chromatin of the maternal PN is more compacted by Hp1β than the paternal PN. This coincides with the enrichment of H3K9me3 maternally, which is the prominent chromatin binding site of the Hp1β CD. Neither euchromatic paternal Hp1β nor the little Hp1β PCH enrichment in late PN5 zygotes is involved in global paternal chromatin compaction. Therefore, Hp1β, putatively bound to maternal H3K9me3, globally compacts maternal chromatin, which results in the relative size difference of the maternal and the paternal PN.

Furthermore, the function of the two other well described H3K9 HMT, G9a and Eset, should be analyzed in respect to PN size. Preliminary analysis revealed that the maternal PN is even bigger than the paternal PN in *G9a*$^{m\text{-}z+}$ deficient zygotes, whereas maternally deficiency for *Eset* did not affect the PN size difference.

The loss of the size difference between maternal and paternal PN in *Hp1β*$^{m\text{-}z+}$ zygotes raised the question whether or not this is a zygotic phenotype. To investigate this, the PN sizes of late wt and *Hp1β*$^{m\text{-}z+}$ zygotes microinjected with either H_2O or with 7.5 ng/µl recombinant Hp1β were analyzed in respect to their PN sizes. The microinjection of 7.5 ng/µl recombinant Hp1β, Hp1β^{I161E} and Hp1α into wt zygotes did not affect the PN size in comparison to H_2O microinjected zygotes (Figure 3.17.A). The maternal PN size compared to the paternal PN size remained (Figure 3.17.B). Microinjection of recombinant Hp1β into *Hp1β*$^{m\text{-}z+}$ zygotes, though,

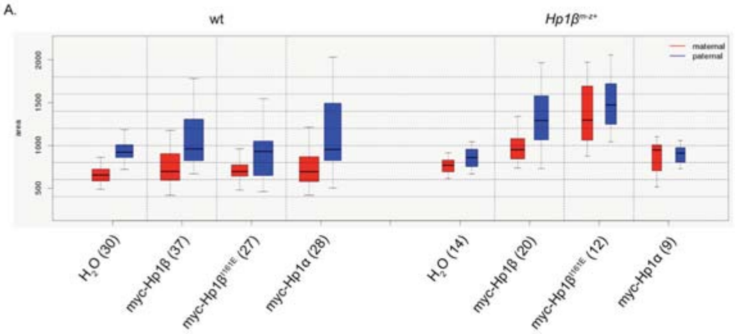

t-test		
wt	H2O mat-pat	4×10^{-12}
	myc-Hp1β mat-pat	2.3×10^{-06}
	myc-Hp1β^{I161E} mat-pat	6.2×10^{-09}
	myc-Hp1α mat-pat	0.0003
Hp1β^{m-z+}	H2O mat-pat	0.18
	myc-Hp1β mat-pat	0.0009
	myc-Hp1β^{I161E} mat-pat	0.47
	myc-Hp1α mat-pat	0.74

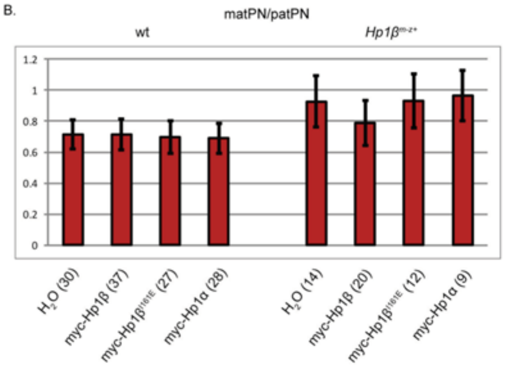

t-test		
wt	H_2O - myc-Hp1β	0.99
	H_2O - myc-Hp1β^{I161E}	0.39
	H_2O - myc-Hp1α	0.9
Hp1β^{m-z+}	H_2O - myc-Hp1β	0.017
	H_2O - myc-Hp1β^{I161E}	0.93
	H_2O - myc-Hp1α	0.73
wt - *Hp1β^{m-z+}*	H_2O - H_2O	0.0004
	myc-Hp1β - myc-Hp1β	0.063
	myc-Hp1β^{I161E} - myc-Hp1β^{I161E}	0.00058
	myc-Hp1α - myc-Hp1α	0.0008

Figure 3.17: Re-establishing the maternal/paternal PN size difference in *Hp1β^{m-z+}* zygotes by exogenously provided Hp1β. **A.** Box plot displaying the effect of microinjected H_2O, Hp1β, Hp1β^{I161E} and Hp1α on the PN size in wt and *Hp1β^{m-z+}* zygotes. Below: p-values. **B.** Relative size differences between maternal and paternal PN (matPN/patPN) of microinjected wt and *Hp1β^{m-z+}* zygotes, including p-values.

affected the size of the maternal PN in *Hp1β^{m-z+}* zygotes. Whereas the size difference of maternal and paternal PN in H_2O, Hp1β^{I161E} and Hp1α injected *Hp1β^{m-z+}* zygotes did not differ significantly, the microinjection of Hp1β resulted in the reestablishment of the significant size difference of the two PN (Figure 3.17.A). It is surprising that only exogenously provided Hp1β and not Hp1α reestablished the mat/pat PN size difference. This might be due to inefficient targeting of the recombinant Hp1α.

Unexpectedly, the actual PN sizes of *Hp1β^{m-z+}* zygotes microinjected with different Hp1 constructs varied (Figure 3.17.A). For the moment, there is no explanation for this. Nevertheless, the differences between the maternal and the paternal PN remained the same, despite the size increase, suggesting that this is a technical issue. Comparison of the matPN/patPN ratio of microinjected *Hp1β^{m-z+}* zygotes revealed a low p-value for H_2O - Hp1β compared to the other p-values of this group. Nevertheless, it is not significant (Figure 3.17.B). Furthermore, the comparison of the matPN/patPN ratio of wt and *Hp1β^{m-z+}* zygotes shows that it is significant for microinjected H_2O, $Hp1\beta^{I161E}$ and Hp1α, but not for microinjected Hp1β (Figure 3.17.B). This strongly suggests that exogenously provided Hp1β is able to reduce the maternal PN size of $Hp1\beta^{m\text{-}z+}$ zygotes and to establish the significant size difference of maternal and paternal PN as observed in wt zygotes, putatively by binding to maternally provided H3K9me3.

Another set of experiments, performed in wt zygotes, suggests that the activity of the SUV39H1 together with Hp1β influences the PN size. Upon microinjection of SUV39H1 mRNA into wt PN0 zygotes, a significant size reduction of the maternal PN was detected at the PN5 zygotic stage. The overexpression of a hyperactive SUV39H1 HMT ($SUV39H1^{H320R}$) then resulted in a significant decrease in PN size of both PN. Interestingly, microinjection of an inactive form of the SUV39H1 HMT ($SUV39H1^{H324L}$) also affected the PN sizes. It led to a significant size decrease of the maternal PN. This might be explained by the maternally inherited H3K9me3, which is the binding site of the SUV39H1 CD, possibly compacting chromatin (Figure 3.18). Surprisingly, the presence and activity of Suv39h2 in zygotes did not significantly reduce the size of neither maternal nor paternal PN (Figure 3.18). Mutational analysis or domain swaps of the two Suv39h HMTs might give insight into this specificity. Finally, the co-microinjection of SUV39H1 together with Hp1β led to a highly significant size decrease of the maternal and the paternal PN (Figure 3.18). Nevertheless, in all these measures, the relative size difference of the two PN was less affected than the actual size. This is in not full agreement with our previous results where maternal *Hp1β* deficiency led to a PN size increase only maternally. It might be explained by the accumulation of H3K9me3 maternally. Possibly, the exogenously provided HMTs are maternally and paternally equally active, leading to similar *de novo* H3K9me3 on both PN, and, therefore, resulting in more maternal H3K9me3 putatively bound by Hp1β and, therefore, compacting chromatin.

Taken together, our results suggest that the maternal PN is smaller than the paternal PN because of Hp1β, putatively bound to maternal H3K9me3, and therefore compacting maternal chromatin to a higher extend than paternal chromatin. In $Hp1\beta^{m\text{-}z+}$ zygotes, this size difference is lost. Microinjection of recombinant Hp1β into $Hp1\beta^{m\text{-}z+}$ zygotes, though, reestablishes the size decrease of maternal PN, suggesting that it is a zygotic phenotype. Furthermore, the maternal and paternal PN sizes of wt zygotes can be decreased by the presence and the enzymatic activity of abundant exogenously provided members of the Suv39h pathway.

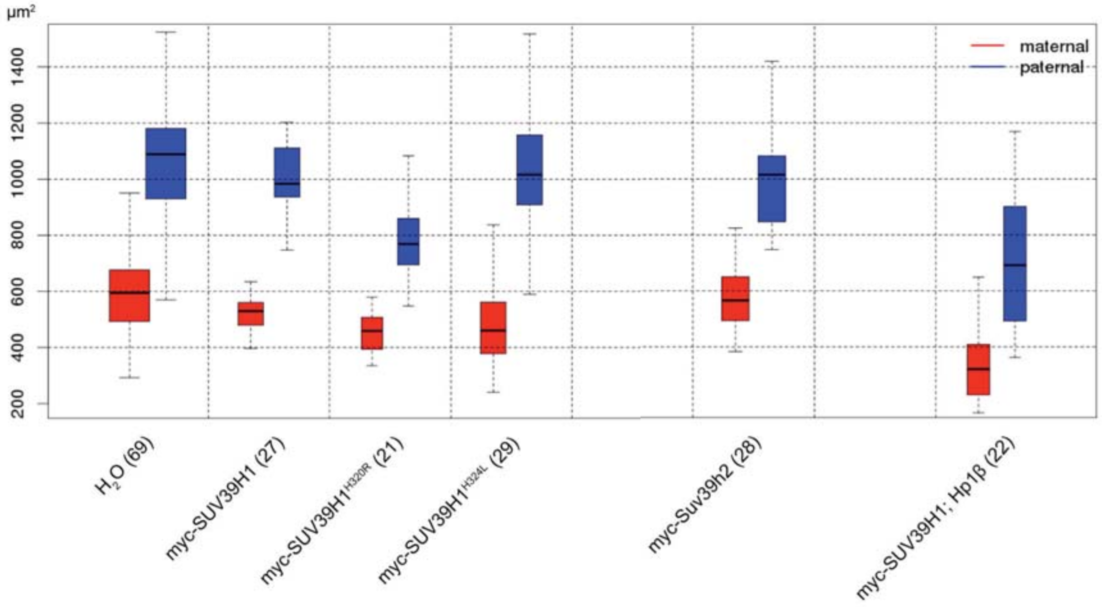

t-test	
wt mat – SUV39H1 mat	0.0076
wt pat – SUV39H1 pat	0.11
wt mat – SUV39H1^{H320R} mat	9.43×10^{-6}
wt pat – SUV39H1^{H320R} pat	3.3×10^{-6}
wt mat – SUV39H1^{H324L} mat	0.0005
wt pat – SUV39H1^{H324L} pat	0.769
wt mat – Suv39h2 mat	0.831
wt pat – Suv39h2 pat	0.85
wt mat – SUV39H1, Hp1β mat	1.45×10^{-8}
wt pat – SUV39H1, Hp1β pat	3.48×10^{-6}

Figure 3.18: The effect of exogenously provided Suv39h and Hp1β on the size of C57BL/6 wt zygotes. The zygotes were microinjected with the constructs indicated right after fertilization. The Suv39h and the Hp1β mRNA were injected at a concentration of 100ng/μl. They were fixed at the PN5 zygotic stage. Below: p-values.

Discussion

The chromatin marks of maternal PN resemble the chromatin signature of ESC and other cell types, whereas the chromatin marks of the paternal PN in the mouse zygote display a more immature chromatin state, hyperacetylated and hypomethylated and therefore less condensed than maternal chromatin. This is visualized by the size difference of the maternal and the paternal PN. Therefore, the mouse zygote is a good model to study determinants of the nuclear size and chromatin compaction. Zygotes maternally deficient for chromatin associated factors can be analyzed for either size increase of maternal PN or size decrease of the paternal PN. Interestingly, we show here experimentally that Hp1β is a determinant factor for the compaction of maternal chromatin. Hp1β IF analysis in wt zygotes displays maternal and paternal euchromatic staining. Despite the euchromatic presence of Hp1β in both PN, the maternal PN is smaller. A major difference between maternal and paternal chromatin is the lack of global paternal H3K9me3, which is the histone mark that is bound by CD of Hp1β with the highest affinity. This suggests that it is Hp1β bound to H3K9me3 that determines the PN size reduction. According to that, the reduction, but not complete loss of H3K9me3 in *Suv39h2*$^{m\text{-}z+}$ zygotes results in an intermediate increase of the maternal PN size, compared to wt and *Hp1β*$^{m\text{-}z+}$ zygotes. Furthermore, exogenously provided SUV39H1 tri-methylates paternal H3K9, which results in the decrease of the paternal PN size.

The results of these experiments show that Hp1β within the Suv39h pathway compacts chromatin globally *in vivo*.

Finally, it would be interesting to analyze the effect of the PN size increase or decrease in respect to global zygotic transcription. Possibly, it also affects the ZGA in 2-cell embryos. Thus, also the developmental potential of these zygotes should be analyzed. Furthermore, the precocious enzymatic activity of the Suv39h HMT in zygotes might lead to early formation of heterochromatin.

Material and Methods

Wild-type and mutant zygotes were obtained, cultured and fixed at the PN5 zygotic stage as described before. Plasmids containing the myc-tagged SUV39H1, Suv39h2 and Hp1β

ORFs were obtained from T. Jenuwein. mRNA was generated as described before. In the rescue experiment, 7.5 ng/µl mRNA was microinjected into the cytoplasm of *in vitro* fertilized wt and *Hp1β*$^{m\text{-}z+}$ C57BL/6 zygotes as described before. In the Suv39h activity experiment, 100 ng/µl mRNA was microinjected into the cytoplasm of *in vitro* fertilized wt C57BL/6 zygotes. Zygotes were fixed at the PN5 zygotic stage. Maternal and paternal PN were determined based on DAPI, H3K9me3, Hp1β and Rnf2 IF stainings. Confocal images of the zygotes at their biggest radius were taken with a LSM700. Images were analyzed with ImageJ.

3.2.3. Impact of Epigenetic Repressors on Zygotic 5mC to 5hmC conversion

Introduction

Within a few hours after fertilization, the paternal genome rapidly loses its global 5mC DNA methylation (Mayer et al., 2000a; Oswald et al., 2000; Santos et al., 2002). The maternal genome remains DNA methylated in the zygote and is only passively DNA demethylated via DNA synthesis. A maternal factor essential for early development called PGC7/Stella was identified to protect the maternal DNA methylation state of several imprinted loci and of the epigenetic asymmetry (Nakamura et al., 2007).

Recently, it was shown that 5mC is converted to 5hmC by the TET proteins (Williams et al., 2011; Wu and Zhang, 2010). Interestingly, 5hmC was detected to appear in the paternal PN, while 5mC diminishes (Iqbal et al., 2011), suggesting that paternal 5mC is not removed, but hydroxymethylated to 5hmC in the zygote. This process has been shown to be dependent on TET3 (Gu et al., 2011). After hydroxymethylation of the paternal 5mC in the zygote, the 5hmC modification is diluted passively via DNA synthesis up to blastocyst embryos, like 5mC maternally (Inoue and Zhang, 2011).

In ESC, Tet1 was shown to convert 5mC to 5hmC (Williams et al., 2011; Wu and Zhang, 2010). Tet1 preferentially binds CpG-rich sequences at promoters of transcriptionally active and also Polycomb-repressed genes (Williams et al., 2011; Wu and Zhang, 2010). In respect to repression, Tet1 contributes to silencing by facilitating recruitment of PRC2 to CpG-rich gene promoters (Wu and Zhang, 2010). Therefore, DNA hydroxymethylation has been linked to PRC2. DNA methylation on the other hand has been associated with the Suv39h pathway. In cells, members of the Suv39h pathway as well as other H3K9 HMTs interact with DNA methyltransferases, linking H3K9 methylation and Hp1β with DNA methylation (Fuks et al., 2003; Smallwood et al., 2007). These results implicate a role of epigenetic modifiers in DNA methylation and DNA hydroxymethylation.

Therefore, we wondered whether or not epigenetic modifiers globally affect DNA methylation or DNA hydroxymethylation. Zygotes, which were maternally deficient for either PcG proteins or members of three H3K9 HMT pathways, were analyzed for their maternal and paternal 5mC and 5hmC content.

Results

In order to determine the 5mC/5hmC content of a zygote, the sum of the signal intensity for either 5mC or 5hmC of a confocal stack was plotted against the maximum area of each zygote (Figure 3.20). The 5mC intensity, 5hmC intensity and the area of the all zygotes from one group were displayed in a box plot (Figure 3.21.A.B.C). The signal intensity of zygotes of one group was then either multiplied by their areas (Figure 3.22.A) or divided by their areas (Figure 3.22.B), determining the signal intensity of 5mC or 5hmC per μm^2. Furthermore, the relative maternal/paternal value for the intensity of the whole area for 5mC and 5hmC was determined (Figure 3.22.C).

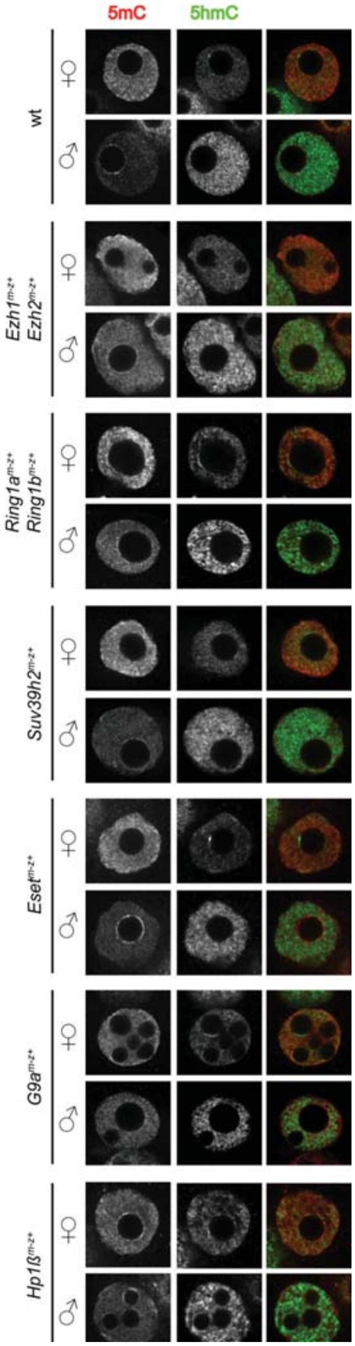

Figure 3.19: Representative confocal images of PN5 zygotes of the seven mouse lines analyzed. Zygotes were stained with antibodies against 5mC and 5hmC.

Wild-type

First, we confirmed that wt PN5 zygotes display an asymmetry for 5mC DNA methylation (Figure 3.19). Maternal PN showed in average 1.7 times more 5mC signal than paternal PN (Figure 3.22.C). This indicates that paternal PN DNA is less methylated than maternal DNA. Nevertheless, paternal DNA is not completely devoid of 5mC. The asymmetry for 5hmC in wt zygotes is more evident with a maternal/paternal ratio of 0.3 (Figure 3.22.C). This difference between 5mC and 5hmC is probably caused by the different antibody properties. The intensity per μm^2 as well as the intensity of the whole area is significantly different for 5mC and 5hmC between maternal and paternal PN in wt zygotes (Figure 3.22.A.B).

PRC2 maternal deficiency

In PRC2 mutants (*Ezh1*$^{m\text{-}z+}$*; Ezh2*$^{m\text{-}z+}$), the maternal and paternal signal intensity for 5mC is similar to wt zygotes (Figure 3.19 and 3.20.A). The 5hmC signal in maternal PN is surprisingly high compared to wt zygotes (Figure 3.20.A). Nevertheless, 5hmC is more enriched paternally (Figure 3.20.A) and also the 5hmC value for the area×intensity between maternal and paternal PN is significantly different (Figure 3.22.A). Furthermore, the maternal/paternal ratio for 5mC is greater than one and for 5hmC it is smaller than 0.5 (Figure 3.22.C).

We conclude from these analyses that maternal deficiency of *Ezh1*$^{m\text{-}z+}$*; Ezh2*$^{m\text{-}z+}$ does not affect the protection of maternal 5mC or the paternal 5mC to 5hmC conversion.

PRC1 maternal deficiency

Ring1a$^{m\text{-}z+}$*; Ring1b*$^{m\text{-}z+}$ PN are small in size compared to wt zygotes. Furthermore, they often contain only one big NPB, unlike wt PN. It must be stated that in our analysis the area of NPBs were not subtracted from the PN area, which might affect the analysis of *Ring1a*$^{m\text{-}z+}$*; Ring1b*$^{m\text{-}z+}$ PN (Figure 3.19). Nevertheless, paternal 5mC and maternal 5hmC are low, as in wt zygotes (Figure 3.20.A). Surprisingly, the enrichment of maternal 5mC and paternal 5hmC as it is observed in wt zygotes is not detected in *Ring1a*$^{m\text{-}z+}$*; Ring1b*$^{m\text{-}z+}$ PN (Figure 3.20.A). This logically reduces the asymmetry of 5mC and 5hmC. Therefore, the comparison of the maternal area×intensity value with the paternal area×intensity value is not significant (Figure 3.22.A). The intensity per μm^2 for maternal and paternal 5mC is significant, though. Furthermore, the maternal/paternal ratio of the intensity of the whole area shows similar relative 5mC signal as wt zygotes, whereas the ratio of the 5hmC signal above 0.5 is higher than in wt PN (Figure 3.22.C).

Ring1a^{m-z+}*; Ring1b*$^{m-z+}$ zygotes are defective in many aspects (Posfai et al, unpublished). Therefore, it is not known for the moment, whether or not the reduced 5mC/5hmC asymmetry compared to wt zygotes is due to the *Ring1a*$^{m-z+}$*; Ring1b*$^{m-z+}$ deficiency directly or indirectly. Rescue experiments would answer this question.

Suv39h2^{m-z+} *zygotes*

Among all mutant lines analyzed, *Suv39h2*$^{m-z+}$ zygotes were most similar to wt zygotes in respect to DNA methylation and DNA hydroxymethylation. Analyses of the 5mC asymmetry in *Suv39h2*$^{m-z+}$ PN show a similar asymmetry as in wt PN. The same is observed for 5hmC (Figure 3.19, 3.20.B). Furthermore, the intensity per μm^2 between maternal and paternal PN is significant for 5mC and 5hmC (Figure 3.22.B). Additionally, it is also significantly different between maternal and paternal PN for the intensity of the whole area for 5hmC (Figure 3.22.A).

These results suggest no effect of the Suv39h pathway on either paternal 5mC to 5hmC conversion or maternal protection of DNA methylation.

Eset^{m-z+} *zygotes*

Zygotes maternally deficient for *Eset* display enhanced paternal 5mC signal (Figure 3.20). This results in a maternal/paternal ratio for the intensity of the whole area for 5mC close to 1 (Figure 3.22). Nevertheless, the intensity per μm^2 between maternal and paternal PN is significant for 5mC. The asymmetry for 5hmC on the other hand is more evident than the asymmetry for 5mC (Figure 3.20.B).

The enhanced maternal/paternal ratio of around 0.5 for 5hmC, and also the very low ratio of 5mC just above 1 (Figure 3.22), suggests a function of Eset in DNA demethylation.

G9a$^{m\text{-}z+}$ *zygotes*

Similar to *Eset*$^{m\text{-}z+}$ zygotes, but more drastic, a low maternal/paternal ratio of the intensity of the whole area for 5mC together with a high maternal/paternal ratio clearly above 0.5 for 5hmC was detected in *G9a* deficient zygotes (Figure 3.22.C). Most evident is the high intensity of the whole area value for maternal 5hmC (Figure 3.22.A), suggesting that *G9a* protects maternal 5mC from conversion to 5hmC. A scatter plot displaying the individual PN shows enhanced 5hmC maternally, but also more 5mC paternally (Figure 3.20.B).

The 5mC to 5hmC conversion in *G9a*$^{m\text{-}z+}$ zygotes is reduced paternally, whereas maternal DNA is enriched for 5hmC compared to wt zygotes.

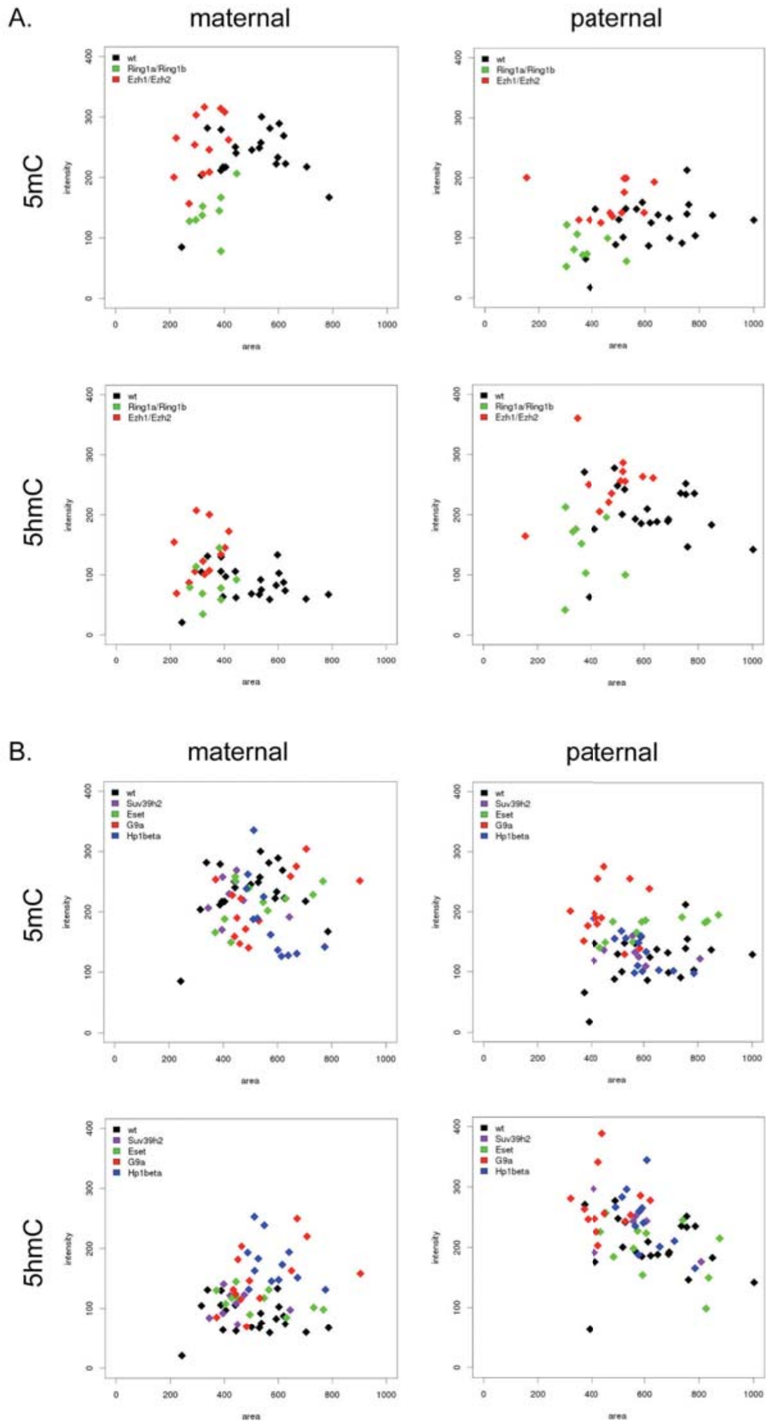

Figure 3.20: Scatter plots displaying the area (X-axis) and the intensity (y-axis) of each PN. **A.** Scatter plots of wt, *Ring1a/Ring1b*$^{m-z+}$ and *Ezh1/Ezh2*$^{m-z+}$ PN. Left: maternal PN; right: paternal PN; top: 5mC signal; bottom: 5hmC signal. **B.** Scatter plots of wt, *Suv39h*$^{m-z+}$, *Eset*$^{m-z+}$, *G9a*$^{m-z+}$ and *Hp1β*$^{m-z+}$ PN. Left: maternal PN; right: paternal PN; top: 5mC signal; bottom: 5hmC signal.

Hp1β$^{m\text{-}z+}$ zygotes

Finally, *Hp1β*$^{m\text{-}z+}$ zygotes display a similar phenotype as *G9a*$^{m\text{-}z+}$ zygotes. Whereas paternal 5mC is like in wt zygotes, maternal 5mC is reduced (Figure 3.20.B). Inversely, 5hmC is enriched maternally, suggesting that Hp1β protects 5mC from conversion to 5hmC. The intensity per μm^2 is not significant for 5mC or for 5hmC (Figure 3.22.B). Interestingly, it is significant for the intensity of the whole area, though (Figure 3.16.A). The maternal/paternal ratio of the intensity of the whole area for *Hp1β*$^{m\text{-}z+}$ zygotes for 5mC and for 5hmC is similar to *G9a*$^{m\text{-}z+}$ zygotes (Figure 3.22).

These results suggest that there is more 5mC to 5hmC conversion in the maternal PN of *Hp1β*$^{m\text{-}z+}$ zygotes.

Discussion

Our initial hypothesis that epigenetic repressors affect maternal 5mC content and paternal 5mC to 5hmC conversion was right. Among the six mutant mouse lines analyzed, we detected abnormalities in at least three lines. The results are all based on IF stainings, which is not the ideal method to quantitatively measure 5mC or 5hmC content. Nevertheless, the limited tissue available (one cell!) urged us to measure 5mC and 5hmC via IF stainings for pre-screening of a possible effect of an epigenetic repressor towards 5mC or 5hmC.

In cell lines, PRC2 has been implicated with the TET proteins and 5hmC. In mouse zygotes maternally deficiency for *Ezh1*$^{m\text{-}z+}$*; Ezh2*$^{m\text{-}z+}$ did not result in the global change of 5hmC. The 5mC to 5hmC conversion occurs in these mutants like in wt zygotes. PRC1 mutants, on the other hand, affect the asymmetry. But not only 5hmC is affected, also 5mC is reduced. Interestingly, it is the maternal 5mC and the paternal 5hmC enrichment that is affected. The development of *Ring1a*$^{m\text{-}z+}$*; Ring1b*$^{m\text{-}z+}$ zygotes is delayed (Posfai et al, unpublished). Therefore, it is possible that the *Ring1a*$^{m\text{-}z+}$*; Ring1b*$^{m\text{-}z+}$ zygotes are not PN5 stage zygotes, but only PN3 stage zygotes. In another step of analysis it needs to be determined whether or not this would influence the analysis. Furthermore, it should be analyzed whether or not this putative phenotype is directly due to the *Ring1a*$^{m\text{-}z+}$*; Ring1b*$^{m\text{-}z+}$ genotype or not. It has been shown that *Ring1a*$^{m\text{-}z+}$*; Ring1b*$^{m\text{-}z+}$ oocytes display the misregulation of thousands of genes (Posfai et al, unpublished). Therefore, it is very well possible that the effect of *Ring1a*$^{m\text{-}z+}$*; Ring1b*$^{m\text{-}z+}$ on 5mC and 5hmC is only an indirect effect. This should be tested by rescue experiments.

Interestingly, maternal deficiency for *Suv39h2* did not result in the loss of 5mC/5hmC asymmetry. The Suv39h HMTs have been shown to interact with Dnmts. During zygotic development, they do not protect maternal 5mC or interact with proteins like PGC7/Stella that protect maternal 5mC. Maternal 5mC is not affected in *Suv39h2*$^{m-z+}$ zygotes. Alike, maternal deficiency for the H3K9 HMT *Eset* does not result in the loss of maternal 5mC. Rather, paternal 5mC is higher than in wt zygotes. This implicates a function of Eset in the 5mC to 5hmC conversion. Interestingly, paternal 5hmC is reduced, which is in agreement with a function of Eset in the 5mC to 5hmC conversion. Therefore, Eset should be tested for interactions with Tet3. The lack of paternal 5mC to 5hmC conversion observed in *Eset*$^{m-z+}$ zygotes is less evident than in *Tet3* mutants (Gu et al., 2011).

The most evident effect on the 5mC to 5hmC conversion in zygotes was observed in maternally deficient *G9a* and *Hp1β* zygotes. In both lines, enhanced conversion of maternal 5mC is observed. This suggests that G9a and even more so Hp1β protect maternal DNA methylation. G9a and Hp1β have been shown to interact (Chin et al., 2007). Thus, their putative function in the protection of maternal DNA might be in the same pathway. The analysis of *G9a* and *Hp1β* double mutants would answer that question. Furthermore, it would be interesting to test, whether or not this protection of DNA methylation by G9a and Hp1β is PGC7/Stella dependent or independent. Altogether, these results suggest that G9a and Hp1β not only interact with the DNA methyltransferases (Esteve et al., 2006; Smallwood et al., 2007), but also protect DNA methylation from its conversion to 5hmC. It remains to be determined though, whether this occurs in a histone methylation dependent or independent manner.

Material and Methods

Zygotes of the different mouse lines were *in vitro* fertilized at once and fixed at the PN5 stage. The fixed zygotes were stained as previously described (Iqbal et al., 2011). 5mC was detected using a monoclonal antibody from eurogentec (1:500). 5hmC was detected using a polyclonal antibody from Active Motif (1:500). Images were analyzed by ImageJ.

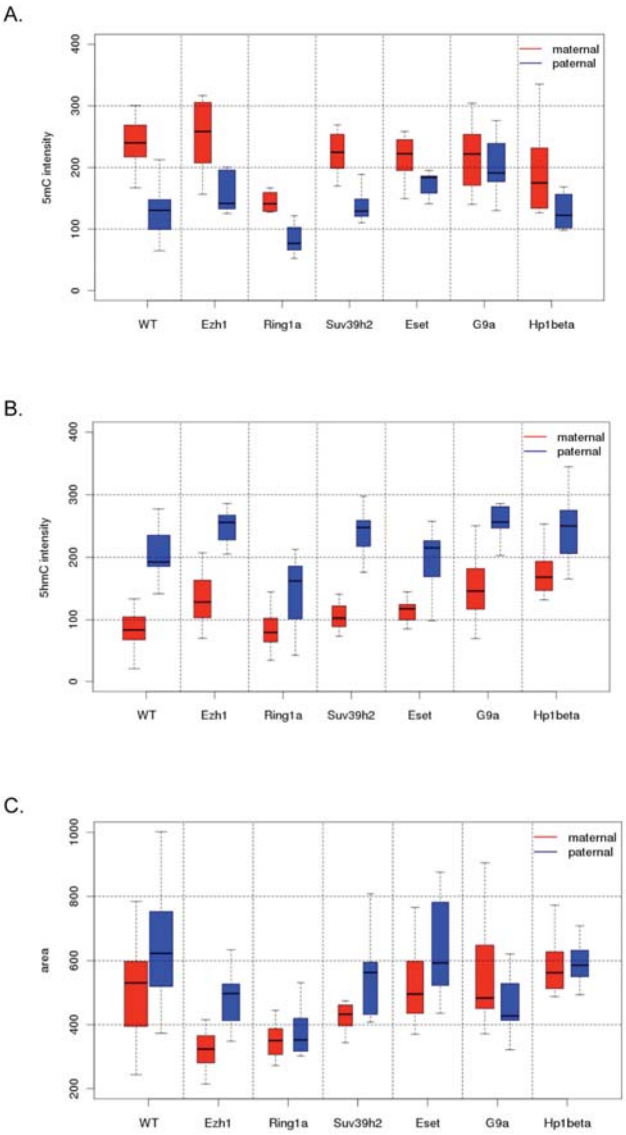

Figure 3.21: Box plots of the 5mC intensity (**A.**), the 5hmC intensity (**B.**) and the area (**C.**) of the zygotes from the seven mouse lines analyzed.

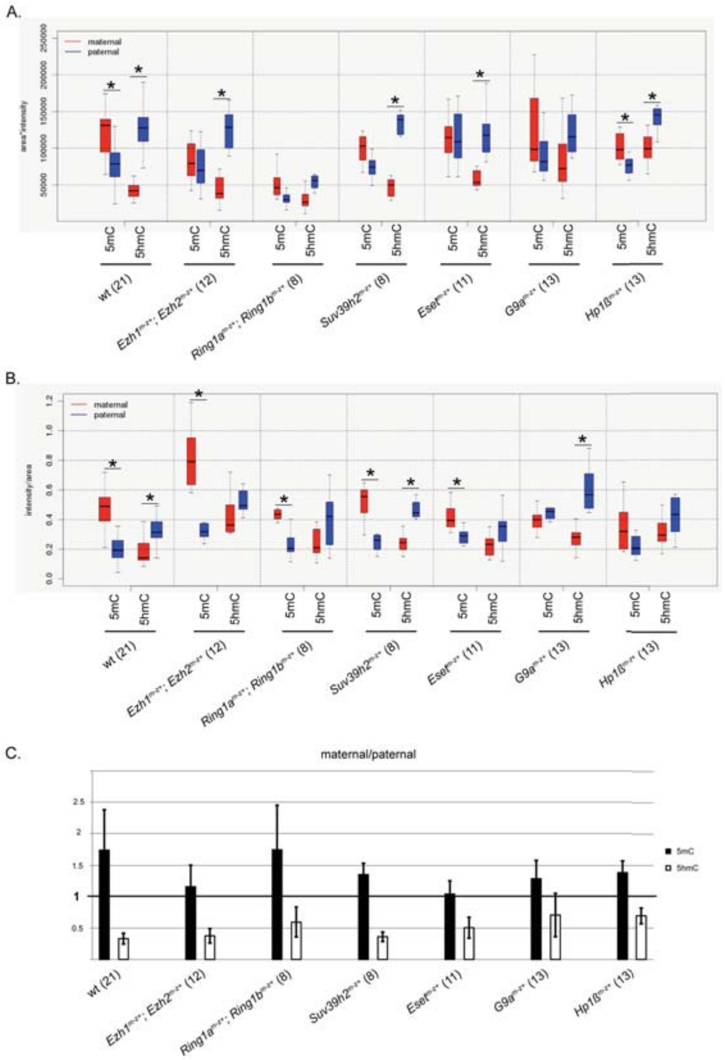

Figure 3.22: A. Box plot displaying the values for area×intensity of maternal and paternal PN of the seven mouse lines. **B.** Box plot displaying the values for intensity/area (µm^2) for the seven mouse lines. **C.** Relative value of the area×intensity between maternal/paternal PN. Red: maternal PN. Blue: paternal PN. Black: 5mC. White: 5hmC.

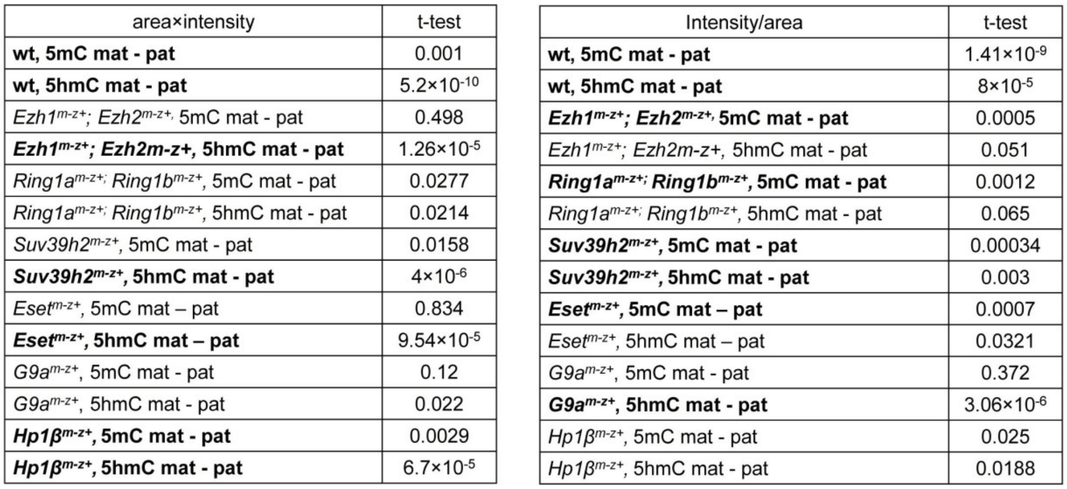

area×intensity	t-test
wt, 5mC mat - pat	0.001
wt, 5hmC mat - pat	5.2×10^{-10}
Ezh1^{m-z+}*; Ezh2*$^{m-z+,}$ 5mC mat - pat	0.498
Ezh1^{m-z+}***; Ezh2m-z+*, 5hmC mat - pat**	1.26×10^{-5}
Ring1a$^{m-z+;}$ *Ring1b*$^{m-z+}$, 5mC mat - pat	0.0277
Ring1a$^{m-z+;}$ *Ring1b*$^{m-z+}$, 5hmC mat - pat	0.0214
Suv39h2^{m-z+}, 5mC mat - pat	0.0158
Suv39h2^{m-z+}**, 5hmC mat - pat**	4×10^{-6}
Eset^{m-z+}, 5mC mat – pat	0.834
Eset^{m-z+}**, 5hmC mat – pat**	9.54×10^{-5}
G9a^{m-z+}, 5mC mat - pat	0.12
G9a^{m-z+}, 5hmC mat - pat	0.022
Hp1β^{m-z+}**, 5mC mat - pat**	0.0029
Hp1β^{m-z+}**, 5hmC mat - pat**	6.7×10^{-5}

Intensity/area	t-test
wt, 5mC mat - pat	1.41×10^{-9}
wt, 5hmC mat - pat	8×10^{-5}
Ezh1^{m-z+}***; Ezh2***$^{m-z+,}$ **5mC mat - pat**	0.0005
Ezh1^{m-z+}*; Ezh2m-z+,* 5hmC mat - pat	0.051
Ring1a$^{m-z+;}$ ***Ring1b***$^{m-z+}$**, 5mC mat - pat**	0.0012
Ring1a$^{m-z+;}$ *Ring1b*$^{m-z+}$, 5hmC mat - pat	0.065
Suv39h2^{m-z+}**, 5mC mat - pat**	0.00034
Suv39h2^{m-z+}**, 5hmC mat - pat**	0.003
Eset^{m-z+}**, 5mC mat – pat**	0.0007
Eset^{m-z+}, 5hmC mat – pat	0.0321
G9a^{m-z+}, 5mC mat - pat	0.372
G9a^{m-z+}**, 5hmC mat - pat**	3.06×10^{-6}
Hp1β^{m-z+}, 5mC mat - pat	0.025
Hp1β^{m-z+}, 5hmC mat - pat	0.0188

Figure 3.23: p-values determined by t-test for the graphs of Figure3.16.A and B. Significant values are written in bold.

4. Discussion

Targeting of PRC1 by Cbx2

Recently, it was shown for BPTF, which is a subunit of the NURF chromatin remodeling complex regulator, that it recognizes H3K4me3 and H4K16 acetylation simultaneously at the mononucleosomal level (Ruthenburg et al., 2011). The C-terminal plant homeodomain (PHD) finger has been described to bind H3K4me3 (Wysocka et al., 2006). This PHD finger is linked by a 15 aa long α-helix with a bromodomain (Li et al., 2006), which exhibits binding selectivity for H4K16 acetylation in combination with H3K4me3 (Ruthenburg et al., 2011). Thus, the authors show that binding of BPTF is dependent on two protein modules that covalently bind modified histone tails. We propose in this study also a bi-modular targeting mechanism of Cbx2 whith one module, the CD, binding the H3K27me3 modified histone tail and with the other module binding AT-rich DNA sequences. These two modules are, similar as in BPTF, linked by 15 aa long linker. In the crystal structure of the human CBX2 CD, the N-terminus of the linker forms an α-helix (Kaustov et al., 2011), like the linker in BPTF. This suggests that the CD and the AT-hook motif together function in a given conformation, whereas the AT-hook motif confers rather unspecific binding to AT-rich DNA sequences, the CD ensures higher specificity. At PCH both modules are sufficient to target Cbx2. Only abrogation of both modules together results in loss of enrichment at heterochromatin. This suggests that the CD and the AT-hook motif display a positive, additive effect on Cbx2 targeting to heterochromatin. This is emphasized by the protein dynamics measured for Cbx2 containing point mutations in either the CD or the AT-hook, which result in a similar increase of Cbx2 mobility at heterochromatin.

It is interesting to note that mitotic chromosomes in the first three cell divisions of the mouse embryo display also an asymmetry for Ring1b and H3K9me3 on chromosomal arms, thus at euchromatic sites, and not only at pericentromeric sites (Puschendorf et al., 2008). It is possible that the banding pattern observed for Ring1b coincide with the AT-rich G-bands observed by Giemsa staining. AT-richness of these bands would implicate a PRC1 targeting mechanism to euchromatin similar as observed in PCH, which would be dependent on the CD and the AT-hook of Cbx2.

Among the Cbx orthologs, Cbx2 is the only one to contain an AT-hook motif. Its expression peaks in oocytes and in preimplantation embryos. This suggests that the targeting mechanism for PRC1 we propose is occurring in a defined developmental time window. Interestingly, the CD and the AT-hook of Cbx2 are conserved in zebrafish. Furthermore, zebrafish Cbx2 has been shown to be maternally provided with putative function during early embryonic development (Kawamura et al., 2002). This suggests conservation of Cbx2 function in respect to its targeting mechanism within a developmental window among vertebrates.

It is evident that PRC1 complexes containing different Cbx orthologs exhibit different chromatin targets. A PRC1 complex containing Cbx2 is enriched at paternal PCH and also in a certain pattern at euchromatic bands in mitotic chromosomes. These chromatin targets are probably specific to Cbx2 due to its AT-hook. In ESCs or in differentiated cells, though, other Cbx orthologs are predominant. They do not only lack the AT-hook, but also display different binding affinities for methylated H3 histone tails. Thus, PRC1 containing different Cbx orthologs will localize to certain chromatin regions due to specific targeting properties. Therefore, it would be interesting to investigate the localization of the Cbx orthologs in a genome wide approach in different cell types. This would not only display the AT-hook dependent Cbx2 targets, but also unravel the target properties of the other Cbx orthologs.

Interdependency of the Suv39h pathway and PRC1

One might ask naively: why have the two major epigenetic repressive pathways besides DNA methylation, not been described to colocalize? Why are they kept separate? What disadvantage would result from such a colocalization to an organism?

I hypothesize that the answer to these questions lies in their targeting mechanism. Different targets display different chromatin features, which facilitate RNA or DNA targeting mechanisms and further silencing. Therefore, the silencing machineries have evolved simultaneously to their targets. The silencing of one chromatin stretch might be efficiently silenced by one pathway, but not by the other pathway, due to a long established linkage of the silencer and its target.

The Suv39h pathway is older than the PcG proteins. It appears already in *S. pombe* and is highly conserved up to humans (Krauss, 2008). In these organisms it is associated with the silencing of PCH. During time, PCH and the Suv39h pathway evolved together. Thus, its targeting mechanism evolved concomitantly. Whereas targeting in *S. pombe* implicates non-coding centromeric transcripts in targeting (Grewal, 2010), non-coding transcripts of the pericentromeric major satellite repeats have been proposed to target Hp1β also to paternal PCH in mouse zygotes (Probst et al., 2010). This is thought to be crucial for heterochromatin maturation and finally recruitment of the Suv39h pathway to paternal chromatin. Thus, in mouse Hp1 is thought to target the Suv39h pathway to PCH via interaction with ncRNA. Based on this model, though, it was surprising that recombinant SUV39H1 microinjected into wt zygotes resulted in paternal establishment of H3K9me3 within a few hours. This raises the question, whether the SUV39H1 targeting to paternal PCH is actually dependent on the interaction of Hp1β with major satellite transcripts, or whether it is not just zygotic Suv39h, which is targeted to paternal PCH by satellite transcripts from the 4-cell stage onwards in mouse. To test, whether Hp1β, as it has been proposed, or the Suv39h HMTs directly are targeted to PCH for *de novo* establishment of heterochromatin, it would be interesting to microinject recombinant SUV39H1 into *Hp1β*$^{m\text{-}z+}$ zygotes and analyze the ability of SUV39H1 in setting H3K9me3 paternally independent of Hp1β. Taken together, unlike the targeting mechanism of Cbx2 to PCH, targeting of the canonical Suv39h pathway is not fully understood yet.

We describe in our evolutionary study Cbx2 paralogs appearing in cnidarians (metazoan). Nevertheless, so far only early bilateral animals have been described to form PRC1 and PRC2 (Whitcomb et al., 2007). Thus, the PcG are young in comparison to the Suv39h pathway. Unlike Suv39h targets, PcG proteins have evolved to maintain the repressed state of facultative heterochromatin or silenced genes. This demands higher specificity than the silencing of repeats, which might has led to the appearance of this pathway, ensuring this specificity. Nevertheless, the maintenance of transcriptional silencing is achieved using similar protein domains, such as SET domains and CDs. I hypothesize that the maintenance of silencing via such domains is simply most efficient. That would explain, why they evolved in this similar way, originally probably by gene or protein domain duplication and further functional separation. Simultaneously, again, a targeting mechanism of PcG must have evolved. This targeting mechanism might, like for the Suv39h pathway, involve ncRNA, as described for HOTAIR and ANRIL (Rinn et al., 2007; Yap et al., 2010). Nevertheless, this ncRNA must display a different feature compared to transcripts of major satellites. Perhaps, secondary RNA structures confer this specificity.

Taken into account that classical PcG targets were described to be genes, it was surprising to detect PRC1 at paternal PCH, a classical Suv39h target, and to unravel a targeting mechanism that is independent on ncRNA. It should be mentioned again that unlike the other Cbx orthologs, Cbx2 has not been described to bind RNA at all. In other words, the ncRNA independent targeting mechanism of Cbx2 to the classical Suv39h target probably evolved in such a way that it does not interfere with the putative targeting mechanism of the Suv39h pathway to paternal PCH. Nevertheless, the similarities of the two pathways do interfere to a certain extent. The binding affinity of the CDs of Hp1β and Cbx2 putatively evolved in a way that inhibits colocalization. The question remains though, why this separation of the two pathways is at all necessary. Why is PRC1 blocked from binding to maternal PCH? And what consequence would colocalization of the two pathways have for preimplantation embryos? This might be due to a quality control for the zygote. Actually, the whole asymmetry of maternal and paternal chromatin might be a quality control for the newly formed organism. After all, entry of the sperm head into an oocyte, that will eventually form an embryo, nurtured by the mother, is a critical moment. Foreign DNA entering a cell is of potential danger. Therefore, it makes sense to mark the ‘intruders’ chromatin differentially than one’s own chromatin, initially. This gives the newly formed embryo a time window to abort development, in case the paternal DNA turns out to be unfavorable for embryonic development. This parent of origin specific epigenetic marking of chromatin enables discrimination of the two genomes even after intermingling of maternal and paternal DNA after the first cell division, beyond the ZGA in late 2-cell embryos and up to the 4-8 cell stage embryos, where the parental chromatin states assimilate. Thus, from my point of view, blocking of PRC1 by Hp1β maintains the parent of origin specific marking of heterochromatin, keeping the highly repetitious paternal major satellite repeats, distinct from the maternal repeats. Finally, it would be interesting to test whether or not this parent of origin specific epigenetic marking is conserved in preimplanation embryos of other species.

Size Difference of Maternal and Paternal Pronuclei

The chromatin marks of maternal PN resemble the chromatin signature of ESC and other cell types, whereas the chromatin marks of the paternal PN in the mouse zygote display a more immature chromatin state, hyperacetylated and hypomethylated and therefore less condensed than maternal chromatin. This is visualized by the size difference of the maternal and the paternal PN. Therefore, the mouse zygote is a good model to study determinants of the nuclear size and chromatin compaction. Zygotes maternally deficient for chromatin associated factors can be analyzed for either size increase of maternal PN or size decrease of the paternal PN. Interestingly, we show here experimentally that Hp1β is a determinant factor for the compaction of maternal chromatin. Hp1β IF analysis in wt zygotes displays maternal and paternal euchromatic staining. Despite the euchromatic presence of Hp1β in both PN, the maternal PN is smaller. A major difference between maternal and paternal chromatin is the lack of global paternal H3K9me3, which is the histone mark that is bound by CD of Hp1β with the highest affinity. This suggests that it is Hp1β bound to H3K9me3 that determines the PN size reduction. According to that, the reduction, but not complete loss of H3K9me3 in *Suv39h2*$^{m\text{-}z+}$ zygotes results in an intermediate increase of the maternal PN size, compared to wt and *Hp1β*$^{m\text{-}z+}$ zygotes. Furthermore, exogenously provided SUV39H1 tri-methylates paternal H3K9, which results in the decrease of the paternal PN size.

The results of these experiments show that Hp1β within the Suv39h pathway compacts chromatin globally *in vivo*.

Impact of Epigenetic Repressors on Zygotic 5mC to 5hmC conversion

We hypothesized that epigenetic repressors affect maternal 5mC content and paternal 5mC to 5hmC conversion. Among the six mutant mouse lines analyzed, we detected abnormalities in at least three lines. Our results are based on IF stainings, which is not the ideal method to quantitatively measure 5mC or 5hmC content. Nevertheless, the limited tissue available (one cell!) urged us to measure 5mC and 5hmC via IF stainings for pre-screening of a possible effect of an epigenetic repressor towards 5mC or 5hmC.

In mouse zygotes maternally deficiency for *Ezh1*$^{m\text{-}z+}$*; Ezh2*$^{m\text{-}z+}$ did not result in the global change of 5hmC. The 5mC to 5hmC conversion occurs in these mutants like in wt zygotes. In PRC1 mutants the maternal 5mC enrichment and the paternal 5hmC enrichment are affected. The development of *Ring1a*$^{m\text{-}z+}$*; Ring1b*$^{m\text{-}z+}$ zygotes is delayed (Posfai et al, unpublished). Therefore, it is possible that the *Ring1a*$^{m\text{-}z+}$*; Ring1b*$^{m\text{-}z+}$ zygotes are not PN5 stage zygotes, but only PN3 stage zygotes. In another step of analysis it needs to be determined whether or not this would influence the analysis. Furthermore, it should be analyzed whether or not this putative phenotype is directly due to the *Ring1a*$^{m\text{-}z+}$*; Ring1b*$^{m\text{-}z+}$ genotype or not. It has been shown that *Ring1a*$^{m\text{-}z+}$*; Ring1b*$^{m\text{-}z+}$ oocytes display misregulation of thousands of genes (Posfai et al, unpublished). Therefore, it is very well possible that the effect of *Ring1a*$^{m\text{-}z+}$*; Ring1b*$^{m\text{-}z+}$ on 5mC and 5hmC is only an indirect effect. This should be tested by rescue experiments.

Interestingly, maternal deficiency for *Suv39h2* did not result in the loss of 5mC/5hmC asymmetry. Therefore, it does not protect maternal 5mC or interact with proteins like

PGC7/Stella that protect maternal 5mC. Alike, maternal deficiency for the H3K9 HMT *Eset* does not result in the loss of maternal 5mC. Rather, paternal 5mC is higher than in wt zygotes. This implicates a function of Eset in the 5mC to 5hmC conversion. Interestingly, paternal 5hmC is reduced, which would be in agreement with a function of Eset in the 5mC to 5hmC conversion. Therefore, Eset should be tested for interactions with Tet3. The lack of paternal 5mC to 5hmC conversion observed in *Eset*$^{m-z+}$ zygotes is less evident than in *Tet3* mutants (Gu et al., 2011).

The most evident effect on the 5mC to 5hmC conversion in zygotes was observed in maternally deficient *G9a* and *Hp1β* zygotes. In both lines, enhanced conversion of maternal 5mC is observed. This suggests that G9a and even more so Hp1β protect maternal DNA methylation. Interestingly, G9a and Hp1β have been shown to interact (Chin et al., 2007). Thus, their putative function in the protection of maternal DNA might be within the same pathway. The analysis of *G9a* and *Hp1β* double mutants would answer that question. Furthermore, it would be interesting to test, whether or not this protection of DNA methylation by G9a and Hp1β is PGC7/Stella dependent or independent. Altogether, these results suggest that G9a and Hp1β not only interact with the DNA methyltransferases (Esteve et al., 2006; Smallwood et al., 2007), but also protect DNA methylation from its conversion to 5hmC. It remains to be determined though, whether this occurs in a histone methylation dependent or independent manner.

5. References

Aagaard, L., Schmid, M., Warburton, P., and Jenuwein, T. (2000). Mitotic phosphorylation of SUV39H1, a novel component of active centromeres, coincides with transient accumulation at mammalian centromeres. J Cell Sci *113 (Pt 5)*, 817-829.

Acevedo, N., and Smith, G.D. (2005). Oocyte-specific gene signaling and its regulation of mammalian reproductive potential. Front Biosci *10*, 2335-2345.

Adenot, P.G., Mercier, Y., Renard, J.P., and Thompson, E.M. (1997). Differential H4 acetylation of paternal and maternal chromatin precedes DNA replication and differential transcriptional activity in pronuclei of 1-cell mouse embryos. Development *124*, 4615-4625.

Ahmad, K., and Henikoff, S. (2002). Histone H3 variants specify modes of chromatin assembly. Proc Natl Acad Sci U S A *99 Suppl 4*, 16477-16484.

Akasaka, T., Kanno, M., Balling, R., Mieza, M.A., Taniguchi, M., and Koseki, H. (1996). A role for mel-18, a Polycomb group-related vertebrate gene, during theanteroposterior specification of the axial skeleton. Development *122*, 1513-1522.

Alder, O., Lavial, F., Helness, A., Brookes, E., Pinho, S., Chandrashekran, A., Arnaud, P., Pombo, A., O'Neill, L., and Azuara, V. (2010). Ring1B and Suv39h1 delineate distinct chromatin states at bivalent genes during early mouse lineage commitment. Development *137*, 2483-2492.

Amirand, C., Viari, A., Ballini, J.P., Rezaei, H., Beaujean, N., Jullien, D., Kas, E., and Debey, P. (1998). Three distinct sub-nuclear populations of HMG-I protein of different properties revealed by co-localization image analysis. J Cell Sci *111 (Pt 23)*, 3551-3561.

Aoki, F., Worrad, D.M., and Schultz, R.M. (1997). Regulation of transcriptional activity during the first and second cell cycles in the preimplantation mouse embryo. Dev Biol *181*, 296-307.

Appels, R., and Hilliker, A.J. (1982). The cytogenetic boundaries of the rDNA region within heterochromatin in the X chromosome of Drosophila melanogaster and their relation to male meiotic pairing sites. Genet Res *39*, 149-156.

Aravin, A., Gaidatzis, D., Pfeffer, S., Lagos-Quintana, M., Landgraf, P., Iovino, N., Morris, P., Brownstein, M.J., Kuramochi-Miyagawa, S., Nakano, T.*, et al.* (2006). A novel class of small RNAs bind to MILI protein in mouse testes. Nature *442*, 203-207.

Aravin, A.A., Hannon, G.J., and Brennecke, J. (2007). The Piwi-piRNA pathway provides an adaptive defense in the transposon arms race. Science *318*, 761-764.

Aucott, R., Bullwinkel, J., Yu, Y., Shi, W., Billur, M., Brown, J.P., Menzel, U., Kioussis, D., Wang, G., Reisert, I.*, et al.* (2008). HP1-beta is required for development of the cerebral neocortex and neuromuscular junctions. J Cell Biol *183*, 597-606.

Aulner, N., Monod, C., Mandicourt, G., Jullien, D., Cuvier, O., Sall, A., Janssen, S., Laemmli, U.K., and Kas, E. (2002). The AT-hook protein D1 is essential for Drosophila melanogaster development and is implicated in position-effect variegation. Mol Cell Biol *22*, 1218-1232.

Auth, T., Kunkel, E., and Grummt, F. (2006). Interaction between HP1alpha and replication proteins in mammalian cells. Exp Cell Res *312*, 3349-3359.

Ayoub, N., Jeyasekharan, A.D., Bernal, J.A., and Venkitaraman, A.R. (2008). HP1-beta mobilization promotes chromatin changes that initiate the DNA damage response. Nature *453*, 682-686.

Badugu, R., Shareef, M.M., and Kellum, R. (2003). Novel Drosophila heterochromatin protein 1 (HP1)/origin recognition complex-associated protein (HOAP) repeat motif in HP1/HOAP interactions and chromocenter associations. J Biol Chem *278*, 34491-34498.

Baker, W.K. (1968). Position-effect variegation. Adv Genet *14*, 133-169.

Bannister, A.J., Schneider, R., Myers, F.A., Thorne, A.W., Crane-Robinson, C., and Kouzarides, T. (2005). Spatial distribution of di- and tri-methyl lysine 36 of histone H3 at active genes. J Biol Chem *280*, 17732-17736.

Bantignies, F., Grimaud, C., Lavrov, S., Gabut, M., and Cavalli, G. (2003). Inheritance of Polycomb-dependent chromosomal interactions in Drosophila. Genes Dev *17*, 2406-2420.

Bardos, J.I., Saurin, A.J., Tissot, C., Duprez, E., and Freemont, P.S. (2000). HPC3 is a new human polycomb orthologue that interacts and associates with RING1 and Bmi1 and has transcriptional repression properties. J Biol Chem *275*, 28785-28792.

Barski, A., Cuddapah, S., Cui, K., Roh, T.Y., Schones, D.E., Wang, Z., Wei, G., Chepelev, I., and Zhao, K. (2007). High-resolution profiling of histone methylations in the human genome. Cell *129*, 823-837.

Bartke, T., Vermeulen, M., Xhemalce, B., Robson, S.C., Mann, M., and Kouzarides, T. (2010). Nucleosome-interacting proteins regulated by DNA and histone methylation. Cell *143*, 470-484.

Bartova, E., Pachernik, J., Kozubik, A., and Kozubek, S. (2007). Differentiation-specific association of HP1alpha and HP1beta with chromocentres is correlated with clustering of TIF1beta at these sites. Histochem Cell Biol *127*, 375-388.

Beisel, C., and Paro, R. (2011). Silencing chromatin: comparing modes and mechanisms. Nat Rev Genet *12*, 123-135.

Bell, S.P. (2002). The origin recognition complex: from simple origins to complex functions. Genes Dev *16*, 659-672.

Bell, S.P., Kobayashi, R., and Stillman, B. (1993). Yeast origin recognition complex functions in transcription silencing and DNA replication. Science *262*, 1844-1849.

Benetti, R., Gonzalo, S., Jaco, I., Munoz, P., Gonzalez, S., Schoeftner, S., Murchison, E., Andl, T., Chen, T., Klatt, P.*, et al.* (2008). A mammalian microRNA cluster controls DNA methylation and telomere recombination via Rbl2-dependent regulation of DNA methyltransferases. Nat Struct Mol Biol *15*, 268-279.

Bernstein, E., Duncan, E.M., Masui, O., Gil, J., Heard, E., and Allis, C.D. (2006). Mouse polycomb proteins bind differentially to methylated histone H3 and RNA and are enriched in facultative heterochromatin. Mol Cell Biol *26*, 2560-2569.

Bhaumik, S.R., Smith, E., and Shilatifard, A. (2007). Covalent modifications of histones during development and disease pathogenesis. Nat Struct Mol Biol *14*, 1008-1016.

Bianchi, A., and Shore, D. (2007). Early replication of short telomeres in budding yeast. Cell *128*, 1051-1062.

Bickmore, W.A., and Sumner, A.T. (1989). Mammalian chromosome banding--an expression of genome organization. Trends Genet *5*, 144-148.

Billur, M., Bartunik, H.D., and Singh, P.B. (2010). The essential function of HP1 beta: a case of the tail wagging the dog? Trends Biochem Sci *35*, 115-123.

Bilodeau, S., Kagey, M.H., Frampton, G.M., Rahl, P.B., and Young, R.A. (2009). SetDB1 contributes to repression of genes encoding developmental regulators and maintenance of ES cell state. Genes Dev *23*, 2484-2489.

Birney, E., Stamatoyannopoulos, J.A., Dutta, A., Guigo, R., Gingeras, T.R., Margulies, E.H., Weng, Z., Snyder, M., Dermitzakis, E.T., Thurman, R.E.*, et al.* (2007). Identification and analysis of functional elements in 1% of the human genome by the ENCODE pilot project. Nature *447*, 799-816.

Birve, A., Sengupta, A.K., Beuchle, D., Larsson, J., Kennison, J.A., Rasmuson-Lestander, A., and Muller, J. (2001). Su(z)12, a novel Drosophila Polycomb group gene that is conserved in vertebrates and plants. Development *128*, 3371-3379.

Blander, G., and Guarente, L. (2004). The Sir2 family of protein deacetylases. Annu Rev Biochem *73*, 417-435.

Borsani, G., Tonlorenzi, R., Simmler, M.C., Dandolo, L., Arnaud, D., Capra, V., Grompe, M., Pizzuti, A., Muzny, D., Lawrence, C.*, et al.* (1991). Characterization of a murine gene expressed from the inactive X chromosome. Nature *351*, 325-329.

Bourc'his, D., and Bestor, T.H. (2004). Meiotic catastrophe and retrotransposon reactivation in male germ cells lacking Dnmt3L. Nature *431*, 96-99.

Boyer, L.A., Plath, K., Zeitlinger, J., Brambrink, T., Medeiros, L.A., Lee, T.I., Levine, S.S., Wernig, M., Tajonar, A., Ray, M.K.*, et al.* (2006). Polycomb complexes repress developmental regulators in murine embryonic stem cells. Nature *441*, 349-353.

Bracken, A.P., Dietrich, N., Pasini, D., Hansen, K.H., and Helin, K. (2006). Genome-wide mapping of Polycomb target genes unravels their roles in cell fate transitions. Genes Dev *20*, 1123-1136.

Brasher, S.V., Smith, B.O., Fogh, R.H., Nietlispach, D., Thiru, A., Nielsen, P.R., Broadhurst, R.W., Ball, L.J., Murzina, N.V., and Laue, E.D. (2000). The structure of mouse HP1 suggests a unique mode of single peptide recognition by the shadow chromo domain dimer. Embo J *19*, 1587-1597.

Breen, T.R., and Duncan, I.M. (1986). Maternal expression of genes that regulate the bithorax complex of Drosophila melanogaster. Dev Biol *118*, 442-456.

Breiling, A., Bonte, E., Ferrari, S., Becker, P.B., and Paro, R. (1999). The Drosophila polycomb protein interacts with nucleosomal core particles In vitro via its repression domain. Mol Cell Biol *19*, 8451-8460.

Brennecke, J., Aravin, A.A., Stark, A., Dus, M., Kellis, M., Sachidanandam, R., and Hannon, G.J. (2007). Discrete small RNA-generating loci as master regulators of transposon activity in Drosophila. Cell *128*, 1089-1103.

Breslauer, K.J., Frank, R., Blocker, H., and Marky, L.A. (1986). Predicting DNA duplex stability from the base sequence. Proc Natl Acad Sci U S A *83*, 3746-3750.

Brockdorff, N., Ashworth, A., Kay, G.F., Cooper, P., Smith, S., McCabe, V.M., Norris, D.P., Penny, G.D., Patel, D., and Rastan, S. (1991). Conservation of position and exclusive expression of mouse Xist from the inactive X chromosome. Nature *351*, 329-331.

Brower-Toland, B., Findley, S.D., Jiang, L., Liu, L., Yin, H., Dus, M., Zhou, P., Elgin, S.C., and Lin, H. (2007). Drosophila PIWI associates with chromatin and interacts directly with HP1a. Genes Dev *21*, 2300-2311.

Brown, C.J., Ballabio, A., Rupert, J.L., Lafreniere, R.G., Grompe, M., Tonlorenzi, R., and Willard, H.F. (1991). A gene from the region of the human X inactivation centre is expressed exclusively from the inactive X chromosome. Nature *349*, 38-44.

Brown, C.J., and Willard, H.F. (1994). The human X-inactivation centre is not required for maintenance of X-chromosome inactivation. Nature *368*, 154-156.

Brown, J.L., Fritsch, C., Mueller, J., and Kassis, J.A. (2003). The Drosophila pho-like gene encodes a YY1-related DNA binding protein that is redundant with pleiohomeotic in homeotic gene silencing. Development *130*, 285-294.

Brown, J.L., Mucci, D., Whiteley, M., Dirksen, M.L., and Kassis, J.A. (1998). The Drosophila Polycomb group gene pleiohomeotic encodes a DNA binding protein with homology to the transcription factor YY1. Mol Cell *1*, 1057-1064.

Brown, J.P., Bullwinkel, J., Baron-Luhr, B., Billur, M., Schneider, P., Winking, H., and Singh, P.B. (2010). HP1gamma function is required for male germ cell survival and spermatogenesis. Epigenetics Chromatin *3*, 9.

Brown, S.W. (1966). Heterochromatin. Science *151*, 417-425.

Brunk, B.P., Martin, E.C., and Adler, P.N. (1991). Drosophila genes Posterior Sex Combs and Suppressor two of zeste encode proteins with homology to the murine bmi-1 oncogene. Nature *353*, 351-353.

Brykczynska, U., Hisano, M., Erkek, S., Ramos, L., Oakeley, E.J., Roloff, T.C., Beisel, C., Schubeler, D., Stadler, M.B., and Peters, A.H. (2010). Repressive and active histone methylation mark distinct promoters in human and mouse spermatozoa. Nat Struct Mol Biol *17*, 679-687.

Buhler, M., and Gasser, S.M. (2009). Silent chromatin at the middle and ends: lessons from yeasts. Embo J *28*, 2149-2161.

Campos, E.I., and Reinberg, D. (2009). Histones: annotating chromatin. Annu Rev Genet *43*, 559-599.

Canzio, D., Chang, E.Y., Shankar, S., Kuchenbecker, K.M., Simon, M.D., Madhani, H.D., Narlikar, G.J., and Al-Sady, B. (2011). Chromodomain-mediated oligomerization of HP1 suggests a nucleosome-bridging mechanism for heterochromatin assembly. Mol Cell *41*, 67-81.

Cao, R., Tsukada, Y., and Zhang, Y. (2005). Role of Bmi-1 and Ring1A in H2A ubiquitylation and Hox gene silencing. Mol Cell *20*, 845-854.

Cao, R., Wang, L., Wang, H., Xia, L., Erdjument-Bromage, H., Tempst, P., Jones, R.S., and Zhang, Y. (2002). Role of histone H3 lysine 27 methylation in Polycomb-group silencing. Science *298*, 1039-1043.

Carmell, M.A., Girard, A., van de Kant, H.J., Bourc'his, D., Bestor, T.H., de Rooij, D.G., and Hannon, G.J. (2007). MIWI2 is essential for spermatogenesis and repression of transposons in the mouse male germline. Dev Cell *12*, 503-514.

Chang, C.C., Ma, Y., Jacobs, S., Tian, X.C., Yang, X., and Rasmussen, T.P. (2005). A maternal store of macroH2A is removed from pronuclei prior to onset of somatic macroH2A expression in preimplantation embryos. Dev Biol *278*, 367-380.

Cheutin, T., McNairn, A.J., Jenuwein, T., Gilbert, D.M., Singh, P.B., and Misteli, T. (2003). Maintenance of stable heterochromatin domains by dynamic HP1 binding. Science *299*, 721-725.

Chin, H.G., Esteve, P.O., Pradhan, M., Benner, J., Patnaik, D., Carey, M.F., and Pradhan, S. (2007). Automethylation of G9a and its implication in wider substrate specificity and HP1 binding. Nucleic Acids Res *35*, 7313-7323.

Cirio, M.C., Ratnam, S., Ding, F., Reinhart, B., Navara, C., and Chaillet, J.R. (2008). Preimplantation expression of the somatic form of Dnmt1 suggests a role in the inheritance of genomic imprints. BMC Dev Biol *8*, 9.

Cleard, F., Moshkin, Y., Karch, F., and Maeda, R.K. (2006). Probing long-distance regulatory interactions in the Drosophila melanogaster bithorax complex using Dam identification. Nat Genet *38*, 931-935.

Conrad, M.N., Wright, J.H., Wolf, A.J., and Zakian, V.A. (1990). RAP1 protein interacts with yeast telomeres in vivo: overproduction alters telomere structure and decreases chromosome stability. Cell *63*, 739-750.

Core, N., Bel, S., Gaunt, S.J., Aurrand-Lions, M., Pearce, J., Fisher, A., and Djabali, M. (1997). Altered cellular proliferation and mesoderm patterning in Polycomb-M33-deficient mice. Development *124*, 721-729.

Cowell, I.G., and Austin, C.A. (1997). Self-association of chromo domain peptides. Biochim Biophys Acta *1337*, 198-206.

Cowieson, N.P., Partridge, J.F., Allshire, R.C., and McLaughlin, P.J. (2000). Dimerisation of a chromo shadow domain and distinctions from the chromodomain as revealed by structural analysis. Curr Biol *10*, 517-525.

Csankovszki, G., Panning, B., Bates, B., Pehrson, J.R., and Jaenisch, R. (1999). Conditional deletion of Xist disrupts histone macroH2A localization but not maintenance of X inactivation. Nat Genet *22*, 323-324.

Cubizolles, F., Martino, F., Perrod, S., and Gasser, S.M. (2006). A homotrimer-heterotrimer switch in Sir2 structure differentiates rDNA and telomeric silencing. Mol Cell *21*, 825-836.

Czermin, B., Melfi, R., McCabe, D., Seitz, V., Imhof, A., and Pirrotta, V. (2002). Drosophila enhancer of Zeste/ESC complexes have a histone H3 methyltransferase activity that marks chromosomal Polycomb sites. Cell *111*, 185-196.

Davey, C.A., Sargent, D.F., Luger, K., Maeder, A.W., and Richmond, T.J. (2002). Solvent mediated interactions in the structure of the nucleosome core particle at 1.9 a resolution. J Mol Biol *319*, 1097-1113.

Davis, T.L., Trasler, J.M., Moss, S.B., Yang, G.J., and Bartolomei, M.S. (1999). Acquisition of the H19 methylation imprint occurs differentially on the parental alleles during spermatogenesis. Genomics *58*, 18-28.

Davisson, M.T.a.R., T. H. (1989). Genetic Variants and Strians of the Laboratory Mouse 416-427.

Dawson, M.A., Bannister, A.J., Gottgens, B., Foster, S.D., Bartke, T., Green, A.R., and Kouzarides, T. (2009). JAK2 phosphorylates histone H3Y41 and excludes HP1alpha from chromatin. Nature *461*, 819-822.

de Kretser, D.M., Loveland, K.L., Meinhardt, A., Simorangkir, D., and Wreford, N. (1998). Spermatogenesis. Hum Reprod *13 Suppl 1*, 1-8.

De La Fuente, R., Viveiros, M.M., Burns, K.H., Adashi, E.Y., Matzuk, M.M., and Eppig, J.J. (2004a). Major chromatin remodeling in the germinal vesicle (GV) of mammalian oocytes is dispensable for global transcriptional silencing but required for centromeric heterochromatin function. Dev Biol *275*, 447-458.

De La Fuente, R., Viveiros, M.M., Wigglesworth, K., and Eppig, J.J. (2004b). ATRX, a member of the SNF2 family of helicase/ATPases, is required for chromosome alignment and meiotic spindle organization in metaphase II stage mouse oocytes. Dev Biol *272*, 1-14.

De Leon, V., Johnson, A., and Bachvarova, R. (1983). Half-lives and relative amounts of stored and polysomal ribosomes and poly(A) + RNA in mouse oocytes. Dev Biol *98*, 400-408.

de Napoles, M., Mermoud, J.E., Wakao, R., Tang, Y.A., Endoh, M., Appanah, R., Nesterova, T.B., Silva, J., Otte, A.P., Vidal, M.*, et al.* (2004). Polycomb group proteins Ring1A/B link ubiquitylation of histone H2A to heritable gene silencing and X inactivation. Dev Cell *7*, 663-676.

Dejardin, J., Rappailles, A., Cuvier, O., Grimaud, C., Decoville, M., Locker, D., and Cavalli, G. (2005). Recruitment of Drosophila Polycomb group proteins to chromatin by DSP1. Nature *434*, 533-538.

del Mar Lorente, M., Marcos-Gutierrez, C., Perez, C., Schoorlemmer, J., Ramirez, A., Magin, T., and Vidal, M. (2000). Loss- and gain-of-function mutations show a polycomb group function for Ring1A in mice. Development *127*, 5093-5100.

Denell, R.E. (1978). Homoeosis in Drosophila. II. a Genetic Analysis of Polycomb. Genetics *90*, 277-289.

Deng, Z., Dheekollu, J., Broccoli, D., Dutta, A., and Lieberman, P.M. (2007). The origin recognition complex localizes to telomere repeats and prevents telomere-circle formation. Curr Biol *17*, 1989-1995.

Deschamps, J., van den Akker, E., Forlani, S., De Graaff, W., Oosterveen, T., Roelen, B., and Roelfsema, J. (1999). Initiation, establishment and maintenance of Hox gene expression patterns in the mouse. Int J Dev Biol *43*, 635-650.

Dietrich, N., Bracken, A.P., Trinh, E., Schjerling, C.K., Koseki, H., Rappsilber, J., Helin, K., and Hansen, K.H. (2007). Bypass of senescence by the polycomb group protein CBX8 through direct binding to the INK4A-ARF locus. Embo J *26*, 1637-1648.

Doenecke, D., Drabent, B., Bode, C., Bramlage, B., Franke, K., Gavenis, K., Kosciessa, U., and Witt, O. (1997). Histone gene expression and chromatin structure during spermatogenesis. Adv Exp Med Biol *424*, 37-48.

Dorigo, B., Schalch, T., Kulangara, A., Duda, S., Schroeder, R.R., and Richmond, T.J. (2004). Nucleosome arrays reveal the two-start organization of the chromatin fiber. Science *306*, 1571-1573.

Dura, J.M., Brock, H.W., and Santamaria, P. (1985). Polyhomeotic: a gene of Drosophila melanogaster required for correct expression of segmental identity. Mol Gen Genet *198*, 213-220.

Eissenberg, J.C., and Hartnett, T. (1993). A heat shock-activated cDNA rescues the recessive lethality of mutations in the heterochromatin-associated protein HP1 of Drosophila melanogaster. Mol Gen Genet *240*, 333-338.

Eissenberg, J.C., Morris, G.D., Reuter, G., and Hartnett, T. (1992). The heterochromatin-associated protein HP-1 is an essential protein in Drosophila with dosage-dependent effects on position-effect variegation. Genetics *131*, 345-352.

Eissenberg, J.C., and Reuter, G. (2009). Cellular mechanism for targeting heterochromatin formation in Drosophila. Int Rev Cell Mol Biol *273*, 1-47.

Erhardt, S., Su, I.H., Schneider, R., Barton, S., Bannister, A.J., Perez-Burgos, L., Jenuwein, T., Kouzarides, T., Tarakhovsky, A., and Surani, M.A. (2003). Consequences of the depletion of zygotic and embryonic enhancer of zeste 2 during preimplantation mouse development. Development *130*, 4235-4248.

Esteve, P.O., Chin, H.G., Smallwood, A., Feehery, G.R., Gangisetty, O., Karpf, A.R., Carey, M.F., and Pradhan, S. (2006). Direct interaction between DNMT1 and G9a coordinates DNA and histone methylation during replication. Genes Dev *20*, 3089-3103.

Evsikov, A.V., Graber, J.H., Brockman, J.M., Hampl, A., Holbrook, A.E., Singh, P., Eppig, J.J., Solter, D., and Knowles, B.B. (2006). Cracking the egg: molecular dynamics and evolutionary aspects of the transition from the fully grown oocyte to embryo. Genes Dev *20*, 2713-2727.

Faust, C., Schumacher, A., Holdener, B., and Magnuson, T. (1995). The eed mutation disrupts anterior mesoderm production in mice. Development *121*, 273-285.

Fischle, W., Tseng, B.S., Dormann, H.L., Ueberheide, B.M., Garcia, B.A., Shabanowitz, J., Hunt, D.F., Funabiki, H., and Allis, C.D. (2005). Regulation of HP1-chromatin binding by histone H3 methylation and phosphorylation. Nature *438*, 1116-1122.

Fischle, W., Wang, Y., Jacobs, S.A., Kim, Y., Allis, C.D., and Khorasanizadeh, S. (2003). Molecular basis for the discrimination of repressive methyl-lysine marks in histone H3 by Polycomb and HP1 chromodomains. Genes Dev *17*, 1870-1881.

Fodor, B.D., Shukeir, N., Reuter, G., and Jenuwein, T. (2010). Mammalian Su(var) genes in chromatin control. Annu Rev Cell Dev Biol *26*, 471-501.

Foss, H.M., Roberts, C.J., Claeys, K.M., and Selker, E.U. (1993a). Abnormal chromosome behavior in Neurospora mutants defective in DNA methylation. Science *262*, 1737-1741.

Foss, M., McNally, F.J., Laurenson, P., and Rine, J. (1993b). Origin recognition complex (ORC) in transcriptional silencing and DNA replication in S. cerevisiae. Science *262*, 1838-1844.

Francis, N.J., Saurin, A.J., Shao, Z., and Kingston, R.E. (2001). Reconstitution of a functional core polycomb repressive complex. Mol Cell *8*, 545-556.

Freitag, M., Hickey, P.C., Khlafallah, T.K., Read, N.D., and Selker, E.U. (2004a). HP1 is essential for DNA methylation in neurospora. Mol Cell *13*, 427-434.

Freitag, M., Lee, D.W., Kothe, G.O., Pratt, R.J., Aramayo, R., and Selker, E.U. (2004b). DNA methylation is independent of RNA interference in Neurospora. Science *304*, 1939.

Fuks, F., Hurd, P.J., Deplus, R., and Kouzarides, T. (2003). The DNA methyltransferases associate with HP1 and the SUV39H1 histone methyltransferase. Nucleic Acids Res *31*, 2305-2312.

Garcia, E., Marcos-Gutierrez, C., del Mar Lorente, M., Moreno, J.C., and Vidal, M. (1999). RYBP, a new repressor protein that interacts with components of the mammalian Polycomb complex, and with the transcription factor YY1. Embo J *18*, 3404-3418.

Gaudet, F., Rideout, W.M., 3rd, Meissner, A., Dausman, J., Leonhardt, H., and Jaenisch, R. (2004). Dnmt1 expression in pre- and postimplantation embryogenesis and the maintenance of IAP silencing. Mol Cell Biol *24*, 1640-1648.

Gehring, M., Huh, J.H., Hsieh, T.F., Penterman, J., Choi, Y., Harada, J.J., Goldberg, R.B., and Fischer, R.L. (2006). DEMETER DNA glycosylase establishes MEDEA polycomb gene self-imprinting by allele-specific demethylation. Cell *124*, 495-506.

Gil, J., Bernard, D., Martinez, D., and Beach, D. (2004). Polycomb CBX7 has a unifying role in cellular lifespan. Nat Cell Biol *6*, 67-72.

Gil, J., Bernard, D., and Peters, G. (2005). Role of polycomb group proteins in stem cell self-renewal and cancer. DNA Cell Biol *24*, 117-125.

Gotta, M., Laroche, T., Formenton, A., Maillet, L., Scherthan, H., and Gasser, S.M. (1996). The clustering of telomeres and colocalization with Rap1, Sir3, and Sir4 proteins in wild-type Saccharomyces cerevisiae. J Cell Biol *134*, 1349-1363.
Govin, J., Caron, C., Lestrat, C., Rousseaux, S., and Khochbin, S. (2004). The role of histones in chromatin remodelling during mammalian spermiogenesis. Eur J Biochem *271*, 3459-3469.
Grau, D.J., Chapman, B.A., Garlick, J.D., Borowsky, M., Francis, N.J., and Kingston, R.E. (2011). Compaction of chromatin by diverse Polycomb group proteins requires localized regions of high charge. Genes Dev *25*, 2210-2221.
Grewal, S.I. (2010). RNAi-dependent formation of heterochromatin and its diverse functions. Curr Opin Genet Dev *20*, 134-141.
Grewal, S.I., and Elgin, S.C. (2007). Transcription and RNA interference in the formation of heterochromatin. Nature *447*, 399-406.
Grewal, S.I., and Jia, S. (2007). Heterochromatin revisited. Nat Rev Genet *8*, 35-46.
Grunstein, M. (1998). Yeast heterochromatin: regulation of its assembly and inheritance by histones. Cell *93*, 325-328.
Gu, T.P., Guo, F., Yang, H., Wu, H.P., Xu, G.F., Liu, W., Xie, Z.G., Shi, L., He, X., Jin, S.G*., et al.* (2011). The role of Tet3 DNA dioxygenase in epigenetic reprogramming by oocytes. Nature.
Guenther, M.G., Levine, S.S., Boyer, L.A., Jaenisch, R., and Young, R.A. (2007). A chromatin landmark and transcription initiation at most promoters in human cells. Cell *130*, 77-88.
Guibert, S.F., T.; Weber, M. (2009). Dynamic regulation of DNA methylation druing mammalian development. Epigenomics *1*, 81-98.
Gunawardane, L.S., Saito, K., Nishida, K.M., Miyoshi, K., Kawamura, Y., Nagami, T., Siomi, H., and Siomi, M.C. (2007). A slicer-mediated mechanism for repeat-associated siRNA 5' end formation in Drosophila. Science *315*, 1587-1590.
Guttman, M., Donaghey, J., Carey, B.W., Garber, M., Grenier, J.K., Munson, G., Young, G., Lucas, A.B., Ach, R., Bruhn, L*., et al.* (2011). lincRNAs act in the circuitry controlling pluripotency and differentiation. Nature *477*, 295-300.
Hall, I.M., Shankaranarayana, G.D., Noma, K., Ayoub, N., Cohen, A., and Grewal, S.I. (2002). Establishment and maintenance of a heterochromatin domain. Science *297*, 2232-2237.
Hamilton, B.A., and Frankel, W.N. (2001). Of mice and genome sequence. Cell *107*, 13-16.
Hammoud, S.S., Nix, D.A., Zhang, H., Purwar, J., Carrell, D.T., and Cairns, B.R. (2009). Distinctive chromatin in human sperm packages genes for embryo development. Nature *460*, 473-478.
Han, Z., Xing, X., Hu, M., Zhang, Y., Liu, P., and Chai, J. (2007). Structural basis of EZH2 recognition by EED. Structure *15*, 1306-1315.
Hasties, N.D. (1998). Highly repeated DNA families in the genome of Mus musculus. Genetic Variants and Strains of the Laboratory Mouse, 559-573.
Hata, K., Okano, M., Lei, H., and Li, E. (2002). Dnmt3L cooperates with the Dnmt3 family of de novo DNA methyltransferases to establish maternal imprints in mice. Development *129*, 1983-1993.
Hatano, A., Matsumoto, M., Higashinakagawa, T., and Nakayama, K.I. (2010). Phosphorylation of the chromodomain changes the binding specificity of Cbx2 for methylated histone H3. Biochem Biophys Res Commun *397*, 93-99.
Haupt, Y., Alexander, W.S., Barri, G., Klinken, S.P., and Adams, J.M. (1991). Novel zinc finger gene implicated as myc collaborator by retrovirally accelerated lymphomagenesis in E mu-myc transgenic mice. Cell *65*, 753-763.
Heitz, E. (1926). Der Nachweis der Chromosomen: Vergleichende Studien über ihre Zahl, Grösse und Form im Pflanzenreich. I Z Bot *18*, 625-681.
Heitz, E. (1928a). Das Heterochrmoatin der Moose. I Jahrb wiss Bot *69*, 762-818.

Heitz, E. (1928b). De bilaterale Bau der Geschlechtschromosomen und Autosomen bei *Pellia fabbrioniana, P. epiphylla* und einigen anderen Iungermanniaceen. Planta *5*, 725-768.
Heitz, E. (1929). Heterochromatin, Chromocentren, Chromomeren (Vorläufige Mitteilung). Ber Dtsch Bot Ges *47*, 274-284.
Heitz, E. (1933a). Die Herkunft der Chromocentren: Dritter Beitrag zur Kenntnis der Beziehung zwischen Kernsturktur und qualitativer Vershciedenheit der Chromosomen in ihrer Längsrichtung. Planta *18*, 571-636.
Heitz, E. (1933b). Über totale und partielle somatische Heteropyknose, sowie strukturelle Geschlechtschromosomen bei Drosophila funebris (Cytologische Untersuchungen an Dipteren, II). Z Zellforsch mikrosk Anat *19*, 720-742.
Hennig, L., Bouveret, R., and Gruissem, W. (2005). MSI1-like proteins: an escort service for chromatin assembly and remodeling complexes. Trends Cell Biol *15*, 295-302.
Hiragami-Hamada, K., Shinmyozu, K., Hamada, D., Tatsu, Y., Uegaki, K., Fujiwara, S., and Nakayama, J. (2011). N-terminal phosphorylation of HP1{alpha} promotes its chromatin binding. Mol Cell Biol *31*, 1186-1200.
Hirasawa, R., Chiba, H., Kaneda, M., Tajima, S., Li, E., Jaenisch, R., and Sasaki, H. (2008). Maternal and zygotic Dnmt1 are necessary and sufficient for the maintenance of DNA methylation imprints during preimplantation development. Genes Dev *22*, 1607-1616.
Hirota, T., Lipp, J.J., Toh, B.H., and Peters, J.M. (2005). Histone H3 serine 10 phosphorylation by Aurora B causes HP1 dissociation from heterochromatin. Nature *438*, 1176-1180.
Honda, S., and Selker, E.U. (2008). Direct interaction between DNA methyltransferase DIM-2 and HP1 is required for DNA methylation in Neurospora crassa. Mol Cell Biol *28*, 6044-6055.
Horsley, D., Hutchings, A., Butcher, G.W., and Singh, P.B. (1996). M32, a murine homologue of Drosophila heterochromatin protein 1 (HP1), localises to euchromatin within interphase nuclei and is largely excluded from constitutive heterochromatin. Cytogenet Cell Genet *73*, 308-311.
Horz, W., and Altenburger, W. (1981). Nucleotide sequence of mouse satellite DNA. Nucleic Acids Res *9*, 683-696.
Huang, D.W., Fanti, L., Pak, D.T., Botchan, M.R., Pimpinelli, S., and Kellum, R. (1998). Distinct cytoplasmic and nuclear fractions of Drosophila heterochromatin protein 1: their phosphorylation levels and associations with origin recognition complex proteins. J Cell Biol *142*, 307-318.
Illingworth, R., Kerr, A., Desousa, D., Jorgensen, H., Ellis, P., Stalker, J., Jackson, D., Clee, C., Plumb, R., Rogers, J*., et al.* (2008). A novel CpG island set identifies tissue-specific methylation at developmental gene loci. PLoS Biol *6*, e22.
Inoue, A., and Zhang, Y. (2011). Replication-dependent loss of 5-hydroxymethylcytosine in mouse preimplantation embryos. Science *334*, 194.
Iqbal, K., Jin, S.G., Pfeifer, G.P., and Szabo, P.E. (2011). Reprogramming of the paternal genome upon fertilization involves genome-wide oxidation of 5-methylcytosine. Proc Natl Acad Sci U S A *108*, 3642-3647.
Iwata, S., Takenobu, H., Kageyama, H., Koseki, H., Ishii, T., Nakazawa, A., Tatezaki, S., Nakagawara, A., and Kamijo, T. (2010). Polycomb group molecule PHC3 regulates polycomb complex composition and prognosis of osteosarcoma. Cancer Sci *101*, 1646-1652.
Jacobs, S.A., and Khorasanizadeh, S. (2002). Structure of HP1 chromodomain bound to a lysine 9-methylated histone H3 tail. Science *295*, 2080-2083.
Jacobs, S.A., Taverna, S.D., Zhang, Y., Briggs, S.D., Li, J., Eissenberg, J.C., Allis, C.D., and Khorasanizadeh, S. (2001). Specificity of the HP1 chromo domain for the methylated N-terminus of histone H3. Embo J *20*, 5232-5241.
Jahner, D., Stuhlmann, H., Stewart, C.L., Harbers, K., Lohler, J., Simon, I., and Jaenisch, R. (1982). De novo methylation and expression of retroviral genomes during mouse embryogenesis. Nature *298*, 623-628.

James, T.C., and Elgin, S.C. (1986). Identification of a nonhistone chromosomal protein associated with heterochromatin in Drosophila melanogaster and its gene. Mol Cell Biol *6*, 3862-3872.

Johansson, A.M., Stenberg, P., Bernhardsson, C., and Larsson, J. (2007). Painting of fourth and chromosome-wide regulation of the 4th chromosome in Drosophila melanogaster. Embo J *26*, 2307-2316.

Jones, K.T. (1998). Ca2+ oscillations in the activation of the egg and development of the embryo in mammals. Int J Dev Biol *42*, 1-10.

Jones, R.S., and Gelbart, W.M. (1990). Genetic analysis of the enhancer of zeste locus and its role in gene regulation in Drosophila melanogaster. Genetics *126*, 185-199.

Joseph, A., Mitchell, A.R., and Miller, O.J. (1989). The organization of the mouse satellite DNA at centromeres. Exp Cell Res *183*, 494-500.

Kagey, M.H., Melhuish, T.A., and Wotton, D. (2003). The polycomb protein Pc2 is a SUMO E3. Cell *113*, 127-137.

Kahn, T.G., Schwartz, Y.B., Dellino, G.I., and Pirrotta, V. (2006). Polycomb complexes and the propagation of the methylation mark at the Drosophila ubx gene. J Biol Chem *281*, 29064-29075.

Kaneda, M., Sado, T., Hata, K., Okano, M., Tsujimoto, N., Li, E., and Sasaki, H. (2004). Role of de novo DNA methyltransferases in initiation of genomic imprinting and X-chromosome inactivation. Cold Spring Harb Symp Quant Biol *69*, 125-129.

Kanellopoulou, C., Muljo, S.A., Kung, A.L., Ganesan, S., Drapkin, R., Jenuwein, T., Livingston, D.M., and Rajewsky, K. (2005). Dicer-deficient mouse embryonic stem cells are defective in differentiation and centromeric silencing. Genes Dev *19*, 489-501.

Kanhere, A., Viiri, K., Araujo, C.C., Rasaiyaah, J., Bouwman, R.D., Whyte, W.A., Pereira, C.F., Brookes, E., Walker, K., Bell, G.W.*, et al.* (2010). Short RNAs are transcribed from repressed polycomb target genes and interact with polycomb repressive complex-2. Mol Cell *38*, 675-688.

Kato, Y., Kaneda, M., Hata, K., Kumaki, K., Hisano, M., Kohara, Y., Okano, M., Li, E., Nozaki, M., and Sasaki, H. (2007). Role of the Dnmt3 family in de novo methylation of imprinted and repetitive sequences during male germ cell development in the mouse. Hum Mol Genet *16*, 2272-2280.

Katoh-Fukui, Y., Tsuchiya, R., Shiroishi, T., Nakahara, Y., Hashimoto, N., Noguchi, K., and Higashinakagawa, T. (1998). Male-to-female sex reversal in M33 mutant mice. Nature *393*, 688-692.

Kaustov, L., Ouyang, H., Amaya, M., Lemak, A., Nady, N., Duan, S., Wasney, G.A., Li, Z., Vedadi, M., Schapira, M.*, et al.* (2011). Recognition and specificity determinants of the human cbx chromodomains. J Biol Chem *286*, 521-529.

Kawamura, A., Yokota, S., Yamada, K., Inoue, H., Inohaya, K., Yamazaki, K., Yasumasu, I., and Higashinakagawa, T. (2002). pc1 and psc1, zebrafish homologs of Drosophila Polycomb and Posterior sex combs, encode nuclear proteins capable of complex interactions. Biochem Biophys Res Commun *294*, 456-463.

Kent, W.J., Sugnet, C.W., Furey, T.S., Roskin, K.M., Pringle, T.H., Zahler, A.M., and Haussler, D. (2002). The human genome browser at UCSC. Genome Res *12*, 996-1006.

Khalil, A.M., Guttman, M., Huarte, M., Garber, M., Raj, A., Rivea Morales, D., Thomas, K., Presser, A., Bernstein, B.E., van Oudenaarden, A.*, et al.* (2009). Many human large intergenic noncoding RNAs associate with chromatin-modifying complexes and affect gene expression. Proc Natl Acad Sci U S A *106*, 11667-11672.

Kireeva, N., Lakonishok, M., Kireev, I., Hirano, T., and Belmont, A.S. (2004). Visualization of early chromosome condensation: a hierarchical folding, axial glue model of chromosome structure. J Cell Biol *166*, 775-785.

Knowles, B.B., Evsikov, A.V., de Vries, W.N., Peaston, A.E., and Solter, D. (2003). Molecular control of the oocyte to embryo transition. Philos Trans R Soc Lond B Biol Sci *358*, 1381-1387.

Kocabas, A.M., Crosby, J., Ross, P.J., Otu, H.H., Beyhan, Z., Can, H., Tam, W.L., Rosa, G.J., Halgren, R.G., Lim, B.*, et al.* (2006). The transcriptome of human oocytes. Proc Natl Acad Sci U S A *103*, 14027-14032.

Krauss, V. (2008). Glimpses of evolution: heterochromatic histone H3K9 methyltransferases left its marks behind. Genetica *133*, 93-106.

Kriaucionis, S., and Heintz, N. (2009). The nuclear DNA base 5-hydroxymethylcytosine is present in Purkinje neurons and the brain. Science *324*, 929-930.

Krouwels, I.M., Wiesmeijer, K., Abraham, T.E., Molenaar, C., Verwoerd, N.P., Tanke, H.J., and Dirks, R.W. (2005). A glue for heterochromatin maintenance: stable SUV39H1 binding to heterochromatin is reinforced by the SET domain. J Cell Biol *170*, 537-549.

Ku, M., Koche, R.P., Rheinbay, E., Mendenhall, E.M., Endoh, M., Mikkelsen, T.S., Presser, A., Nusbaum, C., Xie, X., Chi, A.S.*, et al.* (2008). Genomewide analysis of PRC1 and PRC2 occupancy identifies two classes of bivalent domains. PLoS Genet *4*, e1000242.

Kurihara, Y., Kawamura, Y., Uchijima, Y., Amamo, T., Kobayashi, H., Asano, T., and Kurihara, H. (2008). Maintenance of genomic methylation patterns during preimplantation development requires the somatic form of DNA methyltransferase 1. Dev Biol *313*, 335-346.

Lachner, M., O'Carroll, D., Rea, S., Mechtler, K., and Jenuwein, T. (2001). Methylation of histone H3 lysine 9 creates a binding site for HP1 proteins. Nature *410*, 116-120.

Lane, N., Dean, W., Erhardt, S., Hajkova, P., Surani, A., Walter, J., and Reik, W. (2003). Resistance of IAPs to methylation reprogramming may provide a mechanism for epigenetic inheritance in the mouse. Genesis *35*, 88-93.

Lanzuolo, C., Roure, V., Dekker, J., Bantignies, F., and Orlando, V. (2007). Polycomb response elements mediate the formation of chromosome higher-order structures in the bithorax complex. Nat Cell Biol *9*, 1167-1174.

Larsson, J., Chen, J.D., Rasheva, V., Rasmuson-Lestander, A., and Pirrotta, V. (2001). Painting of fourth, a chromosome-specific protein in Drosophila. Proc Natl Acad Sci U S A *98*, 6273-6278.

Latham, K.E., Garrels, J.I., Chang, C., and Solter, D. (1991). Quantitative analysis of protein synthesis in mouse embryos. I. Extensive reprogramming at the one- and two-cell stages. Development *112*, 921-932.

Lavigne, M., Francis, N.J., King, I.F., and Kingston, R.E. (2004). Propagation of silencing; recruitment and repression of naive chromatin in trans by polycomb repressed chromatin. Mol Cell *13*, 415-425.

Lee, J.K., Moon, K.Y., Jiang, Y., and Hurwitz, J. (2001). The Schizosaccharomyces pombe origin recognition complex interacts with multiple AT-rich regions of the replication origin DNA by means of the AT-hook domains of the spOrc4 protein. Proc Natl Acad Sci U S A *98*, 13589-13594.

Lee, T.I., Jenner, R.G., Boyer, L.A., Guenther, M.G., Levine, S.S., Kumar, R.M., Chevalier, B., Johnstone, S.E., Cole, M.F., Isono, K.*, et al.* (2006). Control of developmental regulators by Polycomb in human embryonic stem cells. Cell *125*, 301-313.

Lees-Murdock, D.J., and Walsh, C.P. (2008). DNA methylation reprogramming in the germ line. Adv Exp Med Biol *626*, 1-15.

Lehnertz, B., Ueda, Y., Derijck, A.A., Braunschweig, U., Perez-Burgos, L., Kubicek, S., Chen, T., Li, E., Jenuwein, T., and Peters, A.H. (2003). Suv39h-mediated histone H3 lysine 9 methylation directs DNA methylation to major satellite repeats at pericentric heterochromatin. Curr Biol *13*, 1192-1200.

Lepikhov, K., and Walter, J. (2004). Differential dynamics of histone H3 methylation at positions K4 and K9 in the mouse zygote. BMC Dev Biol *4*, 12.

Levine, S.S., King, I.F., and Kingston, R.E. (2004). Division of labor in polycomb group repression. Trends Biochem Sci *29*, 478-485.

Lewis, E.B. (1950). The phenomenon of position effect. Adv Genet *3*, 73-115.

Lewis, E.B. (1978). A gene complex controlling segmentation in Drosophila. Nature *276*, 565-570.

Lewis, Z.A., Honda, S., Khlafallah, T.K., Jeffress, J.K., Freitag, M., Mohn, F., Schubeler, D., and Selker, E.U. (2009). Relics of repeat-induced point mutation direct heterochromatin formation in Neurospora crassa. Genome Res *19*, 427-437.

Li, E., Beard, C., and Jaenisch, R. (1993). Role for DNA methylation in genomic imprinting. Nature *366*, 362-365.

Li, E., Bestor, T.H., and Jaenisch, R. (1992). Targeted mutation of the DNA methyltransferase gene results in embryonic lethality. Cell *69*, 915-926.

Li, E.B., A. (2007). DNA methylation in mammals. Epigenetics, 341-356.

Li, H., Ilin, S., Wang, W., Duncan, E.M., Wysocka, J., Allis, C.D., and Patel, D.J. (2006). Molecular basis for site-specific read-out of histone H3K4me3 by the BPTF PHD finger of NURF. Nature *442*, 91-95.

Li, J.Y., Lees-Murdock, D.J., Xu, G.L., and Walsh, C.P. (2004). Timing of establishment of paternal methylation imprints in the mouse. Genomics *84*, 952-960.

Li, Q., Wang, X., Lu, Z., Zhang, B., Guan, Z., Liu, Z., Zhong, Q., Gu, L., Zhou, J., Zhu, B.*, et al.* (2010). Polycomb CBX7 directly controls trimethylation of histone H3 at lysine 9 at the p16 locus. PLoS One *5*, e13732.

Liu, H., Kim, J.M., and Aoki, F. (2004). Regulation of histone H3 lysine 9 methylation in oocytes and early pre-implantation embryos. Development *131*, 2269-2280.

Locke, J., and McDermid, H.E. (1993). Analysis of Drosophila chromosome 4 using pulsed field gel electrophoresis. Chromosoma *102*, 718-723.

Lomberk, G., Bensi, D., Fernandez-Zapico, M.E., and Urrutia, R. (2006). Evidence for the existence of an HP1-mediated subcode within the histone code. Nat Cell Biol *8*, 407-415.

Loo, S., and Rine, J. (1994). Silencers and domains of generalized repression. Science *264*, 1768-1771.

Loupart, M.L., Krause, S.A., and Heck, M.S. (2000). Aberrant replication timing induces defective chromosome condensation in Drosophila ORC2 mutants. Curr Biol *10*, 1547-1556.

Lu, B.Y., Emtage, P.C., Duyf, B.J., Hilliker, A.J., and Eissenberg, J.C. (2000). Heterochromatin protein 1 is required for the normal expression of two heterochromatin genes in Drosophila. Genetics *155*, 699-708.

Luger, K., Mader, A.W., Richmond, R.K., Sargent, D.F., and Richmond, T.J. (1997). Crystal structure of the nucleosome core particle at 2.8 A resolution. Nature *389*, 251-260.

Lyko, F., Beisel, C., Marhold, J., and Paro, R. (2006). Epigenetic regulation in Drosophila. Curr Top Microbiol Immunol *310*, 23-44.

Maison, C., Bailly, D., Peters, A.H., Quivy, J.P., Roche, D., Taddei, A., Lachner, M., Jenuwein, T., and Almouzni, G. (2002). Higher-order structure in pericentric heterochromatin involves a distinct pattern of histone modification and an RNA component. Nat Genet *30*, 329-334.

Maison, C., Bailly, D., Roche, D., Montes de Oca, R., Probst, A.V., Vassias, I., Dingli, F., Lombard, B., Loew, D., Quivy, J.P.*, et al.* (2011). SUMOylation promotes de novo targeting of HP1alpha to pericentric heterochromatin. Nat Genet *43*, 220-227.

Malik, H.S., and Henikoff, S. (2009). Major evolutionary transitions in centromere complexity. Cell *138*, 1067-1082.

Marahrens, Y., Panning, B., Dausman, J., Strauss, W., and Jaenisch, R. (1997). Xist-deficient mice are defective in dosage compensation but not spermatogenesis. Genes Dev *11*, 156-166.

Margueron, R., Li, G., Sarma, K., Blais, A., Zavadil, J., Woodcock, C.L., Dynlacht, B.D., and Reinberg, D. (2008). Ezh1 and Ezh2 maintain repressive chromatin through different mechanisms. Mol Cell *32*, 503-518.

Martelli, A.M., Riccio, M., Bareggi, R., Manfioletti, G., Tabellini, G., Baldini, G., Narducci, P., and Giancotti, V. (1998). Intranuclear distribution of HMGI/Y proteins. An immunocytochemical study. J Histochem Cytochem *46*, 863-864.

Martin, S.L. (1991). LINEs. Curr Opin Genet Dev *1*, 505-508.

Marushige, Y., and Marushige, K. (1975). Transformation of sperm histone during formation and maturation of rat spermatozoa. J Biol Chem *250*, 39-45.

Mayer, W., Niveleau, A., Walter, J., Fundele, R., and Haaf, T. (2000a). Demethylation of the zygotic paternal genome. Nature *403*, 501-502.

Mayer, W., Smith, A., Fundele, R., and Haaf, T. (2000b). Spatial separation of parental genomes in preimplantation mouse embryos. J Cell Biol *148*, 629-634.

Meglicki, M., Zientarski, M., and Borsuk, E. (2008). Constitutive heterochromatin during mouse oogenesis: the pattern of histone H3 modifications and localization of HP1alpha and HP1beta proteins. Mol Reprod Dev *75*, 414-428.

Meissner, A., Mikkelsen, T.S., Gu, H., Wernig, M., Hanna, J., Sivachenko, A., Zhang, X., Bernstein, B.E., Nusbaum, C., Jaffe, D.B.*, et al.* (2008). Genome-scale DNA methylation maps of pluripotent and differentiated cells. Nature *454*, 766-770.

Mendenhall, E.M., Koche, R.P., Truong, T., Zhou, V.W., Issac, B., Chi, A.S., Ku, M., and Bernstein, B.E. (2010). GC-rich sequence elements recruit PRC2 in mammalian ES cells. PLoS Genet *6*, e1001244.

Merico, V., Barbieri, J., Zuccotti, M., Joffe, B., Cremer, T., Redi, C.A., Solovei, I., and Garagna, S. (2007). Epigenomic differentiation in mouse preimplantation nuclei of biparental, parthenote and cloned embryos. Chromosome Res *15*, 341-360.

Micklem, G., Rowley, A., Harwood, J., Nasmyth, K., and Diffley, J.F. (1993). Yeast origin recognition complex is involved in DNA replication and transcriptional silencing. Nature *366*, 87-89.

Min, J., Zhang, Y., and Xu, R.M. (2003). Structural basis for specific binding of Polycomb chromodomain to histone H3 methylated at Lys 27. Genes Dev *17*, 1823-1828.

Minc, E., Allory, Y., Worman, H.J., Courvalin, J.C., and Buendia, B. (1999). Localization and phosphorylation of HP1 proteins during the cell cycle in mammalian cells. Chromosoma *108*, 220-234.

Moehrle, A., and Paro, R. (1994). Spreading the silence: epigenetic transcriptional regulation during Drosophila development. Dev Genet *15*, 478-484.

Morgan, T.H., and Schultz, J. (1942). Investigations on the constitution of the germinal material in relation to heredity. Yearbook Carnegie Inst *41*, 242-245.

Morse, R.H. (1989). Nucleosomes inhibit both transcriptional initiation and elongation by RNA polymerase III in vitro. Embo J *8*, 2343-2351.

Motamedi, M.R., Hong, E.J., Li, X., Gerber, S., Denison, C., Gygi, S., and Moazed, D. (2008). HP1 proteins form distinct complexes and mediate heterochromatic gene silencing by nonoverlapping mechanisms. Mol Cell *32*, 778-790.

Muchardt, C., Guilleme, M., Seeler, J.S., Trouche, D., Dejean, A., and Yaniv, M. (2002). Coordinated methyl and RNA binding is required for heterochromatin localization of mammalian HP1alpha. EMBO Rep *3*, 975-981.

Muller, H.J. (1930). Types of visible varations induced by X-rays in *Drosophila*. J Genetics *22*, 299-334.

Murchison, E.P., Partridge, J.F., Tam, O.H., Cheloufi, S., and Hannon, G.J. (2005). Characterization of Dicer-deficient murine embryonic stem cells. Proc Natl Acad Sci U S A *102*, 12135-12140.

Nakamura, T., Arai, Y., Umehara, H., Masuhara, M., Kimura, T., Taniguchi, H., Sekimoto, T., Ikawa, M., Yoneda, Y., Okabe, M.*, et al.* (2007). PGC7/Stella protects against DNA demethylation in early embryogenesis. Nat Cell Biol *9*, 64-71.

Nakayama, J., Rice, J.C., Strahl, B.D., Allis, C.D., and Grewal, S.I. (2001). Role of histone H3 lysine 9 methylation in epigenetic control of heterochromatin assembly. Science *292*, 110-113.

Nielsen, A.L., Ortiz, J.A., You, J., Oulad-Abdelghani, M., Khechumian, R., Gansmuller, A., Chambon, P., and Losson, R. (1999). Interaction with members of the heterochromatin protein 1 (HP1) family and histone deacetylation are differentially involved in transcriptional silencing by members of the TIF1 family. Embo J *18*, 6385-6395.

Niswander, L., Yee, D., Rinchik, E.M., Russell, L.B., and Magnuson, T. (1988). The albino deletion complex and early postimplantation survival in the mouse. Development *102*, 45-53.
O'Carroll, D., Erhardt, S., Pagani, M., Barton, S.C., Surani, M.A., and Jenuwein, T. (2001). The polycomb-group gene Ezh2 is required for early mouse development. Mol Cell Biol *21*, 4330-4336.
O'Carroll, D., Scherthan, H., Peters, A.H., Opravil, S., Haynes, A.R., Laible, G., Rea, S., Schmid, M., Lebersorger, A., Jerratsch, M.*, et al.* (2000). Isolation and characterization of Suv39h2, a second histone H3 methyltransferase gene that displays testis-specific expression. Mol Cell Biol *20*, 9423-9433.
Okano, M., Bell, D.W., Haber, D.A., and Li, E. (1999). DNA methyltransferases Dnmt3a and Dnmt3b are essential for de novo methylation and mammalian development. Cell *99*, 247-257.
Olek, A., and Walter, J. (1997). The pre-implantation ontogeny of the H19 methylation imprint. Nat Genet *17*, 275-276.
Oswald, J., Engemann, S., Lane, N., Mayer, W., Olek, A., Fundele, R., Dean, W., Reik, W., and Walter, J. (2000). Active demethylation of the paternal genome in the mouse zygote. Curr Biol *10*, 475-478.
Painter, T.S. (1928). A Comparison of the Chromosomes of the Rat and Mouse with Reference to the Question of Chromosome Homology in Mammals. Genetics *13*, 180-189.
Pak, D.T., Pflumm, M., Chesnokov, I., Huang, D.W., Kellum, R., Marr, J., Romanowski, P., and Botchan, M.R. (1997). Association of the origin recognition complex with heterochromatin and HP1 in higher eukaryotes. Cell *91*, 311-323.
Pal-Bhadra, M., Leibovitch, B.A., Gandhi, S.G., Rao, M., Bhadra, U., Birchler, J.A., and Elgin, S.C. (2004). Heterochromatic silencing and HP1 localization in Drosophila are dependent on the RNAi machinery. Science *303*, 669-672.
Palladino, F., Laroche, T., Gilson, E., Axelrod, A., Pillus, L., and Gasser, S.M. (1993). SIR3 and SIR4 proteins are required for the positioning and integrity of yeast telomeres. Cell *75*, 543-555.
Papp, B., and Muller, J. (2006). Histone trimethylation and the maintenance of transcriptional ON and OFF states by trxG and PcG proteins. Genes Dev *20*, 2041-2054.
Paro, R., and Hogness, D.S. (1991). The Polycomb protein shares a homologous domain with a heterochromatin-associated protein of Drosophila. Proc Natl Acad Sci U S A *88*, 263-267.
Partridge, J.F., Borgstrom, B., and Allshire, R.C. (2000). Distinct protein interaction domains and protein spreading in a complex centromere. Genes Dev *14*, 783-791.
Partridge, J.F., Scott, K.S., Bannister, A.J., Kouzarides, T., and Allshire, R.C. (2002). cis-acting DNA from fission yeast centromeres mediates histone H3 methylation and recruitment of silencing factors and cohesin to an ectopic site. Curr Biol *12*, 1652-1660.
Pasini, D., Bracken, A.P., Jensen, M.R., Lazzerini Denchi, E., and Helin, K. (2004). Suz12 is essential for mouse development and for EZH2 histone methyltransferase activity. Embo J *23*, 4061-4071.
Passarge, E. (1979). Emil Heitz and the concept of heterochromatin: longitudinal chromosome differentiation was recognized fifty years ago. Am J Hum Genet *31*, 106-115.
Peng, H., Ivanov, A.V., Oh, H.J., Lau, Y.F., and Rauscher, F.J., 3rd (2009). Epigenetic gene silencing by the SRY protein is mediated by a KRAB-O protein that recruits the KAP1 co-repressor machinery. J Biol Chem *284*, 35670-35680.
Peng, J.C., and Karpen, G.H. (2008). Epigenetic regulation of heterochromatic DNA stability. Curr Opin Genet Dev *18*, 204-211.
Penny, G.D., Kay, G.F., Sheardown, S.A., Rastan, S., and Brockdorff, N. (1996). Requirement for Xist in X chromosome inactivation. Nature *379*, 131-137.
Peters, A.H., Kubicek, S., Mechtler, K., O'Sullivan, R.J., Derijck, A.A., Perez-Burgos, L., Kohlmaier, A., Opravil, S., Tachibana, M., Shinkai, Y.*, et al.* (2003). Partitioning and plasticity of repressive histone methylation states in mammalian chromatin. Mol Cell *12*, 1577-1589.

Peters, A.H., O'Carroll, D., Scherthan, H., Mechtler, K., Sauer, S., Schofer, C., Weipoltshammer, K., Pagani, M., Lachner, M., Kohlmaier, A., *et al.* (2001). Loss of the Suv39h histone methyltransferases impairs mammalian heterochromatin and genome stability. Cell *107*, 323-337.

Platero, J.S., Hartnett, T., and Eissenberg, J.C. (1995). Functional analysis of the chromo domain of HP1. Embo J *14*, 3977-3986.

Platero, J.S., Sharp, E.J., Adler, P.N., and Eissenberg, J.C. (1996). In vivo assay for protein-protein interactions using Drosophila chromosomes. Chromosoma *104*, 393-404.

Plath, K., Talbot, D., Hamer, K.M., Otte, A.P., Yang, T.P., Jaenisch, R., and Panning, B. (2004). Developmentally regulated alterations in Polycomb repressive complex 1 proteins on the inactive X chromosome. J Cell Biol *167*, 1025-1035.

Polo, S.E., Roche, D., and Almouzni, G. (2006). New histone incorporation marks sites of UV repair in human cells. Cell *127*, 481-493.

Powers, J.A., and Eissenberg, J.C. (1993). Overlapping domains of the heterochromatin-associated protein HP1 mediate nuclear localization and heterochromatin binding. J Cell Biol *120*, 291-299.

Prasanth, S.G., Prasanth, K.V., Siddiqui, K., Spector, D.L., and Stillman, B. (2004). Human Orc2 localizes to centrosomes, centromeres and heterochromatin during chromosome inheritance. Embo J *23*, 2651-2663.

Prasanth, S.G., Shen, Z., Prasanth, K.V., and Stillman, B. (2010). Human origin recognition complex is essential for HP1 binding to chromatin and heterochromatin organization. Proc Natl Acad Sci U S A *107*, 15093-15098.

Probst, A.V., and Almouzni, G. (2011). Heterochromatin establishment in the context of genome-wide epigenetic reprogramming. Trends Genet *27*, 177-185.

Probst, A.V., Okamoto, I., Casanova, M., El Marjou, F., Le Baccon, P., and Almouzni, G. (2010). A strand-specific burst in transcription of pericentric satellites is required for chromocenter formation and early mouse development. Dev Cell *19*, 625-638.

Probst, A.V., Santos, F., Reik, W., Almouzni, G., and Dean, W. (2007). Structural differences in centromeric heterochromatin are spatially reconciled on fertilisation in the mouse zygote. Chromosoma *116*, 403-415.

Puschendorf, M., Terranova, R., Boutsma, E., Mao, X., Isono, K., Brykczynska, U., Kolb, C., Otte, A.P., Koseki, H., Orkin, S.H., *et al.* (2008). PRC1 and Suv39h specify parental asymmetry at constitutive heterochromatin in early mouse embryos. Nat Genet *40*, 411-420.

Quivy, J.P., Roche, D., Kirschner, D., Tagami, H., Nakatani, Y., and Almouzni, G. (2004). A CAF-1 dependent pool of HP1 during heterochromatin duplication. Embo J *23*, 3516-3526.

Rea, S., Eisenhaber, F., O'Carroll, D., Strahl, B.D., Sun, Z.W., Schmid, M., Opravil, S., Mechtler, K., Ponting, C.P., Allis, C.D., *et al.* (2000). Regulation of chromatin structure by site-specific histone H3 methyltransferases. Nature *406*, 593-599.

Reeves, R. (2001). Molecular biology of HMGA proteins: hubs of nuclear function. Gene *277*, 63-81.

Reeves, R., and Nissen, M.S. (1990). The A.T-DNA-binding domain of mammalian high mobility group I chromosomal proteins. A novel peptide motif for recognizing DNA structure. J Biol Chem *265*, 8573-8582.

Reik, W. (2007). Stability and flexibility of epigenetic gene regulation in mammalian development. Nature *447*, 425-432.

Reuter, G., and Wolff, I. (1981). Isolation of dominant suppressor mutations for position-effect variegation in Drosophila melanogaster. Mol Gen Genet *182*, 516-519.

Riddle, N.C., and Elgin, S.C. (2006). The dot chromosome of Drosophila: insights into chromatin states and their change over evolutionary time. Chromosome Res *14*, 405-416.

Riddle, N.C., and Elgin, S.C. (2008). A role for RNAi in heterochromatin formation in Drosophila. Curr Top Microbiol Immunol *320*, 185-209.

Riddle, N.C., Shaffer, C.D., and Elgin, S.C. (2009). A lot about a little dot - lessons learned from Drosophila melanogaster chromosome 4. Biochem Cell Biol *87*, 229-241.

Ringrose, L., Ehret, H., and Paro, R. (2004). Distinct contributions of histone H3 lysine 9 and 27 methylation to locus-specific stability of polycomb complexes. Mol Cell *16*, 641-653.

Ringrose, L., and Paro, R. (2007). Polycomb/Trithorax response elements and epigenetic memory of cell identity. Development *134*, 223-232.

Rinn, J.L., Kertesz, M., Wang, J.K., Squazzo, S.L., Xu, X., Brugmann, S.A., Goodnough, L.H., Helms, J.A., Farnham, P.J., Segal, E.*, et al.* (2007). Functional demarcation of active and silent chromatin domains in human HOX loci by noncoding RNAs. Cell *129*, 1311-1323.

Robinson, P.J., Fairall, L., Huynh, V.A., and Rhodes, D. (2006). EM measurements define the dimensions of the "30-nm" chromatin fiber: evidence for a compact, interdigitated structure. Proc Natl Acad Sci U S A *103*, 6506-6511.

Roscic, A., Moller, A., Calzado, M.A., Renner, F., Wimmer, V.C., Gresko, E., Ludi, K.S., and Schmitz, M.L. (2006). Phosphorylation-dependent control of Pc2 SUMO E3 ligase activity by its substrate protein HIPK2. Mol Cell *24*, 77-89.

Rougier, N., Bourc'his, D., Gomes, D.M., Niveleau, A., Plachot, M., Paldi, A., and Viegas-Pequignot, E. (1998). Chromosome methylation patterns during mammalian preimplantation development. Genes Dev *12*, 2108-2113.

Rusche, L.N., Kirchmaier, A.L., and Rine, J. (2002). Ordered nucleation and spreading of silenced chromatin in Saccharomyces cerevisiae. Mol Biol Cell *13*, 2207-2222.

Ruthenburg, A.J., Li, H., Milne, T.A., Dewell, S., McGinty, R.K., Yuen, M., Ueberheide, B., Dou, Y., Muir, T.W., Patel, D.J.*, et al.* (2011). Recognition of a mononucleosomal histone modification pattern by BPTF via multivalent interactions. Cell *145*, 692-706.

Sadaie, M., Iida, T., Urano, T., and Nakayama, J. (2004). A chromodomain protein, Chp1, is required for the establishment of heterochromatin in fission yeast. Embo J *23*, 3825-3835.

Sadaie, M., Kawaguchi, R., Ohtani, Y., Arisaka, F., Tanaka, K., Shirahige, K., and Nakayama, J. (2008). Balance between distinct HP1 family proteins controls heterochromatin assembly in fission yeast. Mol Cell Biol *28*, 6973-6988.

Saito, K., Nishida, K.M., Mori, T., Kawamura, Y., Miyoshi, K., Nagami, T., Siomi, H., and Siomi, M.C. (2006). Specific association of Piwi with rasiRNAs derived from retrotransposon and heterochromatic regions in the Drosophila genome. Genes Dev *20*, 2214-2222.

Santenard, A., and Torres-Padilla, M.E. (2009). Epigenetic reprogramming in mammalian reproduction: contribution from histone variants. Epigenetics *4*, 80-84.

Santenard, A., Ziegler-Birling, C., Koch, M., Tora, L., Bannister, A.J., and Torres-Padilla, M.E. (2010). Heterochromatin formation in the mouse embryo requires critical residues of the histone variant H3.3. Nat Cell Biol *12*, 853-862.

Santos, F., Hendrich, B., Reik, W., and Dean, W. (2002). Dynamic reprogramming of DNA methylation in the early mouse embryo. Dev Biol *241*, 172-182.

Santos, F., Peters, A.H., Otte, A.P., Reik, W., and Dean, W. (2005). Dynamic chromatin modifications characterise the first cell cycle in mouse embryos. Dev Biol *280*, 225-236.

Sanyal, A., Bau, D., Marti-Renom, M.A., and Dekker, J. (2011). Chromatin globules: a common motif of higher order chromosome structure? Curr Opin Cell Biol *23*, 325-331.

Sarmento, O.F., Digilio, L.C., Wang, Y., Perlin, J., Herr, J.C., Allis, C.D., and Coonrod, S.A. (2004). Dynamic alterations of specific histone modifications during early murine development. J Cell Sci *117*, 4449-4459.

Sarot, E., Payen-Groschene, G., Bucheton, A., and Pelisson, A. (2004). Evidence for a piwi-dependent RNA silencing of the gypsy endogenous retrovirus by the Drosophila melanogaster flamenco gene. Genetics *166*, 1313-1321.

Sasaki, H., Ishihara, K., and Kato, R. (2000). Mechanisms of Igf2/H19 imprinting: DNA methylation, chromatin and long-distance gene regulation. J Biochem *127*, 711-715.

Sasaki, H., and Matsui, Y. (2008). Epigenetic events in mammalian germ-cell development: reprogramming and beyond. Nat Rev Genet *9*, 129-140.

Satijn, D.P., Olson, D.J., van der Vlag, J., Hamer, K.M., Lambrechts, C., Masselink, H., Gunster, M.J., Sewalt, R.G., van Driel, R., and Otte, A.P. (1997). Interference with the expression of a novel human polycomb protein, hPc2, results in cellular transformation and apoptosis. Mol Cell Biol *17*, 6076-6086.

Sato, T., Russell, M.A., and Denell, R.E. (1983). Homoeosis in Drosophila: a new enhancer of polycomb and related homoeotic mutations. Genetics *105*, 357-370.

Saurin, A.J., Shiels, C., Williamson, J., Satijn, D.P., Otte, A.P., Sheer, D., and Freemont, P.S. (1998). The human polycomb group complex associates with pericentromeric heterochromatin to form a novel nuclear domain. J Cell Biol *142*, 887-898.

Sawarkar, R., and Paro, R. (2010). Interpretation of developmental signaling at chromatin: the Polycomb perspective. Dev Cell *19*, 651-661.

Schalch, T., Duda, S., Sargent, D.F., and Richmond, T.J. (2005). X-ray structure of a tetranucleosome and its implications for the chromatin fibre. Nature *436*, 138-141.

Schmiedeberg, L., Weisshart, K., Diekmann, S., Meyer Zu Hoerste, G., and Hemmerich, P. (2004). High- and low-mobility populations of HP1 in heterochromatin of mammalian cells. Mol Biol Cell *15*, 2819-2833.

Schmitges, F.W., Prusty, A.B., Faty, M., Stutzer, A., Lingaraju, G.M., Aiwazian, J., Sack, R., Hess, D., Li, L., Zhou, S.*, et al.* (2011). Histone methylation by PRC2 is inhibited by active chromatin marks. Mol Cell *42*, 330-341.

Schones, D.E., Cui, K., Cuddapah, S., Roh, T.Y., Barski, A., Wang, Z., Wei, G., and Zhao, K. (2008). Dynamic regulation of nucleosome positioning in the human genome. Cell *132*, 887-898.

Schoorlemmer, J., Marcos-Gutierrez, C., Were, F., Martinez, R., Garcia, E., Satijn, D.P., Otte, A.P., and Vidal, M. (1997). Ring1A is a transcriptional repressor that interacts with the Polycomb-M33 protein and is expressed at rhombomere boundaries in the mouse hindbrain. Embo J *16*, 5930-5942.

Schotta, G., Ebert, A., Dorn, R., and Reuter, G. (2003). Position-effect variegation and the genetic dissection of chromatin regulation in Drosophila. Semin Cell Dev Biol *14*, 67-75.

Schotta, G., Ebert, A., Krauss, V., Fischer, A., Hoffmann, J., Rea, S., Jenuwein, T., Dorn, R., and Reuter, G. (2002). Central role of Drosophila SU(VAR)3-9 in histone H3-K9 methylation and heterochromatic gene silencing. Embo J *21*, 1121-1131.

Schotta, G., Lachner, M., Sarma, K., Ebert, A., Sengupta, R., Reuter, G., Reinberg, D., and Jenuwein, T. (2004). A silencing pathway to induce H3-K9 and H4-K20 trimethylation at constitutive heterochromatin. Genes Dev *18*, 1251-1262.

Schotta, G., Sengupta, R., Kubicek, S., Malin, S., Kauer, M., Callen, E., Celeste, A., Pagani, M., Opravil, S., De La Rosa-Velazquez, I.A.*, et al.* (2008). A chromatin-wide transition to H4K20 monomethylation impairs genome integrity and programmed DNA rearrangements in the mouse. Genes Dev *22*, 2048-2061.

Schuettengruber, B., and Cavalli, G. (2009). Recruitment of polycomb group complexes and their role in the dynamic regulation of cell fate choice. Development *136*, 3531-3542.

Schuettengruber, B., Chourrout, D., Vervoort, M., Leblanc, B., and Cavalli, G. (2007). Genome regulation by polycomb and trithorax proteins. Cell *128*, 735-745.

Schuettengruber, B., Ganapathi, M., Leblanc, B., Portoso, M., Jaschek, R., Tolhuis, B., van Lohuizen, M., Tanay, A., and Cavalli, G. (2009). Functional anatomy of polycomb and trithorax chromatin landscapes in Drosophila embryos. PLoS Biol *7*, e13.

Schultz, J. (1950). Interrelations of factors affecting heterochromatin-induced variegation in *Drosophila*. Genetics *35*, 134.

Schultz, R.M. (2002). The molecular foundations of the maternal to zygotic transition in the preimplantation embryo. Hum Reprod Update *8*, 323-331.
Schwartz, Y.B., Kahn, T.G., Nix, D.A., Li, X.Y., Bourgon, R., Biggin, M., and Pirrotta, V. (2006). Genome-wide analysis of Polycomb targets in Drosophila melanogaster. Nat Genet *38*, 700-705.
Schwartz, Y.B., and Pirrotta, V. (2007). Polycomb silencing mechanisms and the management of genomic programmes. Nat Rev Genet *8*, 9-22.
Segurado, M., de Luis, A., and Antequera, F. (2003). Genome-wide distribution of DNA replication origins at A+T-rich islands in Schizosaccharomyces pombe. EMBO Rep *4*, 1048-1053.
Selker, E.U. (1998). Trichostatin A causes selective loss of DNA methylation in Neurospora. Proc Natl Acad Sci U S A *95*, 9430-9435.
Selker, E.U., and Stevens, J.N. (1985). DNA methylation at asymmetric sites is associated with numerous transition mutations. Proc Natl Acad Sci U S A *82*, 8114-8118.
Selker, E.U., Tountas, N.A., Cross, S.H., Margolin, B.S., Murphy, J.G., Bird, A.P., and Freitag, M. (2003). The methylated component of the Neurospora crassa genome. Nature *422*, 893-897.
Selker, M.R.E. (2009). Genome defense: the neurospora paradigm. . Epigenomics, pp321-341.
Senthilkumar, R., and Mishra, R.K. (2009). Novel motifs distinguish multiple homologues of Polycomb in vertebrates: expansion and diversification of the epigenetic toolkit. BMC Genomics *10*, 549.
Seum, C., Reo, E., Peng, H., Rauscher, F.J., 3rd, Spierer, P., and Bontron, S. (2007). Drosophila SETDB1 is required for chromosome 4 silencing. PLoS Genet *3*, e76.
Sewalt, R.G., Gunster, M.J., van der Vlag, J., Satijn, D.P., and Otte, A.P. (1999). C-Terminal binding protein is a transcriptional repressor that interacts with a specific class of vertebrate Polycomb proteins. Mol Cell Biol *19*, 777-787.
Shankaranarayana, G.D., Motamedi, M.R., Moazed, D., and Grewal, S.I. (2003). Sir2 regulates histone H3 lysine 9 methylation and heterochromatin assembly in fission yeast. Curr Biol *13*, 1240-1246.
Shao, Z., Raible, F., Mollaaghababa, R., Guyon, J.R., Wu, C.T., Bender, W., and Kingston, R.E. (1999). Stabilization of chromatin structure by PRC1, a Polycomb complex. Cell *98*, 37-46.
Shareef, M.M., King, C., Damaj, M., Badagu, R., Huang, D.W., and Kellum, R. (2001). Drosophila heterochromatin protein 1 (HP1)/origin recognition complex (ORC) protein is associated with HP1 and ORC and functions in heterochromatin-induced silencing. Mol Biol Cell *12*, 1671-1685.
Shearn, A., Hersperger, G., Hersperger, E., Pentz, E.S., and Denker, P. (1978). Multiple Allele Approach to the Study of Genes in DROSOPHILA MELANOGASTER That Are Involved in Imaginal Disc Development. Genetics *89*, 355-370.
Shen, L., Kondo, Y., Guo, Y., Zhang, J., Zhang, L., Ahmed, S., Shu, J., Chen, X., Waterland, R.A., and Issa, J.P. (2007). Genome-wide profiling of DNA methylation reveals a class of normally methylated CpG island promoters. PLoS Genet *3*, 2023-2036.
Shen, X., Liu, Y., Hsu, Y.J., Fujiwara, Y., Kim, J., Mao, X., Yuan, G.C., and Orkin, S.H. (2008). EZH1 mediates methylation on histone H3 lysine 27 and complements EZH2 in maintaining stem cell identity and executing pluripotency. Mol Cell *32*, 491-502.
Shen, Z., Sathyan, K.M., Geng, Y., Zheng, R., Chakraborty, A., Freeman, B., Wang, F., Prasanth, K.V., and Prasanth, S.G. (2010). A WD-repeat protein stabilizes ORC binding to chromatin. Mol Cell *40*, 99-111.
Silver, L.M. (1995). Mouse Genetics.
Sinclair D.A.R, M.R.C., and Grigliatti T.A. (1983). Genes whcih suppress positon effect variegation in *Drosophila melanogaster*. Mol Gen Genet *191*, 326-333.
Sing, A., Pannell, D., Karaiskakis, A., Sturgeon, K., Djabali, M., Ellis, J., Lipshitz, H.D., and Cordes, S.P. (2009). A vertebrate Polycomb response element governs segmentation of the posterior hindbrain. Cell *138*, 885-897.
Singh, P.B., and Georgatos, S.D. (2002). HP1: facts, open questions, and speculation. J Struct Biol *140*, 10-16.

Sinkkonen, L., Hugenschmidt, T., Berninger, P., Gaidatzis, D., Mohn, F., Artus-Revel, C.G., Zavolan, M., Svoboda, P., and Filipowicz, W. (2008). MicroRNAs control de novo DNA methylation through regulation of transcriptional repressors in mouse embryonic stem cells. Nat Struct Mol Biol *15*, 259-267.

Slawson, E.E., Shaffer, C.D., Malone, C.D., Leung, W., Kellmann, E., Shevchek, R.B., Craig, C.A., Bloom, S.M., Bogenpohl, J., 2nd, Dee, J.*, et al.* (2006). Comparison of dot chromosome sequences from D. melanogaster and D. virilis reveals an enrichment of DNA transposon sequences in heterochromatic domains. Genome Biol *7*, R15.

Small, S., Blair, A., and Levine, M. (1992). Regulation of even-skipped stripe 2 in the Drosophila embryo. Embo J *11*, 4047-4057.

Smallwood, A., Esteve, P.O., Pradhan, S., and Carey, M. (2007). Functional cooperation between HP1 and DNMT1 mediates gene silencing. Genes Dev *21*, 1169-1178.

Smit, A.F. (1999). Interspersed repeats and other mementos of transposable elements in mammalian genomes. Curr Opin Genet Dev *9*, 657-663.

Smothers, J.F., and Henikoff, S. (2000). The HP1 chromo shadow domain binds a consensus peptide pentamer. Curr Biol *10*, 27-30.

Souza, P.P., Volkel, P., Trinel, D., Vandamme, J., Rosnoblet, C., Heliot, L., and Angrand, P.O. (2009). The histone methyltransferase SUV420H2 and Heterochromatin Proteins HP1 interact but show different dynamic behaviours. BMC Cell Biol *10*, 41.

Sparmann, A., and van Lohuizen, M. (2006). Polycomb silencers control cell fate, development and cancer. Nat Rev Cancer *6*, 846-856.

Stewart, C.L., Stuhlmann, H., Jahner, D., and Jaenisch, R. (1982). De novo methylation, expression, and infectivity of retroviral genomes introduced into embryonal carcinoma cells. Proc Natl Acad Sci U S A *79*, 4098-4102.

Stitzel, M.L., and Seydoux, G. (2007). Regulation of the oocyte-to-zygote transition. Science *316*, 407-408.

Struhl, G. (1981). A gene product required for correct initiation of segmental determination in Drosophila. Nature *293*, 36-41.

Suetake, I., Shinozaki, F., Miyagawa, J., Takeshima, H., and Tajima, S. (2004). DNMT3L stimulates the DNA methylation activity of Dnmt3a and Dnmt3b through a direct interaction. J Biol Chem *279*, 27816-27823.

Susbielle, G., Blattes, R., Brevet, V., Monod, C., and Kas, E. (2005). Target practice: aiming at satellite repeats with DNA minor groove binders. Curr Med Chem Anticancer Agents *5*, 409-420.

Suto, R.K., Clarkson, M.J., Tremethick, D.J., and Luger, K. (2000). Crystal structure of a nucleosome core particle containing the variant histone H2A.Z. Nat Struct Biol *7*, 1121-1124.

Tachibana, M., Nozaki, M., Takeda, N., and Shinkai, Y. (2007). Functional dynamics of H3K9 methylation during meiotic prophase progression. Embo J *26*, 3346-3359.

Tadros, W., and Lipshitz, H.D. (2009). The maternal-to-zygotic transition: a play in two acts. Development *136*, 3033-3042.

Tagami, H., Ray-Gallet, D., Almouzni, G., and Nakatani, Y. (2004). Histone H3.1 and H3.3 complexes mediate nucleosome assembly pathways dependent or independent of DNA synthesis. Cell *116*, 51-61.

Tahiliani, M., Koh, K.P., Shen, Y., Pastor, W.A., Bandukwala, H., Brudno, Y., Agarwal, S., Iyer, L.M., Liu, D.R., Aravind, L.*, et al.* (2009). Conversion of 5-methylcytosine to 5-hydroxymethylcytosine in mammalian DNA by MLL partner TET1. Science *324*, 930-935.

Takada, Y., Naruse, C., Costa, Y., Shirakawa, T., Tachibana, M., Sharif, J., Kezuka-Shiotani, F., Kakiuchi, D., Masumoto, H., Shinkai, Y.*, et al.* (2011). HP1{gamma} links histone methylation marks to meiotic synapsis in mice. Development *138*, 4207-4217.

Tamaru, H., and Selker, E.U. (2001). A histone H3 methyltransferase controls DNA methylation in Neurospora crassa. Nature *414*, 277-283.

Tanphaichitr, N., Sobhon, P., Taluppeth, N., and Chalermisarachai, P. (1978). Basic nuclear proteins in testicular cells and ejaculated spermatozoa in man. Exp Cell Res *117*, 347-356.

Thanos, D., and Maniatis, T. (1992). The high mobility group protein HMG I(Y) is required for NF-kappa B-dependent virus induction of the human IFN-beta gene. Cell *71*, 777-789.

Thon, G., and Verhein-Hansen, J. (2000). Four chromo-domain proteins of Schizosaccharomyces pombe differentially repress transcription at various chromosomal locations. Genetics *155*, 551-568.

Tie, F., Furuyama, T., and Harte, P.J. (1998). The Drosophila Polycomb Group proteins ESC and E(Z) bind directly to each other and co-localize at multiple chromosomal sites. Development *125*, 3483-3496.

Torres-Padilla, M.E., Bannister, A.J., Hurd, P.J., Kouzarides, T., and Zernicka-Goetz, M. (2006). Dynamic distribution of the replacement histone variant H3.3 in the mouse oocyte and preimplantation embryos. Int J Dev Biol *50*, 455-461.

Trojer, P., and Reinberg, D. (2007). Facultative heterochromatin: is there a distinctive molecular signature? Mol Cell *28*, 1-13.

Tschiersch, B., Hofmann, A., Krauss, V., Dorn, R., Korge, G., and Reuter, G. (1994). The protein encoded by the Drosophila position-effect variegation suppressor gene Su(var)3-9 combines domains of antagonistic regulators of homeotic gene complexes. Embo J *13*, 3822-3831.

Tzeng, T.Y., Lee, C.H., Chan, L.W., and Shen, C.K. (2007). Epigenetic regulation of the Drosophila chromosome 4 by the histone H3K9 methyltransferase dSETDB1. Proc Natl Acad Sci U S A *104*, 12691-12696.

van der Heijden, G.W., Derijck, A.A., Ramos, L., Giele, M., van der Vlag, J., and de Boer, P. (2006). Transmission of modified nucleosomes from the mouse male germline to the zygote and subsequent remodeling of paternal chromatin. Dev Biol *298*, 458-469.

van der Heijden, G.W., Dieker, J.W., Derijck, A.A., Muller, S., Berden, J.H., Braat, D.D., van der Vlag, J., and de Boer, P. (2005). Asymmetry in histone H3 variants and lysine methylation between paternal and maternal chromatin of the early mouse zygote. Mech Dev *122*, 1008-1022.

van der Heijden, G.W., Ramos, L., Baart, E.B., van den Berg, I.M., Derijck, A.A., van der Vlag, J., Martini, E., and de Boer, P. (2008). Sperm-derived histones contribute to zygotic chromatin in humans. BMC Dev Biol *8*, 34.

van der Lugt, N.M., Domen, J., Linders, K., van Roon, M., Robanus-Maandag, E., te Riele, H., van der Valk, M., Deschamps, J., Sofroniew, M., van Lohuizen, M*., et al.* (1994). Posterior transformation, neurological abnormalities, and severe hematopoietic defects in mice with a targeted deletion of the bmi-1 proto-oncogene. Genes Dev *8*, 757-769.

Vandamme, J., Volkel, P., Rosnoblet, C., Le Faou, P., and Angrand, P.O. (2011). Interaction proteomics analysis of polycomb proteins defines distinct PRC1 complexes in mammalian cells. Mol Cell Proteomics *10*, M110 002642.

Vazquez, J., Muller, M., Pirrotta, V., and Sedat, J.W. (2006). The Mcp element mediates stable long-range chromosome-chromosome interactions in Drosophila. Mol Biol Cell *17*, 2158-2165.

Vega-Palas, M.A., Venditti, S., and Di Mauro, E. (1998). Heterochromatin organization of a natural yeast telomere. Changes of nucleosome distribution driven by the absence of Sir3p. J Biol Chem *273*, 9388-9392.

Verdel, A., Jia, S., Gerber, S., Sugiyama, T., Gygi, S., Grewal, S.I., and Moazed, D. (2004). RNAi-mediated targeting of heterochromatin by the RITS complex. Science *303*, 672-676.

Verdel, A., Vavasseur, A., Le Gorrec, M., and Touat-Todeschini, L. (2009). Common themes in siRNA-mediated epigenetic silencing pathways. Int J Dev Biol *53*, 245-257.

Vermeulen, M., Eberl, H.C., Matarese, F., Marks, H., Denissov, S., Butter, F., Lee, K.K., Olsen, J.V., Hyman, A.A., Stunnenberg, H.G*., et al.* (2010). Quantitative interaction proteomics and genome-wide profiling of epigenetic histone marks and their readers. Cell *142*, 967-980.

Veron, N., and Peters, A.H. (2011). Epigenetics: Tet proteins in the limelight. Nature *473*, 293-294.

Vitale, A.M., Calvert, M.E., Mallavarapu, M., Yurttas, P., Perlin, J., Herr, J., and Coonrod, S. (2007). Proteomic profiling of murine oocyte maturation. Mol Reprod Dev *74*, 608-616.

Volpe, T.A., Kidner, C., Hall, I.M., Teng, G., Grewal, S.I., and Martienssen, R.A. (2002). Regulation of heterochromatic silencing and histone H3 lysine-9 methylation by RNAi. Science *297*, 1833-1837.

Voncken, J.W., Roelen, B.A., Roefs, M., de Vries, S., Verhoeven, E., Marino, S., Deschamps, J., and van Lohuizen, M. (2003). Rnf2 (Ring1b) deficiency causes gastrulation arrest and cell cycle inhibition. Proc Natl Acad Sci U S A *100*, 2468-2473.

Walsh, C.P., Chaillet, J.R., and Bestor, T.H. (1998). Transcription of IAP endogenous retroviruses is constrained by cytosine methylation. Nat Genet *20*, 116-117.

Wang, H., Wang, L., Erdjument-Bromage, H., Vidal, M., Tempst, P., Jones, R.S., and Zhang, Y. (2004a). Role of histone H2A ubiquitination in Polycomb silencing. Nature *431*, 873-878.

Wang, L., Brown, J.L., Cao, R., Zhang, Y., Kassis, J.A., and Jones, R.S. (2004b). Hierarchical recruitment of polycomb group silencing complexes. Mol Cell *14*, 637-646.

Watanabe, T., Takeda, A., Tsukiyama, T., Mise, K., Okuno, T., Sasaki, H., Minami, N., and Imai, H. (2006). Identification and characterization of two novel classes of small RNAs in the mouse germline: retrotransposon-derived siRNAs in oocytes and germline small RNAs in testes. Genes Dev *20*, 1732-1743.

Waterston, R.H., Lindblad-Toh, K., Birney, E., Rogers, J., Abril, J.F., Agarwal, P., Agarwala, R., Ainscough, R., Alexandersson, M., An, P.*, et al.* (2002). Initial sequencing and comparative analysis of the mouse genome. Nature *420*, 520-562.

Weber, M., Hellmann, I., Stadler, M.B., Ramos, L., Paabo, S., Rebhan, M., and Schubeler, D. (2007). Distribution, silencing potential and evolutionary impact of promoter DNA methylation in the human genome. Nat Genet *39*, 457-466.

Weiler, K.S., and Chatterjee, S. (2009). The multi-AT-hook chromosomal protein of Drosophila melanogaster, D1, is dispensable for viability. Genetics *182*, 145-159.

Weiss, K., and Simpson, R.T. (1998). High-resolution structural analysis of chromatin at specific loci: Saccharomyces cerevisiae silent mating type locus HMLalpha. Mol Cell Biol *18*, 5392-5403.

Whitcomb, S.J., Basu, A., Allis, C.D., and Bernstein, E. (2007). Polycomb Group proteins: an evolutionary perspective. Trends Genet *23*, 494-502.

Widom, J., and Klug, A. (1985). Structure of the 300A chromatin filament: X-ray diffraction from oriented samples. Cell *43*, 207-213.

Wiederschain, D., Chen, L., Johnson, B., Bettano, K., Jackson, D., Taraszka, J., Wang, Y.K., Jones, M.D., Morrissey, M., Deeds, J.*, et al.* (2007). Contribution of polycomb homologues Bmi-1 and Mel-18 to medulloblastoma pathogenesis. Mol Cell Biol *27*, 4968-4979.

Wiekowski, M., Miranda, M., and DePamphilis, M.L. (1993). Requirements for promoter activity in mouse oocytes and embryos distinguish paternal pronuclei from maternal and zygotic nuclei. Dev Biol *159*, 366-378.

Williams, K., Christensen, J., Pedersen, M.T., Johansen, J.V., Cloos, P.A., Rappsilber, J., and Helin, K. (2011). TET1 and hydroxymethylcytosine in transcription and DNA methylation fidelity. Nature *473*, 343-348.

Williams, S.P., Athey, B.D., Muglia, L.J., Schappe, R.S., Gough, A.H., and Langmore, J.P. (1986). Chromatin fibers are left-handed double helices with diameter and mass per unit length that depend on linker length. Biophys J *49*, 233-248.

Wilson, R.J., Goodman, J.L., and Strelets, V.B. (2008). FlyBase: integration and improvements to query tools. Nucleic Acids Res *36*, D588-593.

Wiren, M., Silverstein, R.A., Sinha, I., Walfridsson, J., Lee, H.M., Laurenson, P., Pillus, L., Robyr, D., Grunstein, M., and Ekwall, K. (2005). Genomewide analysis of nucleosome density histone acetylation and HDAC function in fission yeast. Embo J *24*, 2906-2918.

Wong, A.K., and Rattner, J.B. (1988). Sequence organization and cytological localization of the minor satellite of mouse. Nucleic Acids Res *16*, 11645-11661.
Woodcock, C.L., Skoultchi, A.I., and Fan, Y. (2006). Role of linker histone in chromatin structure and function: H1 stoichiometry and nucleosome repeat length. Chromosome Res *14*, 17-25.
Workman, J.L. (2006). Nucleosome displacement in transcription. Genes Dev *20*, 2009-2017.
Wossidlo, M., Nakamura, T., Lepikhov, K., Marques, C.J., Zakhartchenko, V., Boiani, M., Arand, J., Nakano, T., Reik, W., and Walter, J. (2011). 5-Hydroxymethylcytosine in the mammalian zygote is linked with epigenetic reprogramming. Nat Commun *2*, 241.
Wouters-Tyrou, D., Martinage, A., Chevaillier, P., and Sautiere, P. (1998). Nuclear basic proteins in spermiogenesis. Biochimie *80*, 117-128.
Wu, C., Orozco, C., Boyer, J., Leglise, M., Goodale, J., Batalov, S., Hodge, C.L., Haase, J., Janes, J., Huss, J.W., 3rd*, et al.* (2009). BioGPS: an extensible and customizable portal for querying and organizing gene annotation resources. Genome Biol *10*, R130.
Wu, S.C., and Zhang, Y. (2010). Active DNA demethylation: many roads lead to Rome. Nat Rev Mol Cell Biol *11*, 607-620.
Wustmann, G., Szidonya, J., Taubert, H., and Reuter, G. (1989). The genetics of position-effect variegation modifying loci in Drosophila melanogaster. Mol Gen Genet *217*, 520-527.
Wutz, A. (2011). Gene silencing in X-chromosome inactivation: advances in understanding facultative heterochromatin formation. Nat Rev Genet *12*, 542-553.
Wutz, A., and Jaenisch, R. (2000). A shift from reversible to irreversible X inactivation is triggered during ES cell differentiation. Mol Cell *5*, 695-705.
Wykes, S.M., and Krawetz, S.A. (2003). The structural organization of sperm chromatin. J Biol Chem *278*, 29471-29477.
Wysocka, J., Swigut, T., Xiao, H., Milne, T.A., Kwon, S.Y., Landry, J., Kauer, M., Tackett, A.J., Chait, B.T., Badenhorst, P.*, et al.* (2006). A PHD finger of NURF couples histone H3 lysine 4 trimethylation with chromatin remodelling. Nature *442*, 86-90.
Xhemalce, B., and Kouzarides, T. (2010). A chromodomain switch mediated by histone H3 Lys 4 acetylation regulates heterochromatin assembly. Genes Dev *24*, 647-652.
Yamagata, K., Yamazaki, T., Yamashita, M., Hara, Y., Ogonuki, N., and Ogura, A. (2005). Noninvasive visualization of molecular events in the mammalian zygote. Genesis *43*, 71-79.
Yamazaki, T., Kobayakawa, S., Yamagata, K., Abe, K., and Baba, T. (2007). Molecular dynamics of heterochromatin protein 1beta, HP1beta, during mouse preimplantation development. J Reprod Dev *53*, 1035-1041.
Yap, K.L., Li, S., Munoz-Cabello, A.M., Raguz, S., Zeng, L., Mujtaba, S., Gil, J., Walsh, M.J., and Zhou, M.M. (2010). Molecular interplay of the noncoding RNA ANRIL and methylated histone H3 lysine 27 by polycomb CBX7 in transcriptional silencing of INK4a. Mol Cell *38*, 662-674.
Yeo, S., Lee, K.K., Han, Y.M., and Kang, Y.K. (2005). Methylation changes of lysine 9 of histone H3 during preimplantation mouse development. Mol Cells *20*, 423-428.
Yun, M., Wu, J., Workman, J.L., and Li, B. (2011). Readers of histone modifications. Cell Res *21*, 564-578.
Zacharias, H. (1995). Emil Heitz (1892-1965): chloroplasts, heterochromatin, and polytene chromosomes. Genetics *141*, 7-14.
Zeng, F., Baldwin, D.A., and Schultz, R.M. (2004). Transcript profiling during preimplantation mouse development. Dev Biol *272*, 483-496.
Zhao, T., and Eissenberg, J.C. (1999). Phosphorylation of heterochromatin protein 1 by casein kinase II is required for efficient heterochromatin binding in Drosophila. J Biol Chem *274*, 15095-15100.
Zhao, T., Heyduk, T., and Eissenberg, J.C. (2001). Phosphorylation site mutations in heterochromatin protein 1 (HP1) reduce or eliminate silencing activity. J Biol Chem *276*, 9512-9518.

Zuccotti, M., Piccinelli, A., Giorgi Rossi, P., Garagna, S., and Redi, C.A. (1995). Chromatin organization during mouse oocyte growth. Mol Reprod Dev *41*, 479-485.

Zuccotti, M., Ponce, R.H., Boiani, M., Guizzardi, S., Govoni, P., Scandroglio, R., Garagna, S., and Redi, C.A. (2002). The analysis of chromatin organisation allows selection of mouse antral oocytes competent for development to blastocyst. Zygote *10*, 73-78.

Appendix

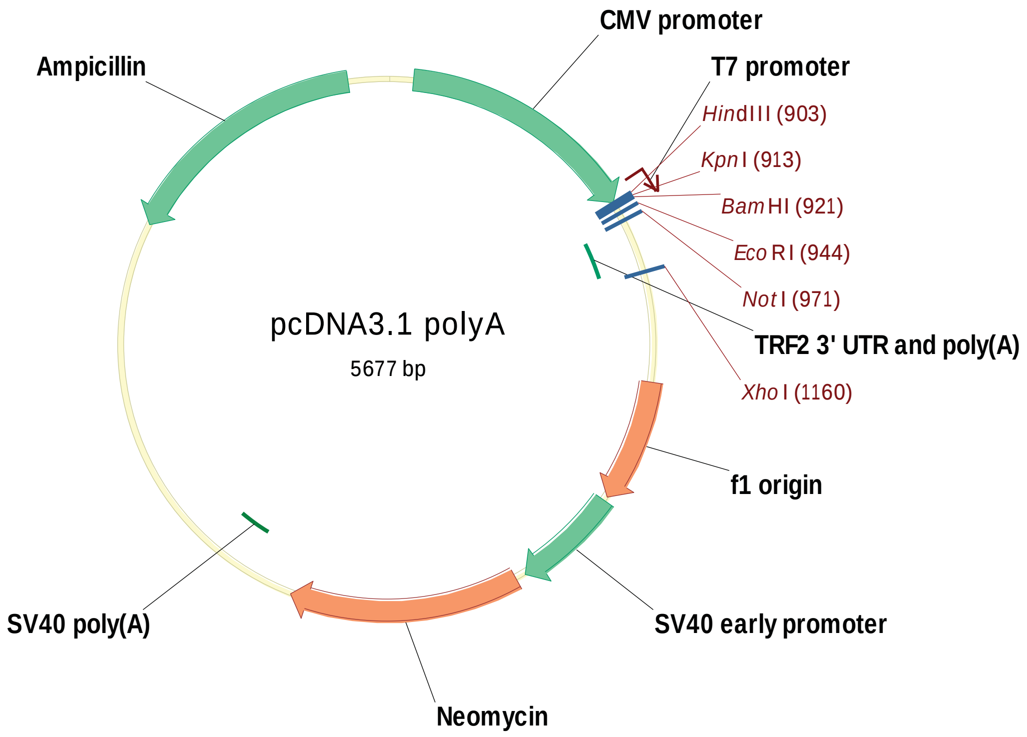
CMV promoter
Ampicillin
T7 promoter
Hind III (903)
Kpn I (913)
Bam HI (921)
Eco R I (944)
Not I (971)
TRF2 3' UTR and poly(A)
Xho I (1160)
pcDNA3.1 polyA
5677 bp
f1 origin
SV40 poly(A)
SV40 early promoter
Neomycin

Sequence pcDNA3.1-polyA: 1-5677

1gacggatcgggagatctcccgatcccctatggtcgactctcagtacaatctgctctgatgccgcatagttaagccagtatctgctccct

gcttgtgtgttggaggtcgctgagtagtgcgcgagcaaaatttaagctacaacaaggcaaggcttgaccgacaattgcatgaagaatc

tgcttagggttaggcgttttgcgctgcttcgcgatgtacgggccagatatacgcgttgacattgattattgactagttattaatagtaatcaatt

acggggtcattagttcatagcccatatatggagttccgcgttacataacttacggtaaatggcccgcctggctgaccgcccaacgaccc

ccgcccattgacgtcaataatgacgtatgttcccatagtaacgccaatagggactttccattgacgtcaatgggtggactatttacggtaa

actgcccacttggcagtacatcaagtgtatcatatgccaagtacgccccctattgacgtcaatgacggtaaatggcccgcctggcattat

gcccagtacatgaccttatgggactttcctacttggcagtacatctacgtattagtcatcgctattaccatggtgatgcggttttggcagtac

atcaatgggcgtggatagcggtttgactcacggggatttccaagtctccaccccattgacgtcaatgggagtttgttttggcaccaaaatc

aacgggactttccaaaatgtcgtaacaactccgccccattgacgcaaatgggcggtaggcgtgtacggtgggaggtctatataagca

gagctctctggctaactagagaacccactgcttactggcttatcgaaattaatacgactcactatagggagacccaagctggctagtta

agcttggtaccgagctcggatccactagtccagtgtggtggaattctgcagatatccagcacagtggcggccgctcgactatgggcac

caaagaacctgtaaacgttatctttttaaattgaatgtgcacaaataaaagtttggaaaagaaaaaaaaaaaaaaaaaaaaaaaaa
aaaaaaaaaaaaaaaaaaaaaaaaaaaaaaaaaaaaaaaaaaaaaaaaaaaaaaaaaaaaaaaaatacgcatcatacgctgtggcgt
acctcgagtctagagggcccttcgaacaaaaactcatctcagaagaggatctgaatatgcataccggtcatcatcaccatcaccattg
agtttaaacccgctgatcagcctcgactgtgccttctagttgccagccatctgttgtttgcccctcccccgtgccttccttgaccctggaagg
tgccactcccactgtcctttcctaataaaatgaggaaattgcatcgcattgtctgagtaggtgtcattctattctggggggtggggtggggc
aggacagcaagggggaggattgggaagacaatagcaggcatgctggggatgcggtgggctctatggcttctgaggcggaaagaa
ccagctggggctctagggggtatccccacgcgccctgtagcggcgcattaagcgcggcgggtgtggtggttacgcgcagcgtgacc
gctacacttgccagcgccctagcgcccgctcctttcgctttcttcccttcctttctcgccacgttcgccggctttccccgtcaagctctaaatc
ggggcatccctttagggttccgatttagtgctttacggcacctcgaccccaaaaaacttgattagggtgatggttcacgtagtgggccatc
gccctgatagacggtttttcgccctttgacgttggagtccacgttctttaatagtggactcttgttccaaactggaacaacactcaaccctat
ctcggtctattcttttgatttataagggattttggggatttcggcctattggttaaaaaatgagctgatttaacaaaaatttaacgcgaattaatt
ctgtggaatgtgtgtcagttagggtgtggaaagtccccaggctccccaggcaggcagaagtatgcaaagcatgcatctcaattagtca
gcaaccaggtgtggaaagtccccaggctccccagcaggcagaagtatgcaaagcatgcatctcaattagtcagcaaccatagtccc
gcccctaactccgcccatcccgcccctaactccgcccagttccgcccattctccgccccatggctgactaattttttttatttatgcagagg
ccgaggccgcctctgcctctgagctattccagaagtagtgaggaggcttttttggaggcctaggcttttgcaaaaagctcccgggagctt
gtatatccattttcggatctgatcaagagacaggatgaggatcgtttcgcatgattgaacaagatggattgcacgcaggttctccggccg
cttgggtggagaggctattcggctatgactgggcacaacagacaatcggctgctctgatgccgccgtgttccggctgtcagcgcaggg
gcgcccggttctttttgtcaagaccgacctgtccggtgccctgaatgaactgcaggacgaggcagcgcggctatcgtggctggccacg
acgggcgttccttgcgcagctgtgctcgacgttgtcactgaagcgggaagggactggctgctattgggcgaagtgccggggcaggat
ctcctgtcatctcaccttgctcctgccgagaaagtatccatcatggctgatgcaatgcggcggctgcatacgcttgatccggctacctgcc
cattcgaccaccaagcgaaacatcgcatcgagcgagcacgtactcggatggaagccggtcttgtcgatcaggatgatctggacgaa
gagcatcaggggctcgcgccagccgaactgttcgccaggctcaaggcgcgcatgcccgacggcgaggatctcgtcgtgacccatg
gcgatgcctgcttgccgaatatcatggtggaaaatggccgcttttctggattcatcgactgtggccggctgggtgtggcggaccgctatc
aggacatagcgttggctacccgtgatattgctgaagagcttggcggcgaatgggctgaccgcttcctcgtgctttacggtatcgccgctc
ccgattcgcagcgcatcgccttctatcgccttcttgacgagttcttctgagcgggactctggggttcgcgaaatgaccgaccaagcgac
gcccaacctgccatcacgagatttcgattccaccgccgccttctatgaaaggttgggcttcggaatcgttttccgggacgccggctggat
gatcctccagcgcggggatctcatgctggagttcttcgcccaccccaacttgtttattgcagcttataatggttacaaataaagcaatagc
atcacaaatttcacaaataaagcatttttttcactgcattctagttgtggtttgtccaaactcatcaatgtatcttatcatgtctgtataccgtcga
cctctagctagagcttggcgtaatcatggtcatagctgtttcctgtgtgaaattgttatccgctcacaattccacacaacatacgagccgg
aagcataaagtgtaaagcctggggtgcctaatgagtgagctaactcacattaattgcgttgcgctcactgcccgctttccagtcgggaa
acctgtcgtgccagctgcattaatgaatcggccaacgcgcggggagaggcggtttgcgtattgggcgctcttccgcttcctcgctcactg
actcgctgcgctcggtcgttcggctgcggcgagcggtatcagctcactcaaaggcggtaatacggttatccacagaatcaggggata
acgcaggaaagaacatgtgagcaaaaggccagcaaaaggccaggaaccgtaaaaaggccgcgttgctggcgtttttccataggc
tccgcccccctgacgagcatcacaaaaatcgacgctcaagtcagaggtggcgaaacccgacaggactataaagataccaggcgtt

tcccccctggaagctccctcgtgcgctctcctgttccgaccctgccgcttaccggatacctgtccgcctttctcccttcgggaagcgtggcg
ctttctcaatgctcacgctgtaggtatctcagttcggtgtaggtcgttcgctccaagctgggctgtgtgcacgaaccccccgttcagcccg
accgctgcgccttatccggtaactatcgtcttgagtccaacccggtaagacacgacttatcgccactggcagcagccactggtaacag
gattagcagagcgaggtatgtaggcggtgctacagagttcttgaagtggtggcctaactacggctacactagaaggacagtatttggt
atctgcgctctgctgaagccagttaccttcggaaaaagagttggtagctcttgatccggcaaacaaaccaccgctggtagcggtggtttt
tttgtttgcaagcagcagattacgcgcagaaaaaaaggatctcaagaagatcctttgatcttttctacggggtctgacgctcagtggaac
gaaaactcacgttaagggattttggtcatgagattatcaaaaaggatcttcacctagatccttttaaattaaaaatgaagttttaaatcaat
ctaaagtatatatgagtaaacttggtctgacagttaccaatgcttaatcagtgaggcacctatctcagcgatctgtctatttcgttcatccata
gttgcctgactccccgtcgtgtagataactacgatacgggagggcttaccatctggccccagtgctgcaatgataccgcgagacccac
gctcaccggctccagatttatcagcaataaaccagccagccggaagggccgagcgcagaagtggtcctgcaactttatccgcctcc
atccagtctattaattgttgccgggaagctagagtaagtagttcgccagttaatagtttgcgcaacgttgttgccattgctacaggcatcgt
ggtgtcacgctcgtcgtttggtatggcttcattcagctccggttcccaacgatcaaggcgagttacatgatcccccatgttgtgcaaaaaa
gcggttagctccttcggtcctccgatcgttgtcagaagtaagttggccgcagtgttatcactcatggttatggcagcactgcataattctctt
actgtcatgccatccgtaagatgcttttctgtgactggtgagtactcaaccaagtcattctgagaatagtgtatgcggcgaccgagttgctc
ttgcccggcgtcaatacgggataataccgcgccacatagcagaactttaaaagtgctcatcattggaaaacgttcttcggggcgaaaa
ctctcaaggatcttaccgctgttgagatccagttcgatgtaacccactcgtgcacccaactgatcttcagcatcttttactttcaccagcgttt
ctgggtgagcaaaaacaggaaggcaaaatgccgcaaaaaagggaataagggcgacacggaaatgttgaatactcatactcttcct
ttttcaatattattgaagcatttatcagggttattgtctcatgagcggatacatatttgaatgtatttagaaaaataaacaaataggggttccg
cgcacatttccccgaaaagtgccacctgacgtc-5677

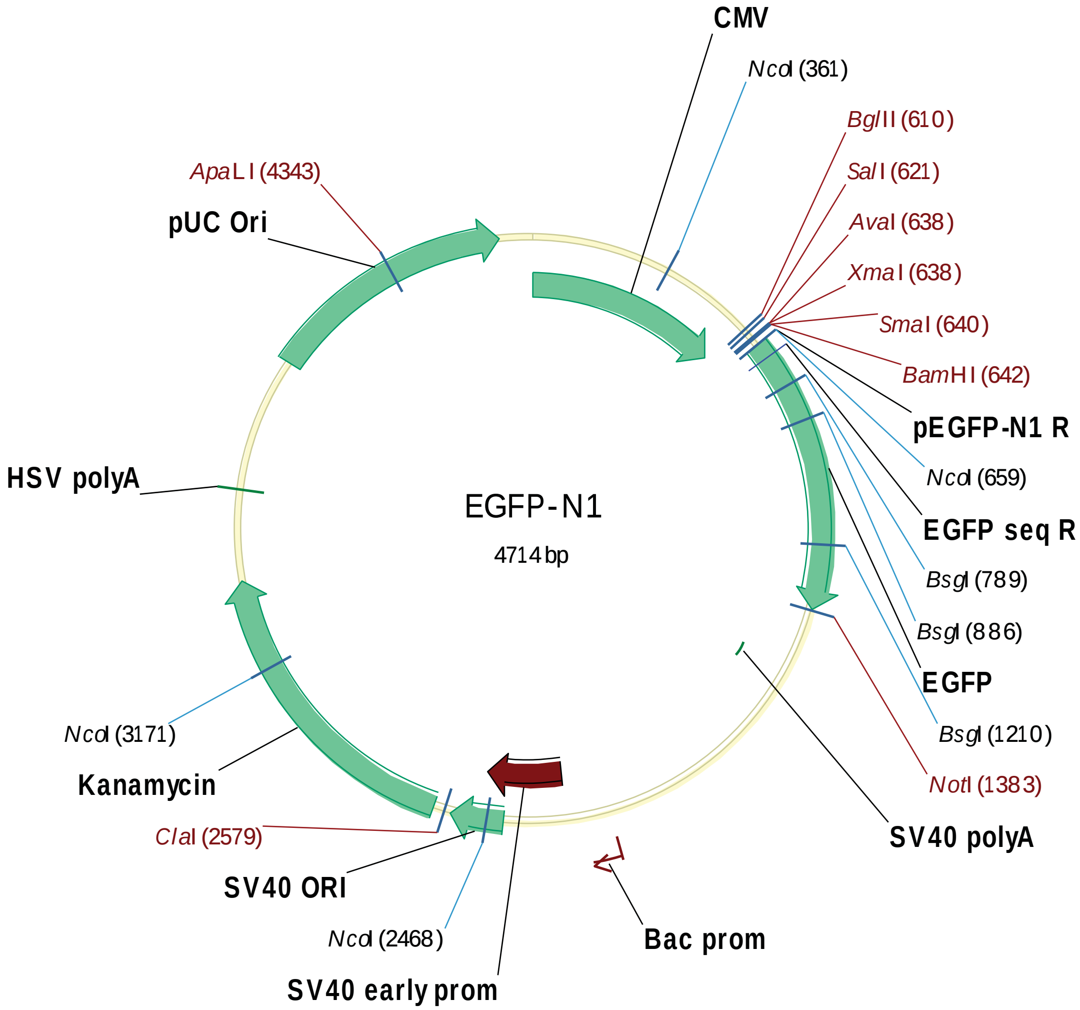
CMV
NcoI (361)
BglII (610)
SalI (621)
AvaI (638)
XmaI (638)
SmaI (640)
BamHI (642)
pEGFP-N1 R
NcoI (659)
EGFP seq R
BsgI (789)
BsgI (886)
EGFP
BsgI (1210)
NotI (1383)
SV40 polyA
Bac prom
SV40 early prom
NcoI (2468)
SV40 ORI
ClaI (2579)
Kanamycin
NcoI (3171)
HSV polyA
pUC Ori
ApaLI (4343)
EGFP-N1
4714 bp

Sequence EGFP-N1: 1-4714

1tagttattaatagtaatcaattacggggtcattagttcatagcccatatatggagttccgcgttacataacttacggtaaatggcccgcct
ggctgaccgcccaacgacccccgcccattgacgtcaataatgacgtatgttcccatagtaacgccaatagggactttccattgacgtc
aatgggtggagtatttacggtaaactgcccacttggcagtacatcaagtgtatcatatgccaagtacgccccctattgacgtcaatgacg
gtaaatggcccgcctggcattatgcccagtacatgaccttatgggactttcctacttggcagtacatctacgtattagtcatcgctattacca
tggtgatgcggttttggcagtacatcaatgggcgtggatagcggtttgactcacggggatttccaagtctccaccccattgacgtcaatgg
gagtttgttttggcaccaaaatcaacgggactttccaaaatgtcgtaacaactccgccccattgacgcaaatgggcggtaggcgtgtac
ggtgggaggtctatataagcagagctggtttagtgaaccgtcagatccgctagcgctaccggactcagatctacccagtcgacggtac
cgcgggcccgggatccaccggtcgccaccatggtgagcaagggcgaggagctgttcaccggggtggtgcccatcctggtcgagct
ggacggcgacgtaaacggccacaagttcagcgtgtccggcgagggcgagggcgatgccacctacggcaagctgaccctgaagtt
catctgcaccaccggcaagctgcccgtgccctggcccaccctcgtgaccaccctgacctacggcgtgcagtgcttcagccgctaccc

cgaccacatgaagcagcacgacttcttcaagtccgccatgcccgaaggctacgtccaggagcgcaccatcttcttcaaggacgacg
gcaactacaagacccgcgccgaggtgaagttcgagggcgacaccctggtgaaccgcatcgagctgaagggcatcgacttcaagg
aggacggcaacatcctggggcacaagctggagtacaactacaacagccacaacgtctatatcatggccgacaagcagaagaac
ggcatcaaggtgaacttcaagatccgccacaacatcgaggacggcagcgtgcagctcgccgaccactaccagcagaacacccccc
atcggcgacggccccgtgctgctgcccgacaaccactacctgagcacccagtccgccctgagcaaagaccccaacgagaagcgc
gatcacatggtcctgctggagttcgtgaccgccgccgggatcactctcggcatggacgagctgtacaagtaaagcggccgcgactct
agatcataatcagccataccacatttgtagaggttttacttgctttaaaaaacctcccacacctccccctgaacctgaaacataaaatga
atgcaattgttgttgttaacttgtttattgcagcttataatggttacaaataaagcaatagcatcacaaatttcacaaataaagcatttttttca
ctgcattctagttgtggtttgtccaaactcatcaatgtatcttaaggcgtaaattgtaagcgttaatattttgttaaaattcgcgttaaatttttgtt
aaatcagctcattttttaaccaataggccgaaatcggcaaaatcccttataaatcaaaagaatagaccgagatagggttgagtgttgttc
cagtttggaacaagagtccactattaaagaacgtggactccaacgtcaaagggcgaaaaaccgtctatcagggcgatggcccacta
cgtgaaccatcaccctaatcaagttttttggggtcgaggtgccgtaaagcactaaatcggaaccctaaagggagcccccgatttagag
cttgacggggaaagccggcgaacgtggcgagaaaggaagggaagaaagcgaaaggagcgggcgctagggcgctggcaagt
gtagcggtcacgctgcgcgtaaccaccacacccgccgcgcttaatgcgccgctacagggcgcgtcaggtggcacttttcggggaaa
tgtgcgcggaacccctatttgtttatttttctaaatacattcaaatatgtatccgctcatgagacaataaccctgataaatgcttcaataatatt
gaaaaaggaagagtcctgaggcggaaagaaccagctgtggaatgtgtgtcagttagggtgtggaaagtccccaggctccccagca
ggcagaagtatgcaaagcatgcatctcaattagtcagcaaccaggtgtggaaagtccccaggctccccagcaggcagaagtatgc
aaagcatgcatctcaattagtcagcaaccatagtcccgcccctaactccgcccatcccgcccctaactccgcccagttccgcccattct
ccgccccatggctgactaattttttttatttatgcagaggccgaggccgcctcggcctctgagctattccagaagtagtgaggaggctttttt
ggaggcctaggcttttgcaaagatcgatcaagagacaggatgaggatcgtttcgcatgattgaacaagatggattgcacgcaggttct
ccggccgcttgggtggagaggctattcggctatgactgggcacaacagacaatcggctgctctgatgccgccgtgttccggctgtcag
cgcaggggcgcccggttctttttgtcaagaccgacctgtccggtgccctgaatgaactgcaagacgaggcagcgcggctatcgtggct
ggccacgacgggcgttccttgcgcagctgtgctcgacgttgtcactgaagcgggaagggactggctgctattgggcgaagtgccggg
gcaggatctcctgtcatctcaccttgctcctgccgagaaagtatccatcatggctgatgcaatgcggcggctgcatacgcttgatccggc
tacctgcccattcgaccaccaagcgaaacatcgcatcgagcgagcacgtactcggatggaagccggtcttgtcgatcaggatgatct
ggacgaagagcatcaggggctcgcgccagccgaactgttcgccaggctcaaggcgagcatgcccgacggcgaggatctcgtcgt
gacccatggcgatgcctgcttgccgaatatcatggtggaaaatggccgcttttctggattcatcgactgtggccggctgggtgtggcgga
ccgctatcaggacatagcgttggctacccgtgatattgctgaagagcttggcggcgaatgggctgaccgcttcctcgtgctttacggtat
cgccgctcccgattcgcagcgcatcgccttctatcgccttcttgacgagttcttctgagcgggactctggggttcgaaatgaccgaccaa
gcgacgcccaacctgccatcacgagatttcgattccaccgccgccttctatgaaaggttgggcttcggaatcgttttccgggacgccgg
ctggatgatcctccagcgcggggatctcatgctggagttcttcgcccaccctagggggaggctaactgaaacacggaaggagacaa
taccggaaggaacccgcgctatgacggcaataaaaagacagaataaaacgcacggtgttgggtcgtttgttcataaacgcggggtt
cggtcccagggctggcactctgtcgataccccaccgagaccccattggggccaatacgcccgcgtttcttccttttccccaccccaccc
cccaagttcgggtgaaggcccagggctcgcagccaacgtcggggcggcaggccctgccatagcctcaggttactcatatatacttta

gattgatttaaaacttcatttttaatttaaaaggatctaggtgaagatcctttttgataatctcatgaccaaaatcccttaacgtgagttttcgttc
cactgagcgtcagaccccgtagaaaagatcaaaggatcttcttgagatcctttttttctgcgcgtaatctgctgcttgcaaacaaaaaaa
ccaccgctaccagcggtggtttgtttgccggatcaagagctaccaactctttttccgaaggtaactggcttcagcagagcgcagatacc
aaatactgtccttctagtgtagccgtagttaggccaccacttcaagaactctgtagcaccgcctacatacctcgctctgctaatcctgttac
cagtggctgctgccagtggcgataagtcgtgtcttaccgggttggactcaagacgatagttaccggataaggcgcagcggtcgggctg
aacggggggttcgtgcacacagcccagcttggagcgaacgacctacaccgaactgagatacctacagcgtgagctatgagaaag
cgccacgcttcccgaagggagaaaggcggacaggtatccggtaagcggcagggtcggaacaggagagcgcacgagggagctt
ccagggggaaacgcctggtatctttatagtcctgtcgggtttcgccacctctgacttgagcgtcgatttttgtgatgctcgtcaggggggcg
gagcctatggaaaaacgccagcaacgcggcctttttacggttcctggccttttgctggccttttgctcacatgttctttcctgcgttatcccct
gattctgtggataaccgtattaccgccatgcat4714

Acknowledgements

First of all, I would like to thank Antoine Peters for his supervision during my PhD. For all the critical comments and the many discussions we had and for his continuous support.

Also, many many thanks to all the current and former lab members of the Peters group. For the great time we spent together at the FMI and also outside the FMI.

I would also like to thank the members of my PhD committee, Susan Gasser, Gunter Reuter and Marc Bühler for helpful discussions and suggestions.

Many thanks to Dirk Schübeler and his lab members for stimulating discussions.

Special thanks also to Susanne, Peter, Vijay, Rabih and Flo from my office, for great atmosphere.

And then of course thanks to the members of at the FMI facilities that supported me: Jens, Laurent, Steve, Heinz, Hans-Ruedi, Michael,…

Thanks thanks thanks…

And especially, thanks to Ula, to my parents, to my family and all of my friends.

Curriculum Vitae

Personal:

Name	Rico Kunzmann
Date of birth	01.02.1977
Place of birth	Zürich, Zürich
Nationality	Swiss
Civil status	single

Language skills:

German, English, French, Italian

Education:

1998	Eidg. Matur Type E (economy) at Gymnasium Zürich Hottingen
1998 – 2000	Studies of German, history and philosophy at the University of Zürich
2001 – 2005	Studies of biology (Bachelor degree) at the University of Zürich
2005 – 2007	Master Thesis at the University of Zürich under supervision of Prof. Dr. Ueli Grossniklaus.
2007 – 2012	PhD at the FMI for Biomedical Research in Basel under supervision of Dr. Antoine Peters